A COMPUTER MODEL OF WATER-IN-OIL EMULSION COAGULATION

LISA SEYMOUR

Thesis Presented for the Degree of

DOCTOR OF PHILOSOPHY

in the

Department of Chemistry

Faculty of Science

University of Cape Town

August 1996

"You will not cease from exploration,
and the end of your exploring will be
to arrive where you started,
and know the place for the first time."

T.S.Eliot

"Arts and sciences are not cast in a mould,
but are formed and perfected by degrees,
by often handling and polishing,
as bears leisurely lick their cubs into form."

Michael de Montaigne. 1533-1592

TO BRUCE

CONTENTS

CHAPTER 3: THE AQUEOUS PHASE

CHAPTER 4: W/O EMULSION EXPERIMENTAL STUDIES

CHAPTER 5: W/O EMULSION COMPUTER MODEL

CHAPTER 6: CONCLUSIONS

APPENDICES

ACKNOWLEDGEMENTS

I would like to thank a few people who have made this work possible:

- My supervisor, Graham Jackson, for his patience, encouragement and guidance and for being both an intellectual role model and a good friend.

- The staff and fellow students of the University of Cape Town Chemistry Department for all their invaluable assistance.

- Fellow members of our research group, for the interesting discussions, helpful suggestions and camaraderie.

- The University of Cape Town Information Technology Services Department for their assistance with computational problems.

- My parents for always having faith in me.

- My husband, Bruce, for his unwavering support and patience.

- Lastly the Foundation for Research and Development and AECI (Pty) Ltd for their financial support.

ABSTRACT

Computer Model of Water-in-Oil Emulsion Coagulation

Lisa Seymour, Department of Chemistry, University of Cape Town, Private Bag, Rondebosch, 7700, South Africa. - *Submitted August 1996*

In this thesis, a stochastic computer model of water-in-oil emulsion coagulation, a two stage process of aggregation and coalescence, is presented. The theoretical basis of the model, including equations for the van der Waals, electrostatic and steric energy barriers between dissimilar droplets, is described. Many of these equations have been derived by the author.

A chemical speciation study of the aqueous phase typically found in emulsion explosives is presented. A potentiometric investigation of the protonation equilibria of propionate, succinate and mono-methyl succinate in tetraethyl ammonium bromide, ammonium nitrate, sodium nitrate, potassium nitrate and calcium nitrate at 25^{o}C and 3 mol/dm^{3} ionic strength was performed. Nuclear Magnetic Resonance titrations for succinate and propionate in varying concentrations of the same salts are also shown. A method of converting thermodynamic stability constants from one ionic strength to another using a modified form of the Pitzer equations is presented with a computer program which performs the conversion. A novel method of obtaining complexation constants from protonation constants in varying media is proposed.

Using optical microscopy, creaming rates and laser particle sizing, the affects of changing surfactant concentration, salt concentration, pH and shearing time for emulsions of ammonium nitrate solution in heptane with CRILL 43 are shown. Equations are derived for converting creaming rate data to droplet size information and a computer program for converting Malvern light intensity data in the anomalous regime (typical of water-in-oil emulsions) to size distribution data is presented.

The computer model is validated against experimental data from this work and the literature and is used to make stability predictions for systems for which no data exists. Further uses for the model are discussed.

PUBLICATIONS

1 L.F.Seymour and G.E.Jackson (1996), "Computer Model of W/O Emulsion Coagulation", *Proceedings of the 33rd Convention of the South African Chemical Institute*, University of Cape Town, Cape Town, South Africa.

2 G.E.Jackson and L.F.Seymour (1995), "Formation Constants at high Ionic Strength - I. Potentiometric determination of Protonation Constants for Succinic, Propionic and Mono-Methyl Succinic Acid in different Ionic Media.", *Talanta*, **42**:5.

3 G.E.Jackson and L.F.Seymour (1995), "Formation Constants at high Ionic Strength - II. The Ionic Strength Correction of Formation Constants using a Simplified Pitzer Equation.", *Talanta*, **42**:9.

4 L.F.Seymour and G.E.Jackson (1994), "Weak Binding Constants in Aqueous Solution.", *Proceedings of the Gordon Research Conference on Water and Aqueous Solutions*, Plymouth, New Hampshire, USA.

5 L.F.Seymour and G.E.Jackson (1993), "The Correction of Formation Constants to High Ionic Strength.", *Proceedings of International Symposium on Metal Ions in Solution*, Malelane Lodge, Transvaal, South Africa.

6 L.F.Seymour and G.E.Jackson (1993), "The Correction of Formation Constants to High Ionic Strength.", *Proceedings of the 23rd International IUPAC Conference on Solution Chemistry*, Leicester, UK.

7 L.F.Seymour and G.E.Jackson (1991), "The effect of Metal Ion Speciation upon Emulsion Stability.", *Proceedings of the South African Chemical Institute 31st Convention*, Rhodes University, Grahamstown, South Africa.

8 L.F.Seymour and G.E.Jackson (1992), "Formation Constants of Weak Complexes at High Ionic Strength". *Proceedings of the University of Cape Town Molecular Recognition and Synthetic Design Conference*, University of Cape Town, Cape Town, South Africa.

LIST OF SYMBOLS, NOTATIONS AND ABBREVIATIONS

[i]	concentration of species i (mol dm^{-3})
α	expansion parameter for surfactant in solvent
$\beta^{(0)}_{ca}$	Pitzer empirical parameter for ion pair ca
$\beta^{(1)}_{ca}$	Pitzer empirical parameter for ion pair ca
β_{pqr}	overall thermodynamic stability constant
$\beta_{m,pqr}$	overall thermodynamic stability constant based on molal activity
γ_i	activity coefficient of ion i
Γ_{pqr}	activity coefficient quotient
$\Delta\rho$	change in density between external and internal emulsion phases (kg m^{-3})
Δ_{clump}	energy barrier to two droplets clumping (J)
Δ_{coal}	energy barrier to two droplets coalescing (J)
ΔG	Gibbs free energy change (J)
ΔH	change in enthalpy (J)
ΔS	change in entropy (J K_{-1})
Δ_T	energy barrier to the coagulation of two droplets (J)
ε_0	permittivity of a vacuum (8.854×10^{-12} C^2 J^{-1} m^{-1})
ε_r	relative permittivity or dielectric constant of medium
η	viscosity of a solution (kg m^{-1} s^{-1})
θ	fraction of droplet surface covered with emulsifier
κ	inverse Debye length (m^{-1})
ν_i	number of surfactant molecules per unit area of surface of droplet i (m^{-2})
ν_{max}	maximum number of surfactant molecules per unit surface area of droplets (m^{-2})
ρ	density of a solution (kg m^{-3})
σ_i	standard deviation of parameter i
ϕ	internal phase volume ratio of an emulsion
ψ_i	surface potential of droplet i (V)
a_i	radius of droplet i (m)
a_i	activity of ion i
A_i	surface area of droplet i
A	Hamaker constant (J)
A_{eff}	Effective Hamaker constant in medium (J)
B_{ca}	Pitzer virial coefficient for ion pair ca (equation 3.*)
B'_{ca}	The derivative of B_{ca}
c_i	concentration of ion i (mol dm^{-3})
C_i	Pitzer virial coefficient for ion pair i
C^{ϕ}_i	Pitzer empirical parameter for ion pair i
C_M	dimensionless osmotic repulsion constant
C_V	dimensionless volume restriction constant
d	a distance parameter (m)
d_s	minimum distance between centres of surfactant molecules on droplet surface (m)
D[3,2]	Equivalent surface area mean diameter (μm)
D[4,3]	Equivalent volume mean diameter (μm)
D[v,0.5]	Particle diameter for which 50% of particles is smaller (μm)

emf	Electromotive force (V)
eqn	equation
E	Electromotive force (V)
E^0	Electromotive force of an electrochemical cell at standard state (V)
E_A	Van der Waals attraction between droplets (J)
E_{cell}	Electromotive force of an electrochemical cell (V)
E_{clump}	interaction energy during droplet clumping (J)
EDTA	ethylenedinitrilo tetraacetic acid
E_M	osmotic repulsion during the coalescence of two droplets (J)
E_R	Electrostatic repulsion between droplets (J)
E_S	Steric energy during the coalescence of two droplets (J)
ESTA	Equilibrium Simulation Titration Analysis program package
E_T	total interaction energy between two droplets (J)
E_V	volume restriction energy during the coalescence of two droplets (J)
f'	a general Debye Hückel term
F	Faraday constant (9.6485×10^4 C mol^{-1})
g	acceleration due to gravity (m s^{-2})
H	theoretical interparticle distance between two perfect spheres, may be positive or negative depending on overlap (m)
HLB	hydrophile-lipophile balance. Balance between the hydrophilic and lipophilic affinities of a surfactant.
h_{min}	minimum thickness of emulsion bilayer (m)
H_{min}	theoretical interparticle separation after which droplet flattening can no longer be calculated due to geometrical constraints (m)
H_{max}	average interparticle separation between neighbouring droplets (m)
I	Ionic strength
I_c	Ionic strength (mol dm^{-3})
I_m	Ionic strength (mol kg^{-1})
I_{SI}	Ionic strength (mol m^{-3})
k	Boltzmann constant (1.381×10^{-23} J K^{-1})
k_{dist}	size distribution constant (μm^5)
KHP	potassium hydrogen phthalate
K_{pqr}	stepwise stability constant
$K_{c,pqr}$	stepwise stability constant expressed in terms of molarity
$K_{m,pqr}$	stepwise stability constant expressed in terms of molality
K_M	osmotic repulsion constant (J m^{-2})
K_V	volume restriction constant (J m^{-2})
K_W	ionic product of water (mol^2 dm^{-6})
l	average head to tail length of surfactant when adsorbed to particle (m)
l_M	length of creaming vessel (m)
L	Avogadro constant (6.022×10^{23} mol^{-1})
log diff	a measure of the correctness of a least squares fitting
m	number of CH_2 groups in hydrocarbon chain of surfactant
m_i	molality of ion i (mol kg^{-1})
Mr_i	molar mass of species i
MS	mono-methyl succinate
$M(H)$	dimensionless osmotic repulsion function

N	total number of droplets
n_i	number of droplets with radius a_i
$n^{20}{}_D$	index of refraction at 20°C relative to air for sodium yellow
NMR	Nuclear Magnetic Resonance
OBJE	optimization module of ESTA
PA	propionic acid
pD	$-\log[a_D]$ where $D = {}^2H^+$
pH	$-\log[a_H]$ where $H = H^+$
P_M	osmotic repulsion constant (J m^{-2})
ppm	parts per million
P_V	volume restriction constant (J m^{-2})
q	a distance parameter (m)
r	maximum distance between centres of colliding droplets (m)
r_M	radius of creaming vessel (m)
R	crystallographic R-factor
R	gas constant (8.314 J K^{-1} mol^{-1})
R[5,3]	a droplet size distribution parameter (μm^2)
s	Nernstian slope of electrochemical cell
s	distance between centres of colliding droplets (m)
SA	Succinic acid
Span	relative spread of particle diameters
t-BuOH	tertiary butyl alcohol
T	temperature (K)
T_i	total concentration of species i (mol dm^{-3})
$V(H)$	dimensionless volume restriction function
V^0	initial volume in titration vessel (dm^3)
V_C	volume of cream (m^3)
V_T	total emulsion volume (m^3)
v	volume titrated (dm^3)
w/o	water-in-oil
x	dimensionless interparticle distance
y	particle size ratio
z_i	charge of ion i
$\bar{Z}_H$	proton formation function
$\bar{Z}_M$	metal formation function

CHAPTER ONE
INTRODUCTION

1.1 EMULSION APPLICATIONS

The importance of emulsions in everyday life can't be understated. Many of the foods we eat, such as butter, margarine, salad dressing and mayonnaise are emulsions. Other than in foodstuffs, emulsions are found in the form of agricultural sprays, bituminous products, cosmetics and pharmaceutical preparations.[1] In fact every day we prepare an emulsion in our daily task of washing dishes. The process is simple, we pour warm water into a sink, add dishwashing liquid, a water soluble surfactant, and then we add our plates, still covered with food residues. Oil is normally immiscible in water, but the dishwashing liquid and some mechanical action, results in the oil residues from the plates becoming intimately mixed in the water in the form of tiny droplets, making the cleaning of plates possible. Extensive research has gone into designing the best surfactant for this task as emulsions are inherently unstable. If we leave the water in the sink after the cleaning process, the droplets of oil will eventually coalesce, forming larger droplets and eventually the two phases will separate out leaving an oil film on the water.

In the chemical industry, emulsions are encountered extensively in stages during preparation or as end products. A great advantage of using emulsions such as cold creams, vanishing creams, deodorant creams and lotions in the cosmetic industry is the ability to apply both water- and oil-soluble ingredients simultaneously to the skin. Polishes are emulsions which are formulated so that they break after application, spreading the polishing ingredient in a smooth, even film. Similarly emulsion paints are formulated with the pigment in the dispersed phase remaining in an even film after the external phase has evaporated. In the field of water-in-oil emulsions considerable research has been done on the demulsification of crude oil. Practically all crude oils contain salt water in a free state or in a water-in-oil emulsion.[2] Recently, in the pharmaceutical and agrochemical industries emulsions have been used to control the release of active substances on application.[3] These complex emulsions are produced so that the active substance is solubilized in the internal phase. Unfortunately much of the research done on emulsions in industry is restricted to the patent literature.

1.2 WATER-IN-OIL EMULSION COAGULATION

An emulsion is a heterogeneous system, consisting of at least one immiscible liquid intimately dispersed in another with a surface active compound partitioned at the interface between the liquids. The outer phase of an emulsion is referred to as the continuous, external or suspending medium and the inner phase of droplets is referred to as the dispersed, internal or suspended medium. Emulsions are a subset of colloids and dispersions.

Emulsions can be divided into two large groups according to the nature of the external phase. These two groups are either water-in-oil (w/o) or oil-in-water (o/w). Although studies on emulsions have been recorded since the Greek physician Galen (131 - *c.*201) recorded the emulsifying power of beeswax, only as recently as 1910 was the distinction made between the common form of emulsions, o/w, and the then extremely uncommon w/o form.[4] For this reason w/o emulsions are often referred to in the literature as reverse emulsions. More recently complex or multiple emulsions such as o/w/o and w/o/w have been recorded and studied.

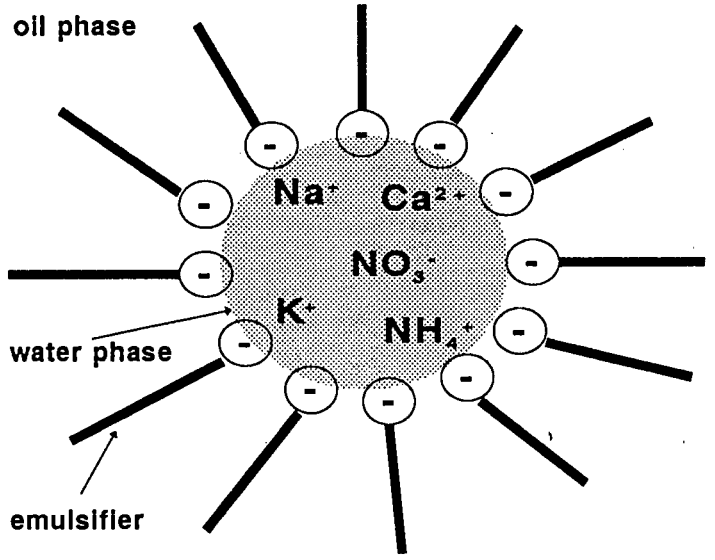

Figure 1.1

Simplistic drawing of a water-in-oil emulsion droplet.

A simplistic drawing of a w/o emulsion droplet is presented in figure 1.1. The surface active compounds that lend stability to emulsions are known as emulsifiers, emulsifying agents or surfactants. Surfactants are either anionic, cationic, nonionic or ampholytic depending on the nature of the emulsion headgroup. Soaps, the salts of long-chain fatty acids, are the most common surfactants.

Emulsions can also be divided according to the droplet size of the dispersed phase. Thus microemulsions are emulsions in which the size of the droplets of the dispersed phase is less than 10nm in diameter, while macroscopic emulsions have droplet sizes in the order of microns. Microemulsions, which were only discovered as recently as 1943, are thermodynamically stable and have a range of actual and potential uses in biotechnology, separation processes, microparticle synthesis and oil technology.[5-7] They form spontaneously and are translucent because of the very small droplet sizes.[8] However, macroemulsions which are more commonly found in industry are thermodynamically unstable. Because of their inherent instability, formation and stabilization of macroemulsions are considered the most important factors in the study of emulsions.[2] This thesis addresses the stability issues pertaining to w/o macroscopic emulsions.

The breakdown, or separation of an emulsion into two separate phases occurs *via* several kinetic mechanisms. Emulsion coagulation refers to the two-step process of aggregation and coalescence of emulsion droplets. Aggregation can be described as the clumping or sticking together of emulsion droplets forming droplet clusters, while coalescence is the joining of droplets to form larger droplets. The process of droplet coagulation is often the main cause of instability in emulsions, ultimately leading to the complete separation of both phases. In present emulsion stability theory, the various states of an emulsion, whether the droplets are stable, aggregated or coagulated, are explained in terms of inter-droplet energy-distance curves. If one is to control the emulsion it is necessary to be able to control these inter-droplet interactions.[3] The bulk stability of an emulsion is predicted to be dependent on the initial droplet coagulation barrier.

The theory of colloid and o/w emulsion stability is well developed, however, quantitative applicability is limited and comparisons between theory and experiment are lacking in the literature.[9,10] In contrast, in the field of w/o emulsions, fundamental understanding is well behind empirical knowledge. A literature review of the stability of w/o emulsions is presented in chapter two.

1.3 RESEARCH MOTIVATION

Emulsion explosives are used in South Africa in the civil engineering and mining industries. Emulsion explosives are high-internal-phase w/o emulsions. Because of the nature of these systems the stability problems are substantial. In the explosive emulsion manufacturing industries, there is a great deal of empirical understanding and companies have their own "rules of thumb" for the systems they work with. However there has been little progress in the scientific understanding of the systems.

The causes of instability which have been reported in these emulsion systems include:

- extended storage times
- changes in pH
- temperature changes
- shock or shearing
- hydrolysis of surfactants in the presence of calcium
- crystallization of the aqueous phase

The aqueous phase, emulsifier and oil phase are the three components that influence these emulsions, although other additives which have no real effect on the emulsion structure are added to make the emulsion explosive detonable. The organic phase is normally a hydrocarbon fuel and the aqueous phase is a supersaturated metastable salt solution, typically high in ammonium nitrate.[11] The most commonly used surfactants are oleic acid esters of sorbitol.[12]

In an emulsion, two immiscible liquids are mixed intimately. This intimate mixture of hydrocarbon fuel, gas bubbles and oxidizers such as ammonium nitrate when detonated, explodes. The stoichiometry of the explosive reaction is:

$$3nNH_4NO_3 + (CH_2)_n \rightarrow nCO_2 + 7nH_2O + 3nN_2 \qquad \text{....1.1}$$

The gas bubbles are needed to ensure detonation. They provide a mechanism through adiabatic compression for the conversion of the energy in the detonation shock wave to the heat energy necessary to produce the chemical reaction and sustain detonation.

An explosion results from a sudden release of energy. The release of energy must happen so rapidly that a local accumulation of energy occurs at the site of the explosion. This energy is then rapidly dissipated in various ways such as by an explosive blast wave or by thermal radiation. The shattering power is directly proportional to the speed of the detonation wave. The energy available for explosive yield can be measured by the Helmholtz free-energy decrease for the explosive process.[13]

$$\textit{energy of explosion} = -\Delta E + T\Delta S \qquad \text{....1.2}$$

The high velocities of detonation are dependent on maintaining the intimately mixed liquid system. The stability requirements are demanding, such as withstanding wide ranges of temperature and long shelf lives. The aqueous phase is often supersaturated and crystallisation of the salts is known to cause film rupture and consequent instability. Curiously crystallization often does not occur because the number of droplets exceeds the number of heterogeneous nuclei present.[12] The storage stability of the emulsion does not always correlate well with initial droplet size.

Because of the complexity of emulsion explosives and the need in industry for a more scientific approach to stability problems, the motivation for this work was to gain a more fundamental understanding of the stability processes at work in emulsion explosives. A two forked approach was selected:

- To perform a chemical speciation analysis of the aqueous phase of typical emulsion explosives. The strong effects that calcium and pH changes have on the stability of these systems gave strong impetus for this study.
- To develop a computer model which would be able to predict the lifetime of a w/o emulsion based on the emulsion formulation and certain physical properties of its components.

It was realized at the start that much of the work that would be done in this area would have relevance outside of emulsion explosives.

1.4 THE SPECIATION OF THE AQUEOUS PHASE

Speciation defines the oxidation state, concentration and composition of each species present in a chemical sample.[14] Emulsion stability effects indicate that speciation could play a critical role in the stability of w/o emulsions. The speciation technique has been widely used to optimize industrial processes, explain drug behaviour and determine the bioavailability of metal ions in food.[14,15]

Therefore, an aim of this work was to determine the speciation of the aqueous phase typically found in emulsion explosives. To this extent it was hoped to quantify all interactions between surfactant headgroups and the various nitrate salts in the aqueous phase. The potentiometric technique was chosen as the primary method for determining the equilibrium constants necessary for the speciation analysis. An overview of the theory of this technique is presented in chapter three.

1.5 THE COMPUTER MODEL

There is a need in industry for a computer model that would be able to predict the lifetime of an emulsion given the formulation and certain physical properties of the emulsion constituents. Such a tool would allow for the rapid testing of different formulations but more importantly could be used to direct experimental work correctly, assisting in the development of emulsions with longer shelf lives. Alternatively the emulsion characteristics could be tailored to suit the application needed. This model would be useful in not only formulating new emulsions but also in understanding the problems of existing formulations. However, it must be noted that there are limitations inherent in modelling real systems. By its nature, a model, although it attempts to represent a real system, never represents reality fully but only represents a subset or simplified version of the real system. The strength of models lie in their ability to assist with the understanding of a system.

The number and size of particles in an emulsion are known to change over time until the emulsion reaches a stable state or separates entirely.[2] When using the current emulsion theory to predict emulsion stability, researchers have looked at the energy barrier between two droplets and determined whether the droplets would coagulate or not. If the droplets are predicted to coagulate, the emulsion is said to be unstable and *visa versa.* Many emulsions have been known to stabilize after a period in which the initial droplets coagulate, therefore the initial rate of coagulation of an emulsion can't be used to calculate the lifetime of the bulk emulsion. A model is needed in which the bulk stability of an emulsion can be determined. Hall and co-workers have devised an elegant solution to this problem for the case of o/w emulsions. Their approach determines the extent of droplet coalescence beyond the critical aggregation point.[17-19]

An aim of this work was to develop a model based on their approach and adapt it for the case of w/o emulsions. This model would be able to assist in the study of any w/o emulsion and would not be restricted purely to the case of explosive emulsions.

1.6 REFERENCES

1. D.J.Shaw (1993), *Introduction to Colloid & Surface Chemistry*, Butterworth-Heinemann Ltd, Oxford, 4th Ed.
2. S.Berkman and G.Egloff (1941), *Emulsions and Foams*, Reinhold Publishing Corporation, New York.
3. Th.F.Tadros (1993), "Industrial Applications of Dispersions", *Adv.Colloid Interface Science*, **46**:1.
4. Paul Becher (1965), *Emulsions: Theory and Practice*, Reinhold Publishing Corporation, New York, 2nd Ed.
5. A.M.Brun and W.H.Wade (1990), "Determination of the Structure of a Water in Oil Microemulsion", *J.Colloid Interface Science*, **139**:93.
6. J.Eastoe, W.K.Young, B.H.Robinson and D.C.Steytler (1990), "Scattering Studies of Microemulsions in Low-density Alkanes", *J.Chem.Soc.Faraday Trans*, **86**:2883.
7. E.B.Abuin, M.A.Rubio and E.A.Lissi (1993), "Solubility of Water in Water-in-Oil Microemulsions stabilized by Cetyltrimethylammonium.", *J.Colloid Interface Science*, **158**:129.
8. M.L.Robbins, J.Bock and J.S.Huang (1988), "Model for Microemulsions. III. Interfacial Tension and Droplet Size Correlation with Phase Behaviour of Mixed Surfactants.", *J.Colloid Interface Science*, **126**:114.
9. J.Th.G.Overbeek (1982), "Strong and Weak Points in the Interpretation of Colloid Stability", *Adv.Colloid Interface Science*, **16**:17.
10. J.Th.G.Overbeek (1977), "Recent Developments in the Understanding of Colloid Stability", *J.Colloid Interface Science*, **58**:408.
11. J.C.Ravey and M.J.Stebe (1994), "Properties of Fluorinated Non-ionic Surfactant-based Systems and Comparison with Non-fluorinated Systems", *Colloids and Surfaces A:*, **84**:11.
12. H.A.Bampfield and J.Cooper (1988), "Emulsion Explosives", in *Encyclopedia of Emulsion Technology*, P.Becher (ed.), Marcel Dekker, New York, vol. 3, p. 281.
13. G.F.Kinney (1962), *Explosive Shocks in Air*, The MacMillan Company, New York.
14. J.R.Duffield and D.R.Williams (1989), "Chemical Speciation", *Chemistry in Britain*:375.

15. D.R.Williams (1989), "Guest Editorial: Speciation and Legislation", *Chemical Speciation and Bioavailability*, **1(1)**:3.

16. P.M.May, P.W.Linder and D.R.Williams (1977), "Computer Simulation of Metal-ion Equilibria: Models for the Low-molecular-weight Complex Distribution of Calcium(II), Magnesium(II), Manganese(II), Iron(III), Copper(II), Zinc(II), and Lead(II) Ions in Human Blood Plasma", *J.Chem.Soc.Dalton Trans.*:588.

17. S.B.Hall, J.R Duffield and D.R.Williams (1991), "A Reassessment of the Applicability of the DLVO Theory as an Explanation for the Schulze-Hardy Rule for Colloid Aggregation", *J.Colloid Interface Science*, **143**:411.

18. S.B.Hall, J.R.Duffield and D.R.Williams (1991), "A Stochastic Computer Simulation of Emulsion Coalescence", *J.Colloid Interface Science*, **143**:416.

19. S.B.Hall, G.W.Gaskin, J.R.Duffield and D.R.Williams (1991), "An Interfacial Equilibria Model for the Electrokinetic Properties of a Fat Emulsion", *Int.J.Pharmaceutics*, **70**:251.

CHAPTER TWO
W/O EMULSION STABILITY THEORY

2.1 INTRODUCTION

Before constructing a computer model to predict w/o emulsion stability, all processes that affect emulsion stability need to be evaluated. A literature review in this area highlighted that the theory of o/w emulsions has been extensively studied while very little work has been done on the stability of w/o emulsions. This is surprising considering the fact that these emulsions are used extensively in industry, especially in the petroleum, explosives, cosmetics and food industries.

Consequently much of the theory for w/o emulsions is presented in this thesis for the first time. What follows is a description of the main processes which affect w/o emulsion stability, partly from literature sources and partly from our own development.

The most important physical property of an emulsion is its stability.[1] However the term 'stable' is only used in the kinetic sense as emulsions are thermodynamically unstable due to the free energy associated with the large interfacial area between the two different phases. Emulsions tend to flocculate, accumulate at an interface or coalesce to reduce the interfacial area. This means that although emulsions spontaneously break down, under certain conditions the kinetic rate of breaking is such that the emulsion can survive for long periods of time.[2] Three main kinetic processes determine the stability of an emulsion, namely "creaming or sedimentation", "clumping, flocculation or aggregation" and "coalescence". Any or all of these phenomena may occur after the emulsion has been prepared.[3]

In our discussion we will be referring to the terms, creaming, clumping, coalescence and coagulation defined as follows:

Creaming is the rise or fall of the droplets of the internal phase due to a difference in density, the droplets remaining separate. This can be reversed by gentle agitation.[4,5]

Clumping is the sticking together of droplets in the formation of three dimensional clusters without the droplets coalescing. This process is normally reversible.[6-8]

Coalescence is the joining of droplets in an emulsion to form larger droplets, which leads to a coarser emulsion and can ultimately lead to two separate liquid layers. Coalescence has to be preceded by clumping.

Coagulation is the process of clumping followed by coalescence.[9]

Within an emulsion the first three kinetic processes can be occurring simultaneously, however the rate-determining process determines the bulk emulsion stability.

A requirement for the formation of w/o emulsions is that the interfacial film should be uncharged and rigid.[10] Uncharged films are found when a nonionic surfactant is used or if an ionic surfactant is associated with ions of the opposite charge found in the aqueous phase. The higher the valency of this counter ion , the stronger the association and the lower the net charge of the film. Polyvalent ions also give rigidity to the interface by interlinking surfactant molecules. The nature of the surfactant and its speciation at the interface can determine the emulsion structure, rheology and stability therefore in an analysis of emulsions the role of chemical interactions should be an important consideration.[11]

This principle is reflected in Bancroft's rule which states that the phase in which the emulsifying agent is the more soluble tends to be the dispersion medium.[1] The HLB system for selecting emulsifiers has a similar basis. The HLB value is a function of the weight percentage of hydrophillic portion of a nonionic surfactant. This has been used extensively in predicting emulsion stability, however some workers have found that none of the methods proposed for determining HLB values give a reliable guide to emulsion stability.[3,12]

Another property of an emulsion is the volume percent of the internal phase. This term is often referred to as the concentration of an emulsion. Emulsions have been formulated over the entire range from 0% to 100% internal phase volume.[13] In concentrated emulsions, with a high internal phase volume, coalescence is the rate-determining step, whereas in dilute emulsions clumping or coalescence can be the rate determining step.[9,12,14] The process which determines the emulsion stability has also been shown to be temperature dependent.[4] An analysis of the factors affecting each rate follows.

2.2 CREAMING

Stability with respect to creaming has been shown experimentally to depend on the droplet-size distribution, the state of aggregation of the droplets and the density difference between the internal and external media. The droplet size distribution is mainly determined by the energy input during emulsification, as well as by the nature and amount of surfactants.[15]

The terminal velocity of a spherical particle settling under gravity in a dense medium is calculated by solving the relevant Navier-Stokes equations and is given in equation 2.1.[16]

$$v = \frac{2}{9\eta} g a^2 \Delta\rho \qquad \text{....2.1}$$

where g = acceleration due to gravity (m s^{-2})

a = droplet radius (m)

η = the viscosity of the external phase (kg m^{-1} s^{-1})

$\Delta\rho$ = density difference between internal and external phase (kg m^{-3})

From equation 2.1 the average mass creaming rate of a dilute emulsion calculated in a tube of infinite length, ds/dt, can be calculated and is depicted in Equation 2.2.[17,18]

$$\frac{ds}{dt} = \sum_i \frac{8\pi}{27\eta\phi V_T} g n_i a_i^5 \Delta\rho \qquad \text{....2.2}$$

where n_i = number of droplets of radius a_i

V_T = total volume of the emulsion (m^3)

ϕ = the internal phase volume ratio of the emulsion

Hence the Stokes law predicts that creaming should increase as the droplet sizes increases, the density difference between the two phases increases, the viscosity of the external phase decreases or if any formulation changes affect any of the above parameters. To prevent creaming emulsion formulators commonly set $\Delta\rho$ to zero or increase the viscosity of the external phase. The viscosity of a pure liquid is known to decrease as the temperature increases according to equation 2.3.[19] Therefore creaming will increase with an increase in temperature.

$$\eta = A_{vis}\, e^{\frac{E_{vis}}{RT}} \qquad \text{....2.3}$$

where A_{vis} = pre exponential factor

E_{vis} = activation energy

The experimental measurement of creaming rates is generally performed in glassware calibrated for volumes such as measuring cylinders. The change in the volume of the cream layer is monitored versus time. Equation 2.2 can then be written as equation 2.4 which predicts that the creaming rate should increase as the width of the cylinder increases.

$$\frac{dV_C}{dt} = \sum_i \frac{8\pi^2 r_M^2 g \Delta\rho}{27\eta\phi V_T}\, n_i a_i^5 \qquad \text{....2.4}$$

where r_M = the radius of the measuring cylinder (m)

V_c = the volume of the creamed layer (m^3)

The equation derived above is in agreement with the prediction that no creaming will occur if the conditions for equation 2.5 are fulfilled.[20]

$$\frac{4}{3}\pi a^3 \Delta\rho g l_M << kT \qquad \text{....2.5}$$

where l_M = length of vessel (m)

Experimentally creaming rates are determined in vessels of finite length. As the particles cream, a Boltzman distribution of particles is set up through the length of the vessel.[18] The environment surrounding each droplet can no longer be considered dilute and hydrodynamic interactions with neighbouring droplets decrease the velocity of each droplet. Experimentally equations 2.2 and 2.4 only apply to the initial creaming rate of the emulsion when the droplet environment can be considered to be dilute. If clumping and coalescence is minimal during the initial creaming state, a plot of the change in the cream volume against time should give a straight line.

Creaming is not necessarily accompanied by clumping or coalescence although it facilitates both processes and the final cream volume depends upon the extent of aggregation or coalescence of the particles.[21] In turn clumping and coalescence of an emulsion enhances creaming as two aggregated particles cream with the effective size of both particles and larger droplets cream faster.[8] The creaming equation does not take into account clumping of the droplets, so creaming results of aggregated droplets will manifest itself as an apparent increase in droplet sizes and a skewing of the size distribution to larger sizes.

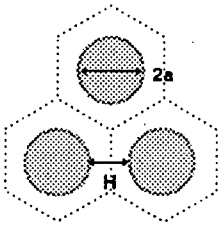

$$\phi_C = \frac{\pi}{3\sqrt{2}} \frac{a^3}{(a+\frac{H}{2})^3} \qquad \text{....2.6}$$

as $H \rightarrow 0$ $\phi_C \rightarrow 0.74$

The internal phase ratio of a cream, ϕ_c, can be calculated for a cream of monodisperse spherical droplets, of radius a, and with the closest interparticle separation being H according to equation 2.6.

If we assume that no association occurs between the droplets, the formation of a cream can be compared to the formation of a heap of hard spheres. An analysis for uniform particles gives a random packing with $0.59<\phi_C<0.65$, however if the particles are non-uniform a random packing with $0.59<\phi_C<0.84$ is obtained.[22,23] Therefore the broader the size distribution the greater the internal phase volume as the smaller droplets can fit into the interstitial spaces between the larger droplets. It is known that there is an interaction between emulsion droplets and if clumping of droplets occurs a cream of monodisperse droplets can be hexagonal close packed with $\phi_C = 0.74$. In fact 0.74 has been quoted as a guide to the concentration of a cream.[14]

$$\phi_C\ (flattened\ sphere) = \frac{\pi}{3\sqrt{2}} \frac{(8a^3 - 18aH^2 - 3H^3)}{(2a + h_{min} + H)^3}$$

$$as\ \ h_{min} \rightarrow 0\ \ and\ \ H \rightarrow H_{min}\ \ \ \phi_C \rightarrow 0.86\ \ \ where\ \ \ H_{min} = -0.114a$$

$$\phi_C\ (rhomboidal\ dodecahedron) = \frac{a^3}{(a + \frac{h_{min}}{\sqrt{2}-})^3} \qquad \text{....2.7}$$

$$as\ \ h_{min} \rightarrow 0\ \ \ \phi_C \rightarrow 1$$

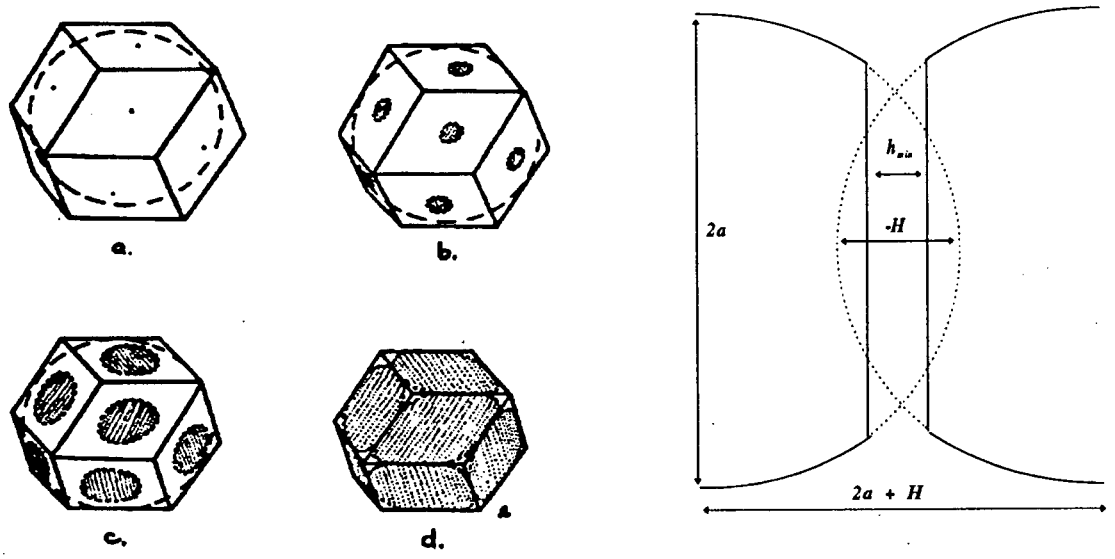

Figure 2.2

Transition from sphere to rhomboidal dodecahedron. Taken from Lissant.[24]

For monodisperse droplets, if ϕ exceeds 0.74 the droplets can no longer be considered to be perfect spheres and their shape would have to be distorted. A geometrical analysis was done of high internal phase ratio emulsions by K.J.Lissant where it was predicted that these emulsions would follow a rhomboidal dodecahedral packing mode when the internal phase contained between 74 to 94%.[24] A rhomboidal dodecahedron has 12 identical rhomboid faces. As the internal volume percent increases above 74%, the spheres become flattened on 12 sides as depicted in figure 2.2 and the internal phase ratio of the cream increases according to equation 2.7.

The variable h_{min} has been added to Lissant's analysis. h_{min} represents the closest interparticle separation or width of surfactant bilayer. Within the floccule or in the cream hydrodynamic forces flatten the droplets.[12] Systematic studies on highly concentrated w/o emulsions have

been almost non-existent until recently when microscopic and conductivity results have confirmed the theory and shown that the emulsions are highly disperse and the droplets are polyhedral in shape.[25]

In most emulsions creaming is not the rate determining step. However the study of creaming rates is invaluable in predicting bulk emulsion stability. Many of the factors that determine emulsion instability affect creaming rates to the same degree. The experimental technique is inexpensive to perform and results are reproducible.

2.3 CLUMPING

The non-Newtonian behaviour of dilute emulsions is a consequence of the clumping of emulsion droplets.[26] In concentrated emulsions often the only indication that the clumping of droplets is occurring is an increase in the viscosity.[4] However clumping can only be measured experimentally in very dilute emulsions in which coalescence is rapid and creaming is avoided. The observed degree of clumping of an emulsion, D, is defined in equation 2.8 and can be determined by counting under a microscope and from the increase in initial creaming rates.[9,26-29]

$$D = \frac{number\ of\ dimers}{number\ of\ monomers + number\ of\ dimers} \qquad \text{....2.8}$$

Experimentally clumping has been found to increase under the following conditions:

- the particle distribution is non uniform;
- the droplets are small;
- in the presence of a velocity gradient in the solution after shearing;
- as the molecular weight of the surfactant increases;
- and as a function of the surfactant concentration, temperature and processing details.[4,9,30]

The net energy of interaction between two particles as they approach one another, E_{clump}, is given as a summation of all attractive and repulsive terms between the particles and is based

on the DLVO (Derjaguin, Landau, Verwey and Overbeek) theory of colloid stability.[31,32] If the energy barrier calculated is less than the thermal energy kT, then two particles are predicted to clump. D.R.Williams *et al.* have reinvestigated this theory for o/w emulsions and what follows is a reinvestigation of the corresponding theory for w/o emulsions.[33]

2.3.1 VAN DER WAALS ATTRACTION

The van der Waals attraction, E_A, between two spherical particles *in vacuo* has been derived by Hamaker and can be expressed by the dimensionless variable x as follows:[7,34]

$$E_A = -\frac{A}{12}\left[\frac{1}{2x+x^2} + \frac{1}{1+2x+x^2} + 2\ln\left(\frac{2x+x^2}{1+2x+x^2}\right)\right] \qquad \text{....2.9}$$

$$\text{where} \quad x = \frac{H}{2a}$$

where a is the radius of the spherical particles in m,

H is the interparticle separation in m and

A is Hamaker's constant in J.

The presence of a liquid dispersion medium between the particles and a layer of stabilising agents both contribute to a significant lowering in the van der Waals interaction energy, and consequently the Hamaker constant needs to be replaced by an effective Hamaker constant for the medium. For an emulsion consisting of a non-homogeneous array of particles, the van der Waals interaction for two particles with different radii can be calculated from the dimensionless interparticle distance, x, and the particle size ratio, y, as follows:[34]

$$E_A = -\frac{A_{eff}}{12}\left[\frac{y}{x^2+xy+x} + \frac{y}{x^2+xy+x+y} + 2\ln\left(\frac{x^2+xy+x}{x^2+xy+x+y}\right)\right] \qquad \text{....2.10}$$

$$\text{where} \quad x = \frac{H}{2a_1} \quad \text{and} \quad y = \frac{a_2}{a_1}$$

A dimensionless form of the van der Waals attraction is plotted in figure 2.4. For the case of a monodisperse system, where y=1, as the radius increases, x decreases resulting in a corresponding increase in the attractive energy. Hence the larger the droplets, the stronger

the van der Waals attraction.

A major problem in calculating the van der Waals attraction is that of evaluating the effective Hamaker constant.[21] A change in this constant will result in a change in the rate of aggregation and from the minimum rate of shear needed to cause redispersion, the effective Hamaker constant can be estimated.[26,30] Using this method Albers *et al.* calculated the value A_{eff} = 4x10^{-22} J for water droplets in benzene, carbon tetrachloride mixtures when using a minimum distance between droplets of 4nm. We have used their effective Hamaker constant for water droplets in hydrocarbon solvents although we should mention that other workers have quoted much larger values.[18]

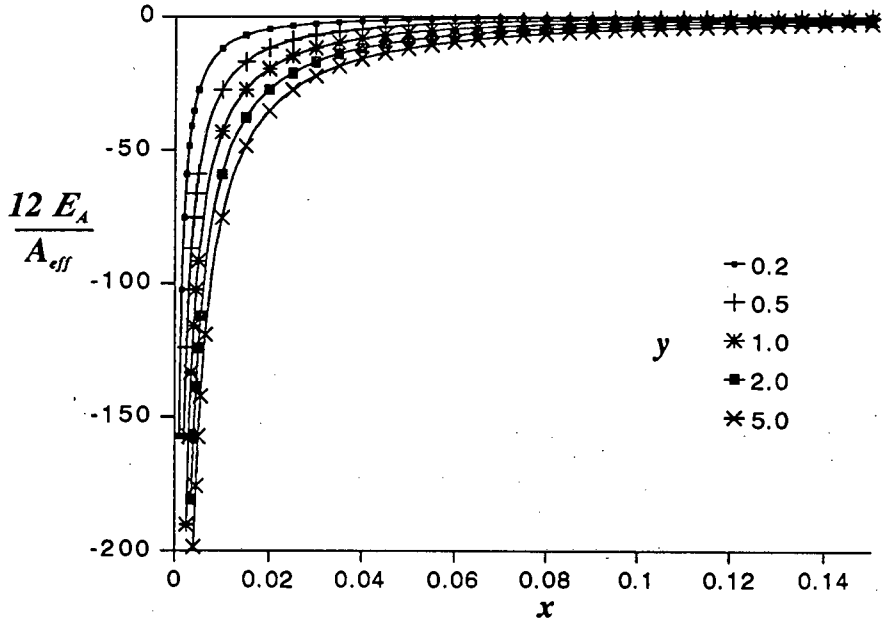

Figure 2.4

Plot of the dimensionless attractive energy against the dimensionless interparticle distance, x, for different particle size ratios.

2.3.2 ELECTROSTATIC REPULSION

Coehn's rule states that a substance will be positively charged when it is in contact with another substance having a lower dielectric charge. A repulsive term, which takes into account the electrostatic interaction between a droplet and its nearest neighbour (with which it is colliding) has been calculated by Albers and Overbeek in a monodisperse, oil continuous system with large double layers (equation 2.11).[18] In this equation the assumption is made that during a collision the surface potential of the drops remain constant.[35]

$$E_R = \frac{\varepsilon_r \varepsilon_0 \psi^2 a^2 e^{-\kappa H}}{H+2a} \qquad \text{....2.11}$$

where ε_r is the dielectric constant or relative permittivity of the organic phase,

ε_0 is the permittivity of a vacuum (8.854×10^{-12} $C^2N^{-1}m^{-2}$)[19]

ψ is the surface potential of the drop in V and

κ^{-1} is the thickness of the electrical double layer or Debye length in m.

The inverse Debye length is given by:[7,36-38]

$$\kappa = \sqrt{\frac{2F^2 I_{SI}}{\varepsilon_r \varepsilon_0 RT}} \qquad \text{....2.12}$$

where R is the gas constant,

F is the Faraday constant and

I_{SI} is the ionic strength of the organic phase in mol m^{-3}.

A dimensionless form of the repulsive interaction is plotted in figure 2.5 according to equation 2.13. As the electrokinetic radius, κa increases so the repulsive interaction between the two droplets increases towards a limiting value.

$$\frac{E_R}{\varepsilon_r \varepsilon_0 \psi^2 a} = \frac{\kappa a \, e^{-\kappa H}}{\kappa H + 2\kappa a} \qquad \text{....2.13}$$

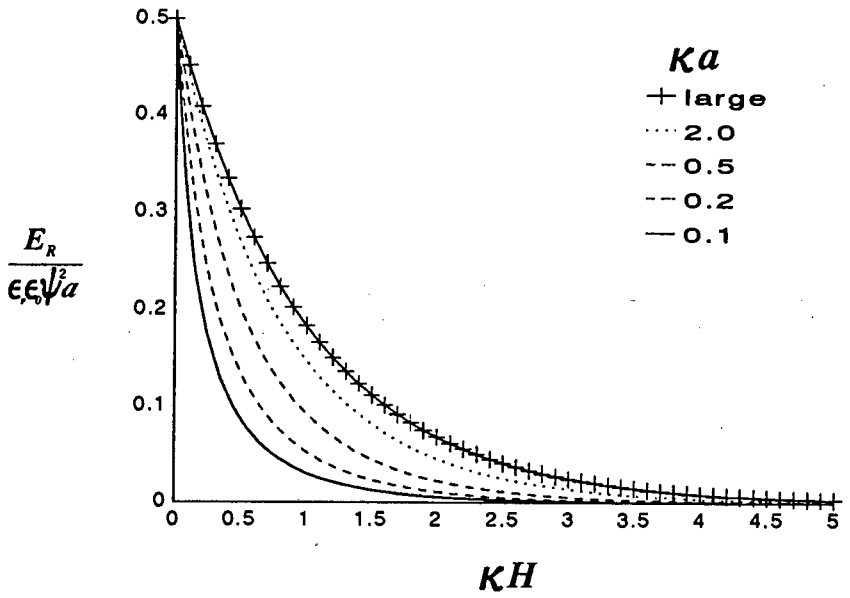

Figure 2.5

Plot of the dimensionless repulsive interaction against κH for varying values of the electrokinetic radius, κa.

The above equations hold for collisions between two droplets of the same size. For collisions between two dissimilar droplets the repulsive term must be modified. The interaction for dissimilar droplets can be calculated as follows:[39]

$$E_R = \frac{\varepsilon_r \varepsilon_0 \psi_1 \psi_2 a_1 a_2 e^{-\kappa H}}{H + a_1 + a_2} \qquad \text{....2.14}$$

the subscripts 1 and 2 refer to the respective properties of the two colliding droplets.

For systems where $\kappa a > 10$ and $\psi < 0.1$V, the Derjaguin approximation simplifies the above equations. However, for most w/o systems equation 2.14 is used.[35,40]

2.3.3 THE EFFECT OF EMULSION CONCENTRATION

In apolar oils, distinct though small ionization occurs and very little charge is needed to obtain appreciable surface potentials. Consequently in w/o emulsions the Debye length is much larger than in o/w emulsions and can sometimes be several microns thick. In o/w

emulsions the repulsive energy of the droplets when equally dispersed is normally zero. In the case of w/o emulsions, however, this is not the case and interactions with many droplets occur. W.Albers and J.Th.G.Overbeek calculated the repulsion energy taking into account long range repulsion for a monodisperse sample of droplets.[41] For a polydisperse emulsion sample in which only the properties of the two colliding droplets and the average properties of the rest of the emulsion are known, equations 2.15 to 2.19 can be derived.

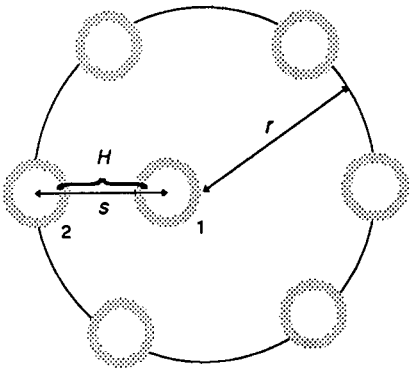

Figure 2.6

Diagram showing the variables used in describing the interactions between droplet 1 and other droplets. Twelve droplets are positioned on the sphere with radius *r*.

$$E_R = \varepsilon_r \varepsilon_0 \psi_1 \psi_2 a_1 a_2 e^{\kappa(a_1+a_2)} \frac{e^{-\kappa s}}{s}$$

$$+ \varepsilon_r \varepsilon_0 \psi_1 \bar{\psi} a_1 \bar{a} e^{\kappa(a_1+\bar{a})} \frac{\{6e^{-\kappa\sqrt{\frac{r^2}{s^2}-\frac{r\bar{r}}{s^2}+\bar{S}^2}} - 6e^{-\kappa(2r-s)}\}}{\kappa r(r-s)} \qquad \text{....2.15}$$

$$+ \varepsilon_r \varepsilon_0 \psi_1 \bar{\psi} a_1 \bar{a} e^{\kappa(a_1+\bar{a})} \frac{8.88e^{-1.3\kappa r}(1.3\kappa r+1)(e^{\kappa(r-s)}-e^{-\kappa(r-s)})}{\kappa^3 r^3 (r-s)}$$

$$s = H + a_1 + a_2 \qquad \text{....2.16}$$

$$H_{max} = \left(\frac{1.81}{\sqrt[3]{\phi}} - 2\right) \bar{a} \qquad \text{....2.17}$$

$$\lim_{r \to \infty} E_R = \varepsilon_r \varepsilon_0 \psi_1 \psi_2 a_1 a_2 e^{\kappa(a_1+a_2)} \frac{e^{-\kappa s}}{s} \qquad \text{....2.18}$$

$$r = H_{max} + a_1 + a_2 \qquad \text{....2.19}$$

where H_{max} is the average interparticle separation between neighbouring droplets.

r is the maximum distance between the centres of colliding droplets,

s is the distance between the centres of the colliding droplets during a collision and a "bar" above a value denotes an average value for all droplets.

During a collision droplet 1 will move from its "equally dispersed" position (when $H = H_{max}$ and $s = r$) towards droplet 2. The repulsion energy that is experienced by droplet 1 can be broken down into three terms. The first term in equation 2.15 is the interaction of droplet 1 with the colliding droplet. The second term is due to the interaction of droplet 1 with the 11 next closest neighbours and the third term is due to the interaction of droplet one with its non-nearest neighbours. The first term is the value of the repulsive energy between the two colliding droplets in an infinitely dilute system (equation 2.14) and is the same as the repulsive energy calculated without considering the effect of emulsion concentration (equation 2.18).

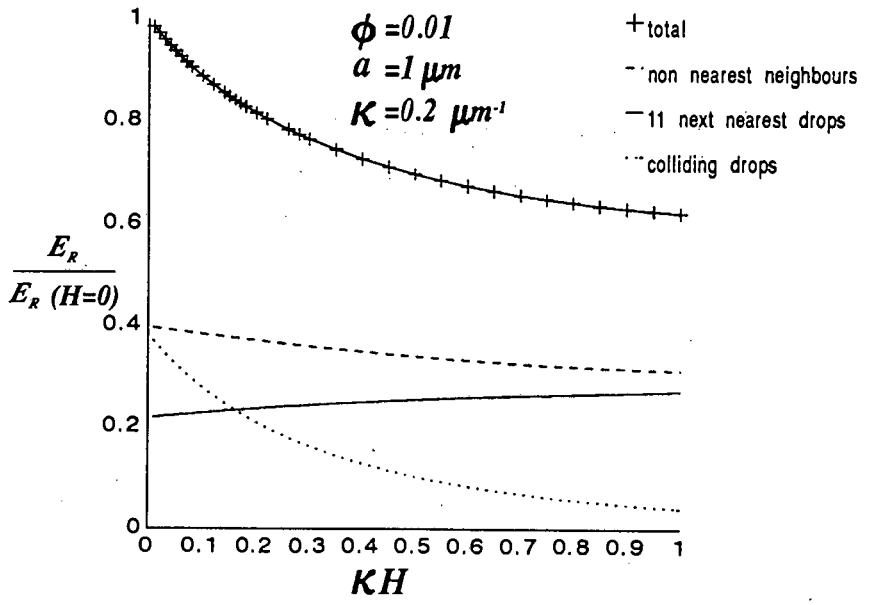

Figure 2.7

Plot of the repulsive interaction between monodisperse droplets with equal surface potential against κH, showing the contribution of the three terms.

For monodisperse droplets with equal surface potential, the contribution of all three terms to

the repulsive energy is shown in figure 2.7. As the two droplets approach each other, their repulsive energy increases, while the repulsive energy with the eleven next nearest neighbours decreases and with the non-nearest neighbours increases. It is apparent that even when the internal phase volume ratio is as low as 0.01 the non-nearest droplets give the maximum contribution to the repulsive energy. However the change in the repulsive energy with interdroplet distance, i.e. the slope of the graph is largely determined by the repulsion energy between the colliding droplets.

In the absence of attractive forces, the repulsive energy that has to be overcome for two droplets to clump is the difference between the repulsive energy when the droplets are at their average distance apart and the repulsive energy when the droplets are touching. In the case of w/o emulsions the droplets have a layer of surfactant molecules protruding into the oil phase. The surfactant tails overlap as the droplets approach one another and the closest interparticle separation is of the range of the surfactant length in the organic phase. The surfactant length can be estimated as follows:

$$l = m*1.26\times10^{-10} + 1.00\times10^{-10} \qquad \text{....2.20}$$

where l is the average surfactant head to tail length when adsorbed in metres and m is the number of CH_2 groups in the hydrocarbon chain of the surfactant.

The repulsion energy experienced by a droplet when the droplets are equally dispersed, $E_R(0)$, is defined in equation 2.21. Hence the repulsive energy barrier for a collision, in the absence of attractive forces, is defined in equation 2.22. This energy barrier is plotted in figures 2.8 to 2.10 for monodisperse droplets with equal surface potential. The maximum contribution to the repulsive energy barrier is due to the colliding droplets. This potential barrier decreases as the phase volume of the aqueous phase increases and increases as the thickness of the double layer increases.

$$E_R(0) = \lim_{s \to r} E_R = \varepsilon_r\varepsilon_0\psi_1 a_1\{\psi_2 a_2 \frac{e^{-\kappa r}e^{\kappa(a_1+a_2)}}{r} + \bar{\psi}\bar{a}\frac{11e^{-\kappa r}e^{\kappa(a_1+\bar{a})}}{r}\} + \varepsilon_r\varepsilon_0\psi_1\bar{\psi}a_1\bar{a}e^{\kappa(a_1+\bar{a})}\frac{17.76e^{-1.3\kappa r}(1.3\kappa r+1)}{\kappa^2 r^3} \qquad \text{....2.21}$$

$$\Delta E_R = E_R(s=a_1+a_2+l) - E_R(0) \qquad \text{....2.22}$$

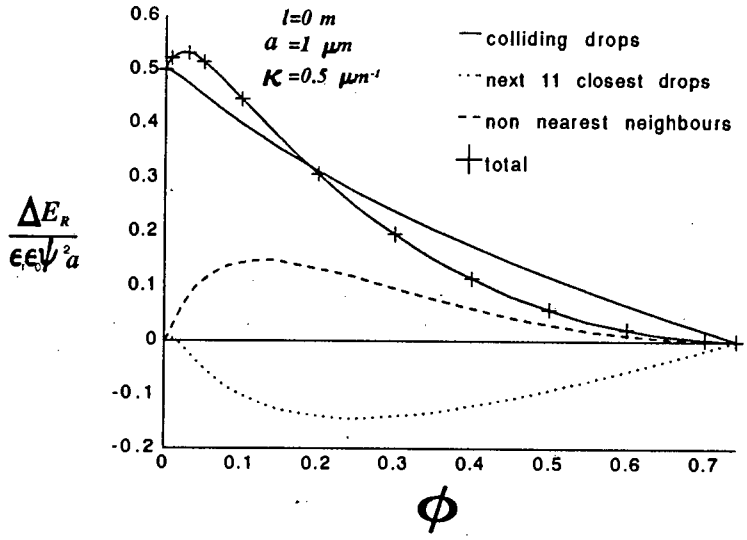

Figure 2.8

Plot of the repulsive energy barrier to a collision against the internal phase volume ratio, ϕ, showing the contribution of the three terms. ($a_1=a_2=\bar{a}$ $\psi_1=\psi_2=\bar{\psi}$)

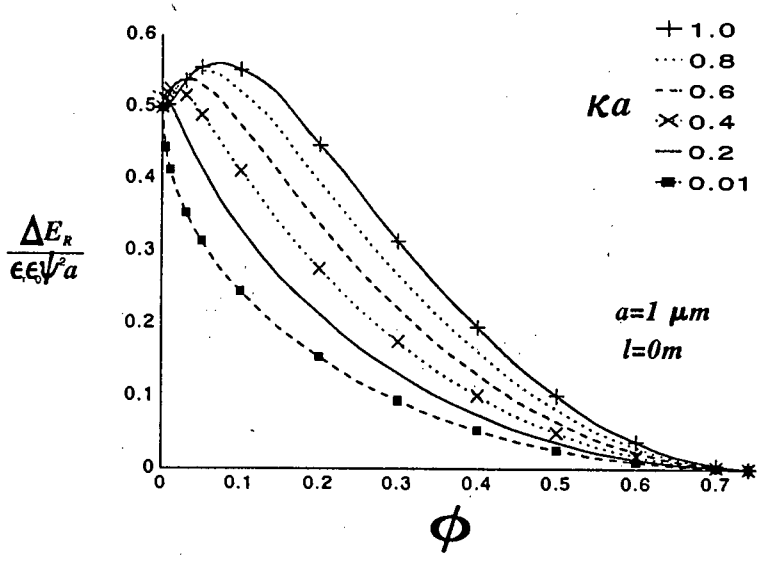

Figure 2.9

Plot of the repulsive energy barrier to a collision against the internal phase volume ratio, ϕ, showing the effect of the thickness of the double layer. ($a_1=a_2=\bar{a}$ $\psi_1=\psi_2=\bar{\psi}$)

Figure 2.10 shows clearly that as the droplet sizes increase so the repulsive energy barrier increases. This would suggest that larger droplets are more stable with respect to clumping than smaller droplets. However as we have shown, as the droplet size increases there is also a corresponding increase in the van der Waals attraction.

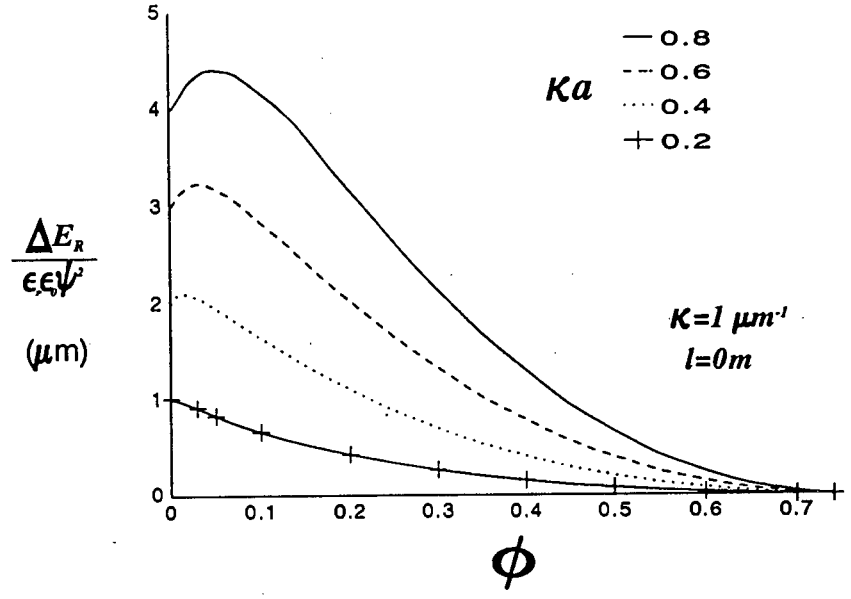

Figure 2.10

Plot of the repulsive energy barrier to a collision against the internal phase volume ratio, ϕ, showing the effect of the droplet size. ($\psi_1=\psi_2=\bar{\psi}$)

2.3.4 OTHER FORCES

Steric stabilization is another term that affects the clumping of emulsion droplets. The interaction of layers of adsorbed surfactant molecules at the phase interphase has been known to lead to repulsion or attraction.[42,43] In the case of w/o emulsions, when the surfactant chains and the solvent interact positively, this term is always repulsive.[37] Thin film experiments have suggested that no significant repulsive forces are generated in hydrocarbon media until the minimum distances of surface separation are less than twice the length of the surfactant (l<H<2l).[21,44]

Another term that promotes clumping of droplets is gravity. The weight of the particles upon one another promotes the increase of concentration in the local cream and subsequently increases flocculation.[29]

2.3.5 ENERGY BARRIER TO CLUMPING

As two droplets approach one another the total interaction is the sum of all repulsive and attractive energies. The predominant forces in the range ($a_1+a_2+l < s < r$) are the van der Waals and electrostatic forces, hence the total interactive energy leading to clumping, E_{clump}, is taken as the sum of these two forces (equation 2.23).

$$E_{clump} = E_A + E_R \qquad \text{....2.23}$$

Figures 2.11 and 2.12 show the change in the total interaction energy as a droplet moves from its average distance apart towards another droplet. As the droplets move together the interaction energy initially increases and then decreases as the attractive forces start playing a role. A secondary minimum is not observed as the repulsive forces predominate at large distances due to the thickness of the Debye length.

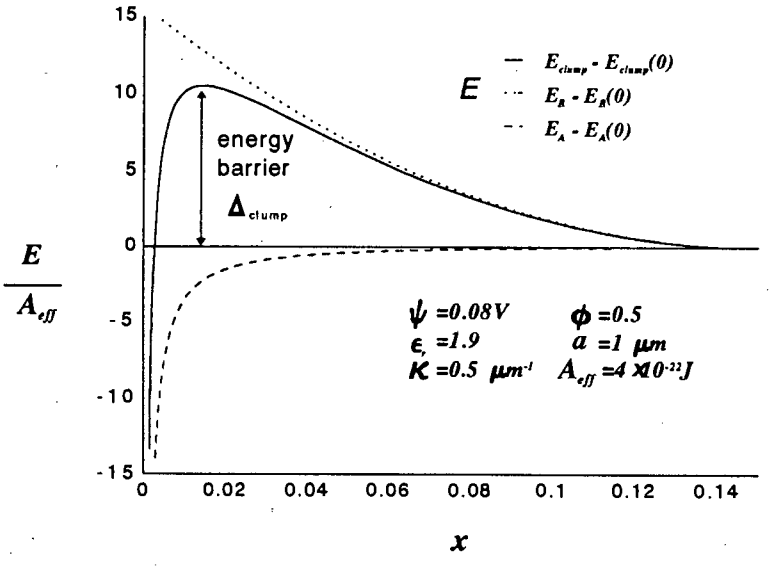

Figure 2.11

Plot of the total repulsive and attractive interactions against the dimensionless interparticle separation. ($a_1=a_2=\bar{a}$ $\psi_1=\psi_2=\bar{\psi}$). The test data used for the energy calculations is included in the plot.

The input parameters used in Figure are depicted in the diagram. The value chosen for the Effective Hamaker Constant (A_{eff}) is a literature estimate for water in benzene.[26] A discussion of the Hamaker Constant is given in section 2.3.1. The dielectric constant for heptane, ε_r, was

determined experimentally (section 4.5.1). The electrostatic parameters, ψ, a and κ were taken from literature values for an emulsion of water and benzene.[41]

$$\Delta_{clump} = E_{clump}(\max) - E_{clump}(0) \qquad \text{....2.24}$$

The energy barrier to clumping, Δ_{clump} is the difference between the maximum total interaction and the interaction when the droplets are equidistant (equation 2.4). This value has to be calculated numerically and is shown graphically in figure 2.12. Included in figure 2.12 is the area in which steric repulsion would play a role. For all phase volumes steric repulsion appears to only start playing a role once the energy barrier is decreasing, and hence does not affect the calculation of the energy barrier to clumping although it would affect the position of the primary energy minimum *i.e.* how close the droplets are in a clump.

Figure 2.12 shows that as the aqueous phase volume approaches 0.74 (maximum value for undistorted monodisperse droplets), the energy barrier approaches zero and the emulsion should clump. This is because $E_{clump} = E_{clump}(0)$. From this figure the energy barrier calculated for a dilute emulsion (ϕ=0.1) can be expressed as 10kT. This ought to retard clumping considerably.

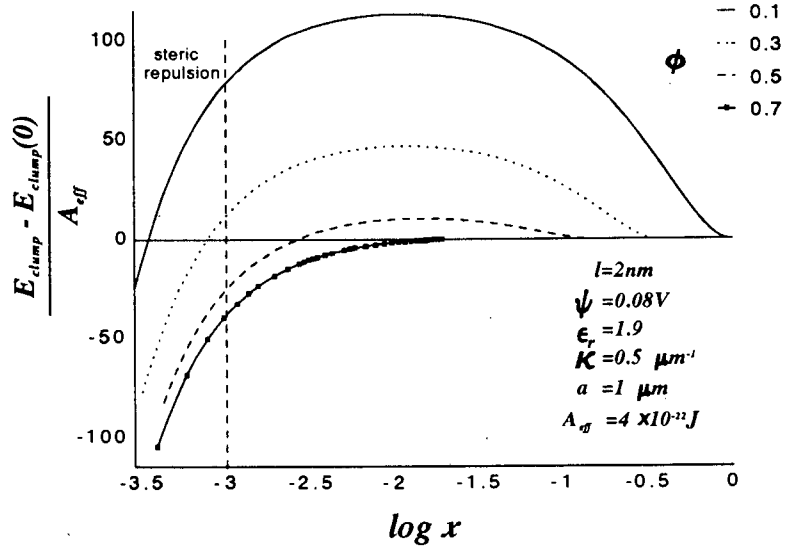

Figure 2.12

Plot of the total repulsive and attractive interactions against the log of the dimensionless interparticle separation, showing the effect of changes in the internal phase volume ratio. ($a_1=a_2=\bar{a}$ $\psi_1=\psi_2=\bar{\psi}$)

As the average droplet size increases there is a corresponding increase in the energy barrier to clumping (figure 2.13). This theory predicts that in w/o macroemulsions, larger droplets are more stable to clumping than smaller droplets.

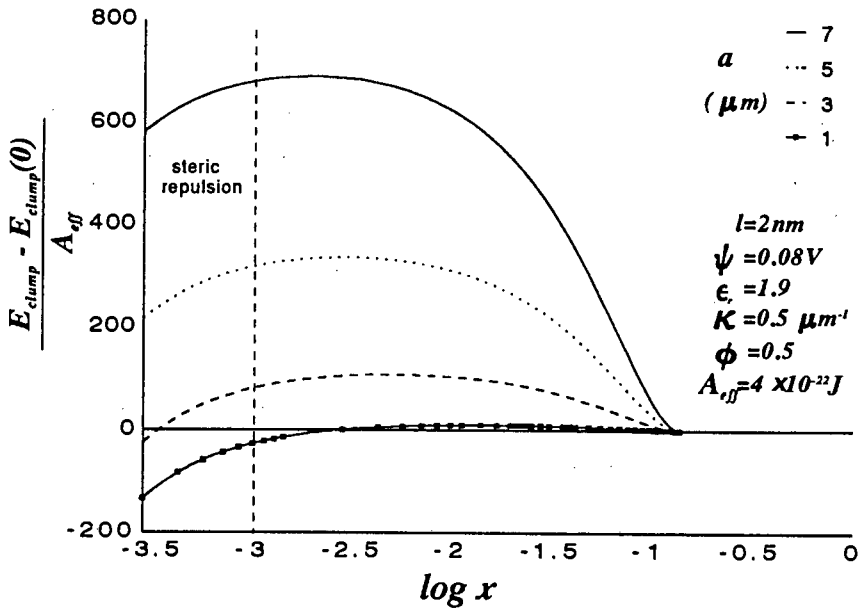

Figure 2.13

Plot of the total repulsive and attractive interactions against the log of the dimensionless interparticle separation, showing the effect of changes in the average droplet sizes. ($a_1=a_2=\bar{a}$ $\psi_1=\psi_2=\bar{\psi}$)

2.3.6 RATE OF CLUMPING

The maximum rate of a diffusion controlled reaction, *i.e.* in the absence of convection currents and creaming, that could occur in liquid systems between two molecules of the same size is proportional to the concentration of the reacting species and can be expressed as follows.[45]

$$\text{Rate of an encounter} = \frac{8\pi a N^2 D_0}{V_T} \qquad \text{....2.25}$$

$$\text{where} \quad D_0 = \frac{kT}{6\pi a \eta}$$

where V_T is the total volume in m^3,

kT is the thermal energy in J,

η is the viscosity of the external phase in kg m^{-1} s^{-1},

N is the total number of molecules

D_0 is the Stokes-Einstein relative diffusion coefficient for two non-interacting spheres

Smoluckowski described coagulation as a bimolecular reaction obeying equation 2.26.[7,46,47] Hence using Smoluckowski's theory the average time for an encounter, whether the collision is successful or not, can be approximated to be:

$$t = \frac{3\eta V_T}{4kTN^2} \qquad \text{....2.26}$$

Experimental results correlate well with this theory as plots of the half-life of a coagulating colloid against $1/N$ have given straight lines.[48]

2.4 COALESCENCE

The forces that dominate emulsion coalescence include electrostatic repulsion, van der Waals attraction and steric repulsion. As the droplets have already clumped, the interparticle distance is small and electrostatic repulsion over such a small distance is negligible.

2.4.1 STERIC REPULSION FOR EQUAL DROPLETS

For droplets to coalesce steric repulsion due to adsorbed surfactant molecules, E_S, has to be overcome (equation 2.26). This steric interaction has two contributions, an osmotic or mixing contribution, E_M, and an elastic, entropic or volume restriction contribution, E_V.[49,50] The osmotic effect in a good solvent, is an increase in free energy due to a local increase in concentration of surfactant molecules when the surfactant layers overlap during a collision. The volume restriction effect is the increase in free energy due to the surfactant molecules losing some of their conformational possibilities when the surfactant layers start overlapping.

$$E_S = E_V + E_M \qquad \text{....2.27}$$

Hesselink solved the energy function for the case of interactions between 2 flat interfaces where the surfactants are treated as interpenetrable and the interface as impenetrable.[42] In this work we will only be considering the simple case where the adsorbed molecules or surfactants are all identical and are attached at the head with a single tail protruding into the nonaqueous solvent.[42]

Equation 2.28 gives the resultant rise in free energy due to volume restriction when two interfaces covered by ν tails per unit area, approach each other.

$$E_V = A\ K_V\ V(H) \qquad K_V = 2\nu kT \qquad \text{....2.28}$$

where ν is the number of surfactant molecules per unit area of surface (m^{-2})

A is the area of the interacting interfaces (m^2)

$V(H)$ is a dimensionless volume restriction function evaluated numerically by the authors as a function of $H\alpha/l$

Equation 2.29 gives the increase in free energy due to osmotic repulsion between surfactant particles as two interfaces approach each other.

$$E_M = A\ K_M\ M(H) \qquad K_M = 2\sqrt{\frac{2\pi}{9}}^{3}(\alpha^2-1)\nu^2 l^2 kT \qquad \text{....2.29}$$

where $M(H)$ is a dimensionless osmotic repulsion function evaluated numerically by the authors as a function of $H\alpha/l$

α is an expansion parameter for the surfactant in the solvent caused by intramolecular interactions; this parameter is an indication of the quality of the solvent, for a good solvent $\alpha > 1$.

Figure 2.14 shows a plot of $M(H)$ and $V(H)$ as a function of $H\alpha/l$. The solid line was calculated through the literature data points, using a non linear regression fitting to an exponential function. To minimize computing time the exponential functions given in equation 2.30 will be used in our computer program. The accuracy of equation 2.30 was

found to be sufficient for our application.

$$V(H) = V_1 e^{-V_2 \frac{H\alpha}{l}} \quad V_1 = 52.51 \quad V_2 = 4.414$$
$$M(H) = M_1 e^{-M_2 \frac{H\alpha}{l}} \quad M_1 = 20.39 \quad M_2 = 2.467 \qquad \text{....2.30}$$

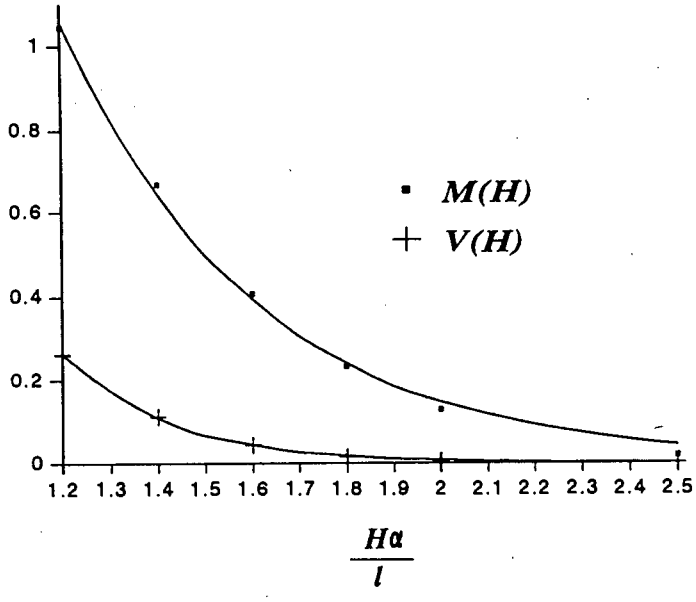

Figure 2.14

Plot of the dimensionless osmotic repulsion function, $M(H)$ and the dimensionless volume restriction function, $V(H)$ against $H\alpha/l$; showing the exponential functions (equations 2.30) as solid lines.

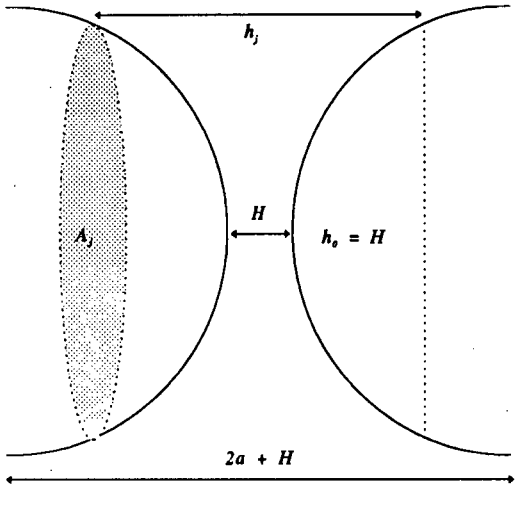

$$E_S = \sum_{j=0}^{N} (A_j - A_{j-1})(K_V V(h_j) + K_M M(h_j))$$
$$E_S = \lim_{N\to\infty} \pi a^2 \int_0^N \frac{2N-2j+1}{N^2} (K_V V(h_j) + K_M M(h_j))\, dj \qquad \text{....2.31}$$

For the case of two droplets at an interparticle distance of H, the area of interaction has to

be calculated. Mathematically the steric energy can be considered as a summation of terms $j = 0$ *to* N, proportional to area, $(A_j - A_{j-1})$, and interparticle distance, h_j. This reduces to a simple integral which can be solved analytically if the exponential terms for $V(H)$ and $M(H)$ are used. (equation 2.31)

Experimental evidence of w/o emulsions shows that as the droplets collide flattening of the droplets occur. In fact most w/o emulsions when viewed under a microscope show flattening. If we let the interparticle distance at which flattening starts occurring to be h_{min}, an equation for steric energy when flattening may occur is given in equations 2.32 to 2.34.

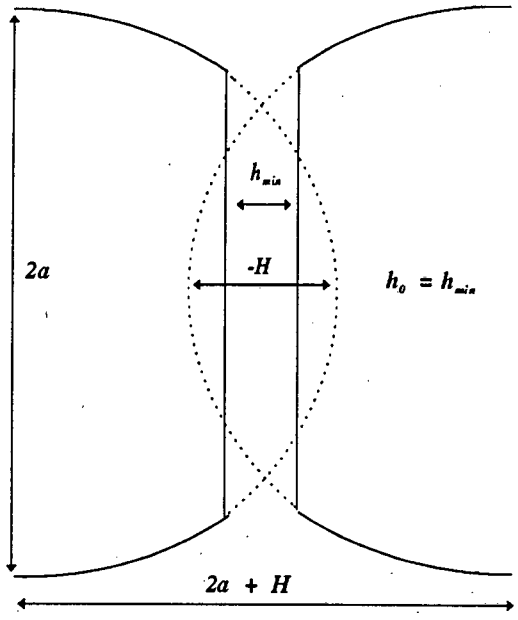

$$E_V = E_{V0} + q^2 \frac{P_V}{C_V^2}(e^{-C_V} + C_V - 1)$$

$$E_{V0} = (4a^2 - q^2)\frac{P_V}{2} \qquad \text{....2.32}$$

$$P_V = \frac{\pi}{2} V_1 K_V e^{-V_2 \frac{h_0 \alpha}{l}} \quad \text{and} \quad C_V = V_2 \frac{q\alpha}{l}$$

$$E_M = E_{M0} + q^2 \frac{P_M}{C_M^2}(e^{-C_M} + C_M - 1)$$

$$E_{M0} = (4a^2 - q^2)\frac{P_M}{2} \qquad \text{....2.33}$$

$$P_M = \frac{\pi}{2} M_1 K_M e^{-M_2 \frac{h_0 \alpha}{l}} \quad \text{and} \quad C_M = M_2 \frac{q\alpha}{l}$$

$$q = 2a + H - h_0$$
$$\text{if } H > h_{min} \text{ then } h_0 = H \text{ (no flattening)} \qquad \text{....2.34}$$
$$\text{if } H \le h_{min} \text{ then } h_0 = h_{min} \text{ (flattening)}$$

these equations are valid for $H >= H_{min}$ where $H_{min} = -0.114a$ (from equation 2.7).

The equations for E_V and E_M are similar and both contain two terms. The first term, denoted with a subscript zero refers to the interaction at the flattened face. The second term is the interaction due to the curved faces, which contains an exponential term. The steric energy, E_S, is plotted in figure 2.17. The function is initially exponential and then flattening of the droplet reduces the function to a straight line *i.e.* the E_{M0} and E_{V0} terms predominate when H is less than h_{min}.

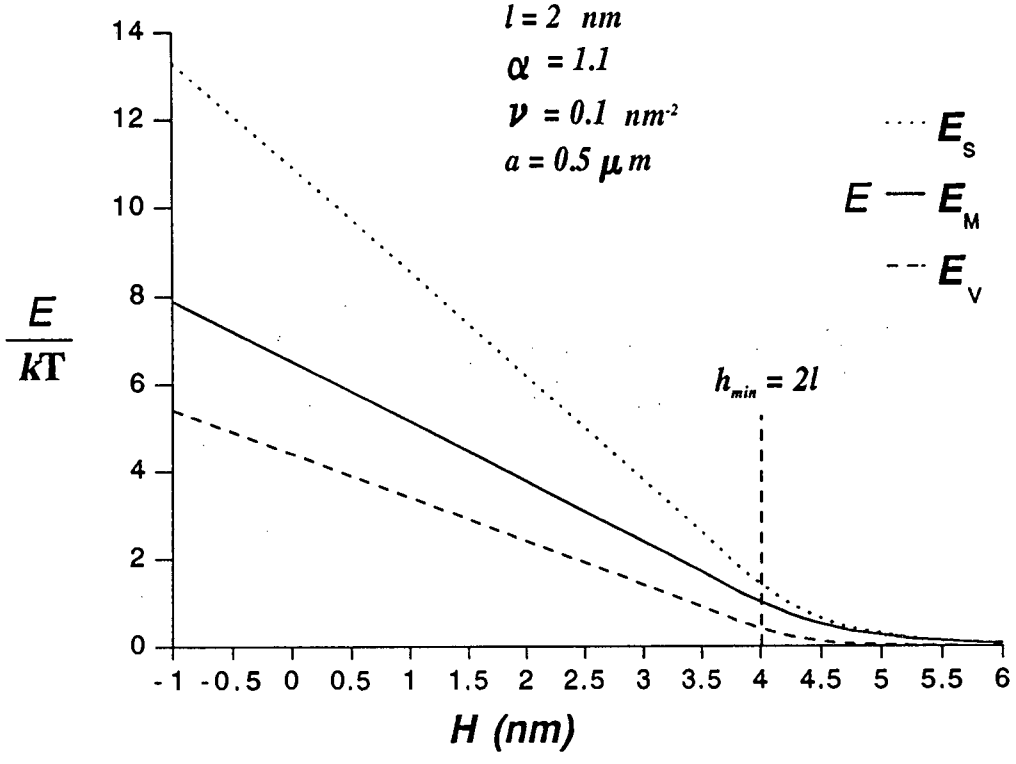

Figure 2.17

Plot of the dimensionless steric energy against the interparticle distance, H, showing the contribution of the E_M and E_V terms.

2.4.2 THE EFFECT OF CHANGING EXPERIMENTAL PARAMETERS

Looking at the terms K_V and K_M defined in equations 2.28 and 2.29 we can see that as the **number of surfactant molecules, ν,** increases, there will be a corresponding increase in E_S, with the increase in the osmotic term, E_M, being greater than that of the volume restriction term, E_V. Increasing **the length of the surfactant, *l*,** as shown in figure 2.18 will result in an increase in K_m with a corresponding increase in the E_{M0} term, the E_{V0} term will remain unchanged giving a net increase in E_S.

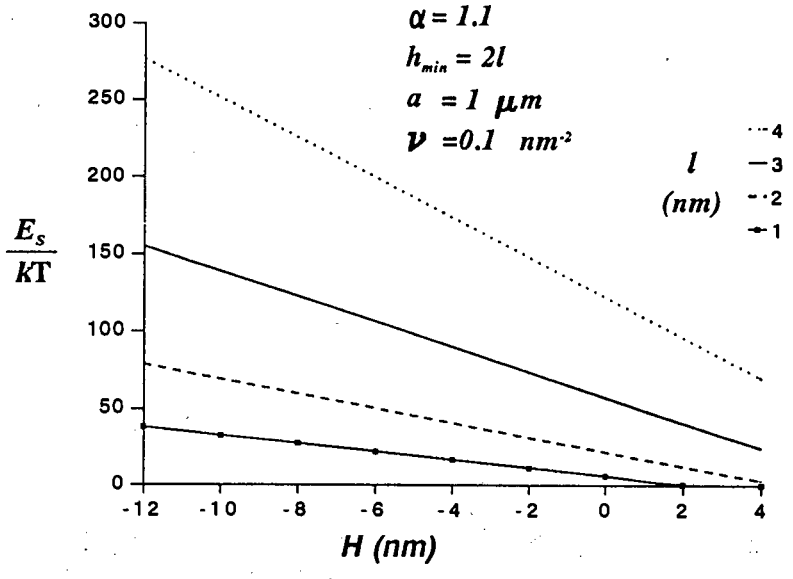

Figure 2.18

Plot of the dimensionless steric energy against the interparticle distance, *H*, showing the effect of an increase in the surfactant length, *l*.

A θ solvent is a solvent in which α = 1. It has been stated that for non-aqueous dispersions to be sterically stabilized, the solvency of the dispersion medium should be better than that of the θ solvent, *i.e.* α > 1.[37,51] A change in the expansion parameter can't be separated experimentally from a change in the average surfactant length. An increase in **the expansion parameter,** α, is seen directly as an increase in the mean surfactant length, *l*. The relationship has not been expressed mathematically, as the average surfactant length when absorbed is dependent on the structure of the surfactant, surfactant-solvent and surfactant-surfactant interactions. Mathematically as α increases the steric energy terms, K_M, C_M and C_V increase and the exponential terms in P_V and P_M decrease. These terms oppose one

another, but generally an increase in the expansion parameter results in a decrease in the steric energy barrier.

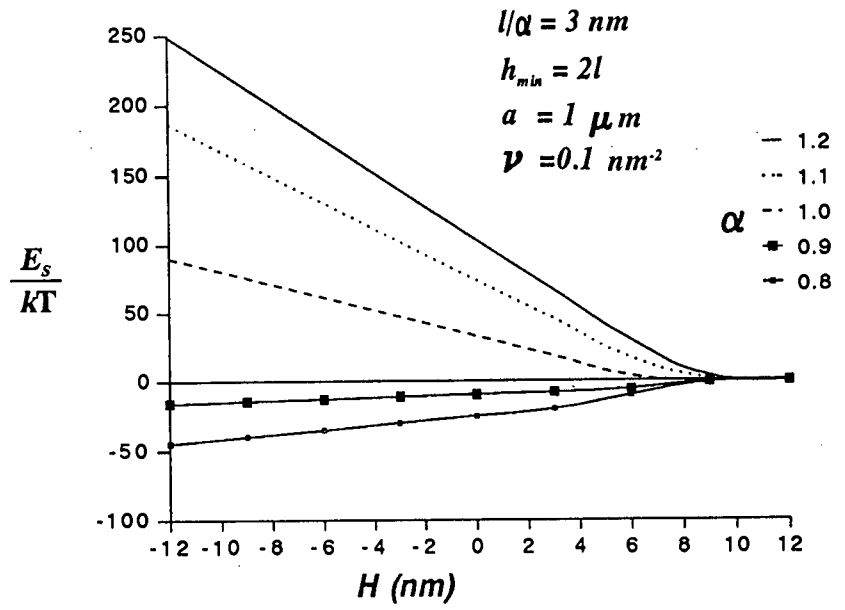

Figure 2.19

Plot of the dimensionless steric energy against the interparticle distance, H, showing the effect of a change in the quality of the non-aqueous solvent, α; E_M dominates E_S.

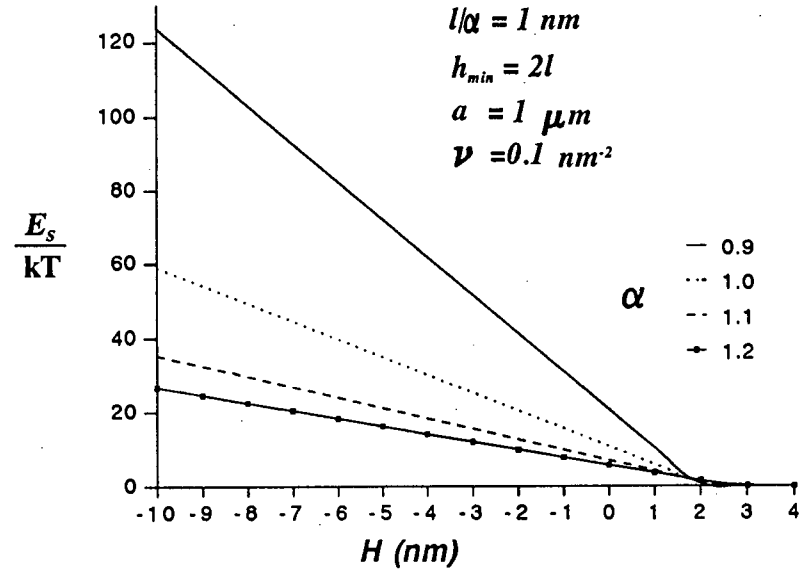

Figure 2.20

Plot of the dimensionless steric energy against the interparticle distance, H, showing the effect of a change in the quality of the non-aqueous solvent, α; E_V dominates E_S.

Experimentally changing the solvent affects the average surfactant length. If a direct relationship is assumed and the ratio l/α is kept constant, an increase in α will translate into a considerable increase in K_m and consequently an increase in E_M. However an increase in l will result in an increase in h_{min} and consequently h_0 with a corresponding decrease in the exponential term of P_V and P_M. This should translate in a decrease in both E_M and E_V. These two trends oppose one another but generally as α increases, E_M increases and E_V decreases. When either the surfactant concentration is low or the surfactant lengths are short, the volume restriction function predominates and an increase in the quality of the solvent can result in a decrease in the steric energy as shown in figure 2.20.

Conversely when the osmotic function predominates, changes in the quality of the solvent has a stronger influence on the steric energy as shown in figure 2.19. An increase in the quality of the solvent increases the steric energy and if the solvent is worse than the θ solvent, the steric energy becomes negative, leading to sensitization of the emulsion.

An increase in **the droplet size, *a*,** as shown in figure 2.21 also results in an increase in the steric energy. The E_{V0} and E_{M0} terms are proportional to the term $(4a^2 - q^2)$ which can be written as $(4a+H-h_0)(h_0-H)$. Therefore as a increases this term will increase, increasing E_S.

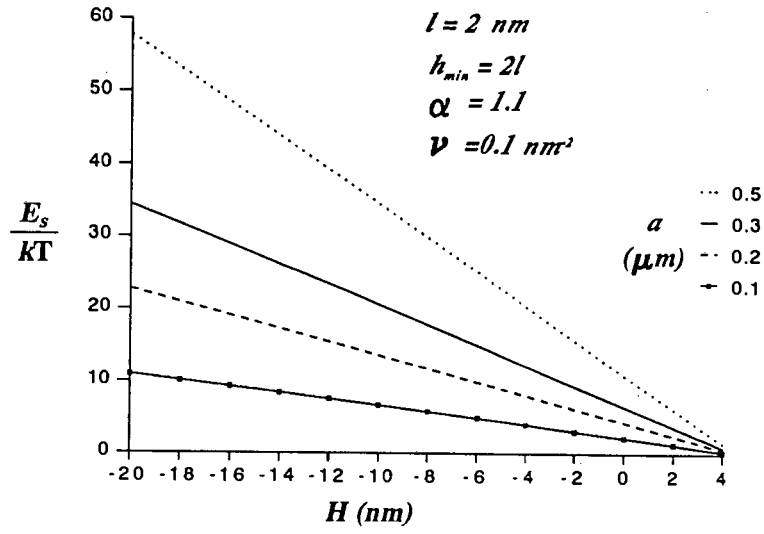

Figure 2.21

Plot of the dimensionless steric energy against the interparticle distance, H, showing the effect of an increase in the droplet radius, a.

2.4.3 STERIC REPULSION FOR DISSIMILAR DROPLETS

For the case of two coalescing spheres which are not identical the above equations need to be adapted. In a typical emulsion the only properties that will vary between droplets will be the droplets radius, a, and the number of surfactant molecules per unit surface area, ν. The coalescing of two droplets of different radii are depicted in figure 2.22. If we label the properties of the smallest droplet with a subscript 2 and those of the larger droplet with a subscript 1, the following equations are derived.

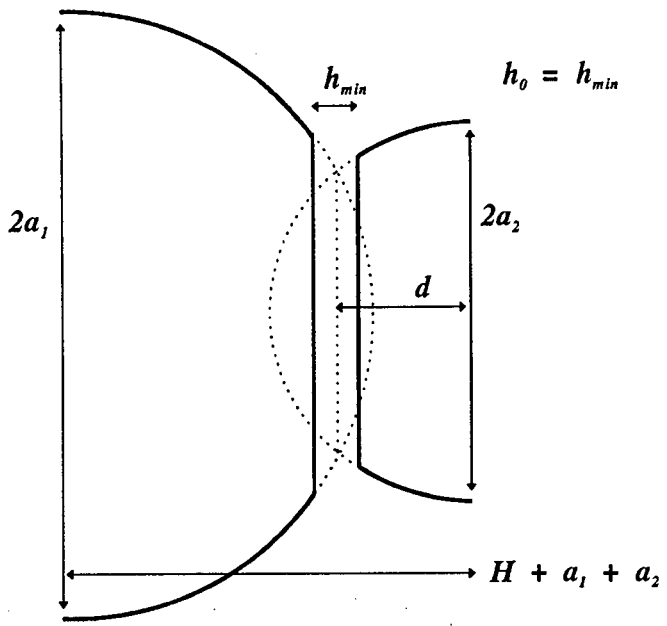

Figure 2.22

Diagram depicting two droplets of unequal radii coalescing.

$$K_V = (\nu_1 + \nu_2)kT \qquad \text{....2.35}$$

$$K_M = 2\left(\frac{2\pi}{9}\right)^{\frac{1}{2}}(\alpha^2 - 1)\nu_1\nu_2 l^2 kT \qquad \text{....2.36}$$

$$q = a_1 + a_2 + H - h_0 \qquad \text{....2.37}$$

$$2d = \frac{(2a_2^2 + 2a_1a_2 + 2a_1H + 2a_2H + H^2)}{(a_1 + a_2 + H)} \qquad \text{....2.38}$$

$$E_M = E_{M0} + \frac{P_M q^2}{C_M^2}\left[e^{-C_M} + \frac{(2d-h_0)}{q}C_M - 1 - \frac{(2d-h_0-q)}{q}C_M e^{-C_M}\right] \quad \text{....2.39}$$

$$E_{M0} = \frac{P_M}{2}\left[4a_2^2 - (2d-h_0)^2\right]$$

$$E_V = E_{V0} + \frac{P_V q^2}{C_V^2}\left[e^{-C_V} + \frac{(2d-h_0)}{q}C_V - 1 - \frac{(2d-h_0-q)}{q}C_V e^{-C_V}\right] \quad \text{....2.40}$$

$$E_{V0} = \frac{P_V}{2}\left[4a_2^2 - (2d-h_0)^2\right]$$

$$H_{\min} = -0.114\,a_2 \quad \text{....2.41}$$

These equations simplify into the equations for similar spheres as when $a_1 = a_2$ the term $(2d - h_0) = q$. The volume restriction constant, K_V, has been set to be proportional to the sum of surfactant molecules on both surfaces and the osmotic repulsion constant is proportional to the product of surfactant concentration on both surfaces. As can be seen in figure 2.22 the surface area experiencing steric repulsion is controlled to the greatest extent by the smallest droplet.

2.4.4 ENERGY BARRIER TO COALESCENCE

The total interaction energy during a collision between two droplets, E_T, is a sum of all interactive energies (equation 2.42). The energy barrier to coalescence is the difference in energy from the minimum at which the droplets are in a clump and the primary energy maximum (equation 2.43). The energy barrier is shown in figure 2.23, included in the plot is the total interaction energy when the droplets are equidistant, $E_T(0)$. As the functions for all interactive energies are complex the energy barrier has to be calculated numerically.

$$E_T = E_A + E_R + E_S \quad \text{....2.42}$$

$$\Delta_{coal} = E_T(1st\ \max) - E_T(1st\ \min) \quad \text{....2.43}$$

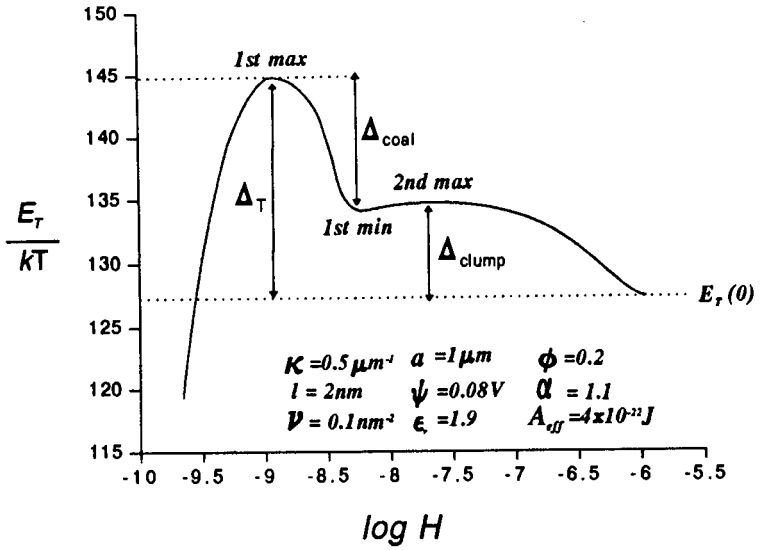

Figure 2.23

Diagram showing the two-stage process of coagulation. $E_T(0)$ is the total interaction energy when $H = H_{max}$.

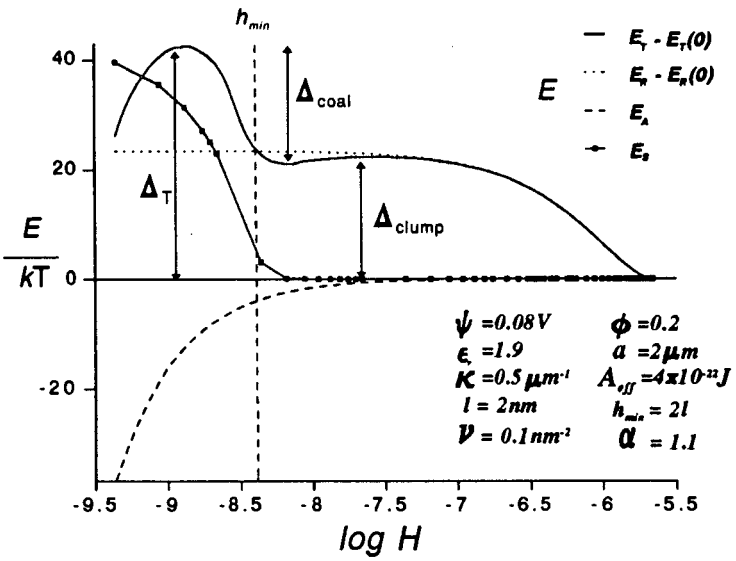

Figure 2.24

Plot of the dimensionless interaction energy against the log of the interparticle distance. (T = 298K)

Figure 2.24 shows the total interaction energy as a function of the interparticle distance, the experimental parameters used are given in the plot. The figure confirms that the effect of electrical repulsion on the energy barrier to coalescence is small and steric repulsion and van der Waals attraction are the predominate forces. In non-aqueous systems repulsion by electrical charge has been quoted to usually be of minor importance and w/o emulsions of moderate concentration have been found to flocculate rapidly through Brownian motion and

gravity and especially under the convective currents produced after shearing.[43] Therefore the bulk stability of moderate concentration w/o emulsions has been quoted to be determined by coalescence.[2,8,27,29]

Looking at figure 2.24 we can see that under certain conditions electrical repulsion can stabilise emulsions considerably, in fact under certain conditions the energy barrier to coagulation is determined predominantly by repulsive charges. However creaming increases the phase volume of the cream decreasing the electrical repulsion between droplets in a cream to zero. Therefore under conditions in which creaming occurs, coalescence would certainly determine the stability of emulsions and this would be independent of electrical repulsion.

Under the conditions given in figure 2.24, the position of the primary energy minimum is to the right of h_{min}, *i.e.* the droplets in a clump are not flattened. However during droplet coalescence considerable flattening will occur. For the system depicted in this plot at the primary maximum, H is 2.7nm less than h_{min}.

2.4.5 RATE OF COALESCENCE

Kinetically, the coalescence of two drops in an emulsion after clumping and flattening has occurred, can be split into two stages:[52]

a) drainage of the thin liquid film to a critical thickness

b) film rupture by surface instability followed by the two droplets uniting.

Experimental observations suggest that the stability of a concentrated emulsion is directly related to the stability of the thin film formed between the droplets and that the stability of this film is determined primarily by its rate of thinning (stage a).

In seeking a correlation between the rate of thinning and the forces responsible, the two forces, capillary pressure and disjoining pressure have been found to govern film lifetimes. Capillary pressure causes the drainage of the film to the plateau borders. The experimentally measurable disjoining pressure is the excess pressure in the thin film relative to the bulk

liquid. This pressure consists of:

a) electrostatic repulsion forces between ions on the two surface layers (for salt concentrations > 10^{-2} M in continuous phase, this component is negligible).

b) van der Waals attractive forces among the molecules of the film

c) steric hindrance forces in closely packed monolayers.

In order to predict the lifetime of a thin emulsion film (between 10 - 100 nm), it is essential to know the rate of drainage as well as the critical thickness at which the film ruptures. Several theoretical and experimental studies have been conducted to understand the behaviour of thin liquid films and to predict the kinetics of emulsion stability. Our approach to the problem as well as the source code of a computer program written to calculate the rate of film thinning is given in appendices 2 and 3.

2.5 COAGULATION

Coagulation is a two stage process of clumping followed by coalescence. It follows that the energy for coagulation is determined by which process has the highest energy barrier and the rate of coagulation is determined by the slowest or rate determining step. The energy for coagulation is a sum of all interactive energies for two droplets (equation 2.42). These equations are modelled in quiescent media with no creaming. To calculate the energy barrier to coagulation the difference between the maximum energy, E_T(max), and the energy when the droplets are equidistant, E_T(0), has to be calculated (equation 2.44 and figure 2.25).

$$\Delta_T = E_T(\text{max}) - E_T(0) \qquad \text{....2.44}$$

Figure 2.25 shows the effect of droplet size changes on the interaction energy between two droplets. The energy barrier to coagulation increases as the droplet size increases. This confirms experimental findings that in polydisperse systems the smaller particles disappear much more quickly than the larger ones.[48]

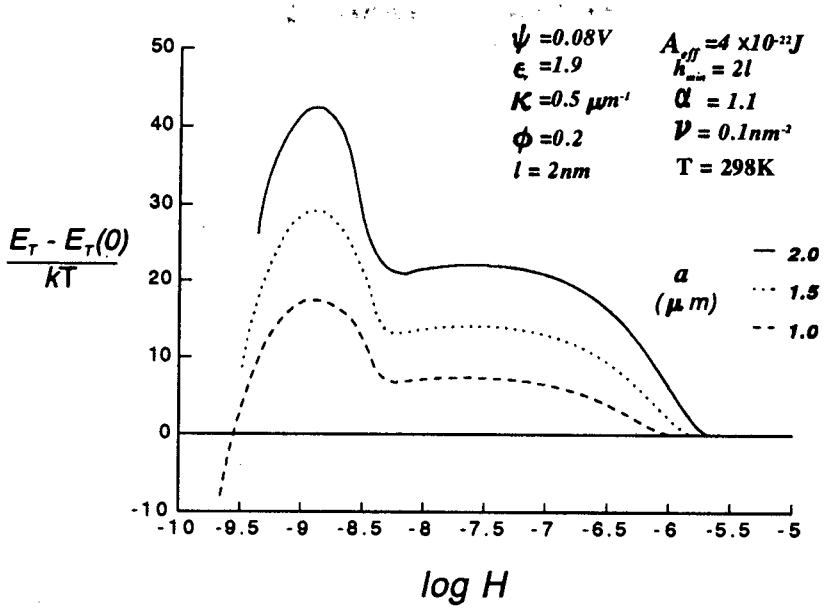

Figure 2.25

Plot of the dimensionless interaction energy against the log of the interparticle distance demonstrating the effect of changes in particle radius, *a*. (T = 298K)

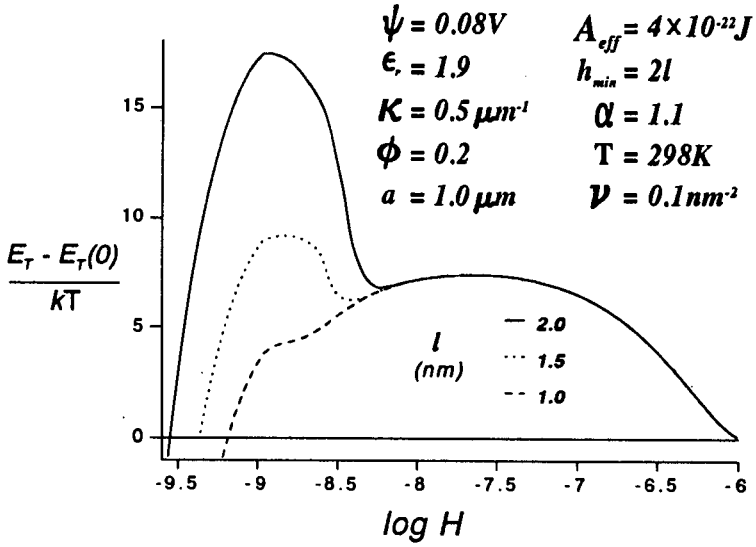

Figure 2.26

Plot of the dimensionless interaction energy against the log of the interparticle distance demonstrating the effect of changes in the surfactant length. (T = 298K)

Experimental coagulation tests performed on polymer colloids stabilized by electrostatic surfactants, have shown a switch in the stabilization mechanism from primarily electrostatic to steric between 9 and 15 ethylene oxide units.[47] Figure 2.26 shows the effect of surfactant length changes on the coagulation energy. A decrease in the surfactant length results in a corresponding decrease in the steric contribution. This trend continues until the steric

repulsion no longer affects the coagulation energy barrier. The primary energy minimum disappears and $\Delta_T = \Delta_{clump}$. The theory agrees with experimental findings that in stabilizing conventional w/o emulsions longer chains are better than short chains.[53]

For the modelling of emulsion coagulation, many experimental parameters are needed. These are given in Table 2.1. Most parameters can be obtained experimentally, however there are problems with calculating the Hamaker constant and the ionic strength is the most difficult parameter to obtain.[54] No method has yet been proposed to measure ionic strength in non-aqueous media.[55]

Table 2.1: List of constants and parameters needed to calculate the interaction between droplets as a function of their interparticle distance, *H*.

	description	value	units
R	gas constant	8.314	$J\ K^{-1}\ mol^{-1}$
F	Faraday constant	9.6485×10^{4}	$C\ mol^{-1}$
k	Boltzman constant	1.381×10^{-23}	$J\ K^{-1}$
ε_0	permittivity of vacuum	8.854×10^{-12}	$C^2\ N^{-1}\ m^{-2}$
A_{eff}	effective Hamaker constant	4×10^{-22}	J
a_i	radius of particle i	1×10^{-6}	m
α	expansion parameter for surfactant in emulsion	1.2	-
ε_r	relative permittivity of organic phase	1.9 (heptane)	-
h_{min}	interparticle distance at which flattening starts occurring	$2l$	m
I_{SI}	ionic strength of organic phase	10^{-7}	$mol\ m^{-3}$
l	average length of surfactant in emulsion		m
N	number of emulsion particles		-
ν_i	number of surfactant molecules per unit area of surface of particle i		m^{-2}
T	temperature of emulsion	298	K
ϕ	internal phase volume ratio of emulsion	0 - 1	-
ψ_i	surface potential of particle i	0.08	V

2.6 REFERENCES

1. D.J.Shaw (1985), *Introduction to Colloid and Surface Chemistry*, Butterworths, London, 3rd Ed.
2. E.Ruckenstein (1977), in *Micellization, Solubilization and Microemulsions*, K.L.Mittal (ed.), Plenum Press, New York, vol. 2.
3. Shun-ichi Noro, Akira Takamura and Masumi Koishi (1979), "Evaluation of Emulsion Stability. Effect of Tween Group Emulsifiers on Stability of o/w Type Emulsions", *Chem. Pharm. Bull.*, **27(2)**:309.
4. D.Fairhurst, M.P.Aronson, M.L.Gum and E.D.Goddard (1983), "Comments on Non-Ionic Surfactant Concentration Effects in o/w Emulsions", *Colloids and Surfaces*, **7**:153.
5. E.G.Cockbain and T.S.McRoberts (1953), *J.Colloid Interface Science*, **8**:440.
6. S.P.Singh, M.Madhuri and P.Bahadur (1982), "Stabilization of Emulsions by Surface Active Agents", *Revue Roumaine de Chimie*, **27**:803.
7. J.Th.G.Overbeek (1977), "Recent Developments in the Understanding of Colloid Stability", *J.Colloid Interface Science*, **58**:408.
8. R.P.Borwankar, L.A.Lobo and D.T.Wasan (1992), "Emulsion Stability - Kinetics of Flocculation and Coalescence", *Colloids and Surfaces*, **69**:135.
9. M.Van den Tempel (1953), "Stability of o/w Emulsions II. Mechanism of coagulation of an Emulsion", *Recueil*, **72**:433.
10. J.H.Schulman and E.G.Cockbain (1940), "Molecular Interactions at Oil/Water Interfaces. Part II. Phase Inversion and Stability of Water in Oil Emulsions.", *Trans. Faraday Soc.*, **36**:661.
11. B.Tezak (1966), "Coulombic and Stereochemical Factors of Colloid Stability of Precipitating Systems", *Disc.Faraday Soc.*, **42**.
12. J.Boyd, C.Parkinson and P.Sherman (1972), "Factors Affecting Emulsion Stability, and the HLB Concept", *J.Colloid Interface Science*, **41**:359.
13. Y.Otsubo and R.K.Prud'homme (1994), "Rheology of o/w Emulsions", *Rheologica Acta*, **33**:29.
14. J.W.McBain (1950), *Colloid Science*, D.C.Heath, p. 26.
15. E.Dickinson (1992), "Interfacial Interactions and the Stability of oil-in-water

Emulsions", *Pure & Appl.Chem.*, **64**:1721.

16. R.J.Hunter (1992), *Foundations of Colloid Science*, Oxford University Press, New York, vol. I.
17. J.L.Cavallo and D.L.Chang (1990), "Emulsion Preparation and Stability", *Chem.Eng.Progress*, **86**.
18. Paul Becher (1965), *Emulsions: Theory and Practice*, Reinhold Publishing Corporation, New York, 2nd Ed.
19. K.J.Laidler and J.H.Meiser (1982), *Physical Chemistry*, The Benjamin/Cummings Publishing Company, California.
20. J.T.Davies and E.K.Rideal (1961), *Interfacial Phenomena*, Academic Press, London.
21. D.J.Shaw (1993), *Introduction to Colloid & Surface Chemistry*, Butterworth-Heinemann Ltd, Oxford, 4th Ed.
22. R.H.Beresford (1969), "Statistical Geometry of Random Heaps of Equal Hard Spheres.", *Nature*, **224**:550.
23. H.H.Kausch, D.G.Fesco and N.W.Tschoegl (1971), "The Random Packing of Circles in a Plane", *J.Colloid Interface Science*, **37**:603.
24. K.J.Lissant (1966), "The Geometry of High-Internal-Phase-Ratio Emulsions", *J.Colloid Interface Science*, **22**:462.
25. C.Solans, R.Pons, S.Zhu, H.T.Davis, D.F.Evans and K.Nakamura (1993), "Statistical Geometry of Random Heaps of Equal Hard Spheres.", *Langmuir*, **9**:1479.
26. W.Albers and J.Th.G.Overbeek (1960), "Stability of Emulsions of Water in Oil III. Floculation and Redispersion of Water Droplets covered by amphipolar Monolayers", *J.Colloid Science*, **15**:489.
27. M. Van den Tempel (1953), "Stability of o/w emulsions III. Measurement of rate of coagulation", *Recueil*, **72**:442.
28. A.Kamel, V.Sadek and S.N.Srivastava (1978), "The Role of Non-ionic Surfactants in Emulsion Stability", *Prog.Colloid & Polymer Science*, **63**:3.
29. W.Albers and J.Th.G.Overbeek (1959), "Stability of Emulsions of Water in Oil. I. The Correlation between Electrokinetic Potential and Stability.", *J.Colloid Science*, **14**:501.
30. B.M.Moudgil, S.Behl and T.S.Prakash (1993), "Effect of Particle Size in Flocculation", *J.Colloid Interface Science*, **158**:511.

31. B.V.Derjaguin and L.Landau (1941), *Acta physicochim. URSS*, **14**:633.

32. E.J.W.Verwey and J.Th.G.Overbeek (1948), "The Interaction of Sol Particles having an Electric Double Layer", *Theory of the Stability of Lyophobic Colloids*, Elsevier, New York.

33. S.B.Hall, J.R Duffield and D.R.Williams (1991), "A Reassessment of the Applicability of the DLVO Theory as an Explanation for the Schulze-Hardy Rule for Colloid Aggregation", *J.Colloid Interface Science*, **143**:411.

34. H.C.Hamaker (1937), "The London - van der Waals Attraction between Spherical Particles", *Physica*, **4**:1058.

35. S.Palkar and A.Lenhoff (1994), "Energetic and Entropic Contributions to the Interaction of Unequal Spherical Double Layers.", *J.Colloid Interface Science*, **165**:177.

36. S.B.Hall, J.R.Duffield and D.R.Williams (1991), "A Stochastic Computer Simulation of Emulsion Coalescence", *J.Colloid Interface Science*, **143**:416.

37. Th.F.Tadros (1993), "Industrial Applications of Dispersions", *Adv.Colloid Interface Science*, **46**:1.

38. R.J.Hunter (1992), *Foundations of Colloid Science*, Oxford University Press, New York, vol. II.

39. H.Ohshima, D.Chan, T.Healy and L.White (1983), "Improvement of the Hogg-Healy-Fuerstenau Formulas for the interaction of Dissimilar Double Layers.", *J.Colloid Interface Science*, **92**:232.

40. E.P.Honig and P.M.Mul (1971), "Tables and Equations of the Diffuse Double layer Repulsion at Constant Potential and at Constant Charge", *J.Colloid Interface Science*, **36**:258.

41. W.Albers and J.Th.G.Overbeek (1959), "Stability of Emulsions of Water in Oil. II. Charge as a Factor of Stabilization against Flocculation.", *J.Colloid Science*, **14**:510.

42. F.Th.Hesselink, A.Vrij and J.Th.G.Overbeek (1971), "On the Theory of the Stabilization of Dispersions by Adsorbed Macromolecules.", *J.Phys.Chem.*, **75**:2094.

43. J.Th.G.Overbeek (1966), "Colloid Stability in Aqueous and Non-Aqueous Media", *Disc.Faraday Soc.*, **42**:7.

44. D.H.Napper (1968), "Flocculation Studies of Non-Aqueous Sterically Stabilized Dispersions of Polymer", *Trans. Faraday Soc.*, **64**:1701.

45. G.M.Barrow (1973), *Physical Chemistry*, McGraw-Hill, Kogakushu, Tokyo, 3rd Ed.

46. K.Danov, I.Ivanov, T.Gurkov and R.Borwankar (1994), "Kinetic Model for the Simultaneous Processes of Flocculation and Coalescence in Emulsion Systems", *J.Colloid Interface Science*, **167**:8.

47. A.Sung and I.Piirma (1994), "Electrosteric Stabilization of Polymer Colloids", *Langmuir*, **10**:1393.

48. J.A.Kitchener and P.R.Mussellwhite (1968), "The Theory of Stability of Emulsions", in *Emulsion Science*, P.Sherman (ed.), Academic Press, London, ch. 2, p. 77.

49. J.Th.G.Overbeek (1982), "Strong and Weak Points in the Interpretation of Colloid Stability", *Adv.Colloid Interface Science*, **16**:17.

50. V.S.Mitlin and M.M.Sharma (1993), "A Local Gradient Theory for Structural Forces in Thin Liquid Films", *J.Colloid Interface Science*, **157**:447.

51. D.H.Napper (1970), "Flocculation Studies of Sterically Stabilized Dispersions", *J.Colloid Interface Science*, **32(1)**:106.

52. G.W.Steven, H.R.C.Pratt and D.R.Tai (1990), "Droplet Coalescence in Aqueous Electrolyte Solutions", *J.Colloid Interface Science*, **136**:470.

53. H.A.Bampfield and J.Cooper (1988), "Emulsion Explosives", in *Encyclopedia of Emulsion Technology*, P.Becher (ed.), Marcel Dekker, New York, vol. 3, p. 281.

54. A.Barbero, A.Rodriguez, J.Fernandez and R.Alvarez (1994), "On the Calculation of Electrokinetic Potential and Hamaker Constant of Model Colloids", *J.Colloid Interface Science*, **162**:257.

55. I.D.Morrison (1993), "Electrical Charges in Nonaqueous Media", *Colloids and Surfaces A*, **71**:1.

CHAPTER THREE
THE AQUEOUS PHASE
- Speciation at High Ionic Strength

3.1 INTRODUCTION

Experimentally the aqueous phase has been found to have an important influence on the stability of w/o emulsions. This evidence includes the following:

- hydrolysis products of surfactant salts and their relative solubility profoundly affects the type of emulsion formed and its relative stability.[1]
- changes in pH and the presence of calcium nitrate in the aqueous phase of emulsion explosives affect the relative stability of emulsions.[2]
- The association of ionic surfactants with counter ions present in the aqueous phase, results in the formation of uncharged films critical for w/o emulsion stability.[2]

All of the above observations can be explained in terms of the chemical speciation occurring in the aqueous phase. In this context chemical speciation refers to the concentration and composition of each chemical species present in solution.[3-6] Very little is known about the interaction of surfactants with metal ions and the consequent effect on emulsion stability. Involved in the speciation would be surfactant headgroups, various salts and water molecules. In the case of emulsion explosives, ammonium, sodium, potassium and calcium nitrate salts are used predominantly although perchlorates are sometimes added. Ionic strengths range from approximately 3*M* to fused salts and temperatures can vary from 0°C to 40°C. Surfactants commonly used are either anionic or non-ionic with common headgroup structures including mono-carboxylate, succinate, succinic anhydride and succinic anhydride derivatives.

To determine the speciation of the aqueous phase, stability constants for the ion association complexes of surfactant headgroups and the cations NH_4^+, Na^+, K^+ and Ca^{++} in solution had to be determined at high ionic strength. Not only was it necessary to study the complex cation / anion interactions in solution but also their interaction with the headgroups of the surfactant molecules. The ligands succinate, propionate and mono-methyl succinate were chosen as model compounds for the headgroups of simple anionic surfactants.

For the purposes of comparison with literature values and ease of experimentation, a temperature of 25°C was chosen at which to determine the stability constants. This is also a reasonable temperature for the use of emulsion explosives.

An important consideration in this work was the ionic strength. Daniele *et al.*, have extensively studied the effect of ionic strength in the range $0M < I < 1M$ upon the protonation equilibria of carboxylic acids.[7-9] Also Belevantsev *et al.* have studied the effect of ionic background upon the dissociation constants of monobasic acids.[10] However, as yet, no study has been reported of the effect of high ionic strength and background medium upon protonation equilibria. Since these data are necessary in order to model the affect of pH upon the speciation of our model polar headgroups, we have undertaken a potentiometric investigation of the protonation equilibria of the above carboxylic acids at an ionic strength of $3M$ (see discussion in section 3.2.1), and in different background electrolytes (KNO_3, $NaNO_3$, NH_4NO_3, $Ca(NO_3)_2$, Et_4NBr). Determining the speciation of such apparently weakly associated complexes at high ionic strengths is not trivial and our varied approaches to this problem are presented in the following section of work.

3.2 EXPERIMENTAL APPROACH

3.2.1 CHOICE OF EXPERIMENTAL METHOD

Very few alkali metal ion/ligand and ammonium ion/ligand stability constants have been published because of the problems associated with their experimental determination. The first problem is the difficulty of distinguishing between activity and complex formation factors when binding is so weak. The second problem is the almost impossible task of keeping the ionic strength constant when measuring weak binding.

Potentiometry is the most convenient and successful technique used for determining stability constants and the use of the glass electrode is recommended because of its high accuracy.[11] Ion selective electrodes were originally used to study these weak complexes.[12] The ion-selective electrode has an advantage over the standard glass electrode as it measures the activity of the metal ions directly, rather than indirectly through the effect their complexation has on the free hydrogen ion activity. However, the precision that can be obtained using ion-selective electrodes is often lower than that obtained using glass electrodes, because of slow response times and memory effects. Ion selective electrodes also tend to deviate from linearity at high concentrations of the determinand ion.[13]

Daniele *et al.* have had success using glass electrodes to study weak alkali metal ion, and ammonium ion, complexation and their results are in good agreement with results obtained by other workers, using ion-selective electrodes and other independent techniques.[8,14] In their work they chose tetraethylammonium halides as background salts, as tetraalkylammonium salts are known to not interact significantly with O-donor ligands. The authors have demonstrated the lack of significant specific interaction between tetraethylammonium and sulphate.[14]

To determine stability constants of alkali-metal/ligand and ammonium/ligand complexes the authors relied on the Lewis-Randall principle according to which in dilute solutions the activity coefficient of a given solute is the same in all solutions of the same ionic strength.[15] Apparent protonation constants were obtained with the halide salt of the metal as the background electrolyte. Complexation constants were then calculated by comparing the apparent protonation constant with that obtained using a solution of the same ionic strength, with tetraethylammonium iodide as background. The difference in the apparent protonation constants in the two media being attributed to metal-ligand complexation.

Following the successes of Daniele *et al.*, glass electrode potentiometry was decided on as the method to determine our stability constants and tetraethylammonium was chosen as the reference background cation. Tetraethylammonium is the preferred alkylammonium ion, as tetramethylammonium ions can still form weak complexes and tetrabutylammonium salts are not sufficiently soluble.[16] In choosing a counter-ion, normally a counter-ion with the weakest electrostatic interaction (*ie.* a singly charged anion with the largest possible radius) is chosen.[17] After perchlorate, nitrate is the largest common counter-ion and since it is the main counter-ion in our model system this counter-ion was chosen.

In potentiometric titrations the activity coefficients should be kept as nearly constant as possible and this is most readily achieved by the use of a very high concentration of bulk electrolyte. This constant ionic medium method is based on Brønsted's principle, which states that the activity coefficient of all solutes present as small fractions of the total electrolyte concentration is constant at constant total electrolyte concentration. An ionic strength of at least $1M$ should be employed, and $3M$ is recommended.[17,18] For the study of weak complexes,

this requirement becomes even more important. The nature of our model system requires the determination of stability constants at very high ionic strengths, but the solubility of potassium nitrate restricts the ionic strength at 25°C to 3*M*. As a reasonable compromise and with the advantage of being able to compare some of our apparent protonation constants with literature values, the recommended ionic strength of 3*M* was chosen. In order to obtain accurate stability constants the concentration of the complex being studied must be of the same order as the free concentration of the most dilute component. To satisfy this requirement, a ligand concentration of less than 0.1*M* was needed.

Because of the difficulty of keeping activity coefficients constant when using solutions of different electrolytes at high concentrations, for comparison, NMR spectroscopy was used as a second method of determining stability constants.

3.2.2 POTENTIOMETRY THEORY

The theory for determining stability constants through potentiometric titrations has been dealt with extensively in the literature, and so only an overview will be given here.[11,17,19,20]

In a solution containing metal ions or cations (*M*), ligands (*L*) and protons (*H*), many complexes may be formed in equilibrium with one another. Each complex has associated with it an equilibrium or stability constant. In general for the reaction

$$pM + qL + rH \rightleftharpoons M_pL_qH_r$$

the thermodynamic stability constant may be defined as:

$$^{T}\beta_{pqr} = \frac{a_{M_pL_qH_r}}{a_M^p a_L^q a_H^r} \qquad \text{....3.1}$$

where *p,q,r* are the stoichiometric coefficients and 'a' denotes activity.
When *r* is negative this refers to the removal of, or addition of, hydrogen or hydroxy ions, respectively.

Owing to its definition, the stability constant is often referred to as a formation constant, as opposed to a dissociation constant. A protonation constant is a stability constant when $p = 0$, $q > 0$ and $r > 0$. To differentiate between the two types of constants to be determined, stability constants where $q > 0$ and $p > 0$ will be referred to as complexation constants.

The basis of many of the variables used in potentiometry varies depending on the composition variable and hence standard state used. In most potentiometric work the standard state is taken as unit molarity. This basis is more convenient as most experimental apparatus are calibrated for the dispensing of volumes. However, at high concentration, molality is more popular as the composition variable, where the standard state is defined as unit molality. This basis has an advantage as it does not change with temperature and pressure.

In this work all the potentiometric experimental work was performed using molarity as the composition variable, which will be referred to as concentration.

In practice, it is easier to determine the concentration of a species than to determine its activity. The activity of a species can be expressed as a product of its composition variable and its activity coefficient, γ, so that as the concentration approaches zero the activity coefficient tends to unity. Depending on the basis used the activity of ion, i, in solution can be expressed as follows:

$$a_{c,i} = \gamma_{c,i} c_i \quad OR \quad a_{m,i} = \gamma_{m,i} m_i \qquad \text{....3.2}$$

where c_i and m_i are the molar and molal composition variables of ion, i, in solution and the basis of the activity and activity coefficients is given as a subscript.[21]

Stability constants, activity and activity coefficients are all dimensionless but vary depending on the basis used. To avoid inconsistency in units the activity should be defined as:

$$a_{c,i}\, c^0 = \gamma_{c,i} c_i \quad OR \quad a_{m,i}\, m^0 = \gamma_{m,i} m_i \qquad \text{....3.3}$$

For convenience the normal convention is to omit the standard state concentration terms, with the understanding that the activity, activity coefficients and stability constants are dimensionless. To prevent confusion care must be taken to define the composition variable used and not to interchange between the different standard states.

Following from the definition of activity, the thermodynamic stability constant can be defined as a product of its stoichiometric stability "constant", β_{pqr}, and its inverse activity coefficient quotient, Γ_{pqr}^{-1}.

$$ {}^{T}\beta_{pqr} = \frac{\beta_{pqr}}{\Gamma_{pqr}} \qquad \text{....3.4} $$

where

$$ \beta_{pqr} = \frac{[M_pL_qH_r]}{[M]^p[L]^q[H]^r} \qquad \text{....3.5} $$

and

$$ \Gamma_{pqr} = \frac{\gamma_M{}^p \, \gamma_L{}^q \, \gamma_H{}^r}{\gamma_{M_pL_qH_r}} \qquad \text{....3.6} $$

The square brackets used in equation 3.5 denote molar concentration. Stability constants can also be expressed in the form of stepwise stability constants represented by the following set of reactions and equations:

$$ \begin{aligned} M + L &\rightleftharpoons ML & K_{110} &= \frac{[ML]}{[M][L]} \\ ML + L &\rightleftharpoons ML_2 & K_{120} &= \frac{[ML_2]}{[ML][L]} \\ &\vdots & & \\ ML_{q-1} + L &\rightleftharpoons ML_q & K_{1q0} &= \frac{[ML_r]}{[ML_{r-1}][L]} \end{aligned} \qquad \text{....3.7} $$

where the cumulative stability constant is the product of the stepwise stability constants.

$$\beta_{01r} = \prod_{i=1}^{r} K_{01i} \qquad \text{....3.8}$$

At constant pressure, each stability constant is related to the Gibbs free energy change, (ΔG), for the reaction it represents, and ΔG is in turn related to the enthalpy change, (ΔH), and entropy change, (ΔS), for the reaction. These relationships are represented by equation 3.9 where R is the gas constant and T the absolute temperature.

$$\begin{aligned} \Delta G &= -RT\ln K \\ &= \Delta H - T\Delta S \end{aligned} \qquad \text{....3.9}$$

In reality, equilibrium reactions represented by stability constants, often involve the displacement of an unknown number of solvent molecules, as represented by the following reaction scheme

$$M(aq) + qL(aq) \rightleftharpoons ML_q(aq) + z_q H_2O \quad \text{where} \quad \beta_{1q0} = \frac{[ML_q(aq)][H_2O]^{z_q}}{[M(aq)][L(aq)]^q} \qquad \text{....3.10}$$

If activity coefficients are kept constant and water is in its standard state, all reference to water in the stability constant can be dropped.[17]

Activity coefficients and hence by definition stoichiometric stability constants vary with temperature, ionic strength and solvent composition. For results to be meaningful these conditions have to be kept constant during the determination of stability constants and have to be given when quoting a stability constant. For the same reasons only stability constants referring to the same activity scale can be directly compared.[19]

According to the IUPAC definition, ionic strength (I) is given by either of the following equations.[21]

$$I_c = \frac{1}{2}\sum_i c_i z_i^2 \quad \text{or} \quad I_m = \frac{1}{2}\sum_i m_i z_i^2 \qquad \text{....3.11}$$

where z_i is the charge number, of the ion, i, in solution.

To hold activity coefficients constant, titrations are performed in the presence of an excess of background electrolyte, under constant temperature conditions and using the same solvent composition throughout. The study of weak complexes is often more difficult because higher values of $[M]$ or $[L]$ are needed which can result in a change in ionic strength during a titration and we may no longer be justified in assuming that activity coefficients remain constant.

The emf measurement of an electrochemical cell containing a reference electrode with a salt bridge, an experimental solution and a glass electrode, gives us a value for the product of the activities of the protons and anions in the experimental solution, as defined by the Nernst equation. Under ideal conditions when activity coefficients are held constant and the solution is in the $-\log[H^+]$ range 2-10, the electrode response can be described in a simpler form.

$$E_{cell} = E^0 + s \log[H^+] \qquad \text{....3.12}$$

where s is the Nernstian slope of the cell which is expected to be 59.16 at 25°C.[22] Internal calibration of the electrode, performed in the test solution, to obtain E^0 and s, is preferable to external calibration, performed in a calibration solution. This is due to the variation of the standard potential of the glass membrane with time and the variation of the liquid-junction potential between solutions.

Calibration and equilibrium constants can be determined from the same set of data. The computational determination of stability constants from a potentiometric titration involves the solving of mass-balance equations at every titration point. Consider the protonation system which was used for the monoprotic ligand, propionic acid. The ligand solution is acidified

with a mineral acid, HA, and a strong base, MOH, is titrated into the solution. At each point in the titration the titre volume of MOH added, (v), and the emf, (E) is measured. The three variables, E^0, s, and β, have to be determined. For every point in the titration we have the following equations.

$$E = E^0 + s\log[H^+] \qquad \textit{eq.}3.12$$

$$\beta_{011} = \frac{[HL]}{[L^-][H^+]} \qquad \textit{by definition}$$

$$[L^-]+[HL] = \frac{[HL]^0V^0}{V^0+v} \qquad \textit{mass balance}$$

$$[H^+]+[HL] = \frac{[HL]^0V^0+[HA]^0V^0-[MOH]v}{V^0+v} - \frac{K_W}{[H^+]} \qquad \textit{mass balance}$$

where at each point in the titration, the following three variables are unknown:

(i) $[HL]$, the current concentration of the protonated ligand

(ii) $[L^-]$, the ligand anion

(iii) $[H^+]$, the free hydrated hydrogen ions

and the following variables are known:

(i) $[MOH]$, the analytical concentration of the base

(ii) $[HL]^0$, the initial analytical concentration of the ligand

(iii) $[HA]^0$, the initial concentration of the mineral acid

(iv) V^0, the initial volume in the titration vessel

K_W, the (concentration) ionic product of water, defined below, can be taken from literature.

$$K_W = [H^+][OH^-] \qquad \textbf{....3.13}$$

So, for a titration of n titration points, there are 3+3n unknowns which can be determined by solving the 4n simultaneous equations.[17,23]

3.2.3 EXPERIMENTAL

3.2.3.1 MATERIALS

As the potentiometric technique is very sensitive to any impurities, chemicals of high purity were used. Materials used are listed in Table 3.1.

Table 3.1: Materials with supplier, and abbreviations used (shown in brackets)

propionic acid (PA)	$C_2H_5CO_2H$	Riedel-de Haën
succinic acid (SA)	$HO_2CC_2H_4CO_2H$	Merck GR
mono-methyl succinate (MS)	$HO_2CC_2H_4CO_2CH_3$	Aldrich-Chemie 95%
ammonium nitrate	NH_4NO_3	Merck GR
calcium nitrate	$Ca(NO_3)_2.4H_2O$	Merck GR
sodium perchlorate	$NaClO_4$	SA Archem
sodium nitrate	$NaNO_3$	Merck GR
potassium nitrate	KNO_3	Merck GR
tetraethylammonium bromide	Et_4NBr	Merck > 99%
(KHP)	$HO_2C.C_6H_4.CO_2K$	BDH AnalaR
sodium tetraborate (borax)	$Na_2B_4O_7.10H_2O$	Merck GR
nitric acid	HNO_3	Merck Titrisol
sodium hydroxide	NaOH	Merck Titrisol
sodium hydroxide pellets	NaOH	Merck GR
potassium hydroxide	KOH	Merck Titrisol
hydrochloric acid	HCl	Merck Titrisol
(EDTA)	$C_{10}H_{14}N_2Na_2O_8.2H_2O$	Merck GR Titriplex III
anion exchange resin	Amberlite IRA 400	Sigma
cation exchange resin	Amberlite IR-120	BDH Chemicals Ltd
soda lime		BDH Chemicals Ltd
phosphorus(V) oxide	P_2O_5	Riedel-de Haën
ethanol	EtOH	BDH AnalaR
acetone	CH_3COCH_3	Merck GR
tert-butyl alcohol (t-BuOH)	$(CH_3)_3COH$	Merck
deuterium oxide	D_2O	Aldrich Chemical Co.

$NaNO_3$ and KNO_3 were dried under vacuum for 12 hours, at 140°C and 70°C respectively.[24] NH_4NO_3 solutions were standardised using a hydrogen form of the cation exchange resin. The eluted HNO_3 being titrated against NaOH using methyl red as an indicator. The NaOH solution was freshly prepared from pellets and standardised against borax using phenolthalein

as an indicator. $Ca(NO_3)_2$ solutions were standardised against EDTA in a substitution titration, using magnesium and solochrome black.[25] The EDTA solution was prepared as a primary standard from its salt. Et_4NBr was recrystallised from ethanol, dried under vacuum at 100°C for 12 days and stored over P_2O_5.[24] Propionic acid was purified by distillation, while the succinic acid and mono-methyl succinate were used without further purification. The NMR reference t-BuOH was dried over sodium and then distilled. Borax was recrystallised from distilled water and stored over a solution saturated with respect to sucrose and sodium chloride.[25] KHP was dried at 120°C and stored in a desiccator. A quantity of the pure salt, Et_4NNO_3, was prepared from Et_4NBr using an anion exchange resin in the nitrate form. The salt was recrystallised from water and gave the following microanalysis: (found: C 49.3, H 10.5, N 14.3. calc($C_8H_{20}N_2O_3$): C 50.0, H 10.5, N 14.6.). Because of time constraints this method could not be used. As a compromise, Et_4NBr (Merck > 99%), was chosen as the background salt.

3.2.3.2 POTENTIOMETRIC METHOD

To obtain protonation constants, an experimental approach was adopted as recommended by workers in this field and following IUPAC guidelines.[23,26] Firstly electrode reliability was established. All available glass electrodes (Metrohm 6.0102) were compared by recording a buffer-line using four Radiometer-Copenhagen buffers. Two glass electrodes were selected to titrate with. They were chosen as they had the fastest response times, were stable and their slopes were closest to 59.16. Both electrodes had slopes within 95% of 59.16. A Ag/AgCl reference electrode (Metrohm 6.0726.100) was used. The inner compartment was filled with saturated KCl and a small amount of $AgNO_3$, and the outer compartment with 3*M* $NaNO_3$. Between titrations, the glass electrodes were stored in a 0.1*M* HNO_3 solution and the reference electrode in a solution of 3*M* $NaNO_3$. These solutions were kept at 25°C.

Potentiometric titrations were carried out under an atmosphere of high purity nitrogen which was passed through a series of wash bottles to remove any residual O_2, CO_2 and to humidify the gas, before passing it over the titration solution. The bottles contained:

1 50% KOH
2 Fieser's solution, prepared according to Vogel[25]
3 Distilled water at 25°C
4 An empty trap at 25°C
5 A 3*M* solution of the background electrolyte at 25°C

To prevent back diffusion, the nitrogen was released to the atmosphere through a trap containing a 3*M* solution of the background electrolyte.

All solutions were made up in glass distilled, deionized water, which had been boiled out to remove dissolved CO_2. All volumetric flasks used in preparing the solutions were calibrated before use.[25] The strong base solutions were prepared under N_2, using Merck titrisols, and were stored in high density polypropylene bottles under an atmosphere of N_2. After preparation all solutions were stored in Metrohm polypropylene bottles which were sealed to the air and soda lime traps were attached to exclude CO_2.

The 50ml Metrohm titration vessel was maintained at 25.00 ± 0.05°C, using a water-bath with a Fried Electric thermostat and pump and the entire titration apparatus kept in a room maintained at a constant temperature of 23 ± 1°C. The titration apparatus used comprises a titration vessel with Metrohm titration head, into which a glass electrode, a reference electrode, a thermometer and a Metrohm burette tip with non-return valve are fitted. The vessel is sealed from the air with an o-ring. A constant stirring rate was maintained using a Kika-Mini-Mr magnetic stirrer with a teflon coated stirrer bar. Volumes were dispensed using a Metrohm automatic burette which was controlled via a RS232 port by a Bondwell XT computer which was interfaced via an 8255 parallel port to a Radiometer Copenhagen phm 84 pH meter. The Pascal software used to control the titration and record titre volumes and emf readings was written in the Department by Adnaan Ederies.

Titrations were repeated using two glass electrodes and a Ag/AgCl reference electrode, connected to the titration solution *via* a salt bridge. The cell used can be represented as follows:

	$AgNO_3$	salt bridge		3*M* titration	standard glass	
(-) | Ag	sat KCl	3*M* $NaNO_3$	⋮ ⋮	solution	electrode	| (+)

Solutions were made up to 3*M* ionic strength with respect to the cation of the background electrolyte. The Et_4NBr system was repeated using a background electrolyte concentration of 2.174*M*. The HNO_3 and strong base solutions were standardised against borax and potassium hydrogen phthalate respectively. With $Ca(NO_3)_2$ and NH_4NO_3 as background electrolyte, however, the HNO_3 solutions could not be standardized against borax and so were standardised against the strong base of the corresponding system.

To convert between molality and molarity, the density of tetraethylammonium bromide solutions ranging in concentration from 0*M* to 3*M*, were measured in a room kept at a constant temperature of 20°C. Solutions were first made up in calibrated volumetric flasks and densities were then measured using a density bottle and density meter (Anton Paar, DMA 35). Both methods gave identical results. A least squares fit of the density data with molarity gave the following equation, where the value in brackets is the standard deviation in the last position for each number.

$$\rho_{Et_4NBr\ soln} = 0.9974(5) + 0.0374(7)[Et_4NBr] + 0.0022(2)[Et_4NBr]^2 \quad \text{....3.14}$$

In all the six systems studied the strong acid was HNO_3. In the case of the sodium and potassium systems, the strong base was NaOH and KOH respectively. In the ammonium and calcium systems, $Ca(OH)_2$ and NH_4OH, could not be used as the strong base, as $Ca(OH)_2$ is insoluble and NH_3/NH_4OH is volatile and has too low a pK_b. Similarly, commercially available Et_4NOH proved to have an unacceptable amount of impurity, probably carbonate and, under strongly basic conditions, hydrolysis of the background salt occurred. In these cases therefore the strong base was 1*M* KOH made up to 3*M* K^+ with KNO_3. Using the base in such a concentrated form resulted in only 0.07% of the background cation being K^+ at the end of a titration.

All titration solutions were first standardised using the Gran method (section 3.3.1). Both primary standards, borax and KHP, were weighed out into the titration vessel using a Sartorius Research R200D Electronic semi-microbalance, with readability up to 0.01 mg. Once both the strong acid and strong base solutions for a system had been standardised, the

ligand solutions were standardised against the standardised strong base solution.

The ligand titrations which were performed to obtain the relevant formation constants, can be divided into six systems, depending on the background electrolyte media. For each system a series of solutions of varying concentration of ligand acidified with a strong acid were titrated with a strong base up to ligand neutralisation. The two glass electrodes were alternated with successive titrations.

The experimental results were processed using the ESTA suite of computer programs (section 3.3.2) to yield electrode parameters and the ligand protonation constant for the system. All experimental data were first refined using ESTA's OBJE task. E^0 was determined *in situ* by refining it simultaneously with β_{01r} from the same experimental titration data. All analytical concentrations and initial volumes were added as input data and fixed. A p*Kw* of 14.18 compiled from 32 refs at 3*M*, was used throughout.[27] Standard deviations, for all parameters associated with random errors, were used to weight the data. They were 0.002 cm^3 for titre volumes, 0.1 for observed emf's, 0.2 for E^0 and 0.02 for the log of stability constants.

When using ammonium nitrate as the background electrolyte experimental points near the endpoint of the ligand were deleted from the titration data as they had high residuals due to the effect deprotonation of the ammonium ions had on the emf of the solution. Inclusion of an ammonia protonation constant would have been merely cosmetic as it would not have improved the value of the protonation constant.

Once E^0 and β_{01r} had been refined the titration data were analyzed using ESTA's ZBAR module. When necessary, data points with high point residuals, found in the unbuffered region near the endpoint and at the start of the titration, were deleted. Two plots showing experimental and calculated protonation curves are shown in figures 3.1 and 3.2. The plots chosen are of the systems with the highest and lowest Hamiltonian *R* value and hence show the best and worst correlation obtained between observed and calculated data points.

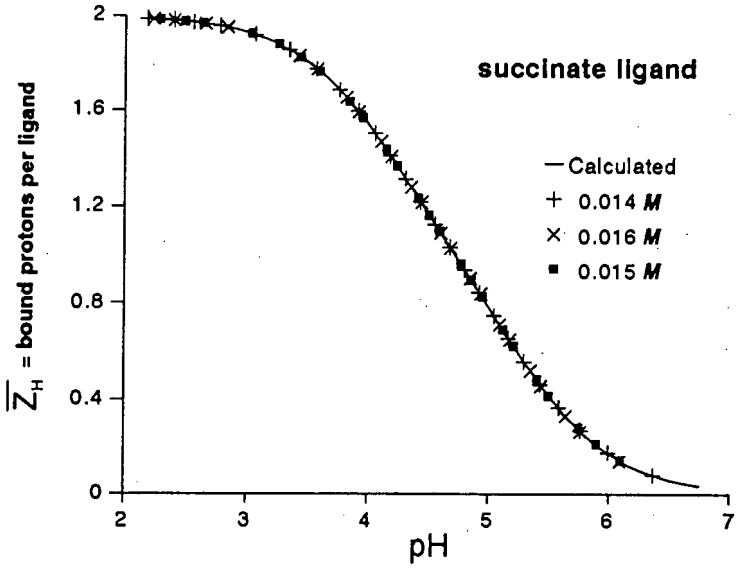

Figure 3.1

Calculated (solid line) and experimental (symbols) protonation curves for succinic acid in KNO_3 (R=0.0006)

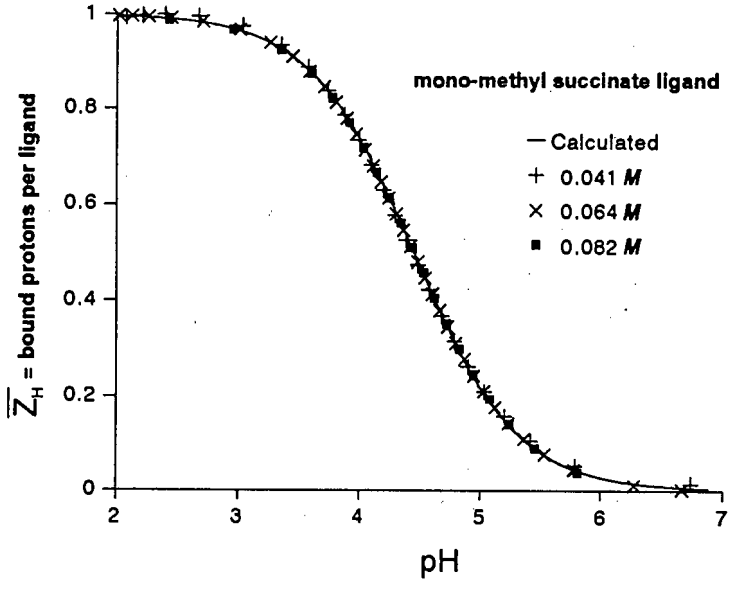

Figure 3.2

Calculated (solid line) and experimental (symbols) protonation curves for mono-methyl succinic acid in $NaNO_3$ (R=0.0088)

A summary of the experimental parameters is given in Table 3.2, as recommended by the IUPAC commission.[28]

Table 3.2: Summary of experimental parameters used in the determination of protonation constants for the ligands succinate, propionate and mono-methyl succinate; T=25°C.

Ligand	Ligand mmol dm^{-3}	Major Electrolyte mol dm^{-3}	pH range	data points	number of titrations
succinate					
	7 - 9	3.00 - 2.93 Et_4NBr	2 - 7	295	5
	5 - 9	2.17 - 2.13 Et_4NBr	2.0 - 7.0	760	7
	14 - 16	3.00 KNO_3	2.0 - 6.4	268	4
	4 - 35	3.00 $NaNO_3$	2.0 - 7.4	1000	9
	6 - 10	3.00 - 2.81 NH_4NO_3	2.0 - 6.1	390	6
	3 - 10	1.00 - 0.97 $Ca(NO_3)_2$	2.1 - 5.8	403	5
propionate					
	7 - 24	3.00 - 2.93 Et_4NBr	2 - 7	166	4
	9 - 17	2.17 - 2.13 Et_4NBr	2.0 - 7.1	629	6
	33 - 37	3.00 KNO_3	2.0 - 6.7	410	5
	37 - 68	3.00 $NaNO_3$	2.0 - 7.3	596	5
	27 - 39	3.00 - 2.93 NH_4NO_3	2.0 - 6.2	767	5
	7 - 21	1.00 - 0.97 $Ca(NO_3)_2$	2.0 - 6.2	751	6
mono-methyl					
succinate	16 - 18	3.00 - 2.94 Et_4NBr	2 - 7	302	5
	10 - 19	2.17 - 2.13 Et_4NBr	2.0 - 6.7	785	7
	35 - 38	3.00 KNO_3	2.0 - 6.0	325	4
	41 - 82	3.00 $NaNO_3$	2.0 - 7.1	811	6
	19 - 26	3.00 - 2.88 NH_4NO_3	2.0 - 5.8	458	4
	11 - 32	1.00 - 0.96 $Ca(NO_3)_2$	2.0 - 5.9	590	5

3.2.3.3 NMR TITRATION METHOD

NMR spectra for most salts were run on a Varian VXR 200 spectrometer at 25°C, using acetone and t-BuOH as internal references and D_2O as solvent. A 0.1*M* solution of ligand in D_2O was prepared and the pD was adjusted to between 8 and 9 by the dropwise addition of a basic solution prepared from NaOH pellets in D_2O. The pD adjustment was monitored using an Ingold microcombination electrode connected to a pH meter (crison microph 2000) which had been calibrated using standard pH 4 and 7 buffers.

For succinate, the NMR titration was performed by successively adding weighed amounts of the salt and recording the resultant chemical shifts. The molality of the solution was converted to molarity using densities of the equivalent aqueous solution (section 3.4.2). The chemical shifts were referenced in ppm relative to t-BuOH.

The large variations in magnetic susceptibility expected for solutions with high metal ion concentrations prevented the use of an external reference as susceptibility corrections become too complicated.

3.3 GRAPHICAL AND COMPUTATIONAL TECHNIQUES

3.3.1 THE GRAN PLOT

Gran's graphical method of end-point determination was used to determine the concentration of all standard solutions.[29] The method is described as the best method for the precise analysis of acids and bases, yielding end-points much more precise than those obtained by the differential method.[30] The Gran function is used to transfer potentiometric data into a linear form before and after the end-point. The point where these lines intersect the x-axis, is the end-point of the titration. Other than obtaining end-points, the analysis gives a good indication of glass electrode performance and possible contamination.[31]

A more accurate extension of the Gran method for the determination of end-points when stability constants are known has been given in the literature.[32] However, in our case, the stability constants were not known and forms of the Gran functions given by Gunnar Gran and F.J.C.Rossotti *et al.* were used and are shown in Table 3.3.[29,30] Data needed for the functions used include the initial volume of acid or base (V^0) and measurements at constant intervals of the cell potential (E) and the volume titrated (v). In all cases a regression line of the Gran function was calculated using SAS STAT and graphs were plotted using SAS GRAPH (section 3.3.3). Examples of Gran plots obtained from potentiometric titrations are shown in figures 3.3 to 3.5.

Table 3.3: Gran functions used to standardise solutions

Titration system	f(E,v) before end-point	f(E,v) after end-point
strong base / strong acid	$(V^0 + v) \times 10^{(E/59.16 - k)}$	$(V^0 + v) \times 10^{(k - E/59.16)}$
strong base / weak acid	$v \times 10^{(E/59.16 - k)}$	$(V^0 + v) \times 10^{(k - E/59.16)}$
weak base / strong acid	$v \times 10^{(k - E/59.16)}$	$(V^0 + v) \times 10^{(E/59.16 - k)}$

The constant "k" is arbitrary and was chosen such that the Gran function before and after the end-point fell into the same range.

When the Gran function deviated from linearity then the points closest to the end-point, where the function was linear, were chosen, otherwise all points were used in the regression calculation. When the x-intercept obtained from data before the endpoint differed from that obtained after the endpoint, an average value was taken. If the difference was greater than 0.005 cm^3, the titration was discarded.

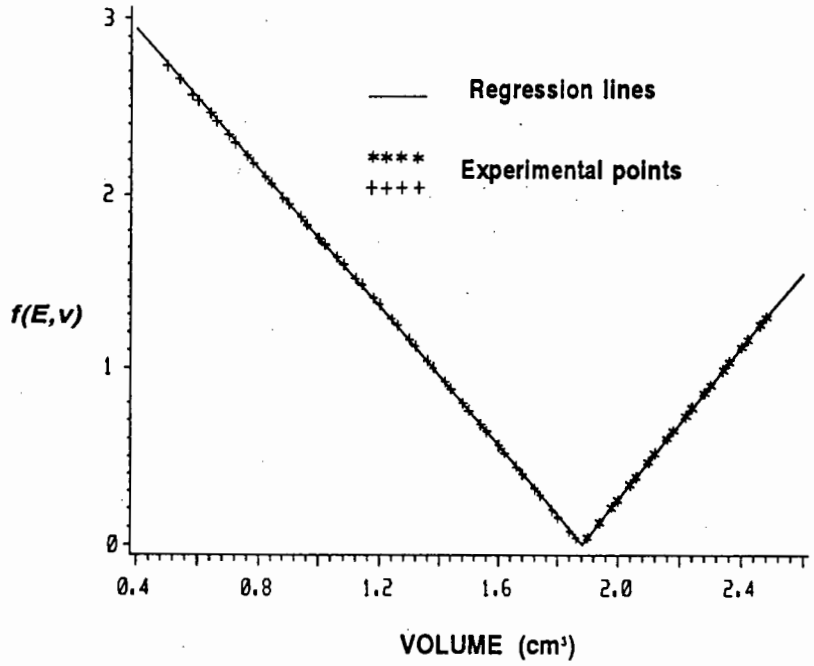

Figure 3.3

Gran plot of HNO_3/NaOH standardisation with $NaNO_3$ electrolyte in both solutions

Figure 3.3 shows a Gran plot which was linear before and after the endpoint of the titration. However this was not always the case. The Gran plot deviated from linearity in the

standardisations using borax and KHP in water, due to the variance of the emf with changes in ionic strength. Electrolyte was not added because of purity and solubility considerations. In these cases, the x-intercept could still be obtained from data before and after the end-point. (see Figure 3.4.)

For the succinate standardisations, nonlinearity before the endpoint was due to the fact that the protonation constants were very close, only one pH unit apart. From the data after the endpoint, only one x-intercept was obtained. (see Figure 3.5)

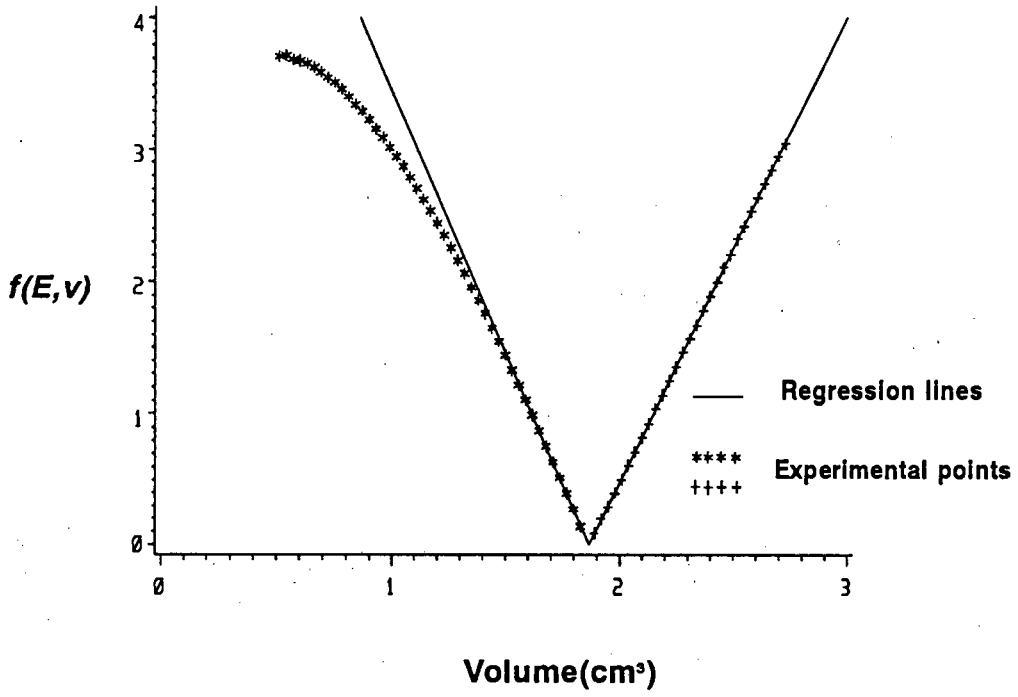

Figure 3.4
Gran plot of KHP/KOH standardisation with NH_4NO_3 electrolyte in base

In the ammonium nitrate system, the Gran plot of the ligand standardisations deviated from linearity after the endpoint due to deprotonation of ammonium ions. The endpoint had to be determined from the x-intercept before the endpoint. In the case of the succinate standardisation, the ligand concentration had to be determined from purity calculated earlier and mass of succinic acid added.

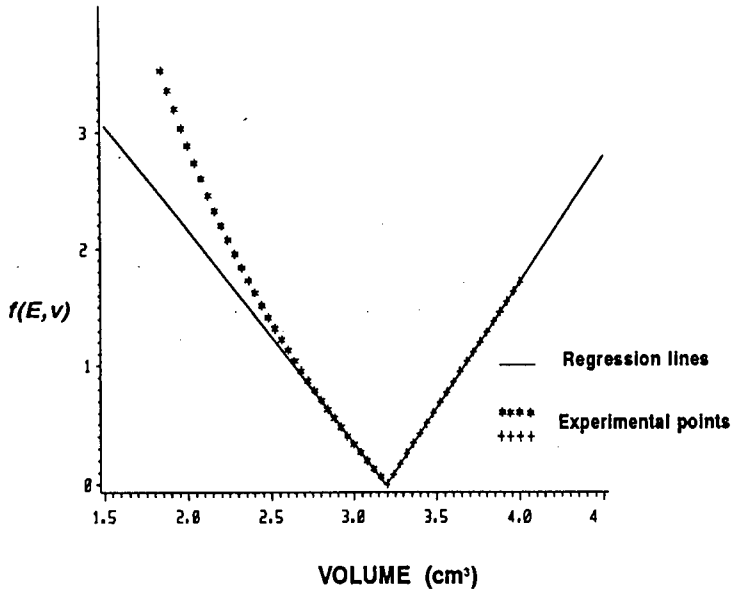

Figure 3.5

Gran plot of SA/NaOH standardisation with $NaNO_3$ electrolyte in both solutions

3.3.2 THE ESTA SUITE OF COMPUTER PROGRAMS

ESTA (Equilibrium Simulation and Titration Analysis) is, as its name implies, a computer program package which can be used for simulating equilibrium distributions of chemical species and for the analysis of potentiometric titration data. ESTA was written by Kevin Murray and Peter M.May of the "University of Wales Institute of Science and Technology". The authors have written several articles on the functions used in the program and a comprehensive overview of all the facilities and the functions used in ESTA is given in the users manual.[33-37] An overview of the ESTA tasks which were used in this study are given here.

3.3.2.1 THE OBJE TASK

ESTA's OBJE optimization and simulation module enables one to refine combinations of the following parameters: β_{pqr}, E^0, s, V^0, c_i^v and c_i^b, where:

c_i^v is the initial vessel concentration of component i and

c_i^b is the initial burette concentration of component i.

This optimization module determines, for one or more parameters, the "best" values, based on a least squares procedure over a whole system of titrations. Equations have been simplified on the assumption that one burette and one standard glass electrode is used. The mass balance equations which are set up for the real and calculated total concentration of each component *i*, at each point are:

$$T_i^r = \frac{c_i^v V^0 + c_i^b v}{V^0 + v} \qquad \text{....3.15}$$

$$T_i^c = [X_i] + \sum_{j=1}^{NJ} r_{ji}\beta_j \prod_{n=1}^{NC} \frac{[X_n]^{r_{jn}}\gamma_n^{r_{jn}}}{\gamma_j} \qquad \text{....3.16}$$

where complex $j = 1,2,...NJ$ and component $n = 1,2,....NC$
^{r} represents experimental or "real" data and ^{c} represents calculated data
$[X_i]$ is the concentration of component i
and r_{ji} is the stoichiometric coefficient of complex j and component i

By putting $T_i^o = T_i^c$, where $i = 1,2,... NC$, one can solve for NC free concentrations. After the NC mass balance equations have been solved, the emf, E_n^c, is calculated from the electrode equation (eqn 3.12). Solving the electrode equation requires a knowledge of the free hydrogen ion concentration, so an iterative solution of the electrode equation and the mass balance equations is implemented.

Simultaneous optimization of n_p parameters is performed by minimizing an objective function, U, defined as:

$$U = (N-n_p)^{-1} \sum_{n=1}^{N} w_n (E_n^r - E_n^c)^2 \qquad \text{....3.17}$$

for experimental titration points $n = 1,2,...N$

where w_n is the weight of the residual at the nth point
E_n is the emf at the nth titration point

A Gauss-Newton method has been adopted in ESTA as the main means of minimizing U. If a failure in the Newton procedure occurs, a secant method is used to solve the equations. The program terminates if it is unable to decrease U before the shift falls below a preset threshold value. When the estimates of the parameters are sufficiently close to the solution, the standard deviation of the parameters being refined is calculated using the formula:

$$\sigma_i = \sqrt{\frac{u \times G_{ii}}{N - n_p}} \qquad \text{....3.18}$$

where G_{ii} is the inverse Hessian for parameter i and

σ_i is the standard deviation of parameter i.

The correlation coefficient between two parameters, i and j, is calculated using the formula:

$$r_{ij} = \frac{G_{ij}}{\sqrt{G_{ii} G_{jj}}} \qquad \text{....3.19}$$

The Hamiltonian or crystallographic R-factor is given by:

$$R = \sqrt{\frac{U}{\sum_{n=1}^{N} w_n (E_n^r)^2}} \qquad \text{....3.20}$$

and the limit by:

$$R_{\text{lim}} = \sqrt{\frac{N}{\sum_{n=1}^{N} w_n (E^r)^2}} \qquad \text{....3.21}$$

3.3.2.2 THE ZBAR TASK

ESTA's ZBAR simulation module calculates the experimental and calculated formation functions on a point-by-point basis.

The proton formation function, $\bar{Z}_H$, is defined as the average number of protons bound to a ligand.

$$\bar{Z}_H = \textit{bound proton / total ligand}$$

$$\bar{Z}_H = \frac{\sum_{j=0}^{NJ} j[H]^j \beta_{01j}}{\sum_{j=0}^{NJ} [H]^j \beta_{01j}} \qquad \text{....3.22}$$

In the absence of metal this equation can be converted into:

$$\bar{Z}_H = \frac{T_H - [H] + \frac{K_W}{[H]}}{T_L} \qquad \text{....3.23}$$

Equation 3.23 is solved for $\bar{Z}_H^r$ and $\bar{Z}_H^c$ from E^r and E^c respectively, using the electrode equation (eqn 3.12) and the mass balance equations for T_L and T_H (eqn 3.15 and 3.16). A printout is generated with the following data for each titration point: E^r; pH^r and pH^c with the residual (pH^r - pH^c); the proton formation functions $\bar{Z}_H^r$ and $\bar{Z}_H^c$ with their residual ($\bar{Z}_H^r$ - $\bar{Z}_H^c$) and a point residual calculated according to equation 3.24.

$$\text{point residual} = \sqrt{(-\log[H^+]^r + \log[H^+]^c)^2 + (\bar{Z}_H^{\,r} - \bar{Z}_H^{\,c})^2} \qquad \text{....3.24}$$

The final sum of squares of each residual type is printed at the end of the last titration. The calculated and experimental protonation curve for the ligand, a plot of $\bar{Z}_H$ versus -log[H^+], can be plotted to evaluate both the calculated and experimental functions.

The metal formation function, $\bar{Z}_M$, is defined for simple mononuclear binary complexes, as the average number of ligand molecules bound to metal according to equation 3.25. A plot of $\bar{Z}_M$ vs -log[L] is termed the formation curve for the system. However the free concentration of proton is measured in the titration, not that of the ligand, so equation 3.25 is converted into equation 3.26:

$$\bar{Z}_M = \textit{total metal bound ligand / total metal}$$

$$\bar{Z}_M = \frac{\sum_{j=0}^{NJ} j[L]^j\beta_{1j0}}{\sum_{j=0}^{NJ} [L]^j\beta_{1j0}} \qquad \text{....3.25}$$

$$\bar{Z}_M = \frac{T_L - A(1+\sum_{j=0}^{NJ}[H]^j\beta_{01j})}{T_M}$$

$$A = \frac{T_H - [H] + \frac{K_W}{[H]}}{\sum_{j=0}^{NJ} j[H]^j\beta_{01j}} \qquad \text{....3.26}$$

Equation 3.26 is solved at every titration point by solving the relevant mass balance equations for T_M, T_L and the electrode equation. The calculated or experimental formation curve is plotted vs -log[A].

3.3.2.3 THE SIME TASK

ESTA's SIME simulation module when used for potentiometric titration calculations, solves the emf's at each point in a titration when given the volume and concentration data and stability constants for the system. The emf is calculated from the electrode equation after the mass balance equations have been solved for all free concentrations. A facility exists whereby an output file of simulated titration data, with a format identical to ESTA input can be generated. This file can be analyzed using the optimization facilities in ESTA.

3.3.2.4 THE SPEC TASK

The speciation of a complex solution gives the exact chemical composition of each chemical species present in solution at equilibrium and their respective concentrations. ESTA's SPEC simulation module, enables the user to calculate the concentration of all species in solution, on a point-by-point basis, given their stability constants and the free or total concentration of each component. The distribution of components amongst all species is determined and can be represented in various graphical formats. In a similar way to the OBJE task, by setting up the mass balance equations $T_i^r = T_i^c$ (eqns 3.15 and 3.16), *NC* free concentrations are solved given *NC* real concentrations. The dimension of the mass balance equations is reduced by the number of free concentrations which are supplied. If corrections for ionic strength are needed, the activity coefficient quotient is calculated using a Debye Hückel equation (section 3.3.4).

3.3.3 NON-LINEAR REGRESSION ANALYSIS

SAS STAT and SAS GRAPH were used in analyzing NMR data, Gran plots and Pitzer equations. All non-linear equations were computed using the least squares methods employed by SAS STAT and SAS GRAPH was used to verify and graphically present the results.

The iterative method most commonly used was the multivariate secant method.[38] An initial estimate was often given and when necessary the estimated parameters were confined to a certain range of values. The multivariate secant method is similar to the Gauss-Newton method, except that the derivatives are estimated from the history of iterations rather than supplied analytically. This method has the advantage in that partial derivatives are not necessary and hence the method is also called the DUD method for Doesn't Use Derivatives. If the convergence criterium is met the procedure prints the parameter estimates, an asymptotically valid standard error of the estimate, an asymptotic 95% confidence interval for the estimate and an asymptotic correlation matrix of the parameters.

3.3.4 IONIC STRENGTH CORRECTIONS

The stoichiometric stability constant can be defined as the product of its thermodynamic stability constant and its activity coefficient quotient Γ_{pqr} (section 3.2.2).

$$\beta_{pqr} = {}^{T}\beta_{pqr}\,\Gamma_{pqr} \qquad \text{....3.27}$$

for the reaction $pM + qL + rH \rightleftharpoons M_pL_qH_r$

The mean activity coefficient for a given solution varies as a function of the ionic strength of the solution and can be determined or calculated from experimental measurements. For a solution containing cations (c) and anions (a), it is defined as follows:

$$\gamma_{\pm} = \sqrt[\nu_a + \nu_c]{\gamma_c^{\nu_c}\,\gamma_a^{\nu_a}} \qquad \text{....3.28}$$

where ν_a and ν_c represent the stoichiometric number of anions and cations in solution

Many equations have been proposed to account for the change in activity coefficients with ionic strength and temperature.[19] These ionic strength equations have been used to project stability constants measured at one ionic strength to another ionic strength. The degree of accuracy obtained in these corrections is strongly dependent on the method chosen and the reliability of the original stability constant.

The extended Debye Hückel equation is the most well known. Its corrected form, also known as the Hückel equation gives the following expression for the mean molal activity coefficient of an electrolyte:[39]

$$-\log\gamma_{\pm} = \frac{A_{\phi}|z_{+}z_{-}|\sqrt{I_m}}{(1+\beta\mathring{a}\sqrt{I_m})} + CI_m \qquad \text{....3.29}$$

where z_+ is the number of charges on the cation

z_- is the number of charges on the anion

C is an empirical constant, characteristic of the electrolyte

$\mathring{a}$ is an ionic size parameter in Angstroms

A_ϕ and β are constants dependent on the solvent density and temperature

For ionic strengths lower than 0.1*m*, relative single-ion activity coefficients and hence the activity coefficient quotient is calculated using equation 3.6.[22] This allows one to estimate ${}^{T}\beta$ by extrapolating to zero ionic strength, where $\Gamma = 1$, or to correct β to any ionic strength, using only one or two data points.

Guggenheim proposed another version of this equation, including an interaction coefficient β which is unrelated to the β of equation 3.29. The molal activity coefficient for an electrolyte *AX* with cations *c* and anions *a* in solution is given by:

$$\log\gamma_{AX} = -\frac{A_\phi|z_+z_-|\sqrt{I_m}}{(1+\sqrt{I_m})} + \frac{2\nu_+}{(\nu_++\nu_-)\ln 10}\sum_a \beta_{Aa} m_a + \frac{2\nu_-}{(\nu_++\nu_-)\ln 10}\sum_c \beta_{cX} m_c \quad \text{....3.30}$$

where A_ϕ is the Debye-Hückel constant

β is the interaction coefficient

ν_- is the number of anions per molecule of electrolyte and

ν_+ is the number of cations per molecule of electrolyte

The β's published by Guggenheim are meant to provide for ionic associations.[40] They state that, for 1-1, 1-2 and 2-1 electrolytes, calculations to 0.1*M* ionic strength should show good accuracy.

Pitzer has developed semi-empirical equations for the convenient and accurate representation and prediction of the thermodynamic properties of aqueous electrolytes including complex mixtures.[41-46] These equations can be extended to high ionic strengths,[47,48] high temperatures [49] and high pressures.[50]

The various forms of the Debye-Hückel calculation show good accuracy up to 0.1*M*. At higher concentrations account must be taken of short range interionic forces that are specific to each solute. These terms which take into account the kinetic effect of the hard core have been included by Pitzer without disturbing the basic pattern of the Debye-Hückel equation and are presented as interaction or virial coefficients for each solute. The three virial parameters

$\beta^{(0)}$, $\beta^{(1)}$ and C^{ϕ} have been evaluated from a wide variety of osmotic or activity coefficient data for pure electrolytes. These parameters take into account any ion pairing or weak association that may take place.

In evaluating activity coefficients in mixtures, it was found that these parameters, determined from the single solutes, are able, in most cases, to define the mixture completely. When mixing solutes the additional combinations of coefficients, θ_{MX}, θ'_{MX} and ψ_{MNX} were added. However, these coefficients were found to be small and frequently negligible. Hence in evaluating activity coefficients in mixtures, it was found that the parameters, determined from the single solutes, are able, in most cases, to define the mixture completely. The Pitzer equation allows the prediction, with considerable accuracy, of the properties of mixtures, if the properties of each pure component are known (eqn 3.31).

The equation is of the same form as that presented by Guggenheim, with the addition of a third virial coefficient. The second virial coefficient B, is now dependent upon ionic strength and the parameters θ and ψ, which have little effect, have been omitted.[45]

$$\ln\gamma_A\gamma_X = (z_A^2 + z_X^2)f^{\gamma} + \sum_a m_a(2B_{Aa} + ZC_{Aa}) + \sum_c m_c(2B_{cX} + ZC_{cX}) + \sum_c \sum_a m_c m_a [(z_A^2 + z_X^2)B'_{ca} + (|z_A| + |z_X|)C_{ca}] \quad \text{....3.31}$$

$$f^{\gamma} = -A_{\phi} \left[\frac{\sqrt{I_m}}{(1 + 1.2\sqrt{I_m})} + \frac{2\ln(1 + 1.2\sqrt{I_m})}{1.2}\right] \quad \text{....3.32}$$

$$B'_{ca} = -2\beta^{(1)}_{ca} \frac{1 - (1 + \alpha\sqrt{I_m} + \frac{\alpha^2 I_m}{2}) e^{-\alpha\sqrt{I_m}}}{\alpha^2 I_m^2} \quad \text{....3.33}$$

$$B_{ca} = \beta^{(0)}_{ca} + 2\beta^{(1)}_{ca} \frac{1 - (1 + \alpha\sqrt{I_m}) e^{-\alpha\sqrt{I_m}}}{\alpha^2 I_m} \quad \text{....3.34}$$

$$C_{ca} = \frac{C^{\phi}_{ca}}{2|z_c z_a|^{\frac{1}{2}}} \qquad \text{....3.35}$$

$$Z = \sum_i m_i |z_i| \qquad \text{....3.36}$$

where f' is the general "Debye Hückel" term for long-range forces,
AX is the monovalent electrolyte kept in excess
B_{ca} and C_{ca} are the second and third virial coefficients and
B'_{ca} is the derivative of B_{ca}.
$\beta^{(0)}_{ca}$, $\beta^{(1)}_{ca}$ and C^{ϕ}_{ca} are empirical parameters for the pair of ions ca,
i represents all ions in solutions, c, all cations and a, all anions,
m_i and z_i represent stoichiometric molality and charge number of species i
and I_m represents the molal ionic strength = $0.5\ \Sigma m_i z_i^2$.
For 1-1 and 2-1 electrolytes $\alpha = 2.0$ and at 25°C $A_{\phi} = 0.391$.
Equations 3.33 and 3.34 only apply to 1-1, 2-1 and 3-1 electrolytes.

In the present study, the single ion form of the Pitzer activity coefficient equation is used.[45] The equations for a positive ion, A, and a negative ion, X, are given in equations 3.37 and 3.38, excluding the terms θ, θ' and ψ.

$$\ln\gamma_A = z_A^2 f^{\gamma} + \sum_a 2m_a B_{Aa} + z_A^2 \sum_c \sum_a m_c m_a B'_{ca} + \sum_a Z m_a C_{Aa} + |z_A| \sum_c \sum_a m_c m_a C_{ca} \qquad \text{....3.37}$$

$$\ln\gamma_X = z_X^2 f^{\gamma} + \sum_c 2m_c B_{cX} + z_X^2 \sum_c \sum_a m_c m_a B'_{ca} + \sum_c Z m_c C_{cX} + |z_X| \sum_c \sum_a m_c m_a C_{ca} \qquad \text{....3.38}$$

The Pitzer parameters $\beta^{(0)}$, $\beta^{(1)}$ and C^{ϕ} for over 120 electrolytes have been published by the author and other workers in this field.[41,51] These parameters allow the equations listed above to be applied to a wide variety of mixed electrolytes at room temperature and at ionic strengths up to 6 molal in many cases and occasionally even higher. If measurements do not extend above 2 molal the third virial coefficient, C, can be omitted.

The Pitzer equation was converted by Millero to an individual ion form using the mean salt convention. Single ion activity coefficients in halide salt solutions have been successfully calculated.[52,53] The mean salt method used to obtain absolute values of ionic activity coefficients, has limitations when applied to nitrate and perchlorate salts which may form ion pairs. The higher the ionic strength the greater these differences become.[52] For these reasons Pitzer's equation involving neutral ion pair parameters was chosen.

Equation 3.6 can be rewritten in the natural logarithmic form:

$$\ln\Gamma_{pqr} = p\ln\gamma_M + q\ln\gamma_L + r\ln\gamma_H - \ln\gamma_{M_pL_qH_r} \qquad \text{....3.39}$$

In the experimental determination of solution equilibrium constants, it is normal practice to keep the ionic strength of the solution constants by using a monovalent background electrolyte, AX, at a concentration much higher than that of the reacting species. Under these conditions, as the interaction between species is weighted by their concentration, it is reasonable to assume that the activity coefficient of a species will depend only on its interaction with the background electrolyte *i.e.* interactions with other species in solution are negligible. Using this approximation, equations 3.37, 3.38 and 3.39 reduce to:

$$\begin{aligned}\ln\Gamma_{pqr} = {} & \xi f^{\gamma} + \xi m_X^2 B'_{AX} + \sigma m_X^2 C_{AX} \\ & + 2qm_X B_{AL} + \xi m_L m_X B'_{AL} + \sigma m_X m_L C_{AL} + 2qm_X I_m C_{AL} \\ & + 2rm_X B_{HX} + \xi m_H m_X B'_{HX} + \sigma m_H m_X C_{HX} + 2rm_X I_m C_{HX} \\ & + 2pm_X B_{MX} + \xi m_M m_X B'_{MX} + \sigma m_X m_M C_{MX} + 2pm_X I_m C_{MX} \\ & - 2m_X B_J + \xi m_S m_X B'_J + \sigma m_X m_S C_J - 2m_X I_m C_J\end{aligned} \qquad \text{....3.40}$$

$$\xi = r + pz_M^2 + qz_L^2 - z_S^2 \qquad \text{....3.41}$$

$$\sigma = r + p|z_M| + q|z_L| - |z_S| \qquad \text{....3.42}$$

for the reaction $pM + qL + rH \rightharpoonup M_pL_qH_r$ *where* $M_pL_qH_r = S$

Depending on the charge of the product, the symbol J refers to the salt parameter of the product, S, with either the anion, A, or the cation, X, of the background electrolyte, *i.e.* if $z_S > 0$ then $J = SX$, if $z_S < 0$ then $J = AS$ and if either z_L, z_M *or* $z_S = 0$ then their relevant virial coefficients are set to zero.

From the activity coefficient quotient and the thermodynamic stability constant, the stoichiometric stability coefficient at any ionic strength can be calculated:

$$\ln \beta_{pqr} = \ln \Gamma_{pqr} + \ln {}^{T}\beta_{pqr} \qquad \text{....3.43}$$

Note that the activity coefficient of the species $M_pL_qH_r$ depends on its concentration and the concentration of the free components in solution *i.e.* it depends on the speciation of the solution. Initial estimates of these concentrations can be estimated from uncorrected β values and then refined iteratively.

Several solutes are known to form ion pairs but this association and the thermodynamic properties of the solute are fitted satisfactorily by the above parameters and equations.

The experimental constants determined were not in the dilute range, therefore, the Pitzer equation had to be used to correct the constants to different ionic strengths. Before using the simplified Pitzer approach, the approximations made were validated by testing the method on experimental data of other well studied systems. These results are given in section 3.4.2.

3.3.4.1 IONIC STRENGTH CORRECTION COMPUTER PROGRAM

A Borland Pascal version 7.0 program has been written to convert stability constants from one ionic strength to other ionic strengths using the simplified Pitzer approach. Seven binary files are associated with the program. These files contain Pitzer parameters and stability constants, mostly literature but some calculated, which can be edited and updated. The program runs interactively and calculates the stability constants at ionic strengths specified as input. Input parameters include p, q and r for the stability constant β_{pqr} and the background electrolyte. The name and concentrations of all species defined in the stability constant are prompted for. The main menu gives details of the format needed in which to enter ligand and cation names and gives a listing of the cations and ligands for which parameters are available. The program is not case sensitive.

All parameters are presented on the screen before an ionic strength correction is performed. The results are then plotted to the screen together with a curve showing the variation of the stability constant with ionic strength. Experimental stability constant values can be plotted simultaneously for an evaluation of the calculated relationship as well as a plot of the Debye Hückel correction term. The graphical data are also saved to a text file which can then be imported into a graphical package at a later date.

The source code of the computer program (the executable file: CORPIT) is given in appendix 4 and the executable and associated files are on disk 1 of the attached 1.44MB diskettes. Instructions on how to use the program as well as a listing of the contents of disk 1, are given in appendix 7.

3.4 RESULTS

3.4.1 PROTONATION CONSTANTS

All experimental protonation constants, together with literature values, are plotted in Figure 3.6 and shown in Table 3.5. A summary of the experimental parameters for each system is given in Table 3.2. The protonation constants were found to follow the general trend K_{011}(SA) > K_{011}(PA) > K_{011}(MS) > K_{012}(SA). The differences in protonation constants are due to the different substituents on the carboxylate groups.

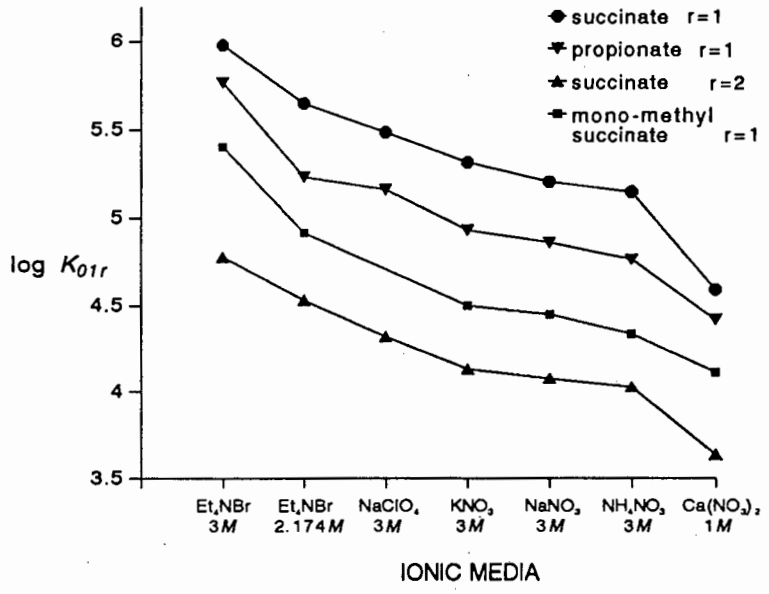

Figure 3.6

Thermodynamic protonation constants K_{011} and K_{012} plotted for the ligands succinate, mono-methyl succinate and propionate in different ionic media. The protonation constants determined in 3*M* $NaClO_4$ were taken from literature.[54,55]

Substituents which are electron donating weaken the carboxylic acid and hence increase K_{01r}, while electron withdrawing groups strengthen the acid and decrease K_{01r}. Therefore we would expect carboxylate groups to increase the protonation constant and carboxylic and ester groups to decrease it. These observations, studied in a wide range of acids, provide the basis for the Taft equations and Taft σ^* constants, which can be used to predict protonation constants.[56] The acid-strengthening ($-\Delta$ log*K*) electrostatic and inductive effects of representative substituents attached to the α-carbon atoms of aliphatic acids have been calculated as a direct function of Taft σ^* constants and have been published for a large number of substituents.[56]

For a dibasic acid such as succinic acid there is also a statistical factor which effects the second protonation constant. When the ligand is completely protonated there are two equivalent ways of losing the first proton, therefore K_{012} should be twice as large as it would be for a closely related monobasic acid. Hence in predicting the protonation constants, log K_{012} should be log 2 (= 0.3) less.

Table 3.4: Comparison of experimental and calculated Δ log K_{01r} for each ligand; where Δ log K_{01r}^{expt} = log K_{01r} - log K_{011} (PA).

substituent	Δ log$K$	ligand	r	Δ log K_{01r}^{calc}	Δ log K_{01r}^{expt}
CH_2COO^-	0.244	SA	1	0.244	0.318
CH_3	0.000	PA	1	0.000	0.000
CH_2COOCH_3	-0.528	MS	1	-0.528	-0.376
CH_2COOH	-0.548	SA	2	-0.848	-0.800

Using the published Δlog$K$ values per substituent and including the statistical effect, Δ log K_{01r}^{calc} can be predicted for the ligands studied. The differences between the experimental protonation constants obtained between the various ligands, Δ log K_{01r}^{expt}, was taken as the difference between the average protonation constant obtained for the ligand in all media and the average value obtained for propionic acid. Values obtained for Δ log K_{01r}^{calc} and Δ log K_{01r}^{expt} are given in Table 3.4. The good correlation obtained between experimental and calculated values lends confidence to our results.

Figure 3.6 shows clearly, that at high ionic strength, the nature of the background medium has a dramatic effect upon the protonation equilibria of carboxylic acids. For all three ligand systems, the protonation constants of the ligands in the different media follow the general trend with respect to the background electrolyte $K_{01r}(Et_4NBr) > K_{01r}(KNO_3) > K_{01r}(NaNO_3) > K_{01r}(NH_4NO_3) > K_{01r}(Ca(NO_3)_2)$. This trend can be seen in Figures 3.7 and 3.8, where the protonation curves for propionic and succinic acid in the different media have been plotted.

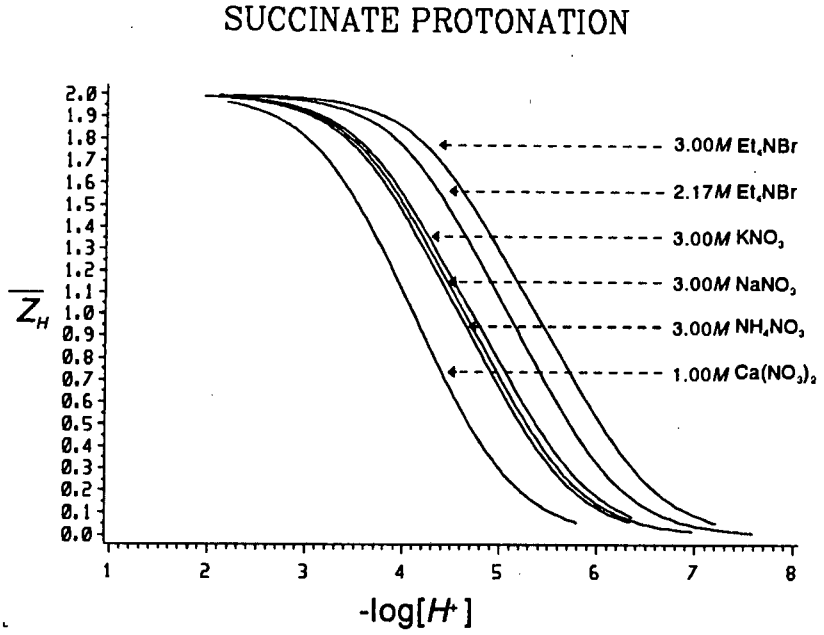

Figure 3.7

Protonation curves obtained for succinic acid in different media

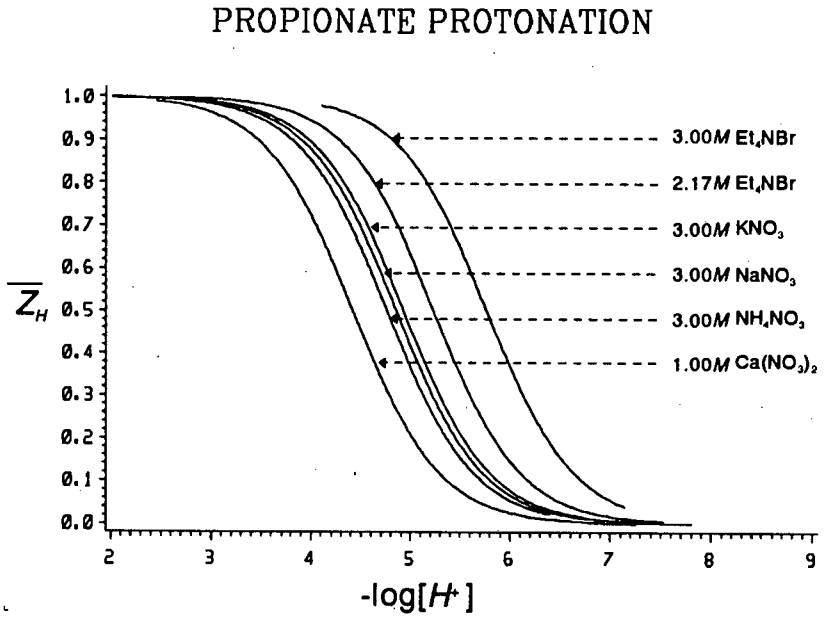

Figure 3.8

Protonation curves obtained for propionic acid in different media

The effect of the ionic medium can be explained in terms of specific or non specific interaction. These two possibilities are explored in the following sections.

Table 3.5: Thermodynamic protonation constants β_{011} and β_{012} for the ligands succinate, propionate and mono-methyl succinate in different ionic media, measured at 25°C; σ is the standard deviation and R the crystallographic R factor. Experimental parameters are given in table 3.2. Literature protonation constants determined in 3*M* $NaClO_4$ have been included for comparison.

Ligand	Medium	R	R_{lim}	$\log K_{011}$	σ	$\log K_{012}$	σ
succinate							
	3*M* Et_4NBr	0.0020	0.0023	5.979	0.0013	4.776	0.0017
	2.17*M* Et_4NBr	0.0023	0.0031	5.649	0.0011	4.533	0.0015
	3*M* $NaClO_4$*			5.485	0.001	4.323	0.001
	3*M* KNO_3	0.0006	0.0025	5.313	0.0003	4.131	0.0005
	3*M* $NaNO_3$	0.0012	0.0014	5.204	0.0004	4.077	0.0007
	3*M* NH_4NO_3	0.0029	0.0015	5.145	0.0022	4.027	0.0026
	1*M* $Ca(NO_3)_2$	0.0067	0.0031	4.590	0.0044	3.635	0.0065
propionate							
	3*M* Et_4NBr	0.0043	0.0037	5.767	0.0028		
	2.17*M* Et_4NBr	0.0027	0.0033	5.232	0.0008		
	3*M* $NaClO_4$*			5.161	0.002		
	3*M* KNO_3	0.0012	0.0023	4.929	0.0004		
	3*M* $NaNO_3$	0.0029	0.0013	4.859	0.0011		
	3*M* NH_4NO_3	0.0026	0.0022	4.762	0.0007		
	1*M* $Ca(NO_3)_2$	0.0035	0.0034	4.418	0.0010		
mono-methyl							
succinate	3*M* Et_4NBr	0.0058	0.0052	5.403	0.0022		
	2.17*M* Et_4NBr	0.0019	0.0029	4.915	0.0006		
	3*M* KNO_3	0.0028	0.0021	4.499	0.0012		
	3*M* $NaNO_3$	0.0088	0.0012	4.448	0.0038		
	3*M* NH_4NO_3	0.0066	0.0027	4.337	0.0023		
	1*M* $Ca(NO_3)_2$	0.0092	0.0024	4.113	0.0034		

*[54,55]

3.4.2 IONIC STRENGTH CORRECTIONS

In order to evaluate the suitability of the simplified Pitzer approach (section 3.3.4) to ionic strength corrections of stability constants, equations 3.40 to 3.43 were tested on some well studied systems.

Most experimental stability constants have been measured with molarity as basis, while the Pitzer approach is based on molality. Hence the literature and experimental stability constants and ionic strengths had to be converted to molality. This conversion is simple if the density of the solution is known. In potentiometric titrations the concentration of the salt is always in excess and the density of the solution approximates to the density of a solution containing the same concentration of pure salt. Molar concentrations were converted to a molal scale using equation 3.44 and the molar based stability constants were converted to a molal scale using equation 3.45.

$$m_{AX} = \frac{[AX]}{\rho_{[AX]} - 0.001\ [AX]\ Mr_{AX}} \qquad \text{....3.44}$$

$$\log K_{m,pqr} = \log K_{c,pqr} + (p+q+r-1)\log(\rho_{[AX]} - 0.001\, Mr_{AX}[AX]) \qquad \text{....3.45}$$

where Mr_{AX} and m_{AX}, are the molar mass and molality, respectively of the salt AX.

Density data (g cm^{-3}) for a range of aqueous electrolyte solutions at 25°C were taken from the literature.[57-59] A least squares fit of the density variation with molality for each electrolyte gave the following equations (equation 3.46), where the value in brackets is the standard deviation in the last position of each number. Similar equations for the salts KCl and KNO_3 have been given in the literature up to 1.7M [60]

The literature Pitzer parameters used in the calculations are given in Table 3.6. Included in the table are the standard deviations quoted and the maximum molality for which the fit was satisfactory.

$$\rho_{KNO_3\ (0-2.8M)} = 0.99713(4) + 0.06181(7)\ [KNO_3] - 0.00099(3)\ [KNO_3]^2$$

$$\rho_{NH_4NO_3\ (0-7.6M)} = 0.9974(1) + 0.03149(7)\ [NH_4NO_3] - 0.000263(9)\ [NH_4NO_3]^2$$

$$\rho_{LiNO_3\ (0-5M)} = 0.9975(6) + 0.0395(6)\ [LiNO_3] - 0.0002(1)\ [LiNO_3]^2$$

$$\rho_{NaNO_3\ (0-7.2M)} = 0.9977(2) + 0.0545(1)\ [NaNO_3] - 0.00053(2)\ [NaNO_3]^2$$

$$\rho_{LiCl\ (0-14M)} = 0.9986(4) + 0.0222(1)\ [LiCl] - 0.00008(1)\ [LiCl]^2$$

$$\rho_{NaCl\ (0-5.3M)} = 0.9973(1) + 0.0400(1)\ [NaCl] - 0.00056(2)\ [NaCl]^2$$

$$\rho_{KCl\ (0-4.1M)} = 0.99729(9) + 0.0461(1)\ [KCl] - 0.00068(3)\ [KCl]^2$$

$$\rho_{LiClO_4\ (0-3M)} = 0.9973(3) + 0.0631(5)\ [LiClO_4] - 0.0006(2)\ [LiClO_4]^2$$

$$\rho_{NaClO_4\ (0-4M)} = 0.9976(8) + 0.078(1)\ [NaClO_4] - 0.0005(2)\ [NaClO_4]^2$$

$$\rho_{Ca(NO_3)_2\ (0-1.8M)} = 0.99716(7) + 0.1207(2)\ [Ca(NO_3)_2] - 0.00371(9)\ [Ca(NO_3)_2]^2$$

....3.46

Table 3.6: Literature Pitzer parameters

salt	$\beta^{(0)}$	$\beta^{(1)}$	C^{ϕ}	max *m*	σ
HBr	0.1960	0.3564	0.00827	3	*
HCl	0.1775	0.2945	0.00080	6	*
HI	0.2362	0.392	0.0011	3	*
$HClO_4$	0.1747	0.2931	0.00819	5.5	0.002
HNO_3	0.1119	0.3206	0.0010	3	0.001
LiCl	0.1494	0.3074	0.00359	6	0.001
NaCl	0.0765	0.2664	0.00127	6	0.001
$NaClO_4$	0.0554	0.2755	-0.00118	6	0.001
$LiNO_3$	0.1420	0.2780	-0.00551	6	0.001
NH_4NO_3	-0.0154	0.1120	-0.00003	6	0.001
$NaNO_3$	0.0068	0.1783	-0.00072	6	0.001
KNO_3	-0.0816	0.0494	0.00660	3.8	0.001
$Ca(NO_3)_2$	0.2108	1.409	-0.02014	2	0.002
Et_4NBr	-0.0176	-0.394	0.0156	4	0.001
Et_4NI	-0.179	-0.571	0.0412	2	0.007
Li Acetate	0.1124	0.2483	-0.00525	4	0.001
Na Acetate	0.1426	0.3237	-0.00629	3.5	0.001

* high accuracy fit.[41]

3.4.2.1 AMMONIA

Figure 3.9 shows the simplified Pitzer approach applied to the protonation of ammonia. The symbols are experimental data points while the solid line is the calculated dependence of the protonation constant upon ionic strength. For the uncharged ligand ammonia, the ξ and σ terms and hence also the Debye-Hückel term are all zero. Only interactions between ions of opposite sign are included in our simplified Pitzer equations, therefore only the *HX* and *SX* interaction coefficients were used in the calculation of the activity coefficients. The resultant activity coefficient reduces to:

$$\begin{aligned} \ln\Gamma_{011} &= \ln\gamma_{H^+} - \ln\gamma_{NH_4^+} \\ &= 2m_X\,(B_{HX} - B_{SX} + IC_{HX} - IC_{SX}) \end{aligned} \qquad \text{....3.47}$$

According to the above equation the cation of the background electrolyte has no effect on the activity coefficient quotient and the same ionic strength relationship was predicted for all nitrate salts. The experimental results for the different nitrates show a similar but not identical trend although the correlation between experimental and calculated results is good for $LiNO_3$ and reasonable for KNO_3 and $NaNO_3$.

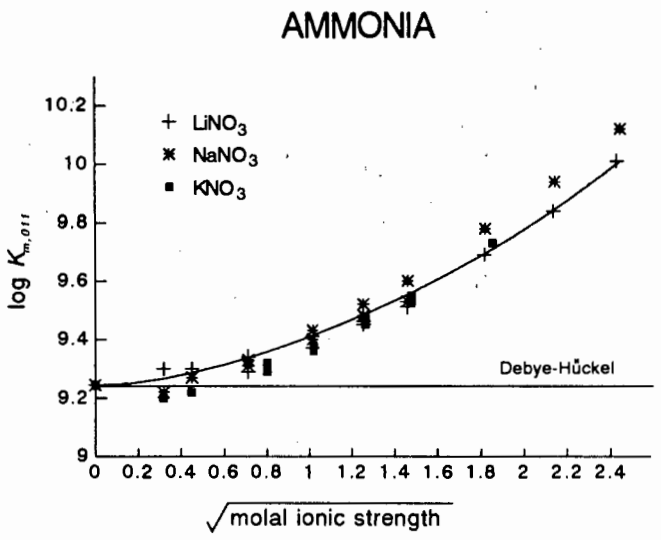

Figure 3.9

The variation in the protonation constant for ammonia as a function of ionic strength for various electrolytes. The symbols are experimental data points obtained from the literature.[59,61] The line was calculated using the simplified Pitzer equation (equations 3.40-3.43), literature Pitzer parameters and a literature K^0 (log K^0 = 9.244)[27]. The Debye Hückel correction term (equations 3.31, 3.32).

3.4.2.2 ACETATE

Figure 3.10 shows the comparison between the experimental and predicted protonation constants for acetate as a function of $NaClO_4$, LiCl and NaCl concentration. In this case both the anion and the cation have an effect on the calculated as well as experimental protonation constant. When analyzing the protonation constants obtained in $NaClO_4$ and NaCl, it can be seen that changing the anion from ClO_4^- to Cl^- results in a decrease in the calculated protonation constant, which is confirmed by the experimental results. This is largely due to varying degrees of ion-pairing of the different electrolytes. When changing the cation from Li^+ to Na^+ an increase in the protonation constant is predicted, this is confirmed by the experimental results. In this case the variation is due to the increase in the acetate Pitzer parameters when changing media (see table 3.6). As is the case with the ammonia system, the correlation between experimental and calculated constants is very good over the ionic strength range 0 to 4 mol kg^{-1}. For comparison, the results of a Debye-Hückel correction are shown. Clearly this correction is not valid above an ionic strength of 0.1 mol kg^{-1}.

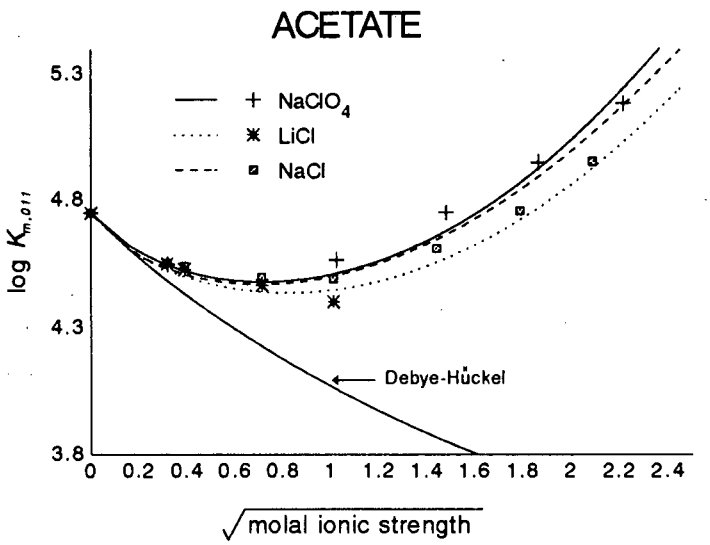

Figure 3.10

The variation in the protonation constant for acetate as a function of ionic strength in various electrolytes. The symbols are experimental data points obtained from the literature.[2,3,4,10] The solid line was calculated using the simplified Pitzer equation (equations 3.40-3.43), literature Pitzer parameters and a literature K^0 (log K^0 = 4.750)[3]. The Debye Hückel correction term (equations 3.31, 3.32) has been included for comparison.

3.4.2.3 PROPIONATE

For the propionate system not all the necessary Pitzer parameters were available in the literature. However, Pitzer noted a general relationship between the two parameters $\beta^{(0)}$ and $\beta^{(1)}$ for various electrolytes and suggested a convenient approximation using this relationship to determine $\beta^{(1)}$ and $\beta^{(0)}$ from experimental data, assuming C to be negligible.[44] At the ligand concentrations used to measure protonation constants of propionate, the contribution of terms involving the third virial coefficient to the overall activity coefficient, are small and so may be neglected.

Many of the metal-ligand parameters were not available and, when only one protonation constant determined at 3*M* ionic strength was available, these Pitzer parameters were calculated using the experimental value, the rough approximation method, and log K^0. When more experimental constants were available, the relevant Pitzer parameters were calculated using a least squares fit of the data. The calculated Pitzer parameters are given in Table 3.7 and the β coefficient relationship used for each electrolyte type is given below the table.

For propionic acid, dimerization is also possible but is only apparent at ligand concentrations greater than 0.05*M* and so was ignored.[65]

Figure 3.11 shows the experimental values of logK_{011} (PA) measured in different ionic media and at different ionic strengths. The solid lines show the calculated dependence of logK_{011} (PA) upon ionic strength and ionic medium, based on the parameters listed in Table 3.7. The experimental protonation constant determined in 3*M* (6.02*m*) Et_4NBr was not used in fitting the curves. The Debye-Hückel curve, the curve for Et_4NI and experimental data obtained from the literature are included in the plot.[66]

From the plot it can be seen that the experimental protonation constants determined in Et_4NBr and $NaClO_4$ are similar at the same molal ionic strength although there is a large difference at the same molar ionic strength. On analyzing the contributions of the various Pitzer terms to the calculated protonation constants one can explain the trends observed.

The protonation constants in Et_4NBr and Et_4NI are greater than those in any other media, largely due to the larger proton (B_{HX}) and salt (B'_{AX}) terms rather than the different ligand (B_{AL}) terms. The protonation constants obtained in $Ca(NO_3)_2$ are smaller mainly due to a smaller concentration of the background salt at the same ionic strength. The differences between the protonation constants in the other nitrate salts are mainly due to the differences between the ligand terms. This could be explained in terms of specific interactions. The larger protonation constants calculated in $NaClO_4$ relative to in $NaNO_3$ are largely due to the different proton terms in going from the one media to the other.

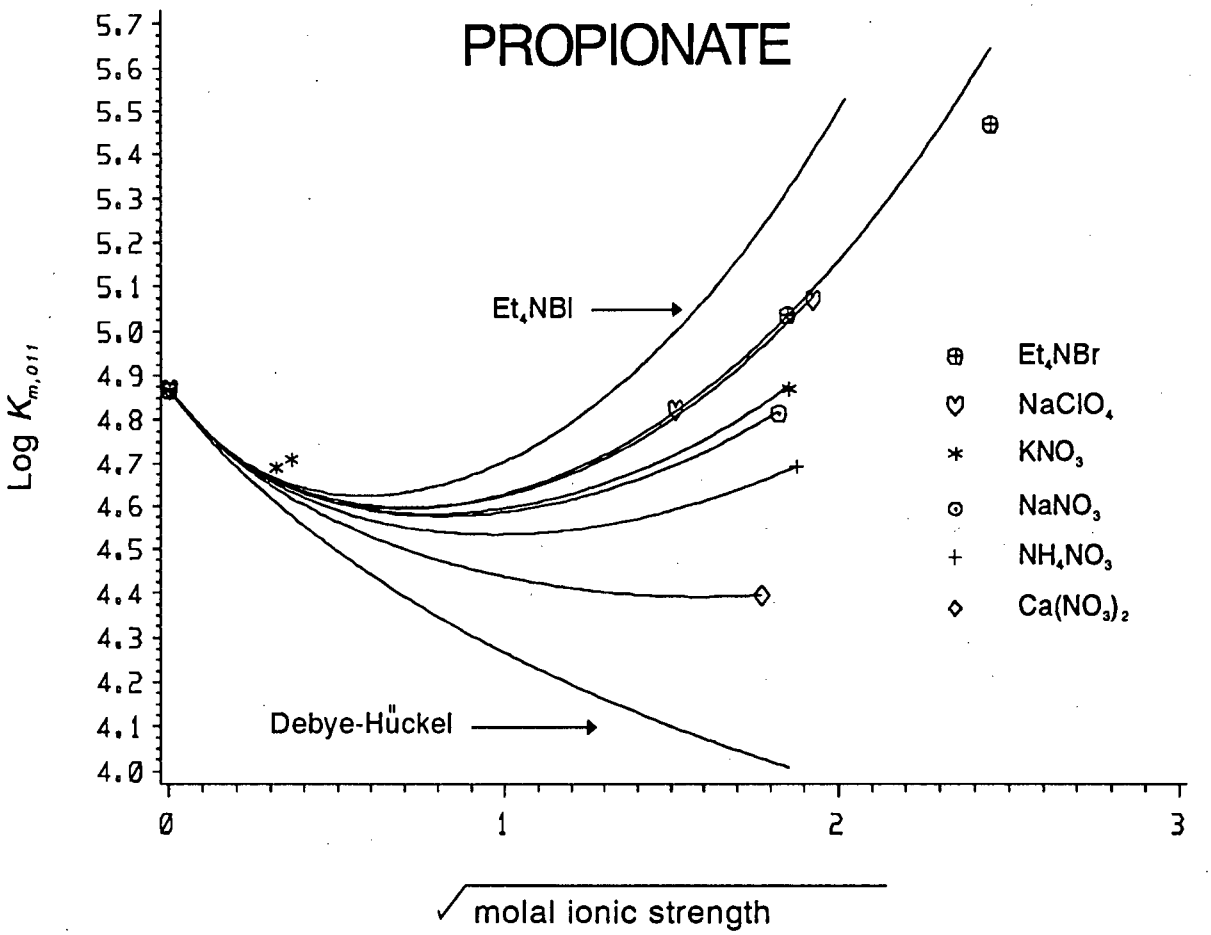

Figure 3.11

Propionates protonation constant as a function of ionic strength for various background electrolytes. The symbols are experimental data points and the solid lines were calculated using the simplified Pitzer equation (equations 3.40-3.43), literature and calculated Pitzer parameters and a literature K^0 ($\log K^0 = 4.868$).

3.4.2.4 SUCCINATE

Succinate presents an interesting example in that the ligand is diprotic and so the solution speciation will depend on the pH of the solution. Once again not all Pitzer parameters were available in the literature and so were estimated from experimental results at 3*M* ionic strength, using the same procedure as before.

The final set of parameters are listed in Table 3.7. Figure 3.12 and 3.13 show the experimental data for this system together with the calculated ionic strength dependence. As in the case of propionate, only the experimental protonation constant in 3.44*m* Et_4NBr was included in the analysis. Experimental data obtained from the JESS (Joint Expert Speciation System) database and from the literature has been included for comparison.[9,67,68] If we compare the succinate data to that obtained for propionate, the same trend is observed for all background media. The curves for the first protonation constant are much steeper than those obtained for the second protonation constant. This is due to a doubling of the ξ term which modulates the Debye-Hückel term, as the charge of the ligand goes from having one negative charge to two negative charges. The smooth trend and similarly shaped curve obtained when plotting our experimental protonation constants determined in NH_4NO_3 with literature values is most gratifying. These curves show that the simplified Pitzer approach is a good representation of the data.

Table 3.7: Calculated parameters used in equations 3.40 - 3.43

salt	$\beta^{(0)}$	$\beta^{(1)}$	salt	$\beta^{(0)}$	$\beta^{(1)}$
Na Propionate	0.1043	0.294	NH_4 Propionate	0.0567	0.218
K Propionate	0.0937	0.278	Et_4N Propionate	0.0046	0.119
Ca Propionate	0.0983	0.793	NH_4H Succinate	0.0312	0.225
NaH Succinate	0.0620	0.227	Et_4NH Succinate	-0.0058	0.096
KH Succinate	0.0538	0.213	CaH Succinate	0.0006	0.522
Na Succinate	0.2383	1.204	NH_4 Succinate	0.1710	1.090
K Succinate	0.2207	1.151	Et_4N Succinate	0.0632	0.694
Ca Succinate*	0.5585	0.5585			

1-1 electrolyte relationship: $\beta^{(0)} = -0.043 + 0.332\beta^{(1)} + 0.574\beta^{(1)}\beta^{(1)}$
1-2 electrolyte relationship: $\beta^{(0)} = -0.20(7) + 0.4(1)\beta^{(1)} - 0.03(6)\beta^{(1)}\beta^{(1)}$
* A relationship was not calculated for 2-2 electrolytes. To fit the curve $\beta^{(1)}$ was made equal to $\beta^{(0)}$.

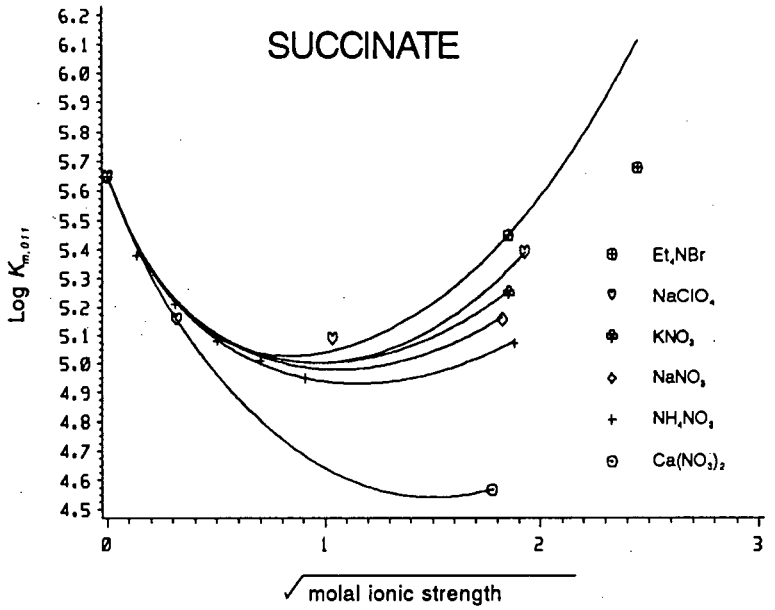

Figure 3.12

The first protonation constant of succinate as a function of ionic strength for various background electrolytes. The symbols are experimental data points and the solid lines were calculated using the simplified Pitzer equation, literature and calculated Pitzer parameters and a literature K^0 ($\log K^0_1$ = 5.648).

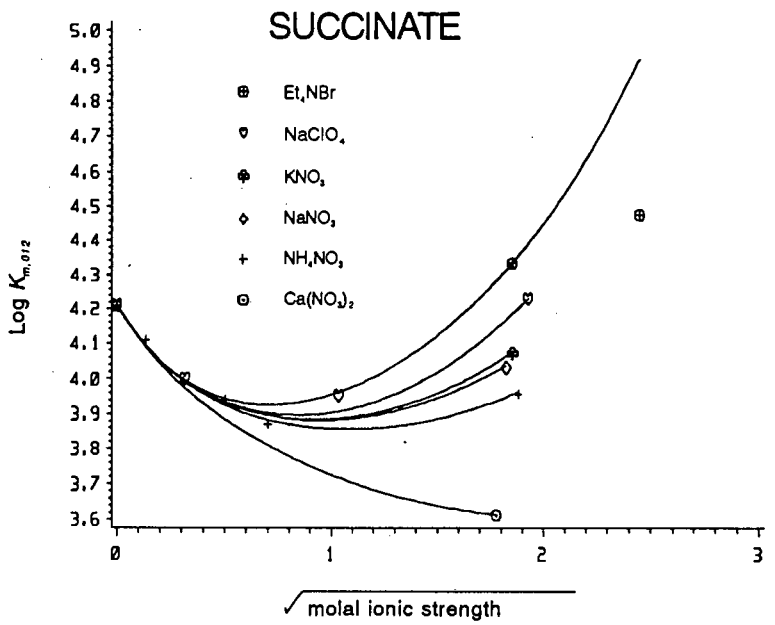

Figure 3.13

The second protonation constant of succinate as a function of ionic strength for various background electrolytes. The symbols are experimental data points and the solid lines were calculated using the simplified Pitzer equation, literature and calculated Pitzer parameters and a literature K^0 ($\log K^0_2$ = 4.209).

3.4.3 COMPLEXATION CONSTANTS OBTAINED FROM POTENTIOMETRIC DATA

At high ionic strength, the nature of the background medium is known to have a dramatic effect upon the protonation equilibria of carboxylic acids. The protonation constants have been found to follow the general trend with respect to background media: $K_{01r}(Et_4NBr) > K_{01r}(NaClO_4) > K_{01r}(KNO_3) > K_{01r}(NaNO_3) > K_{01r}(NH_4NO_3) > K_{01r}(Ca(NO_3)_2)$ (section 3.4.1). As the thermodynamic protonation constant, ${}^{T}K_{01r}$ is a constant, the activity coefficient quotient, Γ_{01r} for the ligands follows the same trend with respect to background media.

The effects of the ionic strength and the ionic medium on the values of the protonation constants can be classified into two main types:

a) the effects of changes in the activity coefficients and
b) specific interactions.

The question arises whether this trend is due to specific interactions between solutes or purely activity coefficient variations. The values of the protonation constants, with the exception of the constants determined in NH_4NO_3, are in the relative order that would be expected from specific interactions between the cation of the electrolyte and the ligand. The smaller the ion and the higher the charge, the more stable the metal ligand complex and the lower the observed protonation constant should be.

The situation is further complicated by the fact that the concentration of water also varies in concentrated electrolyte solutions. The disparity between molarity and molality highlights this problem. The effects arising from the role of water as a component of the equilibrium reactions will appear as an ionic strength dependence. Consequently effects resulting from variations in the water concentration can be attributed to a fictitious equilibrium process.[19]

Ionic strength can be quoted in terms of molar or molal concentration.[21] At low ionic strengths there is little difference between the two units, but molarity is used more frequently as it is more convenient to work in volumes. However at high ionic strengths and when dealing with high molecular weight salts there is a large disparity between the two units. An example being Et_4NBr where a 3 molar aqueous solution is 6.02 molal.

In general for the reaction $pM + qL + rH \rightleftharpoons M_pL_qH_r$ *where* $M_pL_qH_r = S$ the molal stoichiometric stability constant may be defined as

$$\beta_{m,pqr} = \frac{m_S}{m_M{}^p \; m_L{}^q \; m_H{}^r} \qquad \text{....3.48}$$

where m_i represents the molality of species i in mol/kg.

Table 3.8: Protonation constants and apparent protonation constants for the ligands succinate (SA) and propionate (PA) at 25°C and in various concentrations of background electrolytes; I_m is the molal ionic strength.

I_m	medium	log K_{011} (PA)	log K_{011} (SA)	log K_{012} (SA)
3.162	$Ca(NO_3)_2$	4.418	4.590	3.630
3.440	$Ca(NO_3)_2$	4.422	4.605	3.635
3.440	NH_4NO_3	4.757	5.139	4.025
3.535	NH_4NO_3	4.768	5.151	4.033
3.333	$NaNO_3$	4.867	5.208	4.060
3.440	$NaNO_3$	4.883	5.224	4.072
3.440	KNO_3	4.936	5.312	4.132
3.162	$NaClO_4$	5.044	5.355	4.243
3.333	$NaClO_4$	5.081	5.392	4.274
3.440	$NaClO_4$	5.104	5.415	4.293
3.535	$NaClO_4$	5.126	5.437	4.311
3.719	$NaClO_4$	5.167	5.479	4.346
3.162	Et_4NBr	5.177	5.572	4.468
3.333	Et_4NBr	5.201	5.617	4.508
3.440	Et_4NBr	5.233	5.646	4.534
3.535	Et_4NBr	5.253	5.672	4.558
3.719	Et_4NBr	5.291	5.722	4.603

To convert molal based protonation constants determined at one molal ionic strength (m_1) to another (m_2), equation 3.44 was used together with the simplified form of the Pitzer equation (equations 3.40 to 3.43). The resultant protonation constants were then converted back to a

molar base and are shown in Table 3.8.

$$\ln K_{pqr}(m_2) = \ln K_{pqr}(m_1) - \ln \Gamma_{pqr}(m_1) + \ln \Gamma_{pqr}(m_2) \quad \text{....3.49}$$

The Pitzer equations are based on the knowledge that the activity coefficient of an ion is related to its non-ideal behaviour due to ionic interactions with other species in solution.[69] Various ionic interaction models have been used to estimate and explain these activity coefficient variations, the two major types being the ion pairing model and the specific interaction model.[53] Using the protonation constants in Table 3.8 both the ion pairing method and the specific interaction method, as well as a combined method has been used to obtain complexation constants for the cations Na^+, K^+, NH_4^+ and Ca^{++} with the ligands propionate and succinate. A description of these three methods is given in the following sections.

3.4.3.1 THE ION PAIRING MODEL

The ion pairing model defines complexation explicitly. The mean activity coefficient for a solution at a constant temperature and solvent composition varies only as a function of the effective ionic strength.[51] The differences in activity coefficients of salt solutions at the same ionic strength and temperature, are explained by the formation of weak complexes.[70]

Daniele *et al.* have developed an approach to calculate complexation with the cation (*M*) of the background electrolyte.[8,71] When comparing the protonation constants obtained in the various background electrolytes, they made the assumption that these differences are only due to complexation between the ligand and the cation of the background electrolyte. They then made the further assumption that the tetraalkylammonium cation for which the highest protonation constant is obtained, does not form a complex with the ligands. This assumption has been substantiated by other workers in this field who have demonstrated the lack of specific interaction between tetraalkylammonium salts and O-donor ligands.[14] The protonation constants determined in Et_4NI are taken as the stoichiometric constant and by solving the relevant mass balance equations, the metal complexation constants are calculated.[72] The assumption is made that the free metal concentration equals the total metal concentration in solution and that the only

specific binding is due to metal ligand binding, and so estimates of the metal complexation constants can be obtained using equations 3.50 and 3.51. For weak complexes of monoprotic acids and polyprotic acids with very different protonation constants, equation 3.50 can be used, but where the protonation steps are close equation 3.51 must be used.

$$K_{01r} = K'_{01r} (1 + K_{11(r-1)}[M]) \qquad \text{....3.50}$$

$$\frac{\sum r\beta'_{01r}[H]^r}{1 + \sum \beta'_{01r}[H]^r} = \frac{\sum r\beta_{p1r}[M]^p[H]^r}{1 + \sum \beta_{p1r}[M]^p[H]^r} \qquad \text{....3.51}$$

where $K_{11(r-1)}$ is the stability constant for the reaction $M + LH_{(r-1)} \rightleftharpoons MLH_{(r-1)}$
and the superscript, (′), is to denote an apparent value.

Using the approach of Daniele *et al.*, the complexation constants were calculated from the original titration data using the ESTA suite of computer programs (section 3.3.2). The protonation constants determined in Et_4NBr were taken as the stoichiometric constant and the metal complexation constants calculated.

To compare the iterative ESTA technique with the non-iterative technique used by Daniele *et al.*, the complexation constants were recalculated. Equation 3.50 was used for the protonation of propionate and the second protonation of succinate, while equation 3.51 was used for the first protonation of succinate. The constants obtained using this approach were within one standard deviation of those obtained using ESTA.

The complexation constants calculated using these approaches are given in Table 3.9. The Pitzer, and most other, activity coefficient correction methods use equimolal ionic strength.[39] For this reason when calculating metal complexation constants equimolal solutions were compared. The constants presented in Table 3.9 are given for the background salt concentration being 3*M* or 3.44*m*. In all cases the assumption was made that the tetraethylammonium ion does not interact significantly with the ligand.

Table 3.9: Complexation constants calculated for the ligands succinate (SA) and propionate (PA) at 25°C and in various concentrations of the binding cation as background medium. Et_4NBr is taken as the reference medium.

Ligand	r	salt	cation	log K_{11r} equimolal 3.44*m*	log K_{11r} equimolal 3*M*
propionate	0	$NaClO_4$	Na^+	-0.910	-0.958
		$NaNO_3$	Na^+	-0.397	-0.414
		KNO_3	K^+	-0.485	-0.485
		NH_4NO_3	NH_4^+	-0.168	-0.164
		$Ca(NO_3)_2$	Ca^{++}	0.703	0.676
succinate	0	$NaClO_4$	Na^+	-0.156	-0.142
		$NaNO_3$	Na^+	0.333	0.315
		KNO_3	K^+	0.171	0.171
		NH_4NO_3	NH_4^+	0.505	0.528
		$Ca(NO_3)_2$	Ca^{++}	1.900	1.814
succinate	1	$NaClO_4$	Na^+	-0.579	-0.570
		$NaNO_3$	Na^+	-0.212	-0.221
		KNO_3	K^+	-0.294	-0.294
		NH_4NO_3	NH_4^+	-0.119	-0.106
		$Ca(NO_3)_2$	Ca^{++}	0.805	0.770

Figure 3.14 shows the complexation constants for succinate calculated using this method. Literature values have been included in the plot for comparison. The literature values were calculated at an ionic strength of 0.25*M*, comparing the protonation constants in Et_4NI with those obtained in an equimolar solution of the binding cation. All the metal complexation constants calculated are lower than the literature values except for calcium. As these constants are calculated at a higher ionic strength, one would expect the values to be larger, but the reverse is found. Figure 3.11 shows that the protonation constant for propionate is larger in Et_4NI than in Et_4NBr because of the differences in the literature Pitzer coefficients. This is the main reason why the literature protonation constants are higher than the values determined.

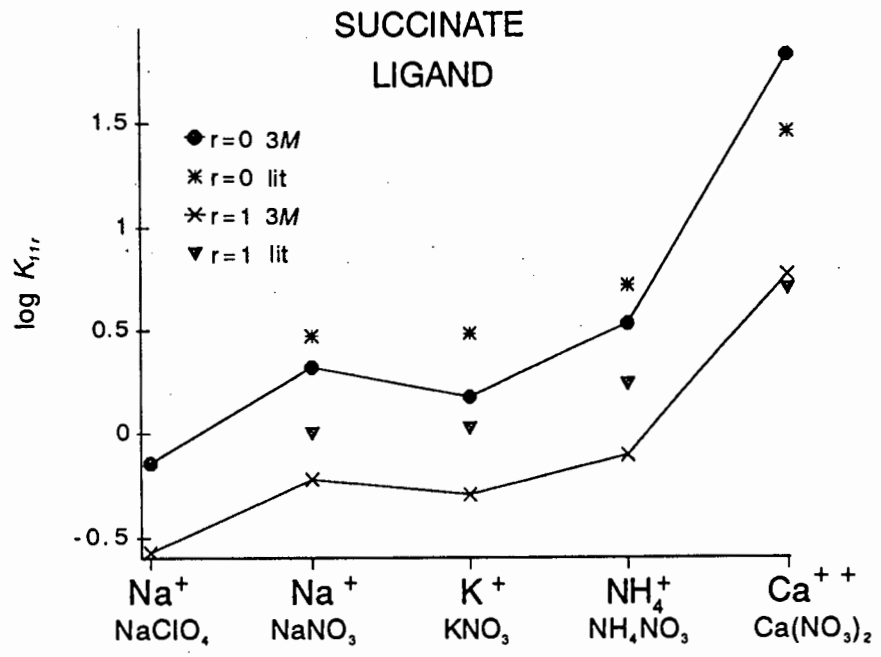

Figure 3.14

Plot of log K_{11r} for the ligand succinate (T=25°C, I=3M) calculated using the ion pairing method; literature values (T=25°C, I=0.25M) have been included in the plot.[8,9]

A major defect of this approach is that it does not account for the consistent difference in protonation constants measured in 3M $NaClO_4$ and 3M $NaNO_3$. The general failing of the ion pairing model above 1M has been attributed to the requirement of ion pairing constants for all species in solution.[53] Without this large number of constants, the model fails to give reasonable estimates of activity coefficients for concentrated electrolyte solutions. This failing has also been attributed to the use of activity coefficients which depend only on ionic strength.[69] It is an experimental fact that above an ionic strength of 1M, γ depends on the relative concentrations of the major solutes in solution.[41,51]

However, the ion pairing model is still favoured by many authors. The deviations in activity coefficients at high ionic strengths are accounted for by adding the formation constants for electrolyte ion pairs, in an iterative process. There is growing physical evidence of electrolyte ion pairing, demonstrated by sound attenuation measurements and Raman spectroscopy.[73] Raman spectra of KNO_3 solutions have given evidence of ion pairs and ion aggregates and at very high concentrations even solutions of NH_4NO_3 have showed anion-cation interactions.[74] At high ionic strengths, large corrections for all possible equilibria in solution have to be applied iteratively

to take into account ion pairing, and the consequent changes in the effective ionic strength. In many cases the constants needed are very difficult to measure, and very few reliable values are available in the literature. On the other hand, Pitzer's ion interaction approach includes interaction coefficients which take into account ion pairing. The approach is much simpler as no ionic strength corrections need to be applied due to ion pairing. Also the interaction coefficients in many media have been measured over a range of stoichiometric ionic strengths and not effective ionic strengths.

3.4.3.2 THE ION INTERACTION MODEL

The ion interaction approach, formulated by Pitzer, accounts for the changes in activity coefficients and hence protonation constants in going from one medium to another in terms of short range interionic forces that are specific to each solute. These forces are taken into account using interaction or virial coefficients. Several solutes are known to form ion pairs and this association is also fitted by these interaction coefficients, hence these virial coefficients take into account changes in activity coefficients as well as specific interactions.

The limitation of the ion interaction model arises when there is a strong association of ions, as in solutions containing weak acids or in which metal ligand complexation takes place. In these cases an association equilibrium should be recognized. According to Pitzer *et al.* there is no difficulty in combining an association equilibrium for particular ions with an ion interaction treatment for all other species. In fact the best representation of the properties of a mixture of solutes is given by a combination of interaction coefficients with one or more association equilibria.[41,69]

The problem is in deciding on a cut off point between using interaction coefficients and an association equilibrium, *i.e.* when is there specific binding. The lower limit for a stability constant, K_{min}, has been estimated to be between $10^{-8}M$ and $10^{-9}M$, however the method used to determine the stability constant puts more severe limitations on K_{min}.[19] Evidence of specific binding for alkali metal and ammonium ions with mono- and dicarboxylics has been reported by Daniele *et al.* in the range $0.02M \leq I \leq 1M$, however Millero has advocated that corrections

for sodium pairing should be avoided as they only add complexity to the model.[53]

Using the Pitzer approach, the association equilibrium for the ligand proton species and the ligand metal species are combined with an ion interaction treatment for all other species. The apparent protonation constant can then be calculated for any mixture of salts (equations 3.40-3.43). Figure 3.15 shows the change in the experimental protonation constant for succinic acid as the 3*M* ammonium nitrate ionic media is gradually replaced with other nitrate salts. The molal ionic strength remains constant throughout. It is evident that calcium has the greatest effect on the protonation constant, depressing the constant, while KNO_3 and $NaNO_3$ have a smaller effect but in the reverse direction, causing an increase in the constant.

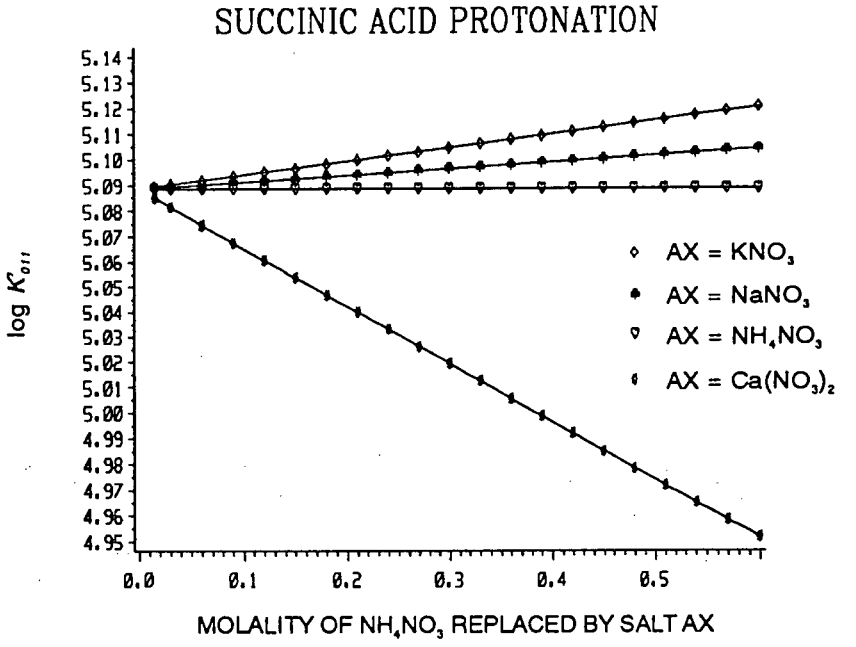

Figure 3.15

Plot of the change in the experimental protonation constant for the ligand succinate as the 3*M* NH_4NO_3 ionic media is gradually replaced by different nitrates; the molal ionic strength remained constant throughout.

The Pitzer equations which have been used up to now to correct stability constants to different ionic strengths, (equations 3.40-3.43) can be rewritten in the form of equation 3.52.

$$\ln K_{m,pqr} = \ln K^{0}_{m,pqr} + \Xi f' + f(AX) + f(AL) + f(HX) + f(MX) + f(J)$$

where

$$\begin{aligned}
f(AX) &= \Xi m_X^2 B'_{AX} + \sigma m_X^2 C_{AX} \\
f(AL) &= 2qm_X B_{AL} + \Xi m_L m_X B'_{AL} + \sigma m_X m_L C_{AL} + 2qm_X I_m C_{AL} \\
f(HX) &= 2rm_X B_{HX} + \Xi m_H m_X B'_{HX} + \sigma m_H m_X C_{HX} + 2rm_X I_m C_{HX} \\
f(MX) &= 2pm_X B_{MX} + \Xi m_M m_X B'_{MX} + \sigma m_X m_M C_{MX} + 2pm_X I_m C_{MX} \\
f(J) &= 2m_X B_J + \Xi m_S m_X B'_J + \sigma m_X m_S C_J - 2m_X I_m C_J
\end{aligned} \qquad \text{....3.52}$$

$\Xi f'$ is the general Debye-Hückel term (equation 3.32 and 3.41).

Equation 3.52 shows that the variation of activity coefficients between different ionic media, at the same molal ionic strength, is due to interactions between:

(i) *f(AL)* the cation of the background electrolyte and the deprotonated ligand,
(ii) *f(AX)* the cation and anion of the background electrolyte,
(iii) *f(HX)* the free proton and the anion of the background electrolyte,
(iv) *f(MX)* the metal and the anion of the background electrolyte
(v) *f(J)* the product and either the cation or anion of the background electrolyte.

In the case of a monoprotic ligand, cation/ligand binding constants can be obtained using the ion pairing approach by subtracting the apparent protonation constant obtained in one media from the protonation constant determined in another. In this case equation 3.50 can be rewritten in the natural logarithmic form:

$$\ln(1 + K_{110}[A]) = \ln K_{011} - \ln K'_{011} \qquad \text{....3.53}$$

By equating equation 3.52 with equation 3.53 we obtain equation 3.54 for a monoprotic acid where the protonated ligand is neutral.

$$\ln(1 + K_{m,110} m_A) = f(AX) - f(AX)' + f(AL) - f(AL)' + f(HX) - f(HX)' \qquad \text{....3.54}$$

In the ion pairing approach we assumed that the difference between protonation constants determined in two different media, at the same molal ionic strength, is due solely to interactions, between the electrolyte cation and the deprotonated ligand. According to the Pitzer approach as shown by equation 3.52, this is incorrect. The differences between the protonation constants obtained in different background media at the same molal ionic strength are due to the differences between the *f(AX)*, *f(HX)* and *f(AL)* terms. Hence the complexation constants calculated using this approach are larger or smaller than the "true" value.

An analysis of the contribution of the various terms to the activity coefficient quotient is given in Table 3.10. From this it appears that in the second protonation of succinate and in the protonation of propionate, the term that contributes the most to the change in activity coefficient is the proton-anion term. In the first protonation of succinate, the largest term is the cation-ligand term, which is to be expected as the ligand has a double negative charge. For this reason it appears that the simple ion pairing model used by Daniele *et al.* and used in section 3.4.3.1 is invalid. To overcome this problem the ion pairing and ion interaction methods have been combined to obtain ion pairing constants.

3.4.3.3 THE COMBINED APPROACH

For the study of emulsion stability, the speciation of Na^+, K^+, NH_4^+ and Ca^{++} with simple carboxylate ligands has to be known. To obtain the ligand speciation, complexation constants for all ligand species are needed. As the ion interaction model does not include complexation constants for alkali metals, a combination of both techniques has been used in an attempt to get improved values for the complexation constants.

An analysis of the anion-ligand terms, *f(AL)*, obtained for all electrolytes showed that the cation which interacts the least with the ligands is sodium (see Table 3.10). It is possible to correct the protonation constant in the absence of non specific interactions by subtracting all interactions except interactions between the ligand and the cation of the electrolyte from our observed protonation constants as shown in the equation below.

$$\ln K^{corr}_{m,01r} = \ln K'_{m,01r} - f(AX) - f(HX) \qquad \text{....3.55}$$

Table 3.10: The contribution of the various activity coefficient terms to the protonation constants as defined in equation 3.52. All protonation constants calculated are in a medium of 3.44 mol kg^{-1} ionic strength of the background salt.

Ligand	Salt	*f(AX)*	*f(AL)*	*f(HX)*	*f(J)*	log $K_{m,011}^{corr}$
propionate	$NaClO_4$	-0.211	0.978	1.558	0	4.432
	$NaNO_3$	-0.136	0.978	1.065	0	4.432
	KNO_3	0.043	0.890	1.065	0	4.394
	NH_4NO_3	-0.081	0.583	1.065	0	4.261
	$Ca(NO_3)_2$	-0.261	0.458	0.706	0	4.207
	Et_4NBr	0.466	0.137	1.760	0	4.067
succinate	$NaClO_4$	-0.406	2.693	1.553	-0.626	4.825
	$NaNO_3$	-0.262	2.693	1.062	-0.626	4.825
	KNO_3	0.007	2.526	1.062	-0.557	4.782
	NH_4NO_3	-0.160	2.131	1.062	-0.413	4.674
	$Ca(NO_3)_2$	-0.485	1.444	0.707	-0.155	4.489
	Et_4NBr	0.744	1.044	1.756	-0.045	4.361
H Succinate	$NaClO_4$	-0.211	0.627	1.557	0	3.621
	$NaNO_3$	-0.136	0.627	1.065	0	3.621
	KNO_3	0.043	0.558	1.065	0	3.591
	NH_4NO_3	-0.080	0.413	1.065	0	3.528
	$Ca(NO_3)_2$	-0.261	0.155	0.707	0	3.416
	Et_4NBr	0.466	0.045	1.760	0	3.368

For a monoprotic acid the differences between the corrected protonation constants in the different media should now only be due to the interaction between the cation of the background electrolyte and the deprotonated ligand (equation 3.56) *i.e.* the assumption made by Daniele *et al.*

$$\ln(1 + K_{m,110} m_A) = \ln K_{011}^{corr} - \ln K'^{corr}_{011} = f(AL) - f(AL)' \qquad \text{....3.56}$$

Using the corrected protonation constants and assuming only non specific interactions for Na^+, the weak metal ligand binding can be calculated as before (equations 3.50, 3.51 and 3.55).

Using this method, we have succeeded in separating out the activity coefficient variations due to interactions between the cation of the salt and the carboxylic ligand from the activity coefficient variations due to interactions between other solutes in solution. The *f(AL)* terms and the complexation constants calculated using this approach are given in Table 3.11 and plotted in Figure 3.16.

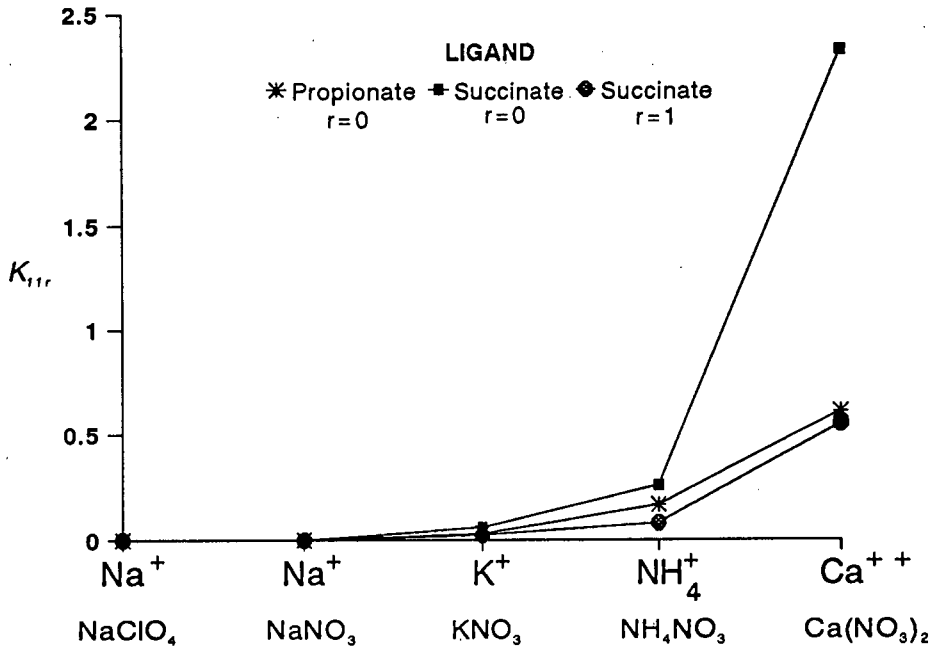

Figure 3.16

Comparison of metal complexation constants calculated at 3*M* ionic strength using the combined approach

Using the same Pitzer parameters, the protonation constants for both ligands were calculated at an ionic strength of 1 molal in the various salts. These constants with the contributions of the various activity coefficient terms are given in Table 3.12. By comparing the *HX* terms we can see the large effect the different cations have on the activity of the proton. The protonation constants in Et_4NI are the highest and the predominant cause of this is the large proton term and not weak binding of the Et_4N^+ species with the different cations, as assumed by Daniele *et al.*[8,71]

Many potentiometric workers have used 3*M* $NaClO_4$ as a standard background electrolyte in which to determine stability constants.[54,55] The assumption is made that this background salt complexes the least with the ligands being studied. The data in Table 3.12 confirm that in this case their assumptions are true and in fact the cation Na^+ is preferable to the cation Et_4N^+ as it binds less.

Table 3.11: Complexation constants calculated using our combined approach for the ligands succinate (SA) and propionate (PA) at 25°C and in various concentrations of the binding cation as background medium.

Ligand	r	cation	*f(AL)* 3.44*m*	K_{11}, 3.44*m*	K_{11}, 3*M*
propionate	0	Na^+	0.978	0	0
		K^+	0.890	0.031	0.031
		NH_4^+	0.583	0.164	0.166
		Ca^{++}	0.459	0.625	0.609
succinate	0	Na^+	2.703	0	0
		K^+	2.535	0.061	0.061
		NH_4^+	2.140	0.257	0.258
		Ca^{++}	1.446	2.281	2.329
succinate	1	Na^+	0.627	0	0
		K^+	0.559	0.024	0.024
		NH_4^+	0.414	0.081	0.081
		Ca^{++}	0.155	0.556	0.548

Table 3.12: The contribution of the various activity coefficient terms to the protonation constants as defined in equation 3.52. All protonation constants calculated are in a medium of 1 mol kg^{-1} ionic strength of the background salt.

Ligand	Salt	*f(AX)*	*f(AL)*	*f(HX)*	*f(J)*	log $K_{m,011}$	log $K_{m,011}^{corr}$
propionate	$NaClO_4$	-0.090	0.383	0.531	0	4.624	4.432
	$NaNO_3$	-0.058	0.383	0.415	0	4.587	4.432
	KNO_3	-0.009	0.352	0.415	0	4.595	4.419
	NH_4NO_3	-0.036	0.242	0.415	0	4.536	4.371
	$Ca(NO_3)_2$	-0.104	0.222	0.276	0	4.437	4.362
	Et_4NBr	0.143	0.080	0.612	0	4.628	4.300
	Et_4NI	0.226	0.080	0.706	0	4.705	4.300
succinate	$NaClO_4$	-0.179	1.188	0.530	-0.258	5.000	4.847
	$NaNO_3$	-0.115	1.188	0.414	-0.258	4.977	4.847
	KNO_3	-0.025	1.122	0.414	-0.234	4.998	4.829
	NH_4NO_3	-0.072	0.987	0.414	-0.196	4.936	4.787
	$Ca(NO_3)_2$	-0.206	0.483	0.276	-0.104	4.641	4.610
	Et_4NBr	0.269	0.537	0.611	-0.045	5.039	4.657
	Et_4NI	0.409	0.537	0.705	-0.045	5.141	4.657
H Succinate	$NaClO_4$	-0.090	0.259	0.531	0	3.911	3.719
	$NaNO_3$	-0.058	0.259	0.415	0	3.874	3.719
	KNO_3	-0.009	0.234	0.415	0	3.885	3.708
	NH_4NO_3	-0.036	0.196	0.415	0	3.856	3.692
	$Ca(NO_3)_2$	-0.104	0.104	0.277	0	3.726	3.651
	Et_4NBr	0.143	0.045	0.612	0	3.954	3.627
	Et_4NI	0.226	0.045	0.706	0	4.031	3.627

3.4.4 COMPLEXATION CONSTANTS FROM NMR

The difficulty of determining stability constants at high ionic strength, as outlined in the previous section, is to convert them from thermodynamic to stoichiometric stability constants *i.e.* to separate specific binding from activity coefficient variations. This problem is circumvented by using NMR which responds to the concentration of a species in solution rather than its activity. In NMR spectroscopy, under conditions of fast chemical exchange, the chemical shift, δ^j, for a particular observable nucleus j is the average of the chemical shifts of that nucleus in the various species present, δ^j_i, weighted by their fractional population.[75]

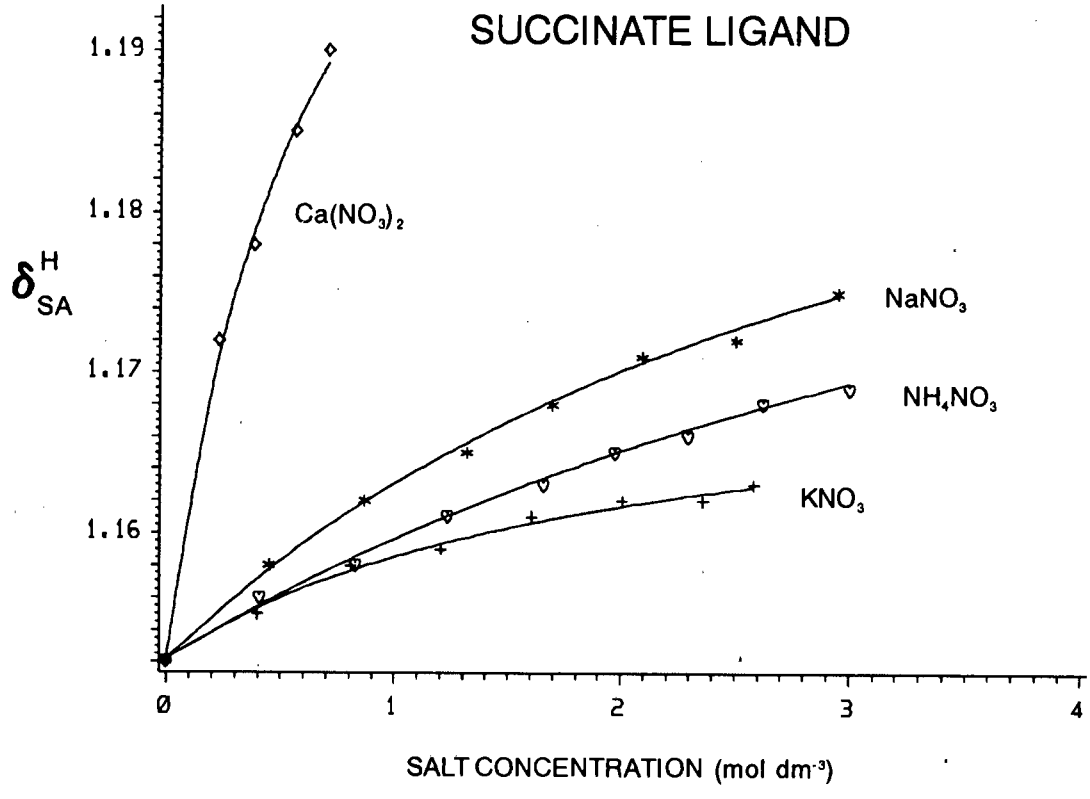

Figure 3.17

Plot of δ^H_{SA} versus MNO_3 addition at pD = 8.0; where δ^H_{SA} is the chemical shift of the equivalent protons of succinate relative to the methyl protons of the internal reference t-BuOH. The symbols represent experimental points and the solid line the calculated function.

Figure 3.17 shows the results of a proton NMR titration curve for succinic acid in D_2O at various background electrolyte concentrations and at a pD value of 8. At this pD, the ligand is fully

deprotonated. As the concentrations of the salts are increased, so the methylene protons are preferentially shifted downfield with respect to the protons of the internal reference. This is a clear indication that there is specific metal ligand binding between the cation and the carboxyl group of the acid. The cation binding to the carboxylate group would withdraw electron density causing relative deshielding and downfield shift of the methylene protons as the salt concentration is increased.

The effect this equilibria has on the chemical shift of the methylene protons of the ligand can be represented by the following equations:

$$\delta_{obs} = P_L\delta_L + P_{ML}\delta_{ML} + P_{NaL}\delta_{NaL} \qquad \text{....3.57}$$

$$\delta_{obs} = \frac{\delta_L + K_{ML}[M]\delta_{ML} + K_{NaL}[Na]\delta_{NaL}}{K_{ML}[M] + K_{NaL}[Na] + 1} \qquad \text{....3.58}$$

where P_L is the mole fraction of free ligand, and the sodium term was added to account for the initial addition of NaOH when adjusting the pH.

It is possible to calculate the strength of this association by performing a least squares fit of the data and refining for the parameters δ_L, δ_{ML}, δ_{NaL}, K_{ML} and K_{NaL}. In Figure 3.17 the chemical shift data are shown as symbols for succinate with the various salts and the least squares fit of the data calculated using equation 3.58 is shown as a solid line. The refined parameters for propionate and succinate are given in Table 3.13. The addition of $NaClO_4$ to succinate solution did not cause any significant shift, and hence no complexation constant could be obtained.

Figure 3.18 shows a proton NMR curve for propionic acid in H_2O. This shows that tetraethylammonium bromide has an unusual effect on the relative chemical shifts of the propionate ligand. Instead of shifting the methylene protons downfield, an upfield shift is seen. Possible causes for this shift could be a hydrophobic interaction between the tetraethylammonium ion and the methyl protons of propionate. This would cause the methyl protons to shift with respect to the methylene protons. Another possibility is an effect due to changes in hydration brought about by the decrease in the concentration of water. At a molarity of 3 mol dm^{-3}

Et_4NBr, there are 9 water molecules for every salt formula unit. However changes in hydration should not be occurring at low ionic strengths so this effect does not explain the shift observed.

As complexation constants vary with ionic strength, the values obtained using this method can only be taken as an average value over the ionic strength range measured. This is shown by the large standard deviations in the values obtained. Because of the small changes in chemical shift, NMR is inherently an insensitive method of measuring equilibrium constants and the values obtained should not be quoted with confidence, however it does give us evidence of specific metal ligand binding which is not always possible to obtain using potentiometric techniques.

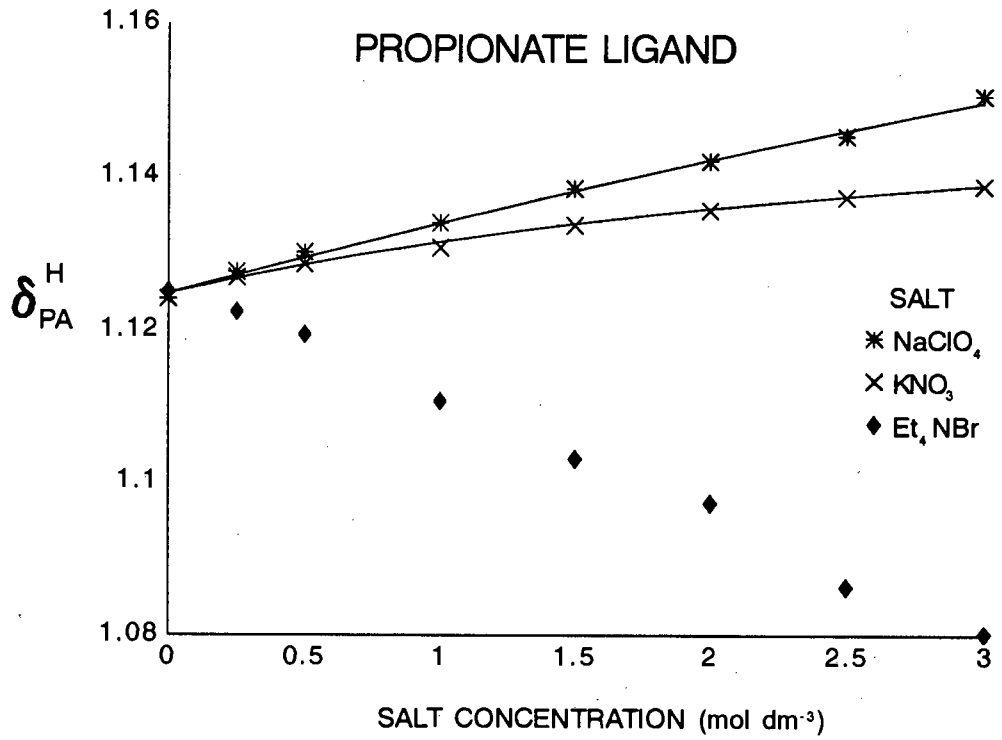

Figure 3.18

Plot of δ^{H}_{PA} versus addition of salt at pH = 9.0; where δ^{H}_{PA} is the chemical shift of the methylene protons of propionate relative to the methyl protons of propionate. The symbols represent experimental points and the solid line , the calculated function.

Table 3.13: Complexation constants for the ligands succinate (pD = 9.0, [NaOH]= 0.098) and propionate (pD = 8.0, [NaOH] = 0.088) measured at 25°C and varying concentrations of background electrolyte; σ is the standard deviation in log K_{110}.

L	M	[electrolyte]	reference	δ_L	δ_{ML}	log K_{110}	σ	solvent
PA	Na^+	0 - 3.0 *M* $NaClO_4$	PA CH_3	1.1238	1.334	-1.34	0.40	H_2O
	Na^+	0 - 2.7 *M* $NaNO_3$	PA CH_3	1.1252	1.435	-1.66	0.53	D_2O
	NH_4^+	0 - 3.6 *M* NH_4NO_3	PA CH_3	1.1252	1.270	-1.19	0.22	D_2O
	K^+	0 - 2.0 *M* KNO_3	PA CH_3	1.1252	1.160	-0.81	0.21	D_2O
	Ca^{++}	0 - 0.8 *M* $Ca(NO_3)_2$	PA CH_3	1.1252	1.207	-0.20	0.23	D_2O
SA	Na^+	0 - 3.0 *M* $NaClO_4$	t-BuOH	1.1539	-	-	-	H_2O
	Na^+	0 - 2.7 *M* $NaNO_3$	t-BuOH	1.1509	1.202	-0.55	0.08	D_2O
	NH_4^+	0 - 3.6 *M* NH_4NO_3	t-BuOH	1.1509	1.224	-0.91	0.25	D_2O
	K^+	0 - 2.0 *M* KNO_3	t-BuOH	1.1539	1.173	-0.39	0.18	H_2O
	Ca^{++}	0 - 0.8 *M* $Ca(NO_3)_2$	t-BuOH	1.1509	1.218	0.26	0.07	D_2O

3.5 DISCUSSION

3.5.1 PITZER'S IONIC STRENGTH CORRECTION METHOD

In recent years chemical equilibrium modelling has developed from an empirical qualitative tool to a sophisticated quantitative tool in the armoury of chemists.[1,3,76] Simultaneous with the development of computer modelling, has grown the realization of chemical speciation as being fundamental to many, if not all, biochemical, and industrial reactions.[4,77] Thus the toxicity of mercury is dependent on its chemical speciation, dimethyl mercury being highly toxic, but mercury in a gold/mercury amalgam being non-toxic.

Fundamental to equilibrium modelling is the availability of a suitable database containing thermodynamic data for all the possible reactions occurring in the model. Several such databases have been constructed.[2,27] However, in order to use these databases, it is necessary to convert the data to the conditions of temperature, pressure and ionic strength applicable to the model. Many attempts have been made to convert equilibrium constants applicable at one ionic strength

to another. Most of these methods are based on the Debye-Hückel equation which only shows good accuracy up to 0.1 mol dm^{-3}. At higher ionic strength it is necessary to add terms for short range interionic forces that are specific to each solute. This is the approach of Pitzer.[41] Because of the large number of virial coefficients needed to evaluate the Pitzer equations this approach has not been generally implemented in equilibrium models even though it works well up to an ionic strength of 6 mol dm^{-3}.

Under the conditions applicable to most simulation models it is possible to simplify the Pitzer equations, which are then easily built into an equilibrium model. In this work an easy method for converting equilibrium data from low to high ionic strength and from one background electrolyte to another is presented. The accuracy of this approach has been evaluated using data for the protonation of ammonia, acetate, propionate and succinate. We have shown that, under the conditions normally used to measure equilibrium constants, that is high background electrolyte concentration relative to reacting species, a simplified Pitzer approach can be used. Using this simplified approach unknown $\beta^{(0)}$ and $\beta^{(1)}$ parameters can be estimated from equilibrium measurements at high ionic strength and then used to predict reliably, equilibrium constants under different modelling conditions. This method should greatly enhance the applicability of chemical equilibrium models.

3.5.2 EVALUATION OF COMPLEXATION CONSTANTS

Calcium, potassium and sodium ions are all commonly present in biological systems, in sea water, in constant ionic media, or when added in a reagent. These ions are major metals in the body and are essential for human life and therefore the study of their chemical speciation should be of great importance.[78] Ammonium ions are also found in large amounts in some biological fluids, such as urine. In biological fluids the formation of weak complexes between alkali or alkali-earth metal ions and organic ligands is highly probable because of the high concentrations of these ions in solution. In fact, many ligands are known to form weak complexes with alkali metal ions, but because of their weak binding they are often ignored.[12]

Table 3.15 lists the complexation constants calculated for succinate and propionate with the cations calcium, ammonium, potassium and sodium. The various techniques used to determine these constants have been discussed previously. For ease of comparison the data points are plotted in figures 3.19 and 3.20 and a description of the methods used in calculating the data are given in Table 3.14.

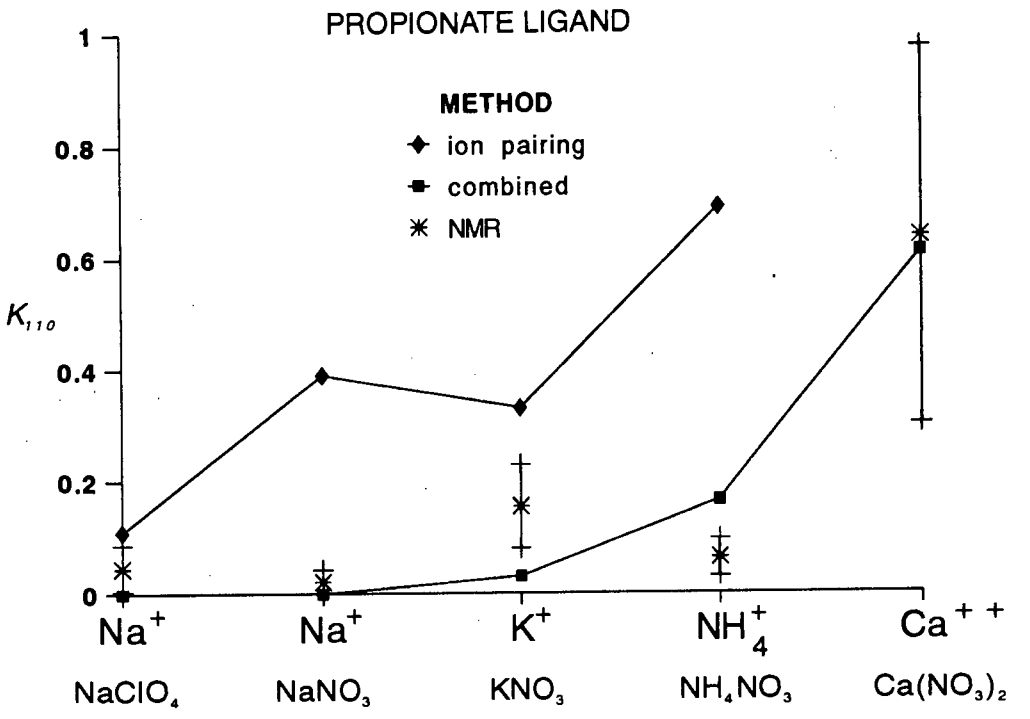

Figure 3.19

Plot of K_{110} for the ligand propionate and various cations, comparing the different values obtained using different techniques.

Comparing the data presented in figures 3.19 and 3.20, it can be seen that the complexation constants obtained using NMR techniques are in the same range as those obtained using the combined method. There are two major differences between these two methods. In the NMR method the ionic strength varies from $0M$ to $3M$, while in the combined method the ionic strength is fixed at $3M$. As a result of this difference one would expect the NMR constants to be lower than those determined using the combined method. The second difference is that in the combined method the complexation constants were calculated with respect to sodium binding in the absence of a suitable reference, whereas the NMR constants are absolute values. This difference should result in the NMR constants being larger than those obtained using the

combined method. As a result of these opposing trends, the close range of the constants obtained is gratifying and serves to confirm the validity of the results.

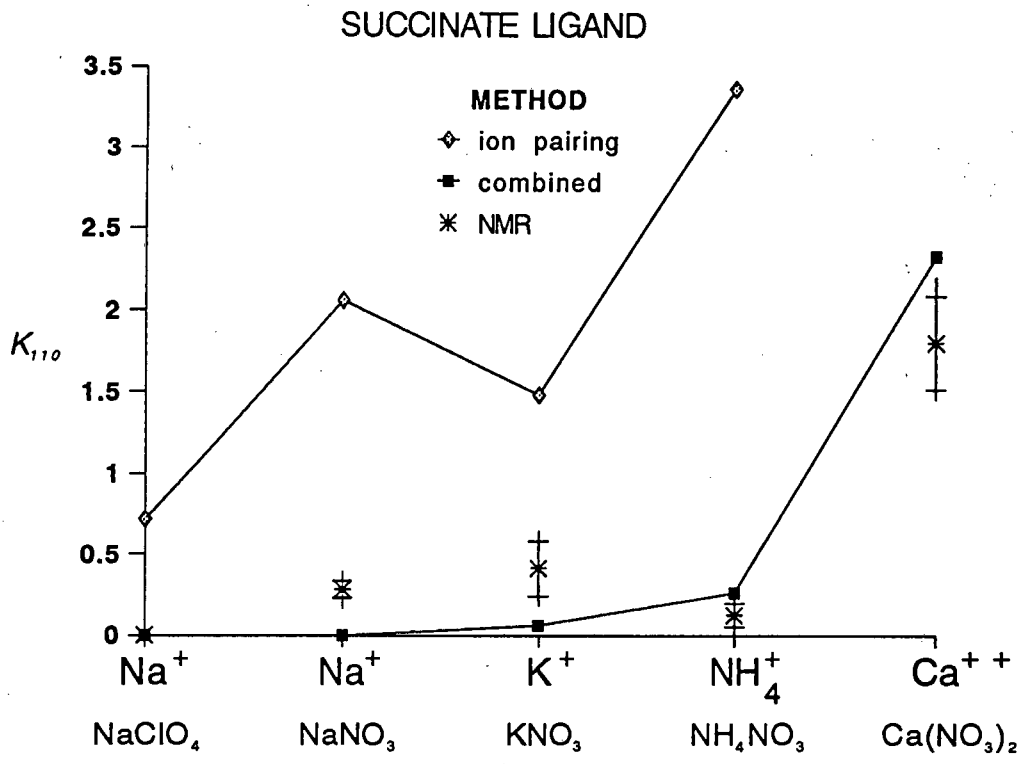

Figure 3.20

Plot of K_{110} for the ligand succinate and various cations, comparing the different values obtained using different techniques.

The constants obtained using the ion pairing method are much larger than those obtained using NMR. Also, there is a large discrepancy between the sodium binding constants obtained in $NaClO_4$ and $NaNO_3$. These differences can't be due solely to ionic strength variations therefore the constants obtained are larger than the "true" value (see discussion section 3.4.3.2).

On analyzing the trends of the complexation constants obtained using the NMR and combined approach, the complexing properties of Na^+ and K^+ appear to be very similar, NH_4^+ forms more stable compounds than Na^+ and K^+ and the Ca^{++} complexes are significantly more stable than those formed with the other three cations.

This trend is the same as that obtained by Daniele *et al.* for a large number of mono- and dicarboxylate ligands in the ionic strength range 0 to 1*M*. They noted that for alkali metal complexation with these ligands, the stability of the metal carboxylates is quite independent of

the ligand.[8] Ring formation was also found to be absent in succinate. This study also highlighted the fact that more work needs to be done on tetraalkylammonium ions, both NMR results and potentiometric analysis has revealed unusual binding effects attributed to these ions.

Table 3.14: Index for methods used in calculating the complexation constants.

Method Title	Reference	Ionic Strength	Section Index	Table Index
ion pairing method	Et_4NBr	3*M*	3.4.3.1	3.9
combined method	Na^+	3*M*	3.4.3.3	3.11
NMR method	absolute	0 - 3*M*	3.4.4	3.13

Table 3.15: Complexation constants calculated for the ligands succinate (SA) and propionate (PA) at 25°C.

constant	salt	cation	Ion Pairing Method	Combined Method	NMR Method
K_{110} (PA)	$NaClO_4$	Na^+	0.110	0	0.05
	$NaNO_3$	Na^+	0.386	0	0.02
	KNO_3	K^+	0.327	0.031	0.15
	NH_4NO_3	NH_4^+	0.685	0.166	0.06
	$Ca(NO_3)_2$	Ca^{2+}	4.741	0.609	0.64
K_{110} (SA)	$NaClO_4$	Na^+	0.721	0	0
	$NaNO_3$	Na^+	2.063	0	0.28
	KNO_3	K^+	1.482	0.061	0.41
	NH_4NO_3	NH_4^+	3.373	0.258	0.12
	$Ca(NO_3)_2$	Ca^{2+}	65.088	2.329	1.80
K_{111} (SA)	$NaClO_4$	Na^+	0.269	0	
	$NaNO_3$	Na^+	0.602	0	
	KNO_3	K^+	0.508	0.024	
	NH_4NO_3	NH_4^+	0.783	0.081	
	$Ca(NO_3)_2$	Ca^{2+}	5.887	0.548	

3.5.3 SPECIATION MODELLING

Very little is known about the interaction of surfactants used in the explosives industry with metal ions and the consequent effect on the emulsion stability. It is known that many of the surfactants show instability with pH change or in the presence of calcium nitrate. Some of the nonionic surfactants used are carboxylic acid derivatives which undergo hydrolysis in the aqueous ammonium nitrate environment, partially converting back to dicarboxylic acid forms. The speciation of propionate and succinate are therefore good models for the speciation of typical anionic or hydrolysed nonionic surfactants used in the explosive industry.

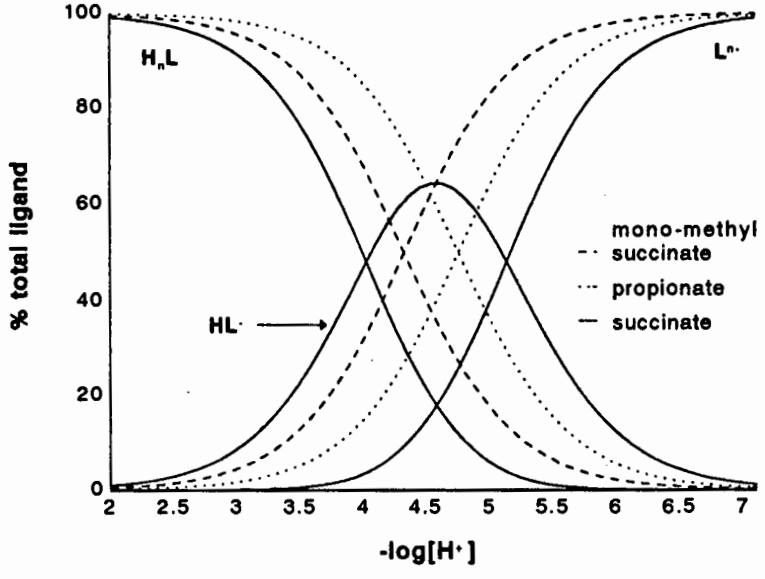

Figure 3.21

The speciation of propionate, succinate and mono-methyl succinate plotted over the pH range 2 to 7 in 3*M* NH_4NO_3. Each species is plotted as a percentage of the total ligand concentration; where n is the number of dissociable protons on the ligand (2 for succinate and 1 for propionate and mono-methyl succinate).

If, as in the ion interaction approach, we assume that there is no specific binding between the carboxylate ligands and the background electrolyte cations, then the carboxylate speciation can be shown using the experimental protonation constants in the different media. Figure 3.21 shows the speciation of the three carboxylate ligands in 3*M* NH_4NO_3 as a function of pH. The effect that the nature of the different polar head groups has on the speciation is clearly shown. In the pH range 2 - 7 the charge of all carboxylate groups changes from neutral to minus one.

Similarly, Figure 3.22 shows how changing the background medium affects the speciation of succinic acid. In an emulsion formulation, these changes will effect the surface packing of the surfactant and may contribute to the observed pH and medium dependence of emulsion stability. These results explain why buffering of explosive emulsions over a narrow pH range is essential.

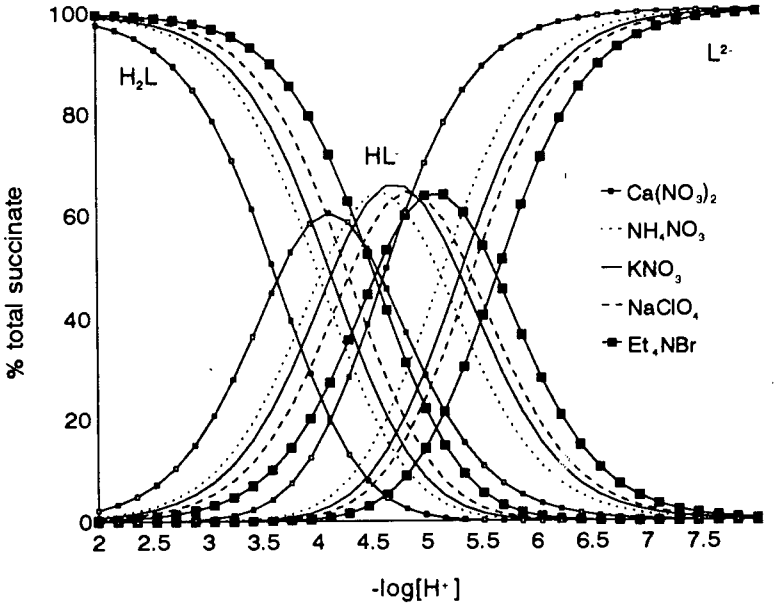

Figure 3.22

The speciation of succinate in various 3*M* background electrolytes over the pH range 2 to 8. Each species is plotted as a percentage of the total ligand concentration.

However, NMR evidence (section 3.4.4) has shown that there is specific binding between the cations of the background media and the carboxylate head groups. Using the stability constants calculated at 25°C using the combined approach (section 3.4.3.2), the speciation of a propionate solution was calculated as a function of pH (figures 3.23 to 3.25).

Figures 3.23 and 3.24 show the effect a 3.44*m* ionic strength media has upon propionate speciation. When the background salt is pure ammonium nitrate, at a pH of 7, 32 percent of the ligand is complexed to NH_4^+ (figure 3.23). If the ammonium nitrate salt media is replaced with calcium nitrate, at the same molal ionic strength and pH, then 40 percent of the propionate would be complexed (figure 3.24).

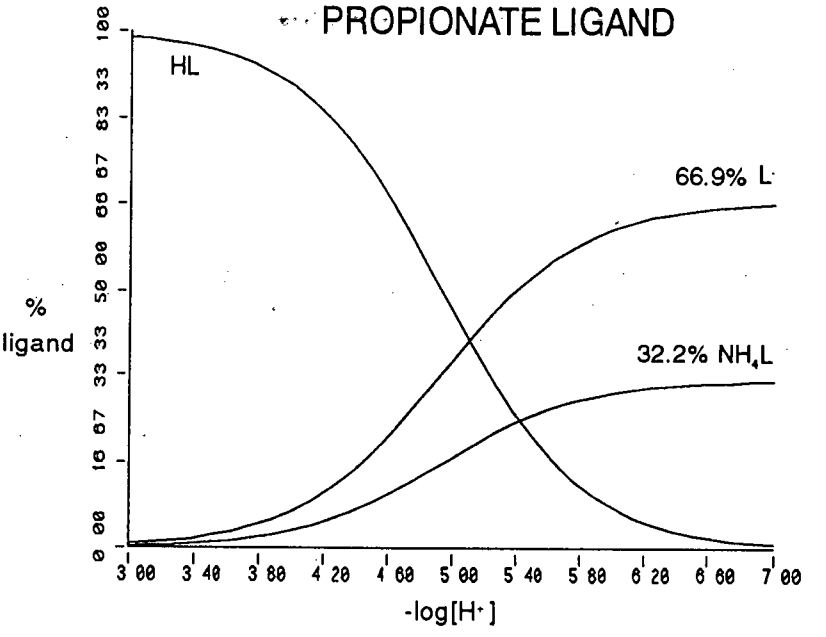

Figure 3.23

The speciation of propionate plotted over the pH range 3 to 7. Each species is plotted as a percentage over the total ligand concentration. The solution contained 0.001*m* ligand and 3.44*m* ammonium nitrate.

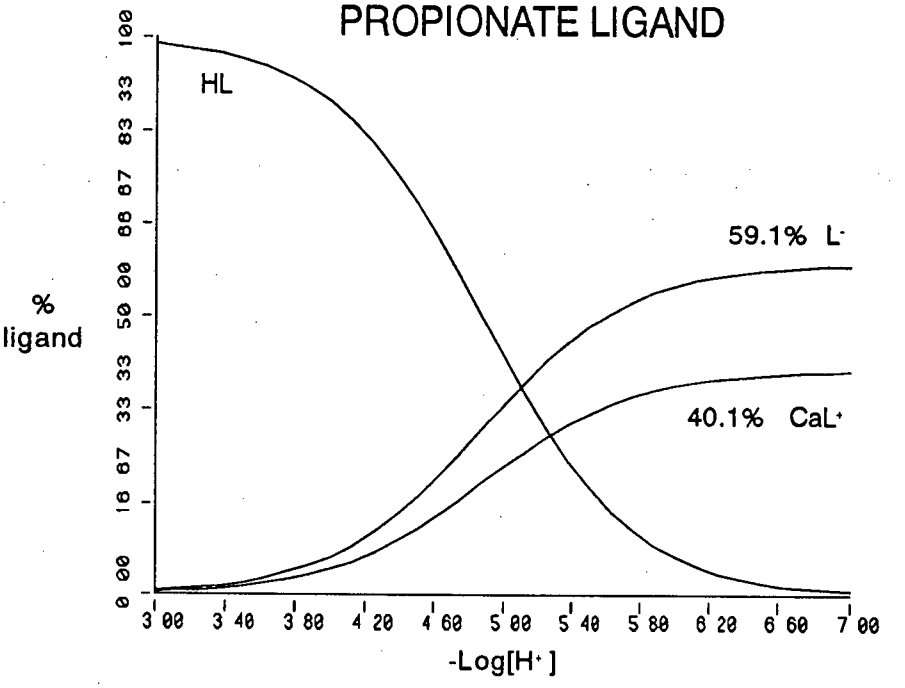

Figure 3.24

The speciation of propionate plotted over the pH range 3 to 7. Each species is plotted as a percentage over the total ligand concentration. The solution contained 0.001*m* ligand and 1.15*m* calcium nitrate.

A typical emulsion formulation contains predominantly ammonium nitrate, certain other salts, an organic phase and surfactant. The concentration of ammonium nitrate is far in excess of the concentration of the surfactant. Occasionally a small amount of calcium nitrate is added to the formulation. The presence of calcium has a destabilising influence on the emulsions and has been known to invert the emulsion type. The effect that a typical formulation of calcium and ammonium nitrate has on the speciation of propionate and succinate is shown in Figures 3.25 and 3.26 respectively. The relative amounts of ligand, ammonium and calcium have been calculated for a typical formulation and an ionic strength of 3.44 molal has been chosen. Although only 0.29 molal calcium nitrate is in the background salt the effect it has on the speciation is considerable. In the case of succinate, at any pH, the amount of ligand bound to calcium is comparable to the amount bound to ammonium, although the concentration of ammonium ions is approximately 9 times that of calcium. These curves also confirm experimental findings that the control of pH is critical in the formulation of an explosive emulsion containing anionic surfactants as the properties of L^- are different to those of LH.

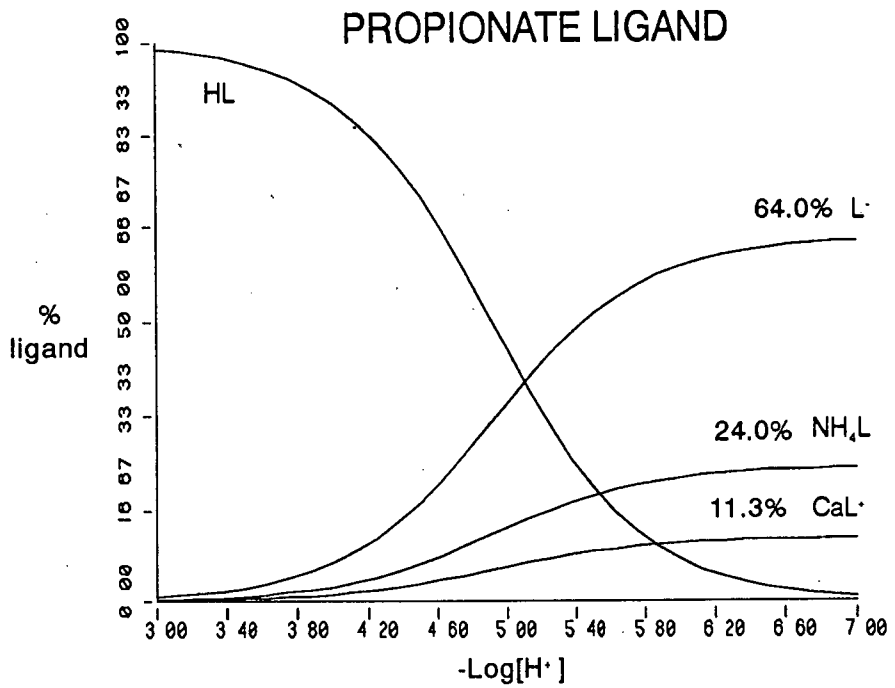

Figure 3.25

The speciation of propionate plotted over the pH range 3 to 7. Each species is plotted as a percentage over the total ligand concentration. The solution contained 0.001*m* ligand, 2.58*m* ammonium nitrate and 0.29*m* calcium nitrate.

The distribution constant values are plotted in figure 4.15 with two data points obtained from malvern experimental results (Table 4.4). The creaming results show that as the surfactant concentration increases, the average droplet size decreases and then gradually this effect levels off. This can be explained in terms of initial coalescence immediately after shearing while the emulsion flow is still turbulent. Droplets with less surfactant would coalesce more resulting in larger droplet sizes.

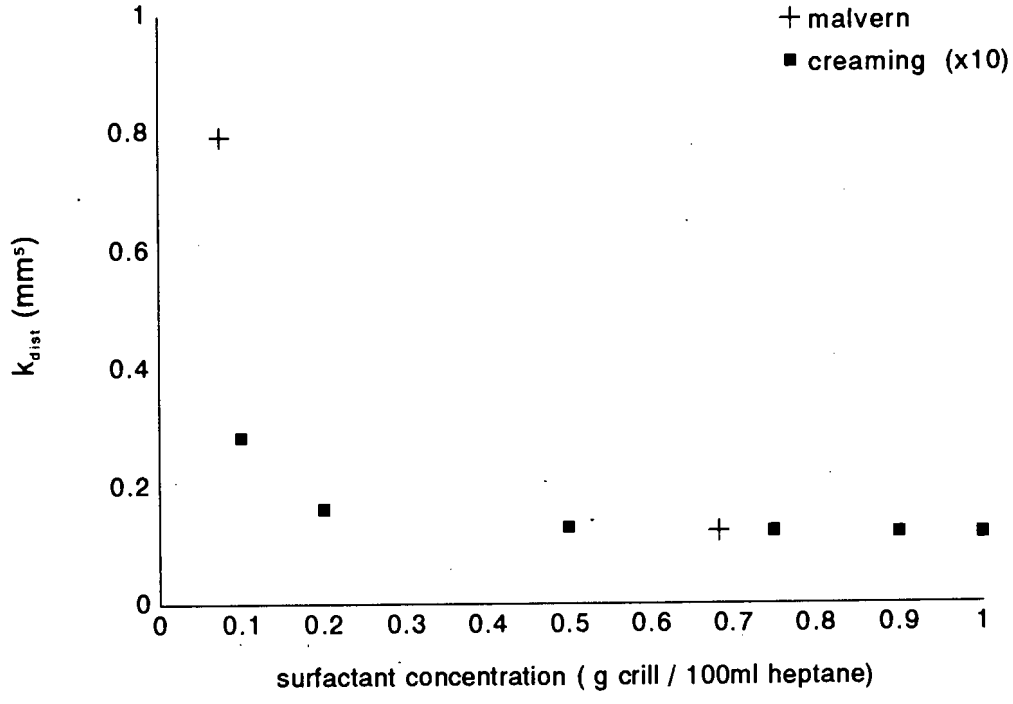

Figure 4.15

Plot of size distribution constants obtained from creaming rate and laser diffraction studies for a series of emulsions where the surfactant concentration was varied. The organic phase contained varying amounts of CRILL in heptane; the aqueous phase contained $5M$ NH_4NO_3 and the shearing time was 1 minute. V_T = 10ml; ϕ = 0.2.

Experimental results of Pons *et al.* have shown that the stability of some w/o emulsions increased and then decreased as the surfactant concentration increased.[28] Surfactants are known to protect droplets from initial coalescence which would experimentally translate as a decrease in droplet size with an increase in surfactant concentration. The decrease in stability with increased surfactant concentration can be due to two factors. Firstly, certain surfactants are known to promote clumping which would be observed as an increase in droplet size.[31] Secondly, when there is sufficient surfactant available to prevent initial coalescence, interfacial tension would be the factor limiting initial droplet size. As the surfactant

The final internal phase volume of the cream for all the emulsions tended to 74%, that of close packed spheres, irrespective of the surfactant concentration.

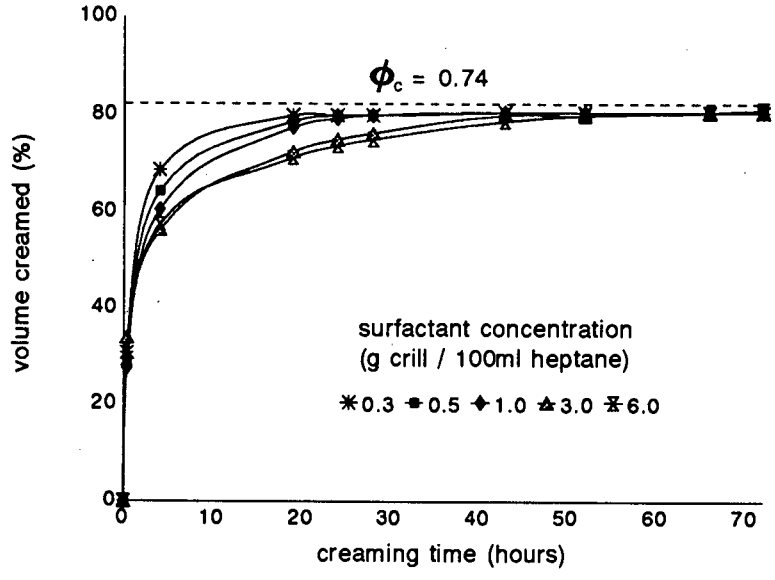

Figure 4.14

Plot of the change in the volume percent creamed with time for a series of emulsions where the concentration of the surfactant was varied. The organic phase contained varying amounts of CRILL in heptane, V_T = 12ml, ϕ = 1/3, the aqueous phase contained 1*M* NH_4NO_3 and the shearing time was 1 minute.

These trends can be explained in terms of micelle formation. Initially increasing the surfactant concentration should not change the density difference between the two phases or the viscosity of the heptane significantly. This is a reasonable assumption as the surfactant should partition itself between the two phases rather than in the one phase. Once the surfactant concentration is increased above the critical micelle concentration, micelles will form in the organic phase affecting both $\Delta\rho$ and η and hence k_{form}. As the surfactant concentration increases, the number of micelles will increase and the time at which the emulsion is no longer considered dilute would decrease thus decreasing the inflexion point in the curve. Micelles are known to form in aliphatic hydrocarbon solvents and solvents with low dielectric constants.[28-30] These changes are hard to determine experimentally and contribute to size distribution data not being obtained from initial creaming rates when the surfactant concentration is above 1g crill per 100ml heptane for this experimental system.

The initial creaming rate before the inflexion point is plotted in figure 4.13 for surfactant concentrations less than 1g crill 43 per 100ml n-heptane and figure 4.12 shows the change in initial creaming time for surfactant concentrations up to 5g crill 43 per 100ml n-heptane. As the surfactant concentration is increased, the initial creaming rate decreases and then at a set concentration it levels off. For this particular system it appears that above a surfactant concentration of 1g Crill per 100ml heptane an increase in surfactant concentration has little effect on the initial creaming rate. Figure 4.13 shows the data points with linear regression lines. From the slopes of these initial linear creaming rates, creaming constants and hence size distribution constants were obtained. The creaming constant values and their analysis to obtain size distribution data are given in Table 4.3. Once the surfactant concentration increased above 1g crill per 100ml heptane, the initial creaming rate was linear only in a small initial region thus preventing reliable creaming constant values from being obtained.

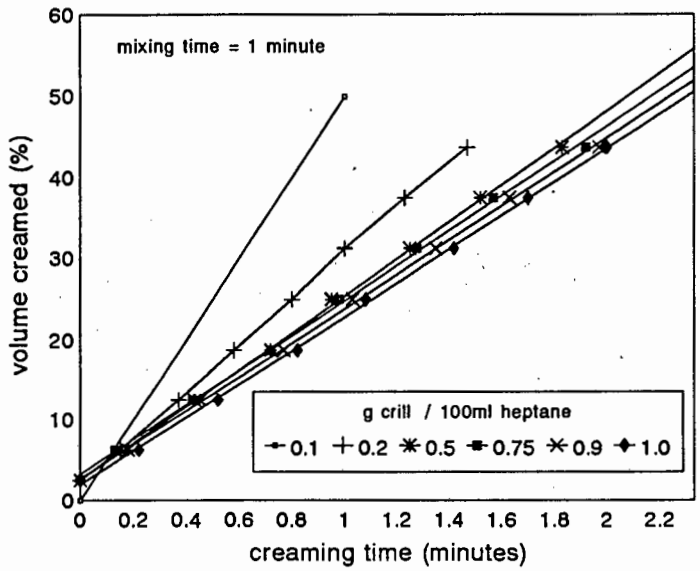

Figure 4.13

Plot of the change in the volume percent creamed with time for a series of emulsions where the concentration of the surfactant was varied. The organic phase contained varying amounts of CRILL in heptane, the aqueous phase contained *5M* NH_4NO_3 and the shearing time was 1 minute. V_T = 10ml; ϕ = 0.2.

Figure 4.14 shows the changes in the final cream volume and the inflexion point as the surfactant concentration increased. If the cream showed signs of breaking it was excluded from this data set. As the surfactant concentration is increased the inflexion point decreases.

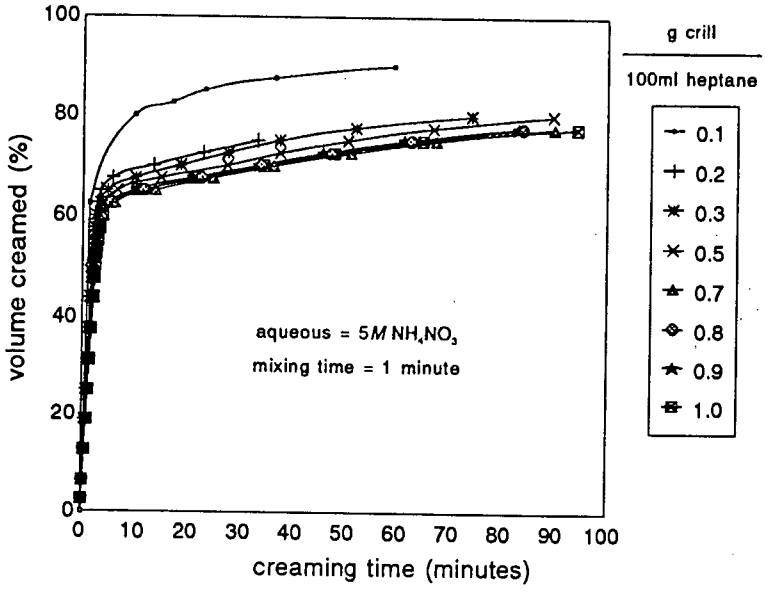

Figure 4.11

Plot of the change in the volume percent creamed with time for a series of emulsions where the concentration of the surfactant was varied. The organic phase contained varying amounts of CRILL in heptane, the aqueous phase contained $5M$ NH_4NO_3 and the shearing time was 1 minute. V_T = 10ml; ϕ = 0.2.

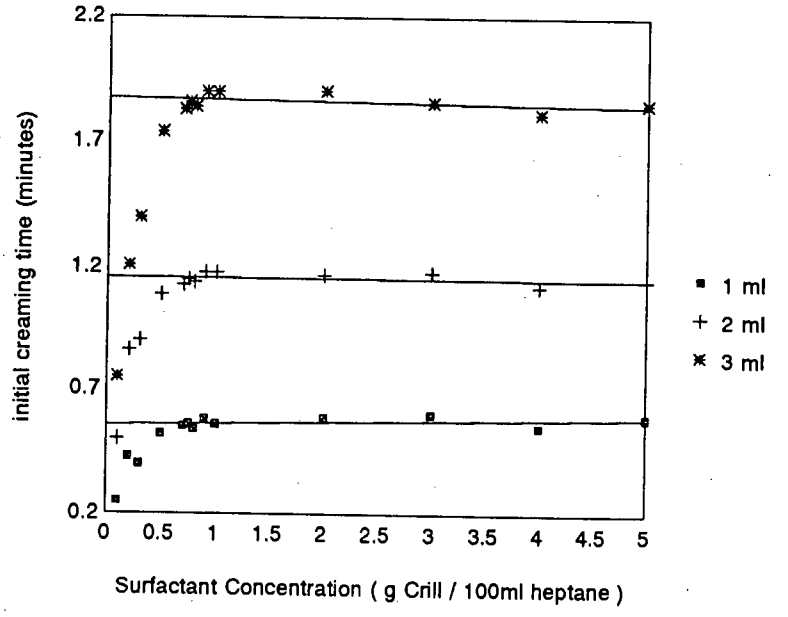

Figure 4.12

Plot of the change in time taken to cream to a set volume for a series of emulsions where the concentration of the surfactant was varied. The organic phase contained varying amounts of CRILL in heptane, the aqueous phase contained $5M$ NH_4NO_3 and the shearing time was 1 minute. V_T = 10ml; ϕ = 0.2.

Table 4.4 Size statistics obtained from particle sizing of emulsions using the Malvern 2600 particle sizer. Emulsions were prepared with crill 43 as the surfactant. ϕ = 0.2; V_T = 10ml. {[AN] represents mol dm^{-3} NH_4NO_3 and H represents n-heptane}

shear time (s)	surfactant concentration (g crill/100ml H)	[AN] (mol/dm^3)	n_D^{20}	log diff	D[3,2] (μm)	D[4,3] (μm)	R[5,3] (μm^2)	Span
5	0.7	1.00	1.343	4.781	13.24	16.12	80.32	1.25
10	0.7	1.00	1.343	4.762	11.73	13.92	60.89	1.00
10	0.7	1.00	1.343	4.121	11.33	13.21	50.81	0.97
30	0.7	1.00	1.343	3.073	6.61	7.91	19.73	1.25
50	0.7	1.00	1.343	2.947	5.00	5.67	9.43	0.93
60	0.7	1.00	1.343	2.417	5.15	5.63	8.76	0.79
120	0.7	1.00	1.343	3.061	4.66	4.98	6.72	0.66
190	0.7	1.00	1.343	2.736	3.85	4.11	4.65	0.63
250	0.7	1.00	1.343	2.492	2.82	3.50	3.77	1.25
60	0.7	0.00	1.333	3.451	5.23	6.16	10.75	0.93
60	0.7	0.45	1.338	2.585	4.86	5.47	8.70	0.88
60	0.7	1.00	1.343	2.417	5.15	5.63	8.76	0.79
60	0.7	1.34	1.346	2.677	4.84	5.31	7.94	0.77
60	0.7	10.74	1.424	3.101	3.96	4.94	7.36	1.25

4.4.3.1 SURFACTANT CONCENTRATION

A series of emulsions were prepared with the only variable being the surfactant concentration. The volume percent creamed was monitored against time (section 4.3.1) and plotted (figure 4.11). The plot indicates that as the surfactant concentration is increased there are changes in the initial creaming rate and the inflexion point of the curve. It should be noted that because of the low surfactant concentration, the emulsion which contained 0.1g crill per 100ml heptane showed signs of breaking in the cream.

Table 4.3 Creaming and size distribution constants obtained from creaming studies done on emulsions prepared with crill 43 as the surfactant. ϕ = 0.2; V_T = 10ml. {[AN] represents mol dm^{-3} NH_4NO_3; np represents the number of experimental points and H represents n-heptane}

shear time	surfactant concentration	[AN]	k_{cream}	np	section	$\Delta\rho$	k_{form}	k_{dist}
s	g crill/100ml H		s^{-1}			kg/m^3	$m^{-5}s^{-1}$	m^5
60	0.1	5	0.8333	2	4.4.3.1	466.5	2.946e+16	2.828e-17
60	0.2	5	0.4750	8	4.4.3.1	466.5	2.946e+16	1.612e-17
60	0.5	5	0.3800	8	4.4.3.1	466.5	2.946e+16	1.290e-17
60	0.75	5	0.3600	8	4.4.3.1	466.5	2.946e+16	1.222e-17
60	0.9	5	0.3517	8	4.4.3.1	466.5	2.946e+16	1.194e-17
60	1	5	0.3467	8	4.4.3.1	466.5	2.946e+16	1.177e-17
60	0.7	0	0.3517	6	4.4.3.2	315	1.989e+16	1.768e-17
60	0.7	0.45	0.3267	8	4.4.3.2	329	2.078e+16	1.572e-17
60	0.7	1.34	0.3050	8	4.4.3.2	357	2.255e+16	1.353e-17
60	0.7	2.69	0.3100	8	4.4.3.2	398	2.514e+16	1.233e-17
60	0.7	5.37	0.3650	8	4.4.3.2	477	3.013e+16	1.212e-17
60	0.7	10.74	0.5417	9	4.4.3.2	626	3.954e+16	1.370e-17
60	0.7	1	0.3117	7	4.4.3.4	346.1	2.186e+16	1.426e-17
60	0.7	1	0.3067	7	4.4.3.4	346.1	2.186e+16	1.403e-17
60	0.7	1	0.3117	7	4.4.3.4	346.1	2.186e+16	1.426e-17
60	0.7	1	0.2750	7	4.4.3.4	346.1	2.186e+16	1.258e-17
60	0.7	1	0.3467	7	4.4.3.4	346.1	2.186e+16	1.586e-17
60	0.7	1	0.2867	7	4.4.3.4	346.1	2.186e+16	1.311e-17
10	0.7	1	0.6217	10	4.4.3.3	346.1	2.186e+16	2.844e-17
30	0.7	1	0.3900	9	4.4.3.3	346.1	2.186e+16	1.784e-17
50	0.7	1	0.3183	9	4.4.3.3	346.1	2.186e+16	1.456e-17
60	0.7	1	0.3064	7	4.4.3.3	346.1	2.186e+16	1.402e-17
120	0.7	1	0.2683	8	4.4.3.3	346.1	2.186e+16	1.228e-17
250	0.7	1	0.2200	8	4.4.3.3	346.1	2.186e+16	1.006e-17

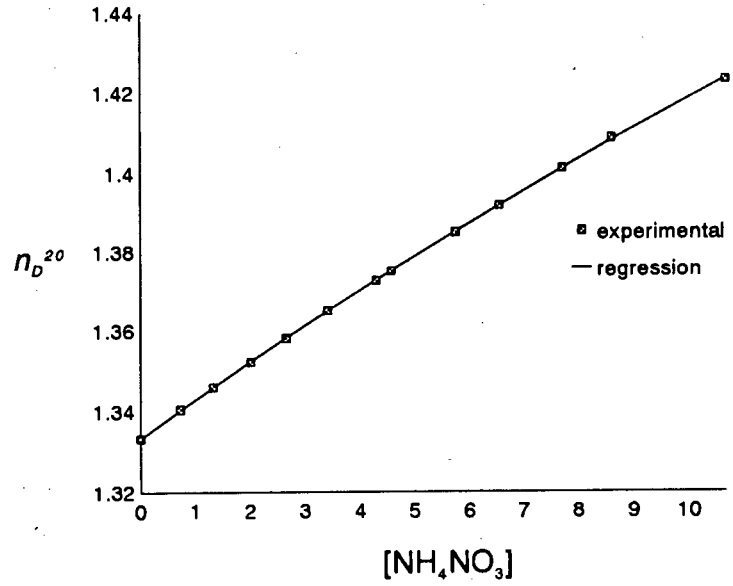

Figure 4.10

Plot of the index of refraction of aqueous ammonium nitrate solutions of various concentration (mol/dm^3). Values were determined at 20°C relative to air for sodium yellow.

4.4.3 EMULSION EXPERIMENTAL RESULTS

For all the emulsion systems studied, a non-ionic surfactant, Crill 43 (Croda Chemicals) was used. Crill 43 consists mainly of a complex mixture of mono-, di-, tri- and tetraesters of sorbitan. The effect that changing the following formulation variables had on the emulsion was studied experimentally.

1 the surfactant concentration

2 the salt concentration

3 the shearing time

4 the pH of the aqueous phase

The results obtained will be discussed in the above order in the following sections. For all systems the size distribution parameters calculated using initial creaming rates and malvern data are given in tables 4.3 and 4.4.

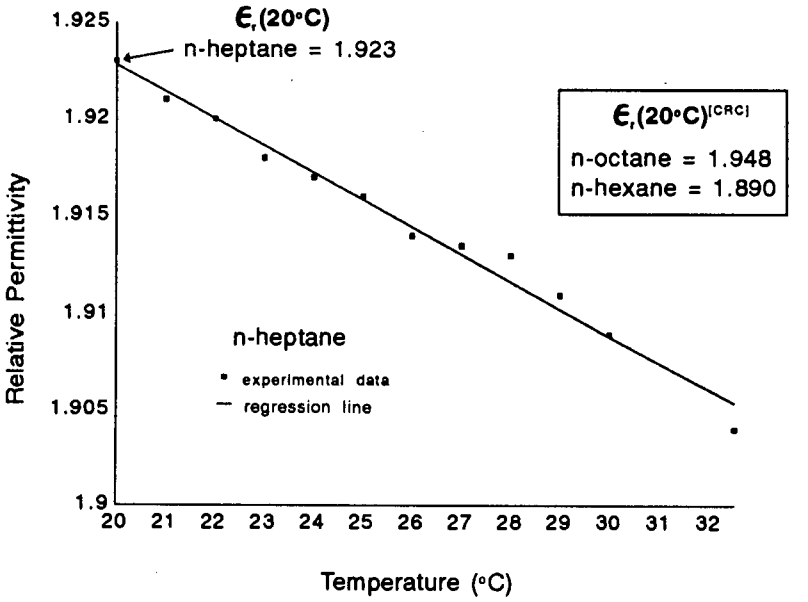

Figure 4.9

Plot of the change in the relative permittivity of n-heptane with temperature. The symbols represent experimental values and the curve a regression line (equation 4.19). The literature values for two n-alkanes are tabulated for comparison.

4.4.2 REFRACTIVE INDEX RESULTS

Refractive indices of both the internal and external phase of the emulsions were needed to convert Malvern light intensity data to droplet size distribution data. Figure 4.10 shows the refractive indices obtained for a series of ammonium nitrate solutions of varying concentration. Included in the plot is the regression line (equation 4.20) which was computed using non-linear regression. The experimental points show little spread, which translates into a small standard deviation in the regression line. This lends confidence to the results.

$$n_D^{20} = 1.3333(2) + 0.00970(8)[NH_4NO_3] - 0.000117(7)[NH_4NO_3]^2 \quad \text{....4.20}$$

where the value in brackets is the standard deviation in the last digit.

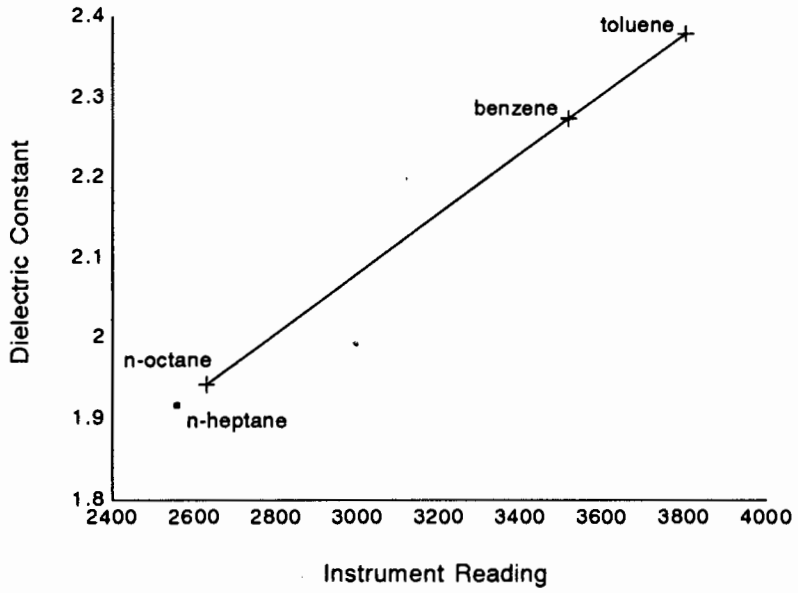

Figure 4.8

The calibration curve for the Dipolemeter.

4.4 DISCUSSION OF EXPERIMENTAL RESULTS

4.4.1 RELATIVE PERMITTIVITY RESULTS

Relative permittivity data for the organic phase of the emulsions studied was needed as input for the emulsion stability computer model. The dielectric constant, or relative permittivity is the capacitance of the solvent relative to the capacitance of the reference condenser in vacuum. Dielectric constants were determined for n-heptane over a temperature range relevant to the emulsion system. Figure 4.9 shows the experimental values obtained. Included in the plot is the regression line (equation 4.19) which was computed using linear regression. Shown in figure 4.9 are dielectric constants at 20°C for n-octane and n-hexane obtained from the literature.[27] The experimental value for n-heptane follows the correct trend with respect to the literature values for the two n-alkanes. Saturating the heptane with water did not result in a significant change in the dielectric constant.

$$\varepsilon_{r,(20-36°C)} = 1.9530(7) - 0.00149(4) \times TEMPERATURE(°C) \qquad \text{....4.19}$$

where the value in brackets is the standard deviation in the last digit.

particle size formed on the glass windows of the sample cell, seriously affecting the particle size results. To solve this problem, the glass windows were replaced by perspex windows. The optical quality of the perspex was found to be comparable with that of the glass.

4.3.5 PERMITTIVITY OF THE ORGANIC SOLVENT

The relative permittivity of the organic phase of the emulsions studied was needed as an input parameter in the emulsion stability computer model. As the literature did not contain sufficient data, experimental determinations were performed.

Relative permittivities or dielectric constants for the organic phase of the emulsions were determined using a Weilheim Dipolemeter type DM01 at 2MHz operating frequency with a DFL1 jacketed sample cell. The temperature was controlled by circulating water around the cell from a thermostatically controlled water bath. Between readings the cell was washed out with AR acetone and dried under nitrogen. Three readings were taken for each sample and the mean quoted.

The instrument was calibrated against solvents with known literature dielectric constants at 25°C (see Figure 4.8). Toluene (BDH AnalaR) and benzene (BDH AnalaR) were first distilled and then stored over sodium wire. n-Octane and n-heptane (Saarchem univAR 99%) were dried over sodium wire and gave one peak in gas chromatography. The calibration curve at 25°C for the instrument is given in equation 4.18 and shown in Figure 4.8.

$$\varepsilon_{r,25} = 0.963(1) + 0.000373(1) \times \text{INSTRUMENT READING} \quad \text{....4.18}$$

where the value in brackets is the standard deviation in the last digit.

the water circulating through the refractometer were thermostatically controlled at 20°C. The ammonium nitrate was dried in a vacuum oven for 60 hours at 65°C prior to preparation.

4.3.4 MALVERN EXPERIMENTAL

The Malvern 2600 particle sizer was set up with a static cell. A constant stirring rate was maintained using the Malvern stirring apparatus. For most of the experiments a 100mm lens was used. All particle sizing was performed in a room thermostatically controlled at 20°C. The solvent, n-heptane, was first added to the solvent cell and a baseline measured. A few drops of the test emulsion were added to the solvent cell and a light measurement performed. Between runs the cell was emptied, rinsed with ethanol and then n-heptane and a new baseline measured. To test reproducibility, three separate measurements were made on an emulsion sample which had been prepared 20 hours prior. The results which were obtained are highly reproducible and are shown in Table 4.2.

Table 4.2 Statistics obtained for 3 separate runs done on a standard emulsion.

Time	D[4,3]	D[3,2]	D[v,0.5]	Span
8.45	9.52	8.41	8.75	0.99
8.50	9.29	8.24	8.53	0.98
8.56	9.35	8.33	8.72	0.95

To obtain size distribution data, the Malvern spreadsheet command was used to output the light intensity data. This data was then interpreted using a computer program written especially for the emulsions used in this study (see section 4.2 for details of the program).

A problem encountered with w/o emulsion particle size determination using the Malvern particle sizer was the effect of the glass windows on the stability of the emulsion. It is known that the wettability of solid surfaces in contact with the emulsion has an influence on the emulsion type. Glass surfaces favour water-continuous emulsions and perspex surfaces strongly favour oil-continuous emulsions.[26] With certain emulsions droplets of a larger

$$volume\ creamed\ (\%) = \frac{volume\ creamed\ (ml)}{volume\ of\ external\ phase\ (ml)} \times 100 \qquad \text{....4.17}$$

$$= ratio\ creamed \times 100$$

4.3.2 OPTICAL MICROSCOPY

To study the emulsion, a Leitz Diaplan stage microscope with Hoffman modulation contrast optics coupled to a photocamera was used. Phase contrast illumination was necessary to observe the samples owing to the small refractive index difference between the continuous and the dispersed phases. In all cases a 100x oil immersion lens was used.

W/o emulsions separate on glass due to capillary action. To prevent this polyethylene sheets were used in place of the conventional glass slides and cover slips. The emulsions were shaken and a 0.2ml aliquot delivered onto the slide using micropipettes with polypropylene disposable tips.

4.3.3 REFRACTIVE INDEX MEASUREMENTS

To convert malvern light intensity data to droplet size data, the real and imaginary component of refractive indices for both the continuous and disperse phase have to be determined. There are known to be difficulties in measuring the imaginary component of the refractive index, but fortunately study of the scattering matrices has shown that precise knowledge of the imaginary component is not required. In most cases all that needs to be known is if particles are transparent, where the imaginary part is given as zero, or opaque where the imaginary part = 0.1.[19]

Refractive indices were determined for a series of 12 ammonium nitrate solutions ranging from 0*M* to saturated at 20°C. Solutions were prepared by accurately weighing the salt and pipetting the solvent. The pipette used was calibrated before use.[25] An Atago Abbe refractometer was used for the refractive index measurements. The room, the solutions and

4.3.1.1 CREAMING EXPERIMENTAL CONDITIONS

Creaming measurements were performed in a room thermostatically controlled at 20°C. Emulsions were sheared in sealed vials using a flat metal impeller (diameter = 18mm; width = 5mm) attached to a modified Moulinex turbomix handblender operating at *ca.* 6200 r.p.m. After shearing, the emulsions were decanted into 10ml measuring cylinders with an internal diameter of 12mm, and the cream level monitored as a function of time. In most studies a total emulsion volume of 10ml was prepared with an internal volume phase ratio, ϕ , of 0.2. Experimentally the final creamed volume was determined using the same experimental conditions used in the standard creaming rate studies with the exception that the internal phase ratio was greater than 0.2.

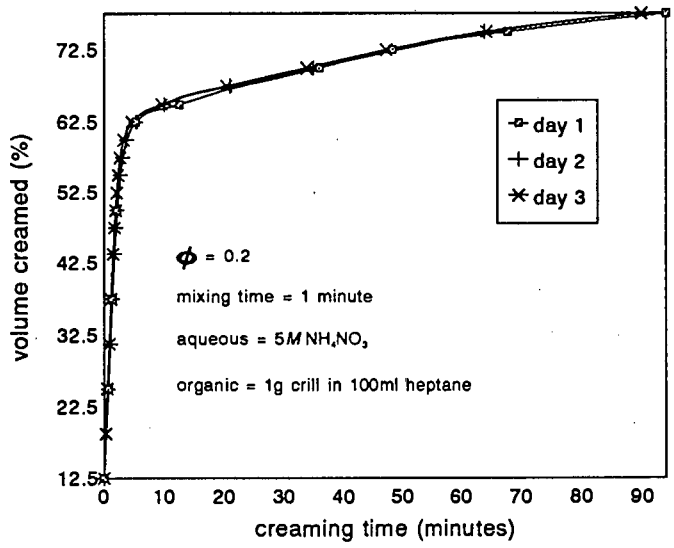

Figure 4.7

Plot of the change in the volume percent creamed with time for a series of identical emulsions prepared on different days. The aqueous phase contained 5*M* NH_4NO_3; the organic phase contained 1g crill 43 per 100ml heptane and the shearing time was 1 minute.

To check reproducibility, measurements of the same system were taken on three separate days. The three creaming runs are shown in figure 4.7, the reproducibility obtained was excellent. However there was a decrease in reproducibility as the bulk emulsion viscosity increased. The greatest experimental error was found to be due to decanting the emulsion. The volume creamed was measured as a percentage according to equation 4.17.

The second creaming parameter, the inflexion point in the curve, is the point at which the plot is no longer linear and Stokes' equations are no longer valid. In this region the environment of the droplets is no longer dilute and information about the formation of micelles or the size and amount of aggregation of the droplets can be obtained.

The third creaming parameter, the final volume of the cream, gives an indication of the extent of clumping of an emulsion; the extent to which the droplets are distorted; and the width of the droplet distribution. If we assume that the amount of internal phase soluble in the external phase is negligible and *vice versa*, then the relationship between the %creamed and the internal phase ratio of the cream is given in equation 4.16. This relationship is shown in figure 4.6 for a standard creaming rate study. The internal phase ratio of the cream is always greater than the internal phase ratio of the emulsion and often tends to 0.74.

$$\%creamed = \frac{100(V_T - V_C)}{V_T(1-\phi)}$$

$$\phi_C = \frac{100\phi}{100 - (1-\phi)\%creamed} \qquad \text{....4.16}$$

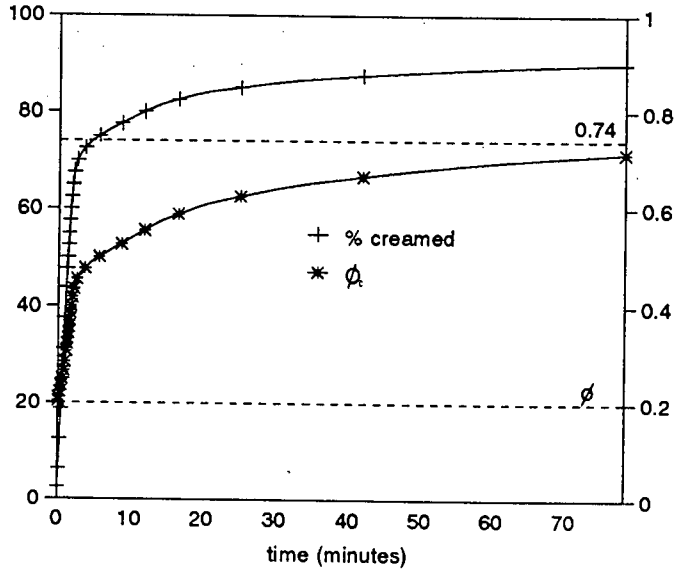

Figure 4.6

The relationship between the % creamed and the internal phase ratio of the creamed layer during a standard creaming rate study

As the constant k_{form} can be calculated for each experimental system, the constant k_{dist} which represents the size distribution of droplets at the onset of creaming can be determined from the initial experimental creaming rate. By comparing the initial creaming rates for a series of emulsions, the changes in the initial size distributions can be compared.

$$\frac{d\ \%creamed}{dt} = k_{cream} = k_{form} \times k_{dist}$$

$$\text{where} \quad k_{form} = \frac{800\pi^2 g \Delta\rho r_M^2}{27\eta V_T^2 \phi(1-\phi)} \quad \text{and} \quad k_{dist} = \sum_i n_i a_i^5 \qquad \text{....4.14}$$

To experimentally validate that the relationship between k_{form} and r_M holds, two identical emulsions were prepared and allowed to cream in measuring cylinders with different internal radii. Using the data from one run the creaming rate for the second was predicted using equation 4.15. The calculated and experimental creaming runs are plotted in figure 4.5 and confirm the theory.

$$V_c(r_{M_2}) = V_c(r_{M_1}) \times \frac{r_{M_1}^2}{r_{M_2}^2} \qquad \text{....4.15}$$

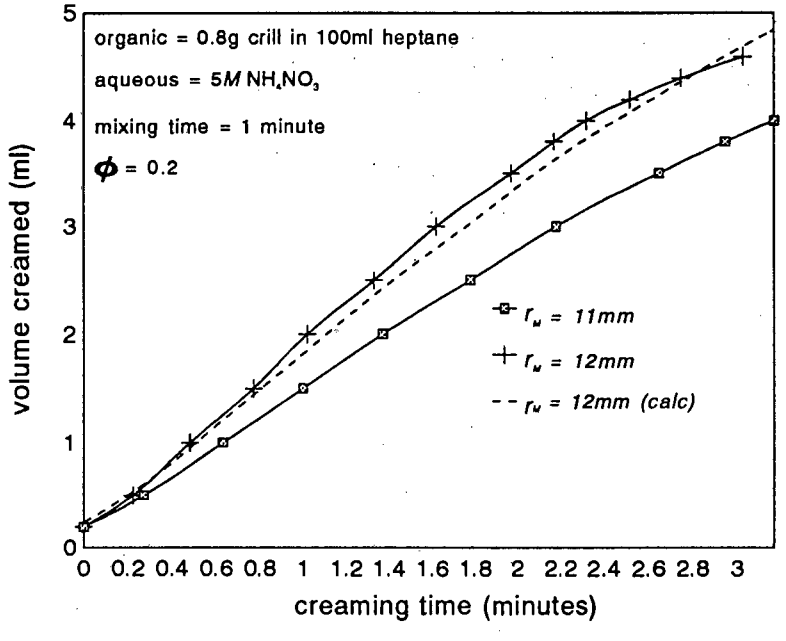

Figure 4.5

Plot of the change in the cream volume versus time for two identical emulsions which were allowed to cream in 10ml measuring cylinders of differing diameters. The broken line was calculated according to equation 4.15

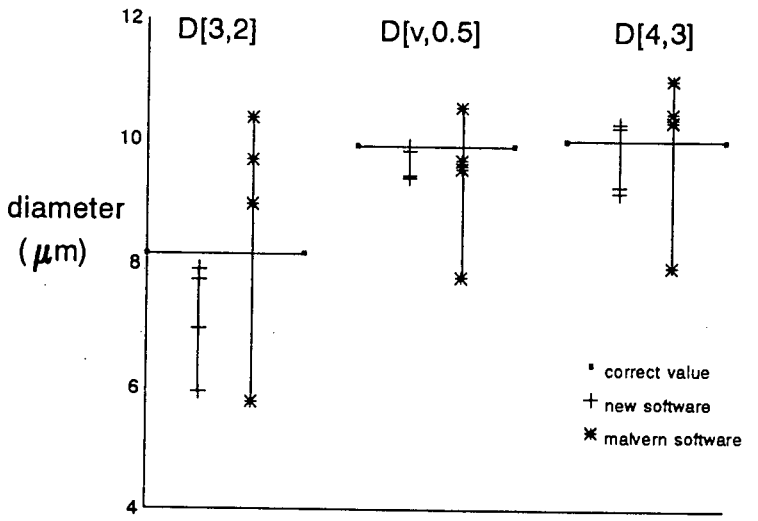

Figure 4.4

Comparison of statistics obtained using our software and the on-line software. Input light data was simulated for a gaussian distribution (μ=10 and σ=4), refractive-index ratios (0.959, 0.980, 0.995, 1.023) and a 100mm lens.

4.3 EXPERIMENTAL TECHNIQUES

4.3.1 CREAMING STUDIES

When comparing the experimental plots of creaming rates for different emulsions, three main creaming results can be compared: the initial slope of the graph or initial creaming rate, the inflexion point in the curve and the final cream volume. These three parameters are shown in figure 4.6.

The first creaming parameter, the initial creaming rate is when Stokes' equations are considered valid. If clumping and coalescence is minimal during initial creaming, a plot of the change in the volume creamed versus time should yield a straight line. This has been observed in the experimental results (figure 4.7). The slope of the graph, derived from the creaming rate equation (equation 2.4), can be expressed as a product of two constants, k_{form} and k_{dist} (equation 4.14).

Figure 4.2 and 4.3 show the light energy patterns on the detector rings that were simulated for a specified gaussian distribution and a 100mm lens. The light energy patterns were computed for several refractive-index ratios. It is clear from both figures that a change in the refractive-index ratio has a great effect on the light intensity and that one scattering matrix is insufficient for all refractive-index ratios. The shifting of the main light peak to the outer detectors as the mean droplet diameter decreases from 15μm to 10μm is also apparent.

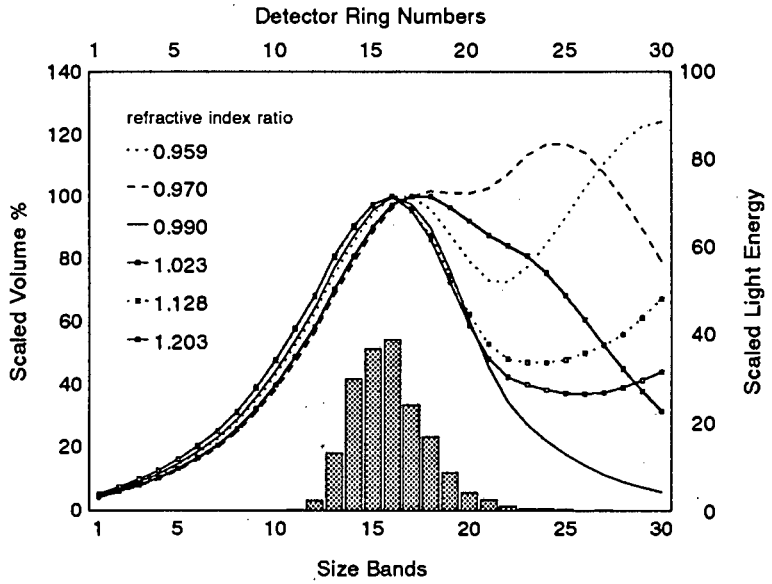

Figure 4.3

The light energy patterns computed for several refractive index ratios. The Guassian distribution specified as input (μ = 15 and σ = 4) is shown. Lens = 100mm.

The matrix inversion software was used to analyze four simulated light scattering patterns for a guassian distribution (μ=10 and σ=4) and refractive-index ratios applicable to our system (0.959, 0.980, 0.995, 1.023). In each case the correct matrix for the system was used. The same light scattering data was then used as input and was analyzed using the on-line Malvern software. Figure 4.4 shows a comparison of the statistics obtained using the two different software inversions. Included in the plot is the correct statistic for the distribution which was used as input for the simulation program. For each refractive index ratio, the statistic obtained using our software was closer to the real value than the value obtained using the Malvern software.

Table 4.1 Comparison of size statistics produced by analyzing the light energy distribution obtained for a standard emulsion using the Malvern on-line software and our software. Parameters used in the table have been described in section 4.2.2.

Software	log diff	Span	D[4,3]	D[3,2]	D[v,0.1]	D[v,0.5]	D[v,0.9]
Malvern	3.817	1.02	7.40	6.46	4.26	6.89	11.28
New	3.696	0.98	8.81	7.65	4.99	8.42	13.27

Using J.Knight's simulation program the effect changes in the refractive index ratio had on the light scattered were tested. Various bimodal and Gaussian distributions were tested in the refractive index range 0.95 to 1.20. One hundred data points were used for each simulation. The Gaussian distribution function is as follows:

$$y = \frac{e^{\frac{-(x-\mu)^2}{2\sigma^2}}}{\sigma\sqrt{2\pi}} \qquad \text{....4.13}$$

where μ is the mean value (μm) and

σ is the standard deviation (μm)

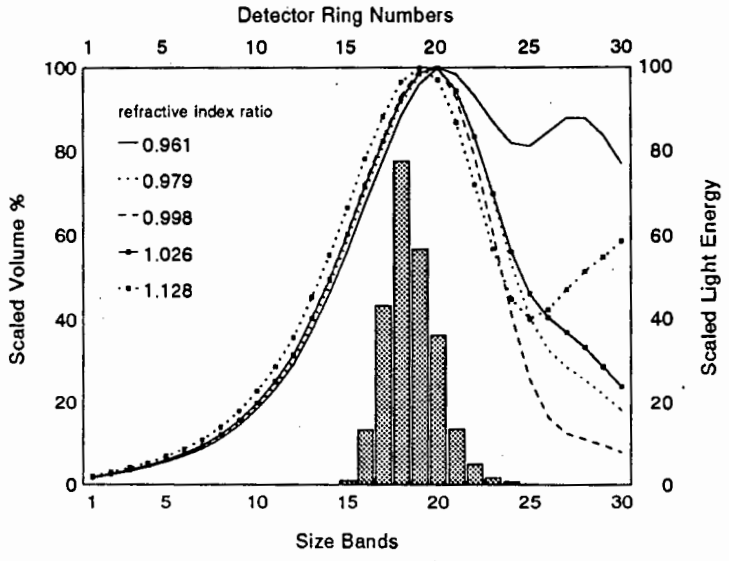

Figure 4.2

The light energy patterns computed for several refractive index ratios. The Guassian distribution specified as input (μ = 10 and σ = 2) is shown. Lens = 100mm.

The source code of the resulting computer program, is given in appendix 5 and the executable file (MALVERN.EXE) is on disk 2 of the included 1.44Mb diskettes. Instructions on how to execute the program as well as a listing of the files on disk 2 are given in appendix 7.

4.2.4 EVALUATION OF COMPUTER PROGRAM

In Figure 4.1 the size distribution obtained from analyzing a standard emulsion using a 100mm lens and the on-line Malvern software and the new software is shown. Table 4.1 compares the same size distributions results. It is clear that the new software gives the expected Gaussian distribution while the on-line software gives a bimodal distribution.

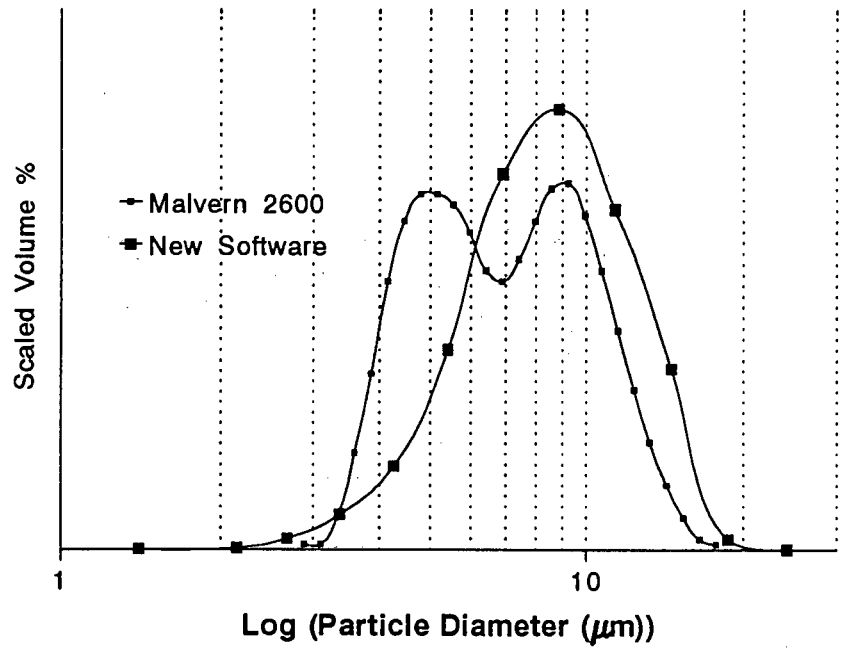

Figure 4.1

Comparison of the size distributions of emulsion droplets obtained using a 100mm lens and two different model independent computational fitting procedures. Comparative statistics are given in Table 4.1.

The volume distribution is initially estimated using the following equations

$$q[i] = \frac{I_m[i]}{a[i,i]} \quad \text{where } i = 1...15$$
$$q[16] = 1.5*(2*q[15] - q[14]) \qquad \text{....4.8}$$

The value then enters two iteration loops where in each loop it is recalculated until the fitting error obtains a minimum. In the first iteration the volume distribution is calculated using the following equation

$$q[i]^{k+1} = q[i]^k * q[i]^k \quad \text{where } i = 1...16 \qquad \text{....4.9}$$

where k represents the iteration number

In the final iteration loop the volume distribution is calculated using equation 8.

$$q[i]^{k+1} = q[i]^k * \left[\left(\frac{I_m[i]}{I_c[i]^k}\right)^2 + \left(\frac{I_m[i+1]}{I_c[i+1]^k}\right)^2 \right]$$
$$q[16]^{k+1} = q[16]^k * 2 * \left(\frac{I_m[16]}{I_c[16]^k}\right)^2 \qquad \text{....4.10}$$

The size distribution and minimum fitting error that entered the last iteration are then presented as the final solution.

An addition to the program was the calculation of the R[5,3] statistic. This value can be used to calculate k_{dist}, the size distribution constant needed for analyzing creaming rate studies (see section 4.3.1). R[5,3] and it's relationship to k_{dist} is shown in equations 4.11 and 4.12.

$$R[5,3] = \frac{\sum_i q[i]\times d[i]^2}{4} = \frac{\sum_i n_i a_i^5}{\sum_i n_i a_i^3} \qquad \text{....4.11}$$

$$k_{dist} = \sum_i n_i a_i^5 = \frac{3V_T\ R[5,3]}{4\pi} \qquad \text{....4.12}$$

$$I_m[16] = 2 * I_m[15] - I_m[14] \qquad \text{....4.4}$$

A least squares fitting procedure is then applied to calculate the size distribution that gives the closest fitting scattering pattern. During the fitting procedure the volume distribution is continually recalculated after which it is normalized with its cumulative sum equal to 1. The calculated light energy pattern is recalculated from the new volume distribution using the following equation

$$I_c[i] = \sum_{j=1}^{16} a[i,j] * q[j] \qquad \text{where } i = 1...15 \qquad \text{....4.5}$$

where $q[j]$ is the volume fraction of size class j,

$I_c[i]$ is the calculated light energy on detector rings $2i$ and $2i$-1 and

$a[i,j]$ is the matrix coefficient representing the light scattered by size class j on the detector elements $2i$-1 and $2i$.

The scattering matrix used has 15 rows corresponding to 15 detector element pairs and 16 columns corresponding to 16 size classes. All matrices were calculated using J.Knight's matrix program.

The calculated light intensity is then normalized with its peak value set to 2047. The sixteenth number is calculated according to equation 4.6, in a similar way as the corresponding measured value is calculated.

$$I_c[16] = 2 * I_c[15] - I_c[14] \qquad \text{....4.6}$$

The fitting error, log diff, is the logarithm of the least squares error between the measured and calculated scattered-light energy data and is calculated as follows

$$\log \text{ diff} = \log\left(\sum_{i=1}^{16} (I_c[i] - I_m[i])^2 \right) \qquad \text{....4.7}$$

log diff — is the measure of correctness of the least squares fit (eqn. 4.7)

D[v,x] — is the particle diameter in μm for which x volume fraction of the particles is smaller

Span — is the relative spread = (D[v,0.9] - D[v,0.1])/D[v,0.5]

D[4,3] — is the De Broucker mean or equivalent volume mean diameter in μm

D[3,2] — is the Sauter mean or equivalent surface area mean diameter in μm

$$D[4,3] = \sum_i q[i] * d[i] = \frac{2\sum_i n_i a_i^4}{\sum_i n_i a_i^3} \qquad \text{....4.2}$$

$$D[3,2] = \frac{1}{\sum_i q[i]/d[i]} = \frac{2\sum_i n_i a_i^3}{\sum_i n_i a_i^2} \qquad \text{....4.3}$$

where $d[i]$ is the diameter size representing the ith size class

$q[i]$ is the volume percent contained in the ith size class

n_i are the number of particles of radius a_i

4.2.3 THE COMPUTER PROGRAM

The program is similar to the fitting procedure used in the Malvern 2600 Particle Sizer which has been described in the literature.[17,24] The measured light energy pattern which is obtained from the Malvern using the spreadsheet command, contains 30 numbers corresponding to the energy of the scattered light on each detector. These numbers are paired to obtain fifteen numbers ($l_m[i]$ where i = 1 to 15), which represent the measured light energy on detector rings $2i$ and $2i$-1. These numbers are initially normalized with their peak value set to 2047. The sixteenth number which represents the light energy from particles smaller than the lower limit of the detectors is calculated according to the following equation:

scatter light on the outermost detectors (large detector ring numbers) and *vice versa.*[18]

At large scattering angles, when particles are less than 1μm, diffraction and anomalous diffraction, no longer completely describe the light scattering and the Mie theory has to be used.[19] The Mie and anomalous diffraction theory both require knowledge of the refractive-index ratio. This ratio has a real and imaginary part, the real part controlling how light is deflected by the particle and the imaginary part determining how much light is absorbed in the particle. For many emulsions and when particles are crystals in saturated solutions, the refractive-index ratio will be close to unity. If anomalous effects are ignored this can result in serious skewing of particle size information. As the refractive index ratio is reduced there is a relative move of light energy to the outer detector rings, resulting in a false interpretation of a decrease in particle size.[15]

Mathematically, if the particles causing the scattering are divided into discrete size classes, the recorded scattering pattern can be written as a set of linear equations which in vector notation reads

$$L = A \times Q \qquad \text{....4.1}$$

where L is the light energy vector,

Q is the particle size volume distribution vector and

A is the scattering matrix

To obtain particle size measurements an inversion process is needed to determine the size distribution, Q from the scattering distribution, L. Different algorithms such as matrix inversion and iterative techniques have been used in commercial instruments. However, the inversion of the equation is strongly ill-conditioned and a straightforward matrix inversion fails to restore the correct size distribution. An iterative inversion appears to be the method of choice.[20,21]

There are many terms used to describe the distribution of particle sizes, the most common of which are: [13,17,22,23]

4.2 LASER DIFFRACTION COMPUTER PROGRAM

4.2.1 INTRODUCTION

For w/o emulsions the Malvern particle sizer gave incorrect size distributions. Typically the Malvern on-line software gives bimodal size distributions for standard emulsions which according to theoretical and experimental results should have Guassian distributions.

To solve the size distribution problem encountered with the Malvern on-line software, it was necessary to write new software for the Malvern 2600 instrument. A Pascal program was written which fits the measured light energy pattern obtained from the Malvern particle sizer to a size distribution using the scattering matrix specific for the lens being used and the refractive-index ratio of the emulsion being studied. Other than this pascal program, two Fortran 77 programs, a matrix calculation and a light simulation program, were written by J.Knight, a doctoral student in the University of Cape Town Physics Department, and run under VMS on an Alpha Vax system. Both programs incorporate the Mie theory as described in the literature.[17] The simulation program was used to calculate the light scattering of a specified distribution of particles with a given refractive-index ratio, through a specified lens. The scattering matrix program was used to calculate the scattering matrix for the refractive index and lens specified.

4.2.2 LASER DIFFRACTION THEORY

Particle size analysis by laser light scattering requires that particles are passed through a laser beam and that light scattered by these particles is intercepted by a silicon detector array. The signals from the detector may then be analyzed mathematically to produce a volume/size distribution. The Malvern 2600D detector consists of 31 semi-circular detector rings with a small hole in the centre. All particles present in the optical measuring volume contribute to the scattering pattern received by the photo diode array detector. For spherical particles with a diameter greater than the wavelength of the He/Ne laser (λ = 0.6328μm), the diameter of the diffraction pattern is inversely proportional to the particle diameter i.e. small particles

separation after a fixed time period; or changes in the mean droplet volume, emulsion interface or droplet-size distribution with time.[5,9-14]

In this study bulk emulsion stability measurements were made of the change in the droplet size distribution with time. Initial droplet sizing information was obtained using creaming study results and relative trends in droplet sizes were determined using optical microscopy. To obtain droplet size distributions with time and to validate the creaming results obtained, a convenient sizing technique had to be found. The nature of the w/o emulsion system precludes the use of most sizing techniques available today. Sieving can't be used on liquids; optical microscopy is slow, inaccurate and underestimates the number of small particles giving a bias error; and the Coulter technique needs an aqueous electrolyte solution as the external phase. Laser diffraction spectrometry is known to be a useful non-intrusive technique for studying aggregation phenomena and it also allows for rapid and reliable on-line measurements, hence it was chosen for determining droplet size distributions.

The Malvern 2600 laser diffraction instrument available to us, determines the size distribution of particles using the Fraunhofer diffraction theory. This theory adequately describes the scattering of particles larger than 3 μm when using a He/Ne laser, if the refractive-index ratio (the ratio of the refractive index of the particle to the suspending medium) is large.[15] When the apparatus is used to size systems with refractive-index ratios near unity, refraction of the light through the particle contributes significantly to forward scattering and produces so-called anomalous diffraction. For refractive index ratios between 0.9 and 1.1, it is advisable to process the measured scattering patterns with the corresponding calculated scattering matrix instead of the standard Malvern scattering matrix which is more applicable to a refractive-index ratio of approximately 1.2.[16,17] For this reason a computer program was written to analyze the malvern light intensity data in terms of droplet size. A modification of this program is now in commercial use. The theory behind the program is given in the following section.

4.1 INTRODUCTION

The theoretical explanation of colloid and w/o emulsion stability has been developed in chapter three. However, quantitative comparisons have to be made between theory and experiments.[1] The theoretical predictions made by the emulsion stability computer model have to be validated by experimental results before the model can have any practical applications and be used predictively.

The theory predicts that the stability of a bulk emulsion depends on which factors influence the rate determining step. The measurement and prediction of emulsion stability has been based on a variety of experimental techniques. Measurements of the emulsion volume after a fixed time, the volume of the cream phase or the change in density at a fixed depth have all been quoted as measurements of bulk emulsion stability.[2-4] However, many of these experimental techniques only measure stability with respect to one of the kinetic processes involved in emulsion break down, such as creaming or clumping. Depending on the experimental technique performed contradictory results have been reported. For example it has been found that increasing the surfactant concentration increases the stability of an emulsion with respect to coalescence but for some systems can decrease emulsion stability with respect to clumping through chemical bonding between surfactant films.[3]

The stability of an emulsion left undisturbed may also be very different to its stability under stress. Thus techniques such as the initial rate of separation of the liquid from the internal phase in a centrifuge or when exposed to severe temperature changes should be used with caution.[5] Temperature changes are known to change the rate determining step in emulsion coagulation and therefore this technique is not recommended unless stability with respect to temperature change is a major concern of the formulator. Ultracentrifugation on the other hand does not measure stability in the true sense since it only provides information on coalescence.[6] Similarly coalescence rates of droplets at planar oil/water interfaces are not good predictors of bulk stability.[7,8]

Experimental techniques which give a good indication of bulk emulsion stability include measurement of the breaking time of an emulsion; the storage time in days; the phase

CHAPTER FOUR
W/O EMULSION
EXPERIMENTAL STUDIES

72. A.De Robertis, C De Stefano, S.Sammartano and C.Rigano (1987), "The Determination of Formation Constants of Weak Complexes by Potentiometric Measurements: Experimental Procedures and Calculation Methods", *Talanta*, **34**:933.

73. K.S.Johnson and R.M.Pytkowicz (1978), "Ion Association of Cl- with H^+, Na^+, K^+, Ca^{++}, and Mg^{++} in Aqueous Solutions at 25 degrees Celsius.", *Am.J.Science*, **278**:1428.

74. R.L.Frost and D.W.James (1982), "Ion-Ion-Solvent Interactions in Solution. Part 4.", *J.Chem.Soc.Faraday Trans.I.*, **78**:3235.

75. B.de Castro, J.Pereira, P.Gameiro and J.L.F.C.Lima (1992), "Multinuclear NMR and Potentiometric Studies on the Interaction of Zinc and Cadmium with Cytidine and Glycylglycine.", *J.Inorg.Biochem.*, **45**:53.

76. Y-H.Li (1991), "Distribution Patterns of the Elements in the Ocean: A Synthesis", *Geochim.CosmochimActa*, **55**:3223.

77. P.W.Linder, A.Voye and S.Cocks (1990), *NATO ASI Series*, **G23**:91.

78. P.M.Harrison and R.J.Hoare (1980), *Metals in Biochemistry*, Chapman and Hall, London.

79. A.E.Martell, R.M.Smith and R.J.Motekaitis, *NIST Critical Stability Constants of Metal Complexes Database*, Garthersburg, MD.

80. G.E.Jackson and L.F.Seymour (1995), "Formation Constants at high Ionic Strength - I. Potentiometric determination of Protonation Constants for Succinic, Propionic and Mono-Methyl Succinic Acid in different Ionic Media.", *Talanta*, **42**:5.

81. G.E.Jackson and L.F.Seymour (1995), "Formation Constants at high Ionic Strength - II. The Ionic Strength Correction of Formation Constants using a Simplified Pitzer Equation.", *Talanta*, **42**:9.

82. S.L.Marshall, P.M.May and G.T.Hefter (1995), "Least-Squares Analysis of Osmotic Coefficient Data at 25°C According to Pitzer's Equation. 1. 1:1 Electrolytes.", *J.Chem.Eng.Data*, **40**:1041.

83. G.T.Hefter and P.M.May (1991), "Ionic strength lives!", *Chemistry in Britain*, **27**:620.

58. R.H.Perry and D.Green (1988), *Perry's Chemical Engineer's Handbook*, McGraw-Hill, Singapore, 6th Ed.

59. M.Maeda, G.Nakagawa and G.Biedermann (1983), "Estimation of Medium Effect on Dissociation Constant of Ammonium Ion and Formation Constants of Silver(I)-Ammine Complexes in Aqueous Solution", *J.Phys.Chem.*, **87**:121.

60. R.Herrero, I.Brandariz, S.Fiol and M.E.Sastre de Vicente (1993), "Pitzer and Thermodynamic Parameters of Triethanolamine and Glycine in Aqueous Saline Solutions", *Collect.Czech.Chem.Commun.*, **58**:1269.

61. K.Szabo, I.Nagypal and I.Fabian (1983), "Unexpected Dependence of the Protonation Constant of 2,2-Bipy on ionic strength", *Talanta*, **30**:801.

62. R.K.Cannan and A.Kibrick (1938), "Complex Formation between Carboxylic Acids and Divalent Metal Cations.", *J.Am.Chem.Soc.*, **60**:2314.

63. A.De Robertis, C.De Stefano, S.Sammartano and R.Scarcella (1985), "Studies on Acetate Complexes. Part I. Formation of Proton, Alkali-Metal, and Alkaline-Earth-Metal Ion Complexes at Several Temperatures and Ionic Strengths.", *J.Chem.Research(M)*:629.

64. O.Johansson and W.Wedborg (1985), "Determination of the Stability for Acetic Acid in Synthetic Seawater Media at Various Temperatures and Salinities", *J.Solution Chemistry*, **14**:431.

65. D.L.Martin and F.J.C.Rosotti (1959), "The Hydrogen-bonding of Monocarboxylates in Aqueous Solution", *Proc.Chem.Soc.*:60.

66. E.Dübler, U.Haring, K.Scheller, P.Baltzer and H.Sigel (1984), "Dependence of an Intramolecular Aromatic-Ring Stacking.", *Inorg.Chem.*, **23**:3785.

67. P.M.May and K.Murray (1991), "Jess, a Joint Expert Speciation System- I.", *Talanta*, **38**:1409.

68. P.M.May and K.Murray (1991), "Jess, a Joint Expert Speciation System - II. The Thermodynamic Database.", *Talanta*, **38**:1419.

69. F.J.Millero (1985), "The Physical Chemistry of Natural Waters", *Pure & Appl.Chem.*, **57**:1015.

70. C.W.Davies (1962), *Ion Association*, Butterworths, London.

71. A.De Robertis, C.De Stefano, R.Scarcella and C.Rigano (1984), "Thermodynamics of Formation of Magnesium(II), Calcium(II), Strontium(II) and Barium(II)-Succinate Complexes in Aqueous Solution", *Thermochimica Acta*, **80**:197.

43. K.S.Pitzer and J.J.Kim (1974), "Thermodynamics of Electrolytes. IV. Activity and Osmotic Coefficients for Mixed Electrolytes.", *J.Am.Chem.Soc.*:5701.

44. K.S.Pitzer (1973), "Thermodynamics of Electrolytes. I. Theoretical Basis and General Equations.", *J.Phys.Chem.*, **77**:268.

45. K.S.Pitzer (1986), "Theoretical considerations of solubility with emphasis on mixed aqueous electrolytes", *Pure & Appl.Chem.*, **58**:1599.

46. K.S.Pitzer (1987), "A Thermodynamic Model for Aqueous Solutions of Liquid-Like Density", *Reviews in Mineralogy*, **17**:97.

47. R.T.Pabalan and K.S.Pitzer (1990), "Models for Aqueous Electrolyte Mixtures for Systems Extending from Dilute Solutions to Fused Salts.", *ACS Symp.Ser.*, **416**:44.

48. K.S.Pitzer (1984), "Ionic Fluids", *J.Phys.Chem.*, **88**:2689.

49. K.S.Pitzer (1989), "Fluids, both Ionic and Nonionic, over Wide Ranges of Temperature and Composition.", *Pure & Appl.Chem.*, **61**:979.

50. D.J.Bradley and K.S.Pitzer (1979), "Thermodynamics of Electrolytes. 12. Dielectric Properties of Water and Debye-Hückel Parameters to 350 degrees and 1 kbar.", *J.Phys.Chem.*, **83**:1599.

51. C.E.Harvie, N.Moller and J.H.Weare (1984), "The Prediction of Mineral Solubilities in Natural Waters: The Na-K-Mg-Ca-H-Cl-SO4-OH-HCO3-CO3-CO2-H2O System to High Ionic Strengths at 25 degrees Celsius", *Geochim.Cosmochim.Acta*, **48**:723.

52. F.J.Millero and D.R.Schreiber (1982), "Use of the Ion Pairing Model to Estimate Activity Coefficients of the Ionic Components of Natural Waters.", *Am.J.Science*, **282**:1508.

53. F.J.Millero and D.J.Hawke (1992), "Ionic Interactions of Divalent Metals in Natural Waters", *Marine Chemistry*, **40**:19.

54. A.Hamman, A.Olin and P.Svanstrom (1977), "The Complex Formation between Pb^{++} and Dicarboxylic Acids", *Acta Chem.Scand.*, **31**:384.

55. F.J.C.Rossotti and R.J.Whewell (1977), "Structure and Stability of Carboxylate Complexes. Part 16. Stability constants of some Mercury(II)Carboxylates", *J.Chem.Soc.Dalton Trans*:1223.

56. D.D.Perrin, B.Dempsey and E.P.Serjeant (1981), *pKa Prediction for Organic Acids and Bases*, Chapman and Hall, London.

57. E.W.Washburn (Ed) (1928), *International Critical Tables of Numerical Data*, McGraw, London, vol. III.

28. D.G.Tuck (1989), "IUPAC Commission on Equilibrium Data. A Proposal for the Use of a Standard Format for the Publication of Stability Constant Measurements.", *Pure & Appl.Chem.*, **61**:1161.

29. G.Gran (1952), "Determination of the Equivalence Point in Potentiometric Titrations. Part II.", *Analyst*, **77**:661.

30. F.J.C.Rossotti and H.Rossotti (1965), "Potentiometric Titrations Using Gran Plots. A Textbook Omission", *J.Chem.Ed.*, **42**:375.

31. P.M.May, D.R.Williams, P.W.Linder and R.G.Torrington (1982), "The Use of Glass Electrodes for the Determination of Formation Constants - I: A Definitive Method for Calibration.", *Talanta*, **29**:249.

32. F.Ingram and E.Still (1966), "Graphic Method for the Determination of Titration End-points", *Talanta*, **13**:1431.

33. P.M.May, K.Murray and D.R.Williams (1985), "The Use of Glass Electrodes for the Determination of Formation Constants - II: Simulation of Titration Data.", *Talanta*, **32**:483.

34. P.M.May, K.Murray and D.R.Williams (1988), "The Use of Glass Electrodes for the Determination of Formation Constants - III: Optimization of Titration Data: The Esta Library of Computer Programs.", *Talanta*, **35**:825.

35. P.M.May and K.Murray (1988), "The Use of Glass Electrodes for the Determination of Formation Constants - IV: Matters of Weight.", *Talanta*, **35**:927.

36. P.M.May and K.Murray (1988), "The Use of Glass Electrodes for the Determination of Formation Constants - V: Monte Carlo Analysis of Error Propagation.", *Talanta*, **35**:933.

37. K.Murray and P.M.May (1984), *ESTA Users Manual. ver 1.0*, University of Wales.

38. M.L.Ralston and R.I.Jennrich (1978), "DUD, A Derivative free Algorithm for Nonlinear Least Squares Regression", *Technometrics*, **20**:7.

39. J.F.Zemaitis, D.M.Clark, M.Rafal and N.C.Scrivner (1986), *Handbook of Aqueous Electrolyte Thermodynamics - Theory & Appl.*, AIChE, DIPPR, New York.

40. F.A.Guggenheim and J.C.Turgeon (1955), *Trans. Faraday Soc.*, **51**:747.

41. K.S.Pitzer in (1979), in *Activity Coefficients in Electrolyte Solns*, R.M.Pytkowicz (ed.), CRC Press, Florida, vol. 1, p. 157.

42. K.S.Pitzer (1977), "Electrolyte Theory - Improvements since Debye and Hückel", *Acc.Chem.Research*, **10**:371.

13. E.P.Serjeant (1984), *Potentiometry and Potentiometric Titrations. Chem.Analysis*, Wiley-Interscience, New York, vol. 69.

14. P.G.Daniele, C.Rigano and S.Sammartano (1982), "Studies on Sulphate Complexes. Part I. Potentiometric Investigations of Li^+, Na^+, K^+, Rb^+ and Cs^+ Complexes at 37 degrees C and 0.03<I<0.5", *Inorganica Chimica Acta*, **63**:267.

15. G.N.Lewis and M.Randall (1921), "The Activity Coefficient of Strong Electrolytes", *J.Am.Chem.Soc.*, **43**:1112.

16. R.M.Smith and R.A.Alberty (1956), "The Apparent Stability Constants of Ionic Complexes of Various Adenosine Phosphates with Monovalent Cations.", *J.Phys.Chem.*, **60**:180.

17. H.Rossotti (1978), *The Study of Ionic Equilibria: An Introduction.*, Longman Grp. Ltd., London.

18. G.Anderegg (1982), "Critical Survey of Stability Constants of NTA Complexes.", *Pure & Appl.Chem.*, **54**:2693.

19. M.T.Beck and I.Nagypal (1990), *Chemistry of Complex Equilibria*, Wiley, New York.

20. F.R.Hartley, C.Burgess and R.M.Alcock (1980), *Solution Equilibrium*, Horwood, Chichester.

21. I.Mills (Ed) (1989), *Quantities, Units and Symbols in Physical Chemistry (IUPAC)*, Blackwell Scientific, Oxford.

22. P.W.Linder and K.Murray (1982), "Correction of Formation Constants for Ionic Strength, from only one or two Data Points: An Examination of the Use of the Extended Debye-Hückel Equation.", *Talanta*, **29**:377.

23. P.W.Linder, R.G.Torrington and D.R.Williams (1984), *Analysis using Glass Electrodes*, Open University Press, Belfast.

24. D.D.Perrin and W.L.F.Armarego (1988), *Purification of Laboratory Chemicals*, Pergamon Press, London, 3rd Ed.

25. G.H.Jeffery, J.Bassett, J.Mendham and R.C.Denney (1989), *VOGEL's Textbook of Quantitative Chemical Analysis*, Longman Scientific & Technical, London, 5th Ed.

26. G.H.Nancollas and M.B.Tomson (1982), "IUPAC Commission on Equilibrium Data. Guidelines for the Determination of Stability Constants.", *Pure & Appl.Chem.*, **54**:2675.

27. A.E.Martell and R.M.Smith (1989), *Critical Stability Constants*, Plenum Press, New York, vol. 1-6.

3.7 REFERENCES

1. J.W.McBain (1950), *Colloid Science*, D.C.Heath, Boston.
2. J.H.Schulman and E.G.Cockbain (1940), "Molecular Interactions at Oil/Water Interfaces. Part II. Phase Inversion and stability of W/O Emulsions. *Trans.Faraday Soc.*,**36**:661.
3. D.R.Williams (1989), "Guest Editorial: Speciation and Legislation", *Chemical Speciation and Bioavailability*, **1(1)**:3.
4. J.R.Duffield and D.R.Williams (1989), "Chemical Speciation.", *Chemistry in Britain*:375.
5. G.E.Jackson (1990), "Al, Ga, In in biological fluids. Computer model.", *Polyhedron*, **9**:163.
6. P.M.May, P.W.Linder and D.R.Williams (1977), "Computer Simulation of Metal-ion Equilibria: Models for the Low-molecular-weight Complex Distribution of Calcium(II), Magnesium(II), Manganese(II), Iron(III), Copper(II), Zinc(II), and Lead(II) Ions in Human Blood Plasma", *J.Chem.Soc.Dalton Trans.*:588.
7. A.De Robertis, C.De Stefano, C.Rigano and S.Sammartano (1990), "Thermodynamic Parameters for the Protonation of Carboxylic Acids in Aqueous Tetraethylammonium Iodide Solutions", *J.Solution Chemistry*, **19**:569.
8. P.G.Daniele, A.De Robertis, C.De Stefano and S.Sammartano (1985), "On the Possibility of Determining the Thermodynamic Parameters for the Formation of Weak Complexes using a Simple Model for the Dependence on Ionic Strength of Activity Coefficients: Na^+, K^+ and Ca^{++} Complexes of Low Molecular Weight Ligands in Aqueous Solution.", *J.Chem.Soc.Dalton Trans*:2353.
9. A.De Robertis, C.De Stefano, S.Sammartano and R.Scarcella (1985), "Formation and Stability of Some Dicarboxylate-ammonium Complexes in Aqueous Solution at 25°C.", *J.Chem.Research(S)*:322.
10. V.I.Belevantsev, I.V.Mironov and B.I.Peschevitskii (1982), "Influence of Changes in the Ionic Background on the Dissociation Constant of a Monobasic Acid", *Russ.J.Inorg.Chem.*, **27**:29.
11. A.E.Martell and R.J.Motekaitis (1988), *Determination and use of Stability Constants.*, VCH Publishers.
12. D.Midgley (1975), "Alkali-metal Complexes in Aqueous Solution.", *Chem.Soc.Rev.*, **4**:549.

3.6 CONCLUSIONS

The study of the aqueous phase of w/o emulsions was performed because of the importance of this phase on the stability of these emulsions. The speciation of the polar surfactant headgroups has been found to be critical in the stability of w/o emulsion explosives.[1-2] The study of the polar headgroup speciation is dependent on the ionic strength and the formulation, necessitating a detailed analysis of high ionic strength media.[80] In this regard, an adapted version of Pitzer's ionic strength equations was found to satisfy our needs.[81] Since this work other workers have confirmed the importance of the nature of the electrolyte at high ionic strength and the usefulness of the Pitzer approach to cater for these effects.[82] These results confirm that weak interactions can't be ignored at high ionic strength.[83]

The results and theoretical discussions presented in this chapter confirm many empirical observations made in industry. The stability of emulsions and the speciation of the aqueous phase are both effected by:

- pH changes,
- temperature changes
- the nature of the surfactant headgroup,
- the concentration of the surfactant and
- the concentration and mix of salts in the formulation.

Other effects that would contribute to w/o emulsion stability include crystallisation and solubility effects. Depending on the nature and charge of the surfactant ion complex, its solubility in the organic phase could change. Neutral species may migrate into the organic phase forming micelles and reducing the stability of the interface. Because of the high ionic strengths in the aqueous phase, crystallisation of salts could occur, rupturing interfaces and resulting in emulsion instability.

Because our results have shown that the speciation of model surfactant headgroups changes depending on the formulation of an emulsion, we have investigated the effect of speciation on emulsion stability. The results of these studies are given in chapters 4 and 5.

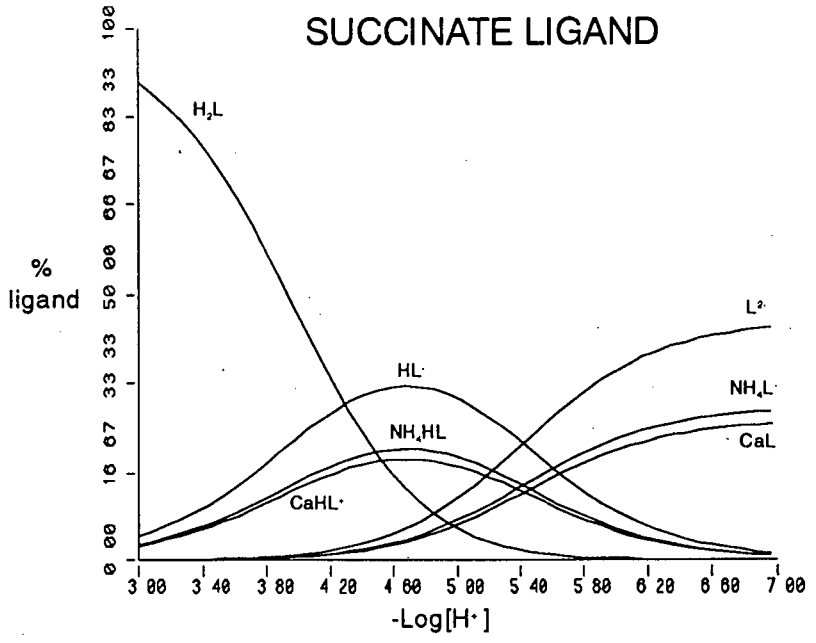

Figure 3.26

The speciation of succinate plotted over the pH range 3 to 7. Each species is plotted as a percentage over the total ligand concentration. The solution contained 0.001*m* ligand, 2.58*m* ammonium nitrate and 0.29*m* calcium nitrate.

The protonation constant for ammonia has been determined experimentally in 3*M* ammonium nitrate at 25°C (log K_{011} = 9.631).[79] The addition of the constant would not effect the speciation in the pH range being studied and therefore the constant was not added to the speciation calculations.

The speciation studies performed show that although the complexation constants for sodium, ammonia and calcium with mono- and di-carboxylate ligands are very small, when large amounts of the cation are available in solution a considerable amount of the ligand is bound. In the case of 0.001*m* propionate in 3.44*m* NH_4NO_3, when the ligand is deprotonated (pH > 7), 32 percent of the ligand is bound to ammonium. However the amount of ammonium bound to the ligand is minimal and hence the effect this weak binding has on the effective ionic strength of the solution is negligible.

concentration increases it will result in increased interfacial tensions and more energy would be needed during shearing to break the emulsion films and obtain smaller droplet sizes.[28,32]

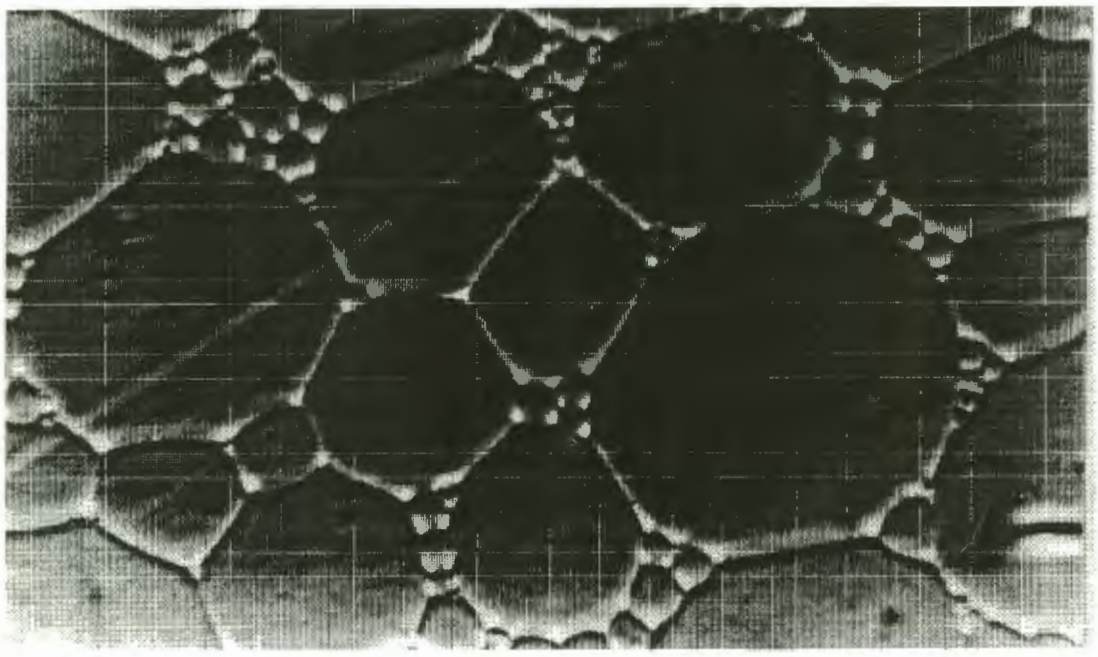

Figure 4.16

Scanned photograph of the droplets of an emulsion (scale = 130:1). Emulsion formulation: aqueous phase = 1*M* NH_4NO_3; organic phase = 0.2g crill per 100ml heptane; shearing time = 10s; V_T = 10ml; ϕ = 0.2.

Figures 4.16 and 4.17 show the affect changing the surfactant concentration from 0.2g crill per 100ml heptane to 0.7 g crill per 100ml heptane has on the emulsion droplets. The droplets prepared with the lower surfactant concentration showed coalescence under the microscope and the average droplet size was larger. The photographs clearly show the polydispersity of the droplets and their polyhedral shape with flattened faces. The larger droplets are closely packed and highly ordered confirming dynamic simulation results obtained by Heyes and Melrose which show regions of hexagonal ordering in model dense suspensions.[33] Malvern and optical microscopy results both confirm the theory predictions that w/o emulsion droplets are polydisperse with log-normal population distributions. The microscopy results confirm the trends shown by malvern and creaming results, that the droplets size initially decreases as the surfactant concentration increases. In this case the surfactant appears to stabilize the emulsion from coalescing rather than cause sensitisation of the emulsions.

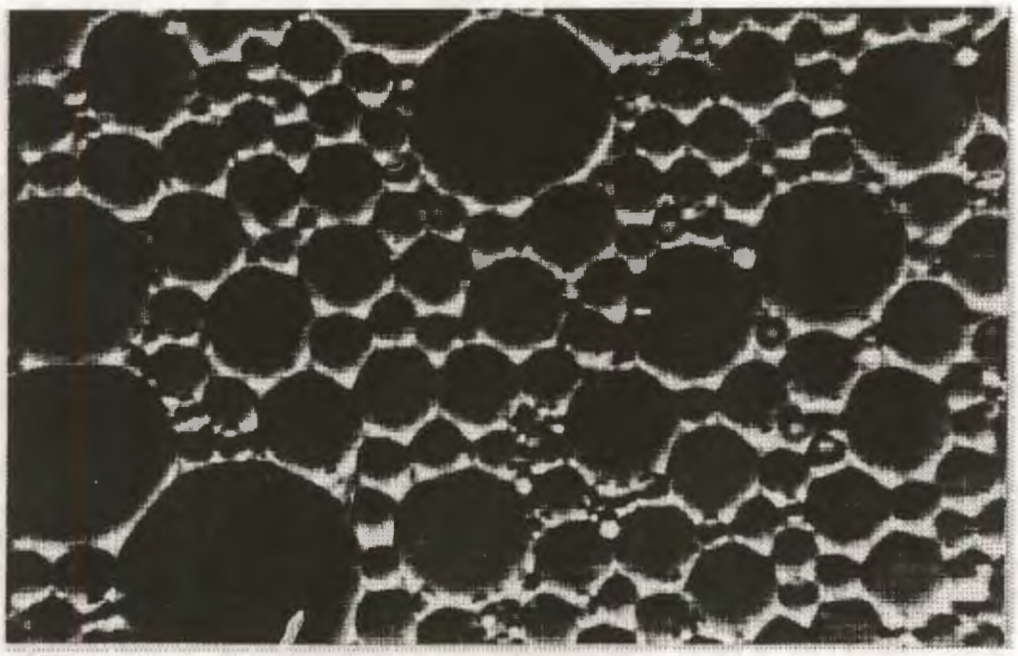

Figure 4.17

Scanned photograph of the droplets of an emulsion (scale = 130:1). Emulsion formulation: aqueous phase = 1*M* NH_4NO_3; organic phase = 0.7g crill per 100ml heptane; shearing time = 10s; V_T = 10ml; ϕ = 0.2.

4.4.3.2 SALT CONCENTRATION

The creaming results obtained for a series of emulsions where the only formulation variable was a change in the salt concentration are plotted in figure 4.18. The plot clearly indicates that changing the salt concentration affects the initial creaming rate, the inflexion point and the final cream volume.

Figure 4.19 shows the change in time to cream as a function of salt concentration. For salt concentrations greater than 1 mol/dm^3, the initial creaming rate increases as the salt concentration increases. This is expected as an increase in the salt concentration of the aqueous phase will result in an increase in the density difference between the external and internal phases and a consequent increase in the creaming rate. However below 1 mol/dm^3 ionic strength other factors appear to be involved.

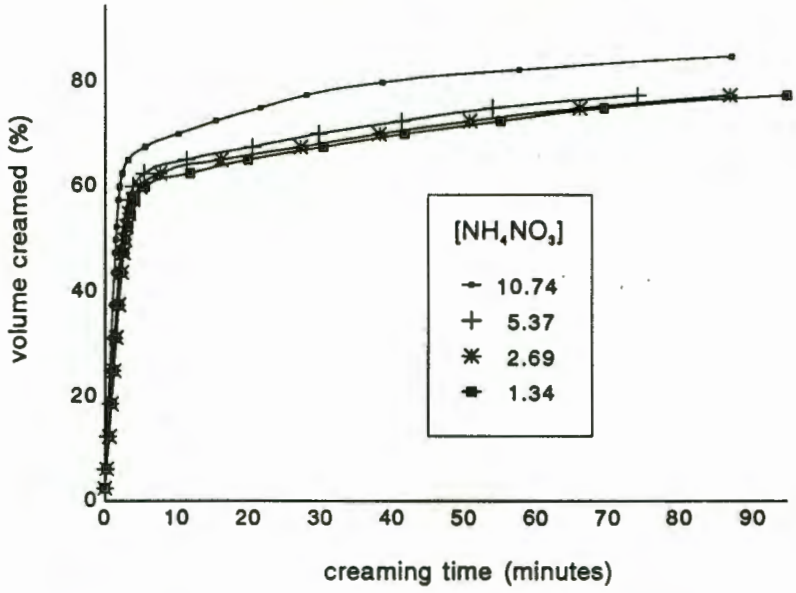

Figure 4.18

Plot of the change in the volume percent creamed with time for a series of emulsions where the ionic strength of the ammonium nitrate aqueous phase was varied. The organic phase contained 0.7g CRILL per 100ml heptane and the shearing time was 1 minute. V_T = 10ml; ϕ = 0.2.

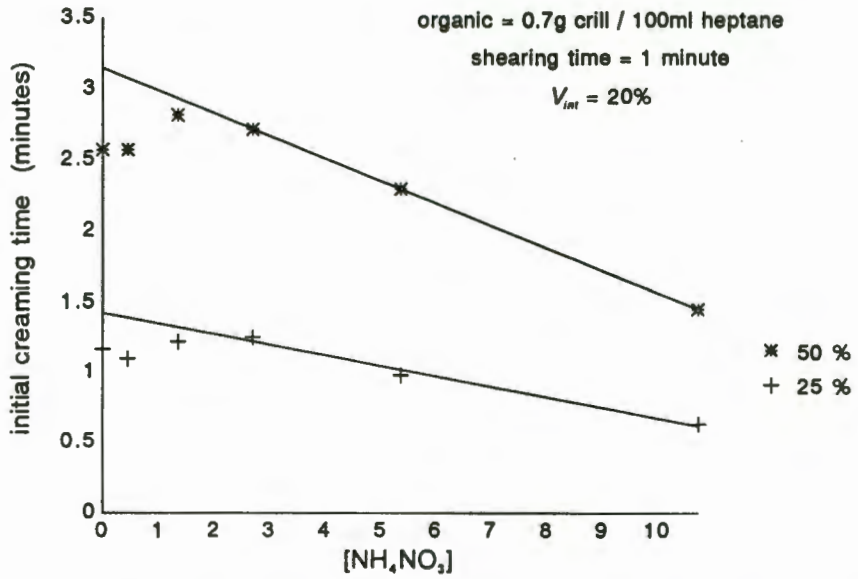

Figure 4.19

Plot of the change in the time taken to cream to a set volume for a series of emulsions where the ionic strength of the ammonium nitrate aqueous phase was varied. The organic phase contained 0.7g CRILL per 100ml heptane and the shearing time was 1 minute. V_T = 10ml; ϕ = 0.2.

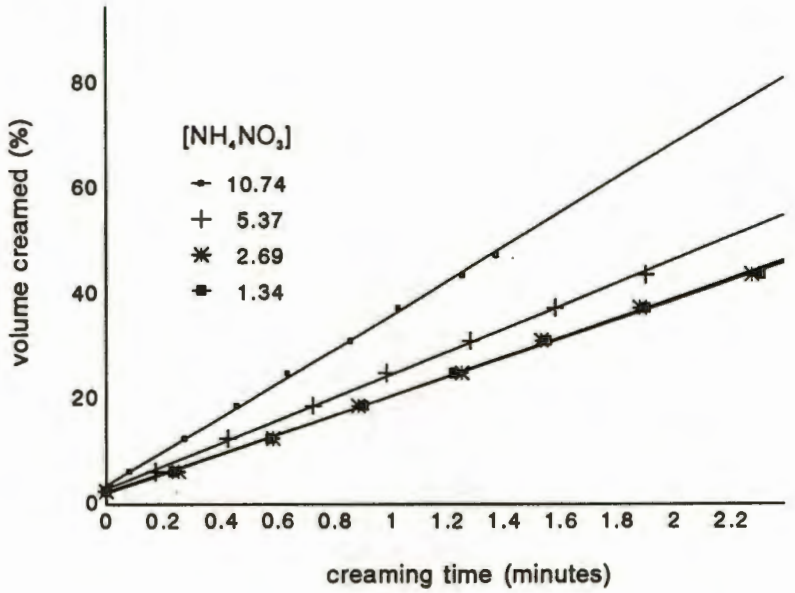

Figure 4.20

Plot of the change in the volume percent creamed with time for a series of emulsions where the ionic strength of the ammonium nitrate aqueous phase was varied. The organic phase contained 0.7g CRILL per 100ml heptane and the shearing time was 1 minute. V_T = 10ml; ϕ = 0.2.

Size distribution constants were obtained from the initial creaming rates shown in figure 4.20. The affect of density difference upon the initial creaming was corrected for and the size distribution constants shown in Table 4.3 obtained. These constants together with the same constants obtained from Malvern experimental measurements are plotted in figure 4.21. Both methods show that an increase in the salt concentration appears to result in an initial decrease in the average droplet size and then an increase. The correlation between the results obtained using the different techniques is most gratifying.

The final cream volumes for the same series of emulsions are plotted in figure 4.22. The final cream volume decreases and then increases as the salt concentration of the aqueous phase increases. The final internal phase volume appears to increase above 74% which tends to confirm that the droplets in the cream are 100% aggregated.

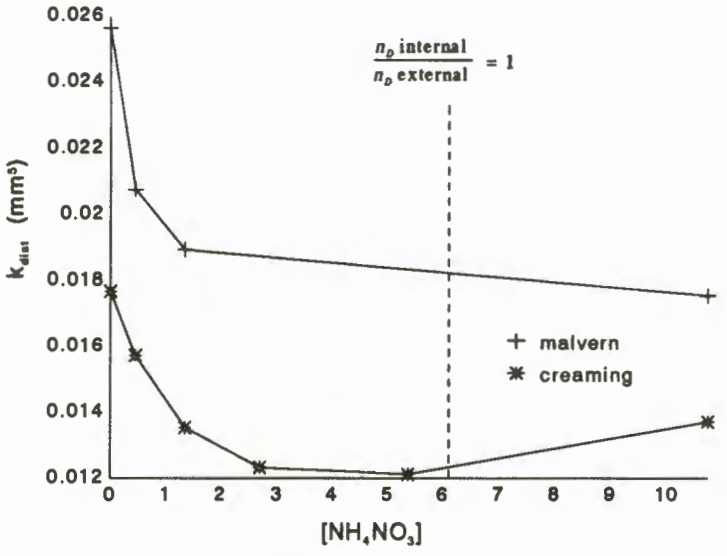

Figure 4.21

Plot of the size distribution constants obtained from malvern and creaming rate studies for a series of emulsions where the ammonium nitrate concentration of the aqueous phase was varied. The organic phase contained 0.7g CRILL per 100ml heptane and the shearing time was 1 minute. V_T = 10ml; ϕ = 0.2.

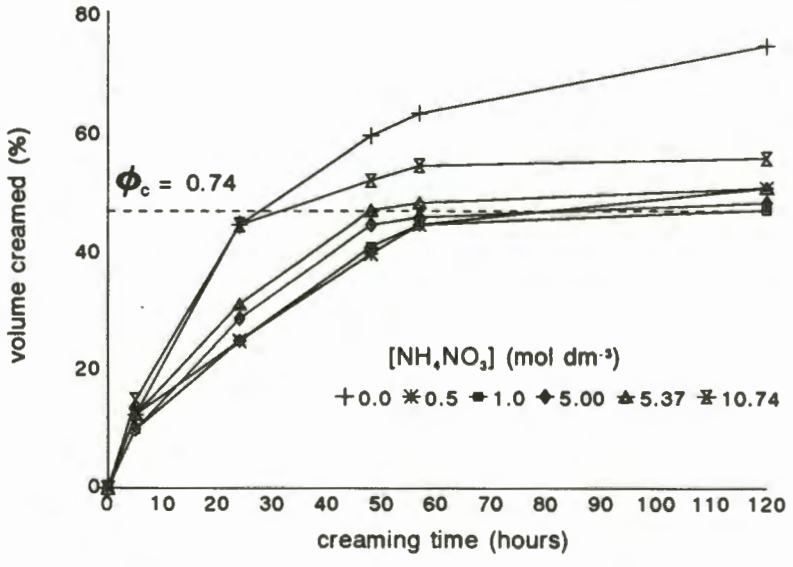

Figure 4.22

Plot of the change in the volume percent creamed with time for a series of emulsions where the ionic strength of the ammonium nitrate aqueous phase was varied. The organic phase contained 2.0g CRILL per 100ml heptane, V_T = 10ml, ϕ = 0.6 and the shearing time was 1 minute.

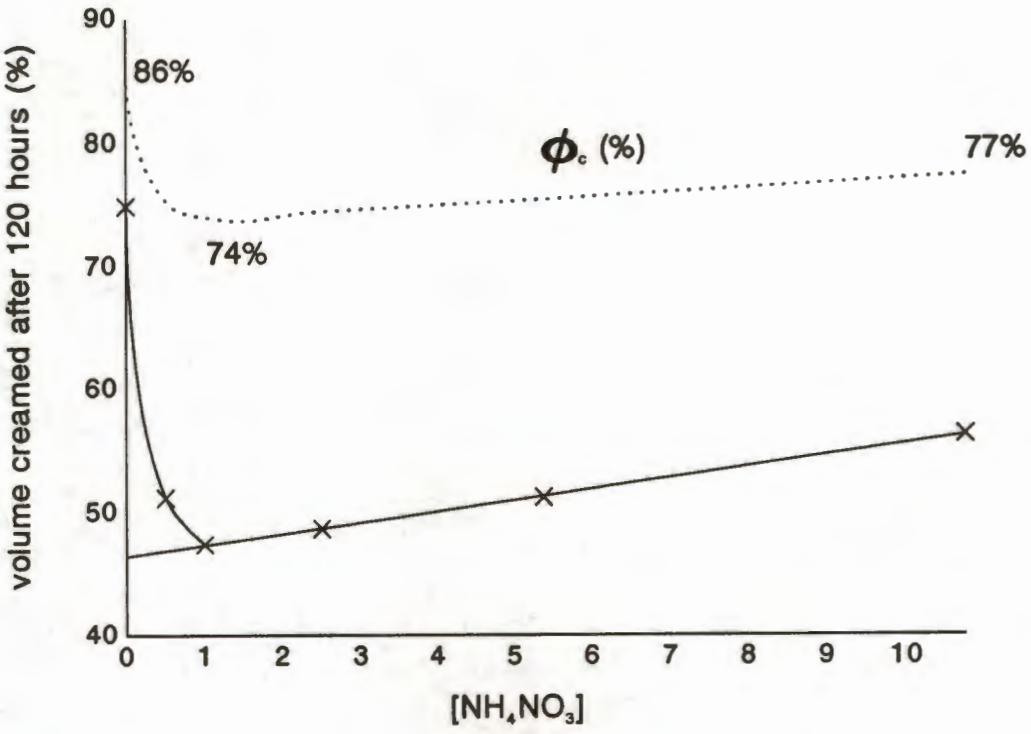

Figure 4.23

Plot of the change in the volume percent creamed after 120 hours for a series of emulsions where the ionic strength of the ammonium nitrate aqueous phase was varied. The organic phase contained 2.0g CRILL per 100ml heptane, V_T = 10ml, ϕ = 0.6 and the shearing time was 1 minute.

The initial decrease in droplet size can be explained in terms of initial clumping or coalescence. In the absence of salt the droplets will clump and coalesce more easily due to a decrease in electrostatic repulsion. As the salt concentration increases this affect will diminish. The increase in droplet sizes at high salt concentrations is due to the shearing process itself. As the density of the aqueous phase is increased it will increase the bulk viscosity of the solution and the association of ions in the Stern layer at the interface will result in the formation of a rigid film with a corresponding increase in interfacial shearing. Both of these factors will result in less efficient shearing and larger droplets. These results correlate well with results from other workers in this field.[32]

The creaming rate data also correlates well with final cream volumes. The larger the droplets, the more easily they can be deformed and hence the higher the internal phase volume will be.

The creaming results suggest that creaming with resultant clumping proceeds at a faster rate than coalescence confirming theoretical predictions that creaming reduces the energy barrier to clumping. When the density difference between the two phases is large, creaming is significant and coalescence is the rate determining step.

Figures 4.24 to 4.26 show the changes in the emulsion as the salt concentration is increased. As the salt concentration increases the amount of aggregation and distortion of the droplets increases. The cream containing droplets of saturated ammonium nitrate appeared to be distorted into hexagonal type packing. Creaming results showed that the internal phase volume of the final cream increased as the salt concentration increased, confirming the trend visible from the photographs.

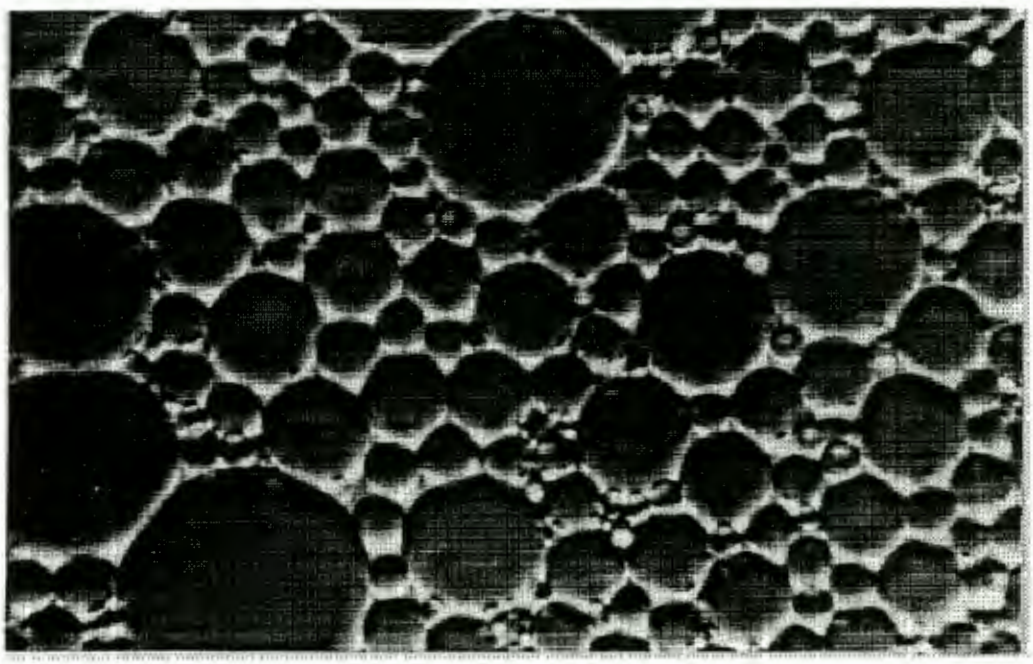

Figure 4.24

Scanned photograph of the droplets of an emulsion (scale = 130:1). Emulsion formulation: aqueous phase = 1*M* NH_4NO_3; organic phase = 0.7g crill per 100ml heptane; shearing time = 10s; V_T = 10ml; ϕ = 0.2.

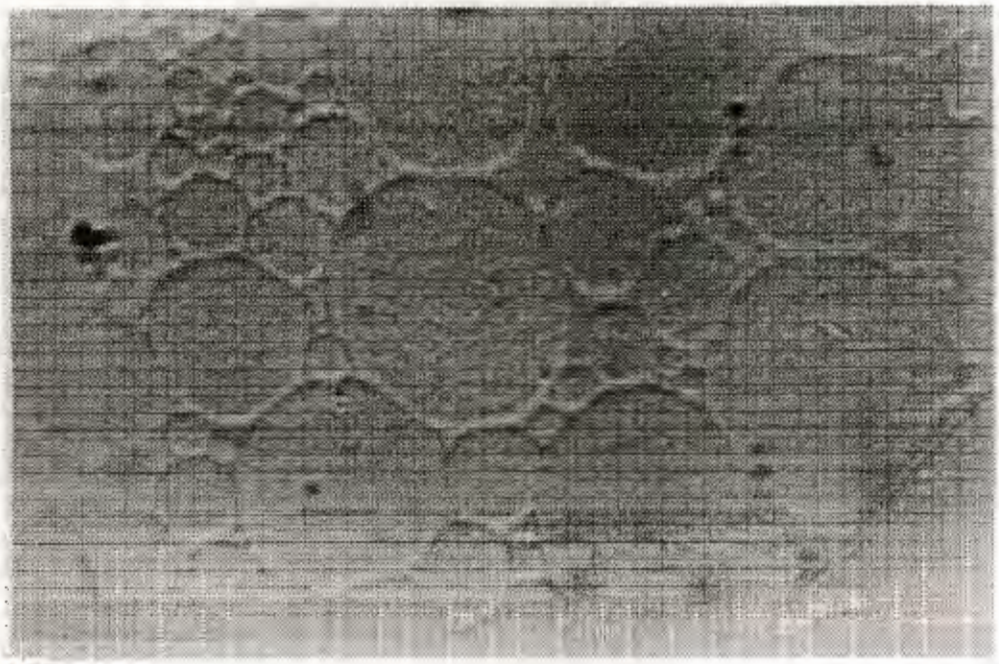

Figure 4.25

Scanned photograph of the droplets of an emulsion (scale = 130:1). Emulsion formulation: aqueous phase = 5*M* NH_4NO_3; organic phase = 0.7g crill per 100ml heptane; shearing time = 10s; V_T = 10ml; ϕ = 0.2.

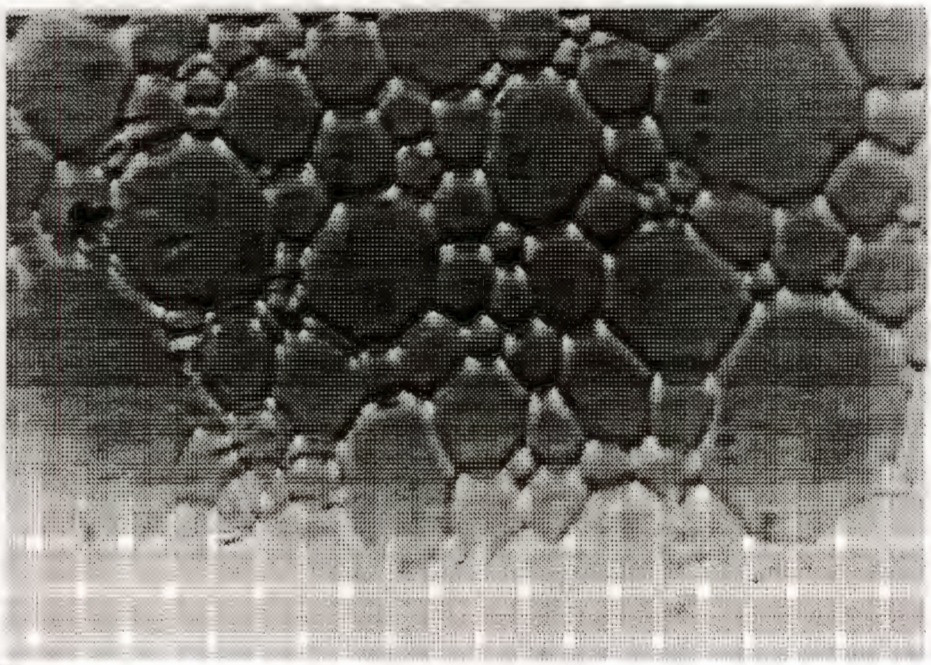

Figure 4.26

Scanned photograph of the droplets of an emulsion (scale = 130:1). Emulsion formulation: aqueous phase = saturated NH_4NO_3; organic phase = 0.7g crill per 100ml heptane; shearing time = 10s; V_T = 10ml; ϕ = 0.2.

4.4.3.3 SHEARING TIME

Changing the shearing as shown in figure 4.27 has a dramatic affect on the creaming rate of an emulsion. The initial creaming rate, the inflexion point and the final cream volume all change with a change in shearing time.

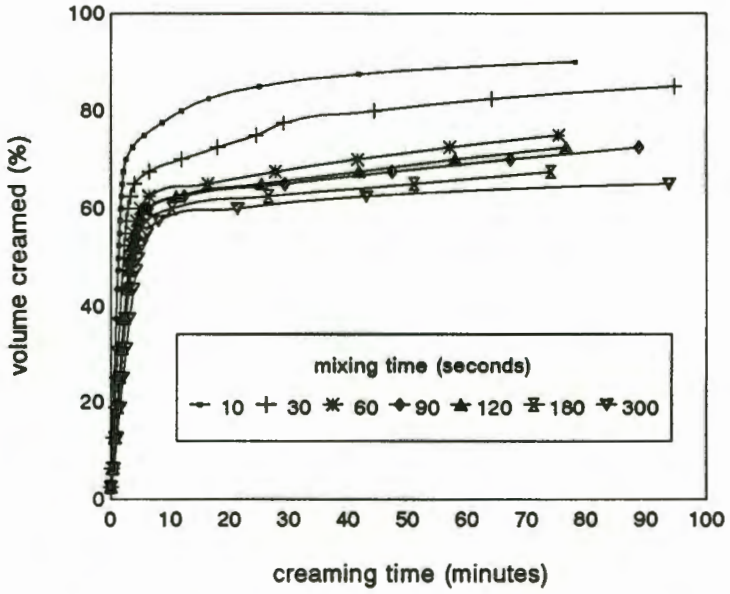

Figure 4.27

Plot of the change in the volume percent creamed with time for a series of emulsions where only the shearing time was varied. The organic phase contained 0.7g CRILL per 100ml heptane and the aqueous phase contained 1*M* NH_4NO_3. V_T = 10ml; ϕ = 0.2.

Figure 4.28 illustrates that as the shearing time is increased, the initial creaming rate decreases. As the formulation of the emulsions in the study are identical the formulation constant should be constant as the shearing time is increased. Therefore the changes in the initial creaming rate can be unambiguously assigned to changes in the droplet size distribution and the distribution constant. As the shearing time is increased theory would predict that the mean droplet size and hence k_{dist} would decrease and the creaming rate would decrease. The experimental results confirm this. The size distribution constants calculated from figure 4.29 are given in Table 4.3. Both Malvern and creaming results show that this affect is most pronounced when the shearing time is initially increased but the affect gradually levels off. The close correlation between malvern and creaming results when considering that the size

parameter is multiplied five times is gratifying.

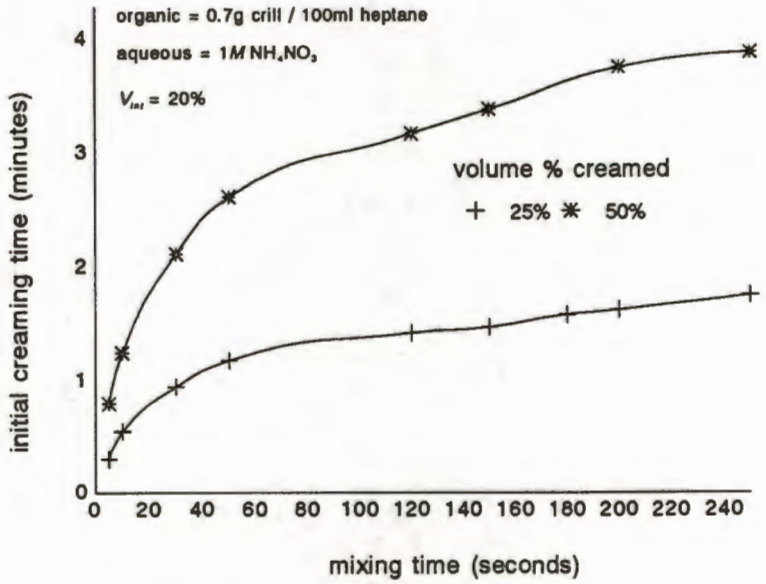

Figure 4.28

Plot of the time taken to cream to a set volume for a series of emulsions where only the shearing time was varied. The organic phase contained 0.7g CRILL per 100ml heptane and the aqueous phase contained 1*M* NH_4NO_3. V_T = 10ml; ϕ = 0.2.

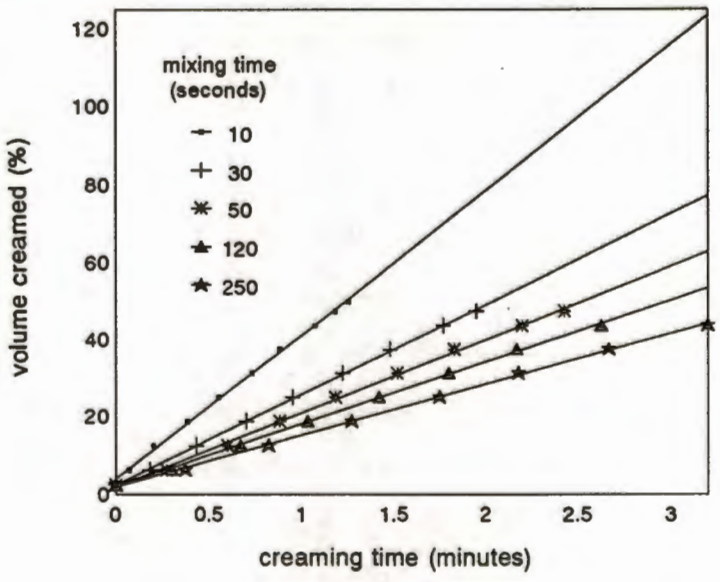

Figure 4.29

Plot of the volume percent creamed versus time for a series of emulsions where only the shearing time was varied. The organic phase contained 0.7g CRILL per 100ml heptane and the aqueous phase contained 1*M* NH_4NO_3. V_T = 10ml; ϕ = 0.2.

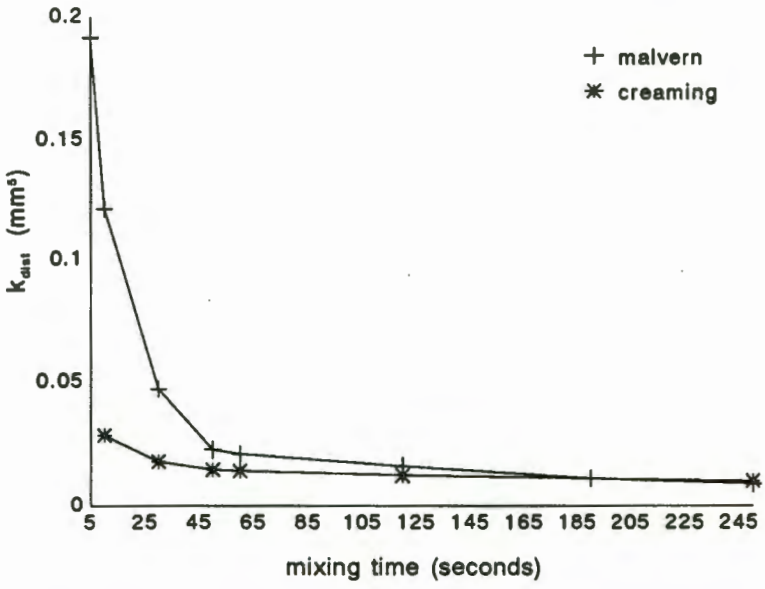

Figure 4.30

Plot of the size distribution constants obtained from malvern and creaming rate studies for a series of emulsions where the shearing time was varied. The organic phase contained 0.7g CRILL per 100ml heptane and the aqueous phase contained 1*M* NH_4NO_3. V_T = 10ml; ϕ = 0.2.

Figure 4.32 illustrates that as the shearing time increases, so the volume at the inflexion point decreases and the final volume decreases. The change in the inflexion point can be explained as follows. As the shearing time increases, so the number of droplets increases and their average size decreases, therefore the probability that droplets will interact or collide increases. The internal phase volume ratio of the cream varies between 71 and 81% (see figure 4.31). As the size of a droplet increases the ease with which it can be distorted geometrically increases and hence the concentration of the cream should increase. The correlation between the trends observed in figure 4.31 and 4.32 confirms this. The flattening of large droplets explains the decrease in the concentration of the cream as the shearing time is increased. When the final cream volume is below 74% the droplets can no longer be considered to be completely aggregated. It appears that in previous results the reason the internal cream volume tended to 74% can be assigned to the size of droplets obtained when shearing times of 60 seconds were used.

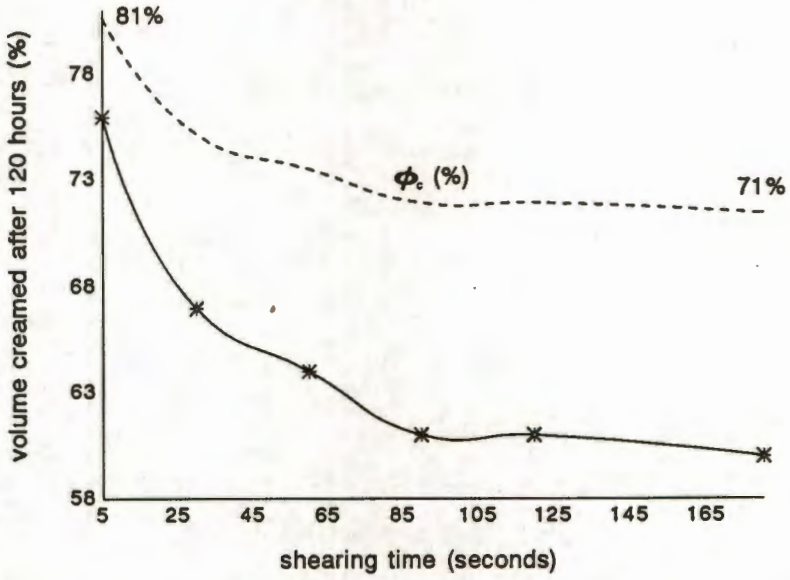

Figure 4.31

Plot of the change in the volume percent creamed after 120 hours for a series of emulsions where the shearing time was varied. The organic phase contained 1.2g CRILL per 100ml heptane, V_T = 10ml, ϕ = 0.5 and the aqueous phase contained 1*M* NH_4NO_3.

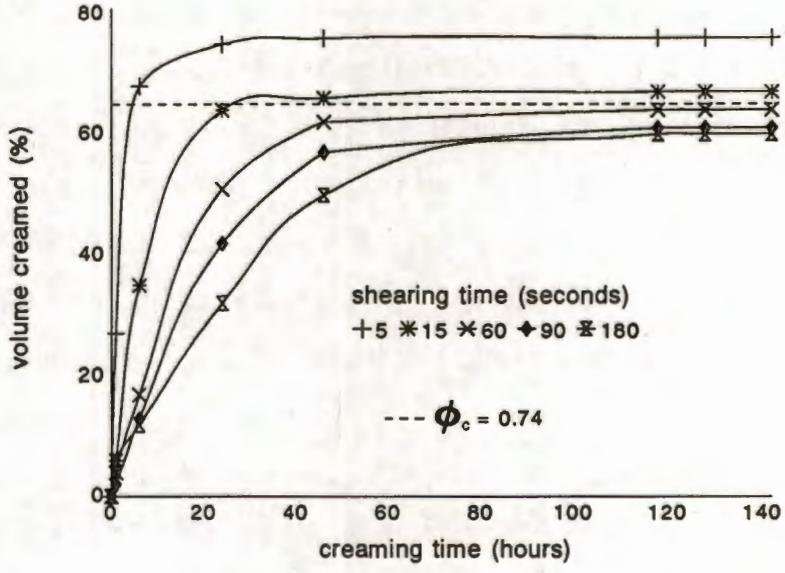

Figure 4.32

Plot of the change in the volume percent creamed with time for a series of emulsions where the shearing time was varied. The organic phase contained 1.2g CRILL per 100ml heptane, V_T = 10ml, ϕ = 0.5 and the aqueous phase contained 1*M* NH_4NO_3.

Optical Microscopy results show that as the shearing time increased the affect on the average droplet size was very marked. After shearing for 1 minute the droplets were so small they tested the resolution of this technique. Figures 4.33 to 4.35 show the changes in the emulsion droplets as the shearing time for an emulsion is increased. These results are in agreement with stochastic modelling results obtained by Mendibourne *et al.* The author predicted a log normal droplet distribution with the geometric mean and standard deviation both decreasing as the speed of rotation of the mixer increased.[34]

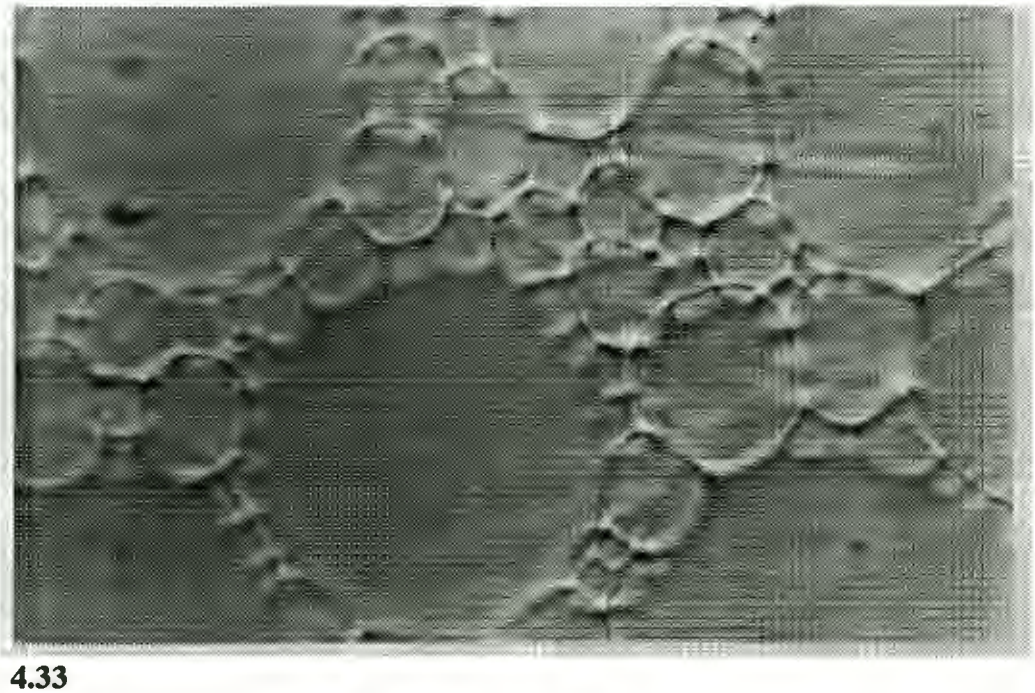

Figure 4.33

Scanned photograph of the droplets of an emulsion (scale = 130:1). Emulsion formulation: aqueous phase = 1*M* NH_4NO_3; organic phase = 1.0g crill per 100ml heptane; shearing time = 5s; V_T = 10ml; ϕ = 0.2.

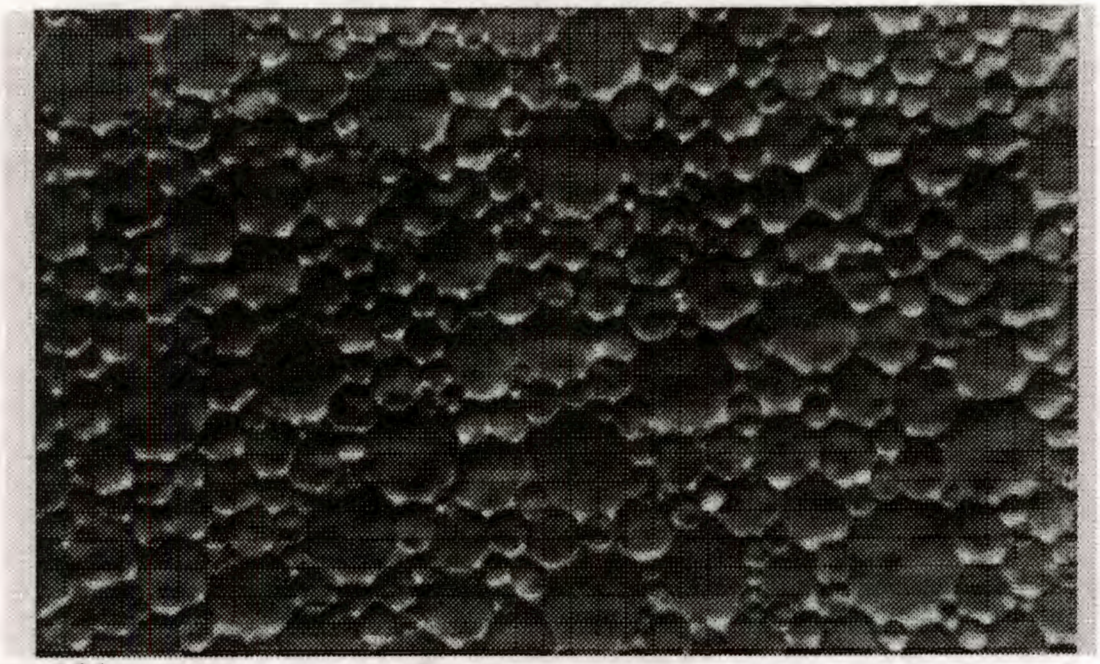

Figure 4.34

Scanned photograph of the droplets of an emulsion (scale = 130:1). Emulsion formulation: aqueous phase = 1*M* NH_4NO_3; organic phase = 1.0g crill per 100ml heptane; shearing time = 15 seconds; V_T = 10ml; ϕ = 0.2.

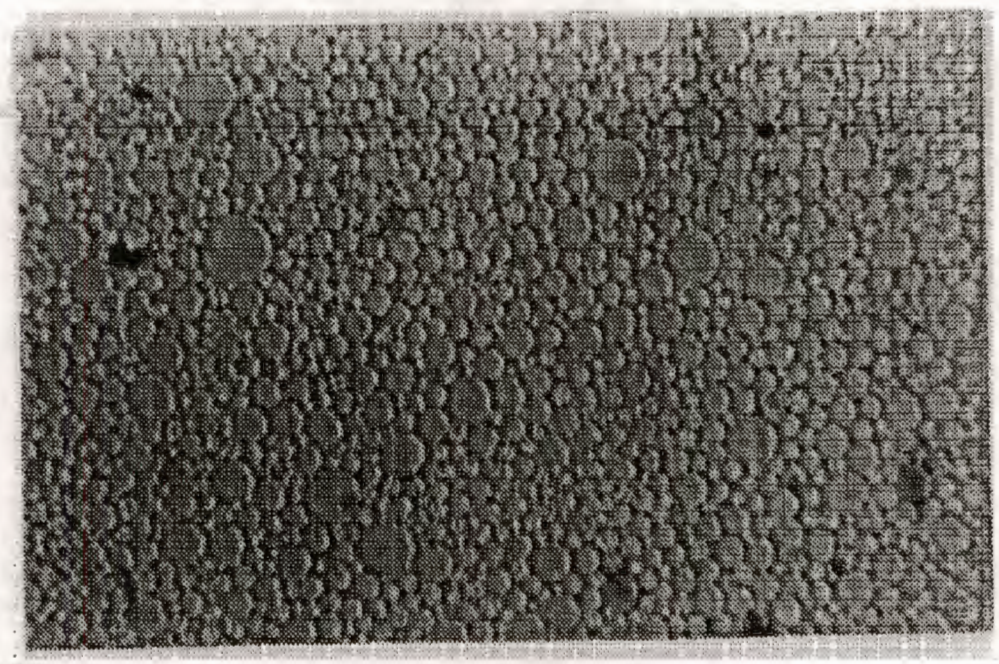

Figure 4.35

Scanned photograph of the droplets of an emulsion (scale = 130:1). Emulsion formulation: aqueous phase = 1*M* NH_4NO_3; organic phase = 1.0g crill per 100ml heptane; shearing time = 2 minutes; V_T = 10ml; ϕ = 0.2.

4.4.3.4 PH OF AQUEOUS PHASE

Figures 4.36 to 4.39 display creaming results obtained for a series of emulsions where the only formulation change was a change in the pH. These results indicate that there is no significant change in the creaming rate of these emulsions as the pH is changed. However experimentally it was observed that as the pH decreased below neutral, the organic phase became progressively more cloudy. This affect was probably due to some form of precipitation, however the species involved were not identified.

The spread in values which is noticeable in figure 4.39 can be attributed to the changes in density of the aqueous phase and corresponding changes in initial creaming times with the addition of ammonia or nitric acid. These results show the insensitivity of emulsion stability to changes in pH. This correlates well with results from other workers who have shown that o/w emulsions stabilized by non-ionic surfactants are not pH sensitive.[35]

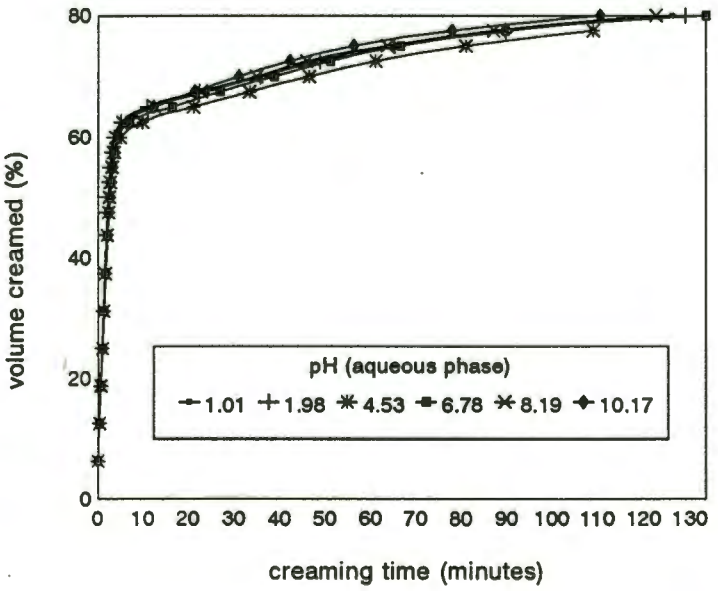

Figure 4.36

Plot of the change in the volume percent creamed with time for a series of emulsions where the pH of the 1*M* ammonium nitrate aqueous phase was varied. The organic phase contained 0.7g CRILL per 100ml heptane and the shearing time was 1 minute. V_T = 10ml; ϕ = 0.2.

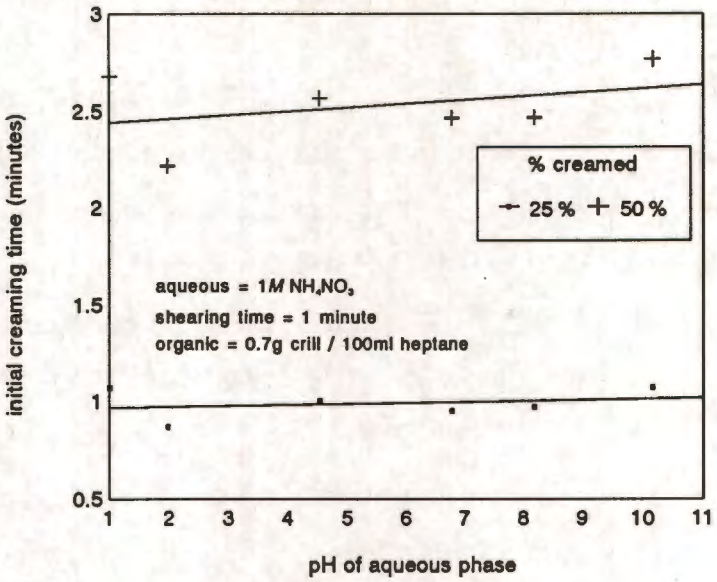

Figure 4.37

Plot of the change in the time taken to cream to a set volume percent for a series of emulsions where the pH of the 1*M* ammonium nitrate aqueous phase was varied. The organic phase contained 0.7g CRILL per 100ml heptane and the shearing time was 1 minute. V_T = 10ml; ϕ = 0.2.

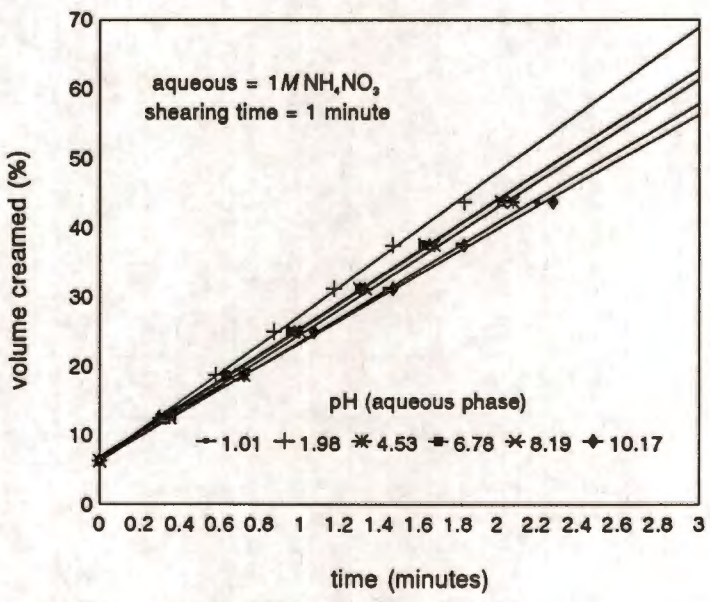

Figure 4.38

Plot of the change in the volume percent creamed with time for a series of emulsions where the pH of the 1*M* ammonium nitrate aqueous phase was varied. The organic phase contained 0.7g CRILL per 100ml heptane and the shearing time was 1 minute. V_T = 10ml; ϕ = 0.2.

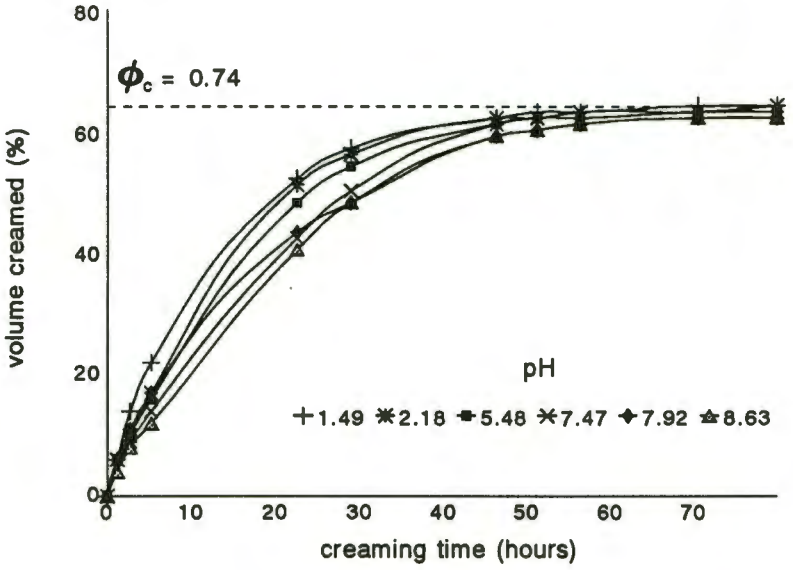

Figure 4.39

Plot of the change in the volume percent creamed with time for a series of emulsions where the pH of the 1*M* ammonium nitrate aqueous phase was varied. The organic phase contained 1.2g CRILL per 100ml heptane and the shearing time was 1 minute. V_T = 10ml; ϕ = 0.5.

4.4.3.5 STORAGE TIME

Figures 4.40 - 4.43 show the change in two emulsion droplet distributions as each emulsion is allowed to cream for 9 days. The change in droplet size distribution due to the coalescing of droplets in the cream is quite evident. These results confirm theoretical predictions that if the density difference between two phases is significant and a good surfactant is used, the rate of creaming will be greater than the rate of coalescence. As creaming decreases the energy barrier to clumping, the rate determining step will be emulsion coalescence and the emulsion stability will be determined by the rate of emulsion coalescence.

For both emulsions the formulations were the same although the shearing time varied resulting in different initial droplet sizes. The emulsion that had been sheared for 2 minutes appeared to be quite stable after 9 days storage while the emulsion that had only been sheared for 5 seconds showed signs of breaking up. These results indicate that a decrease in the initial droplet size results in an increase of stability.

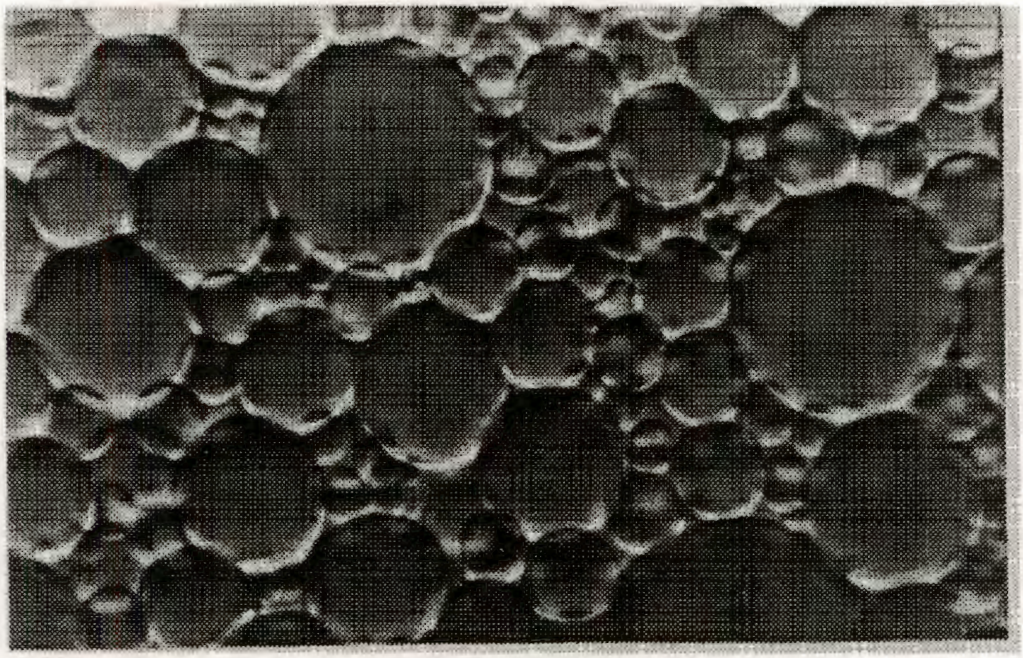

Figure 4.40

Scanned photograph of the droplets of an emulsion (scale = 130:1). Emulsion formulation: aqueous phase = 1*M* NH_4NO_3; organic phase = 1.0g crill per 100ml heptane; shearing time = 5 seconds; V_T = 10ml; ϕ = 0.2. Stored for 4 hours.

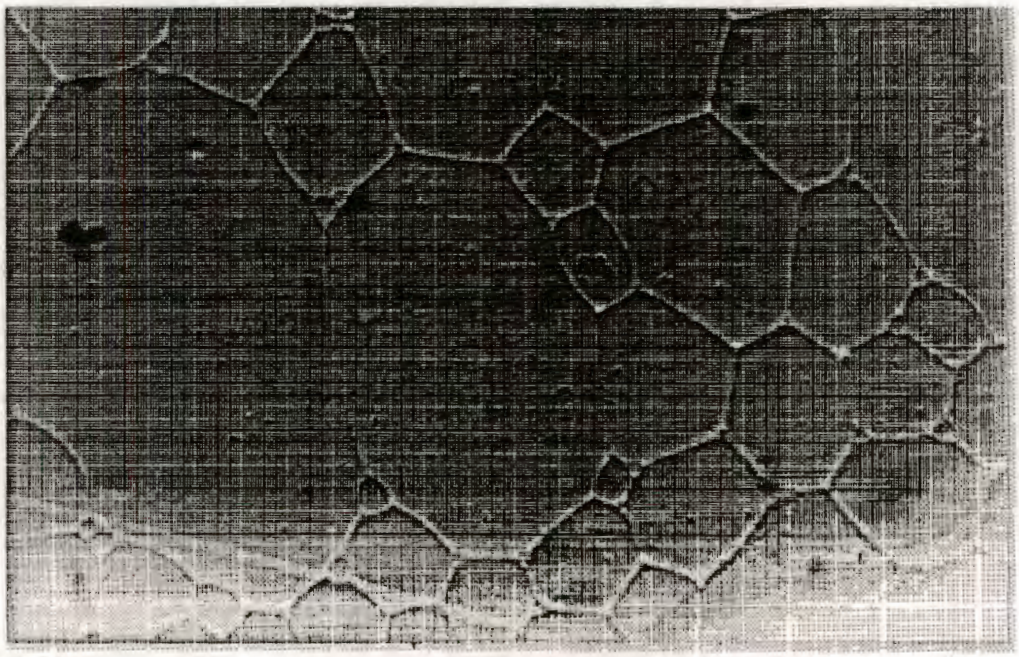

Figure 4.41

Scanned photograph of the droplets of an emulsion (scale = 130:1). Emulsion formulation: aqueous phase = 1*M* NH_4NO_3; organic phase = 1.0g crill per 100ml heptane; shearing time = 5 seconds; V_T = 10ml; ϕ = 0.2. Stored for 9 days.

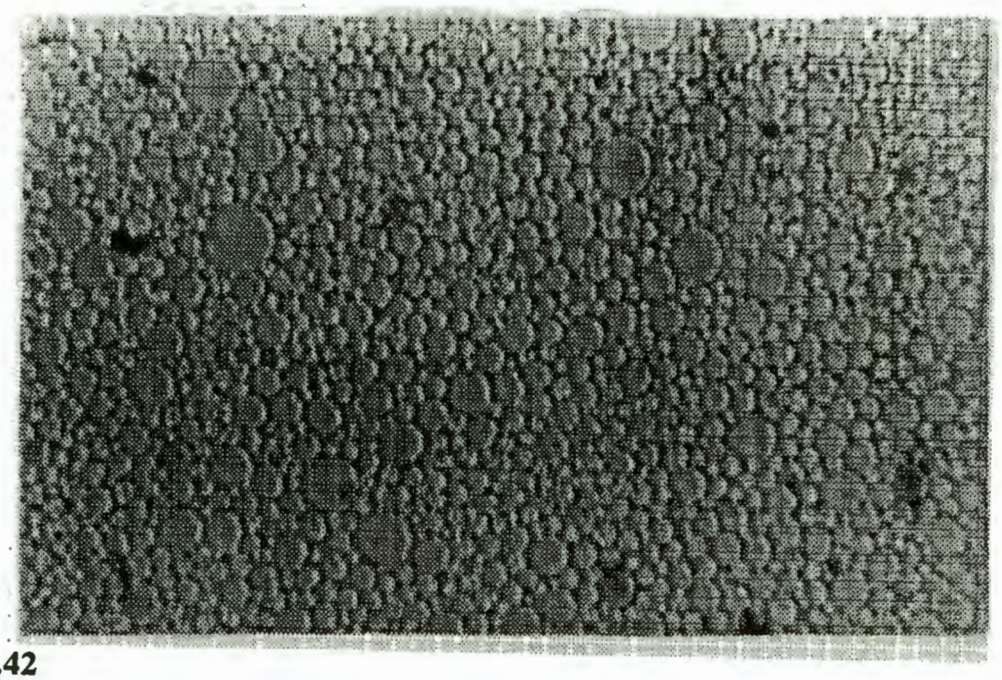

Figure 4.42

Scanned photograph of the droplets of an emulsion (scale = 130:1). Emulsion formulation: aqueous phase = 1*M* NH_4NO_3; organic phase = 1.0g crill per 100ml heptane; shearing time = 2 minutes; V_T = 10ml; ϕ = 0.2. Stored for 3 hours.

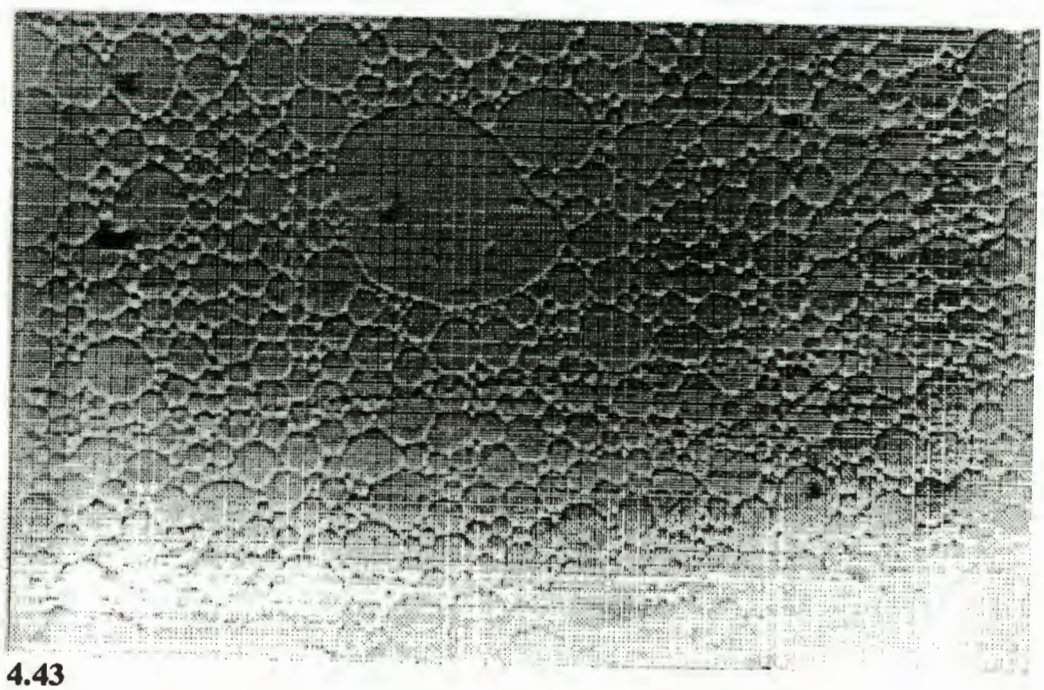

Figure 4.43

Scanned photograph of the droplets of an emulsion (scale = *:1). Emulsion formulation: aqueous phase = 1*M* NH_4NO_3; organic phase = 1.0g crill per 100ml heptane; shearing time = 2 minutes; V_T = 10ml; ϕ = 0.2. Stored for 9 days.

4.5 CONCLUSIONS

These results indicate that creaming rate measurements are simple, fast, inexpensive and effective in studying emulsion stability. The equations developed here to obtain size distribution data from creaming data were of great use and the correlation of size data from creaming and malvern studies was pleasing. Optical microscopy and laser particle sizing are two useful complementary techniques. Optical microscopy is not recommended as an accurate technique in particle sizing because it underestimates the number of small particles and is slow and inaccurate, however it is invaluable in observing relative trends and giving a visual picture of the droplet structure. The Malvern particle sizer is the recommended instrument for studying w/o emulsion particles. Unfortunately because of the close refractive indexes of our aqueous and organic phase a lot of work had to be done in converting the light data appropriately. When the refractive index ratio of the two phases was too close to unity the technique became unreliable. Of the three experimental techniques used the Malvern and creaming techniques could only be used on dilute emulsions, whereas optical microscopy could give images of concentrated emulsions.

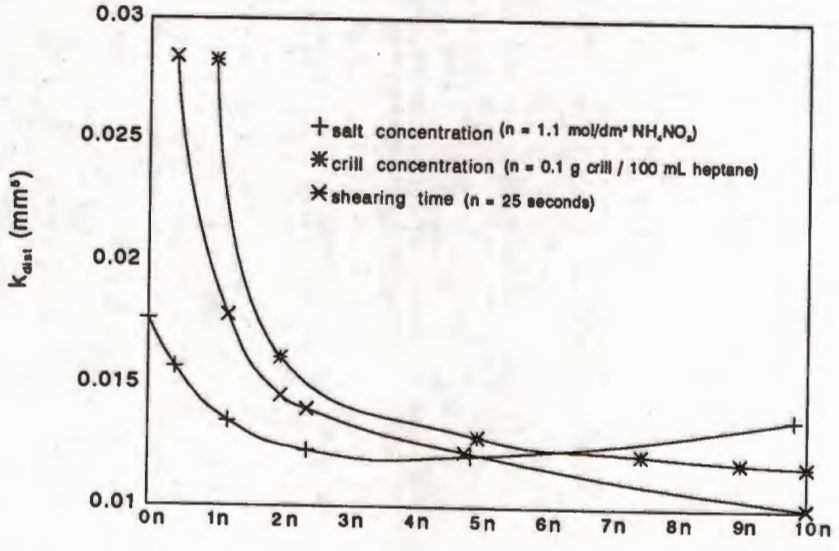

Figure 4.44

Plot of the change in the droplet distribution constant, k_{dist}, against the change in different formulation properties. The experimental results are given in table 4.3. In all cases V_T = 10ml and ϕ = 0.2.

The emulsion experimental studies performed were limited to a simple w/o emulsion system. The nonionic surfactant blend, crill 43 which was used, is used industrially. The aqueous phase of the emulsion was an ammonium nitrate solution and the organic phase was n-heptane. The affect of changes in stability with regard to changing the following four variables was studied:

- ionic strength
- pH
- surfactant concentration
- shearing time.

Changes in pH for this system appeared to have no affect on the stability of the emulsion. Figure 4.44 shows how changes in salt concentration, surfactant concentration and shearing time affect the droplet size distribution data obtained from creaming results. The droplet size distribution appears to be determined to the greatest extent by the shearing time and the surfactant concentration.

Having demonstrated the applicability of these experimental techniques to the study of the effects of pH, surfactant concentration, shearing time and salt concentration on w/o emulsion stability these techniques can now be used to study other effects. The creaming technique is a useful technique for obtaining size distribution data from creaming rate studies of emulsions or dispersions where the two phases have different densities. Where the two phases have different refractive indexes, the laser particle sizing technique can be used. However, in situations where the continuous and dispersed media have similar refractive indexes, the software developed in this thesis has to be used or erroneous results are obtained.

4.6 REFERENCES

1. J.Th.G.Overbeek (1977), "Recent Developments in the Understanding of Colloid Stability", *J.Colloid Interface Science*, **58**:408.
2. D.E.Tambe and M.M.Sharma (1993), "Factors Controlling the Stability of Colloid-Stabilized Emulsions", *J.Colloid Interface Science*, **157**:244.
3. P.Pithayanukul and N.Pilpel (1982), "Stabilization of Some Emulsions with Nonionic Surfactants", *J.Colloid Interface Science*, **89**:494.
4. Shun-ichi Noro, Akira Takamura and Masumi Koishi (1979), "Evaluation of Emulsion Stability. Effect of Tween Group Emulsifiers on Stability of o/w Type Emulsions", *Chem. Pharm. Bull.*, **27(2)**:309.
5. J.L.Cavallo and D.L.Chang (1990), "Emulsion Preparation and Stability", *Chem.Eng.Progress*, **86**:54
6. P.Sherman (1968), "General Properties of Emulsions and their Constituents", in *Colloid Science*, P.Sherman (ed.), Academic Press, London, ch. 3, p. 131.
7. S.S.Davis and A.Smith (1976), "The Stability of Hydrocarbon Oil Droplets at the Surfactant/Oil Interface", *Colloid & Polymer Science*, **254**:82.
8. L.E.Nielsen, R.Wall and G.Adams (1958), "Coalescence of Liquid Drops at Oil-Water Interfaces", *J.Colloid Science*, **13**:441.
9. E.Dickinson (1992), "Interfacial Interactions and the Stability of oil-in-water Emulsions", *Pure & Appl.Chem.*, **64**:1721.
10. J.W.McBain (1950), *Colloid Science*, D.C.Heath, Boston, p. 26.
11. R.Buscall (1978), "The properties of o/w Emulsions stabilised with a non-ionic surfactant-polymer mixture", *Prog.Colloid & Polymer Science*, **63**:15.
12. O.D.Velev, T.D.Gurkov, S.K.Chakarova, I.B.Ivanov and R.Borwankar (1994), "Experimental Investigations on Model Emulsion Systems Stabilized with Non-ionic Surfactant Blends", *Colloids and Surfaces A:*, **83**:43.
13. Paul Becher (1965), *Emulsions: Theory and Practice*, Reinhold Publishing Corporation, New York, 2nd Ed.
14. D.Fairhurst, M.P.Aronson, M.L.Gum and E.D.Goddard (1983), "Comments on Non-Ionic Surfactant Concentration Effects in o/w Emulsions", *Colloids and Surfaces*, **7**:153.

15. D.J.Brown, E.J.Weatherby and K.Alexander (1988), "Shape, Concentration and Anomalous Diffraction Effects in Sizing Solids in Liquids", in *Optical Particle Sizing. Theory and Practice*, G.Gouesbet and G.Grehan (ed.), Plenum Press, New York, p. 351.

16. K.A.Kusters, J.G.Wijers and D.Thoenes (1990), "Determination of Particle Size Distributions of Ice Crystals in Aqueous Solutions using Laser Diffraction Spectrometry", *Proc.2nd Int.Congress Optical Particle Sizing*, Arizona State University:585.

17. K.A.Kusters, J.G.Wijers and D.Thoenes (1991), "Particle Sizing by Laser Diffraction in the Anomalous Regime", *Applied Optics*, **30**:4839.

18. A.Boxman, H.G.Merkus, P.J.T.Verheijen and B.Scarlett (1990), "Enhanced Deconvolution of Light Scattering Patterns by Observing Intensity Fluctuations", *Proc.2nd Int.Congress Optical Particle Sizing*, Arizona State University:178.

19. N.S.Lightfoot (1990), "The Effect of Optical Properties of Particles and Dispersing Media on Particle Size Analysis by Laser Diffraction", *Proc.2nd Int.Congress Optical Particle Sizing*, Arizona State University:511.

20. J.C.Knight, D.Ball and G.N.Robertson (1990), "Characterization of Monodisperse and Multimodal Size Distributions by Measurement of Forward Scattered Light", *Proc.2nd Int.Congress Optical Particle Sizing*, Arizona State University:580.

21. M.N.Treiner, P.J.Freud and E.L.Weiss (1990), "Particle Size Measurement-Impulse Response Model for Inversion of Scattered Light", *Proc.2nd Int.Congress Optical Particle Sizing*, Arizona State University:169.

22. T.Allen (1981), *Particle Size Measurement*, Chapman and Hall, London, 3rd Ed.

23. A.Raule (1993), "The Importance of Particle Sizing in the Coatings Industry", *First International Paint Congress, Technopinturas, Buenos Aires*, Argentina.

24. D.Lisiecki, P.Allano and M.Ledoux (1988), "Some Aspects of Utilization of Malvern Diffraction Granulometer", in *Opticle Particle Sizing. Theory and Practice*, G.Gouesbet and G.Grehan (ed.), Plenum Press, New York, p. 559.

25. G.H.Jeffery, J.Bassett, J.Mendham and R.C.Denney (1989), *VOGEL's Textbook of Quantitative Chemical Analysis*, Longman Scientific & Technical, London, 5th Ed.

26. J.T.Davies and E.K.Rideal (1961), *Interfacial Phenomena*, Academic Press, London.

27. R.C.Weast (1982), *CRC Handbook of Chemistry and Physics*, CRC Press, Florida,

63rd Ed.

28. R.Pons, J.C.Ravey, S.Sauvage, M.J.Stebe, P.Erra and C.Solans (1993), "Structural Studies on Gel Emulsions", *Colloids and Surfaces A*, **76**:171.

29. S.G.Frank and G.Zografi (1969), "Solubilization of Water by Dialkyl Sodium Sulfosuccinates in Hydrocarbon Solutions", *J.Colloid Interface Science*, **29**:27.

30. A.K.Chattopadhyay, M.Drifford and C.Treiner (1985), "Evidence for Aggregates of Cationic Surfactants in Dilute Methanolic Solution of Benzene", *J.Phys.Chem.*, **89**:1537.

31. F.A.M.Leermakers, Y.S.Sdranis and R.D.Groot (1994), "On the Colloidal Stability of W/O Emulsions", *Colloids and Surfaces A*, **85**:135.

32. C.Solans, R.Pons, S.Zhu, H.T.Davis, D.F.Evans and K.Nakamura (1993), "Statistical Geometry of Random Heaps of Equal Hard Spheres.", *Langmuir*, **9**:1479.

33. D.M.Heyes and J.R.Melrose (1993), "Brownian Dynamics Simulations of Model Hard-Sphere Suspensions", *J.Non-Newtonian Fluid Mechanics*, **46**:1.

34. B.Mendiboure, A.Graciaa, J.Lachaise, G.Marion and M.Bourrel (1991), "Influence of the Intensity of Mixing on the Droplet Size Distribution of emulsions", *Prog.Colloid & Polymer Science*, **84**:338.

35. A.Kamel, V.Sadek and S.N.Srivastava (1978), "The Role of Non-ionic Surfactants in Emulsion Stability", *Prog.Colloid & Polymer Science*, **63**:3.

CHAPTER FIVE
W/O EMULSION COMPUTER MODEL

5.1 INTRODUCTION

Up to now, most industrial emulsions are prepared using a trial and error approach which, apart from being time consuming and expensive, does not lead to producing general rules which could be applied to other systems.[1] The advantages of having a predictive computer model which could determine the stability of an emulsion when given the formulation and certain physical properties of the emulsion constituents are many. The model would be able to direct the experimental work of formulators in the correct direction and identify the predominant causes of instability. Inherent in the nature of a model is the fact that it is not a full representation of reality, but it has great power in assisting with the fundamental understanding of complex systems.

When trying to predict emulsion stability, researchers have looked at the energy barrier between droplets and determined whether the droplets would coalesce or not. If the droplets are predicted to coalesce, the emulsion is said to be unstable and *visa versa*. In the field of w/o emulsions, no previous consideration has been given to the consequences of coalescence, namely the stability characteristics of new droplets arising from the coalescence of the original droplets.

When droplets coalesce, the volume of the new droplet is a summation of the volumes of the precursor droplets. The surface area of the new droplet is also greater than that of the precursor droplets, but the relative increase is less. This results in an increase in surface potential and surfactant surface coverage per droplet with coalescence. The increase implies that the new droplets are more stable than the original droplets. Hence the initial coagulation energy barrier and rate cannot completely describe the phenomena of emulsion coagulation.

Hall and co-workers have applied an elegant solution to this problem. Their recursive and stochastic model for o/w emulsions is similar to von Smoluchowski's coagulation equation and determines the extent of coalescence beyond the critical aggregation point.[2-4] A program based on their approach for o/w emulsions has been developed here for the case of w/o emulsions. The program is referred to as STREAC, an acronym for "Stochastic Reverse Emulsion Aggregation and Coalescence". The stability theory for the case of w/o emulsions

is outlined in chapter three. Because of the large differences between the two emulsion types, many changes in methodology have had to be adopted. The following sections deal with the methodology, validation and use of this computer model.

5.2 COMPUTATIONAL METHODOLOGY

The stochastic computational model developed, considers interactions between randomly selected pairs of droplets from an emulsion particle size distribution with statistical weighting depending on the total volume of the particles within each radius interval. For two droplets to coagulate, the net energy for clumping has to be overcome, as well as the minimum energy necessary for coalescence. If the total energy barrier, Δ_T, is less than the thermal energy, kT then the two droplets are predicted to coagulate.

Initially an emulsion of mono-disperse particles, with an initial radius, a_1, surface potential, ψ_1 and surfactant surface coverage, ν_1, is considered. An array of X particle size channels is set up based on volume conservation. Due to memory constraints the particle distribution is restricted to X=300 potential channels. The volume (V), surface area (A), radius (a), surfactant surface coverage (ν) and surface potential (ψ) of the particles in each channel is calculated as a function of the initial particles (eqn. 5.1).

$$V_x = \tfrac{4}{3}\pi a_1^3 x \quad , \quad A_x = 4\pi a_1^2 x^{\frac{2}{3}} \quad , \quad a_x = a_1 x^{\frac{1}{3}} \quad , \quad \nu_x = \nu_1 x^{\frac{1}{3}}$$

$$\psi_x = \frac{a_{x-1}\psi_{x-1}(1+\kappa a_{x-1}) + a_1\psi_1(1+\kappa a_1)}{a_x(1+\kappa a_x)} \qquad \text{....5.1}$$

where $x = 2,3,4,.....X$

Figure 5.1 shows how the volume, radius, surface area, surfactant surface coverage and surface potential increase as a function of the particle size channel. Although the volume increases linearly the increase in the radius, surface area and surface coverage is not as steep. The increase in the surface potential is considerably more than the increase in the radius.

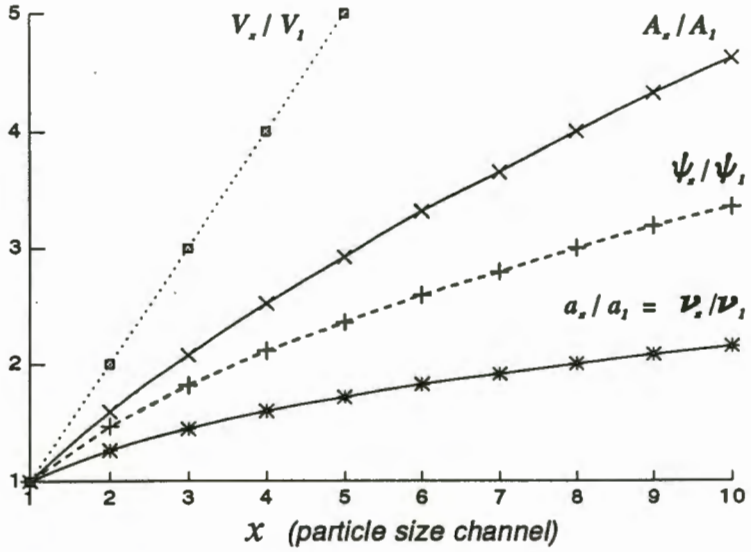

Figure 5.1

Plot of the increase in volume, radius, surfactant surface coverage and surface potential versus the particle size channel

Upon coalescence of two droplets, the array is modified to account for the formation of the new droplet and the removal of the interacting pair of droplets. The interactions between pairs of droplets are considered recursively and produce volume histograms. The program continues until the emulsion is declared stable or unstable. The conditions under which the emulsion is determined to be stable or unstable are discussed in section 5.3.2. These changes in the droplet size distribution curve with time, leading to a distribution with higher diameters are a measure of the instability of an emulsion.[5]

To calculate the coalescence energy barrier for two droplets, the maximum total energy has to be determined. This is done using two different numerical methods. The first procedure calculates a triplet of points, a < b < c, that bracket a maximum, such that f(a) < f(b) > f(c).[6] The second procedure, is a variant of the Brent's method and is used to calculate the maxima once given the bracketing triplet.[6] The energy function has at most two maxima, both of which have to be found. The procedure is first started to the left of the function ($\log H$ = -12) and steps H to the right increasing each step by a constant factor until the function decreases. If the maxima (E_T/kT) is found to be less than one, the search is started from the right of the function where $r=s$, stepping to the left. If the maxima obtained from the right is also less than one, then only do we exit the relevant subroutines, declaring the collision to be successful.

The adapted Brent's method, is a parabolic interpolation method which makes use of the first derivative of the function. The sign of the derivative at the central point of the bracketing triplet a < b < c indicates uniquely whether the next point should be taken in the interval (a,b) or in the interval (b,c). Assuming the interval (b,c) is selected, the procedure ends when either b and c are $2x$.TOL apart. Where x is the abscissa whose ordinate is the best minimum and TOL is the square root of the machine's floating precision. The first and second derivative of E_T with respect to s, were calculated analytically and are represented in appendix 6.

The procedures are written so as to evaluate the energy function (E_T/kT) and its first derivative as few times as possible. If for any value of H, the function (E_T/kT) is found to be larger than one the subroutines are exited and the collision is declared unsuccessful. Similarly to minimize computation, the repulsive energy component of the total interaction energy is calculated first and if $(E_R - E(0))/kT$ is found to be greater than one the other energy components are not calculated and the subroutines are exited and the collision is declared unsuccessful.

This computer program is written for the case in which clumping is the rate determining step and coalescence occurs rapidly. The time of each collision is calculated from the rate of clumping according to equation 2.26. For this reason the computer model is not applicable to emulsions in which the internal phase volume is above 74%. Once the internal phase occupies over 74.05% of the total volume, the emulsion droplets can no longer be considered spherical due to geometrical constraints, and the coalescence theory of Smoluchowski cannot be applied to these very high internal phase volume emulsions.

For small values of the inverse Debye length (κ), the repulsive energy contribution becomes ill conditioned. The limiting values for κ are ill defined and hence a limiting value of 1000 was given for κ. For our system (heptane at 25°C) this translates into an ionic strength of $2\text{x}10^{-15}$ M. An ionic strength below this would in fact be chemically meaningless. Because of the large number of exponential functions used in the repulsive energy calculations, numerical limitations were imposed on these functions so that values would fall within the range of the real type variable used.

5.3 THE COMPUTER PROGRAM - STREAC.EXE

STREAC is an acronym for "Stochastic Reverse Emulsion Aggregation and Coalescence", this modelling program was compiled in Borland Pascal version 7. The program makes extensive use of Turbo Vision, Borland Pascal's object-orientated application framework for windowing programs. The program has a windows feel, with overlapping windows, dialog boxes, pull-down menus and mouse support. The program is very easy to use and instructions are included in the on-line Help. The main features of the program are listed in the following Table and are accessible by either selecting the title of the option using a mouse, using the pull-down menu or pressing the relevant function keys or key combinations.

Table 5.1 Description of the features of the w/o computer program.

Keys	Title	Description
F1	HELP	To display Instructions on how to navigate around the program and to perform a computational run
F2	DATA	To open the Data Input Window
F3	SAVE	To save the values in the Data Input window to the input text file
F9	GO	To start a computational run using the input values from the Data Input window
F10	MENU	To access the Menu options
Alt-X	EXIT	To exit the program

Figure 5.2 depicts the screen with the Data Input window open. When the program starts, the input parameters are read in from a input text file (EMUL_IN.DAT). If the file is not found the program will produce the default input parameters as depicted in Figure 5.2. At any point selecting SAVE will result in the values currently in the Data Input window to be saved in the input text file. This file also includes comprehensive descriptions of the input parameters.

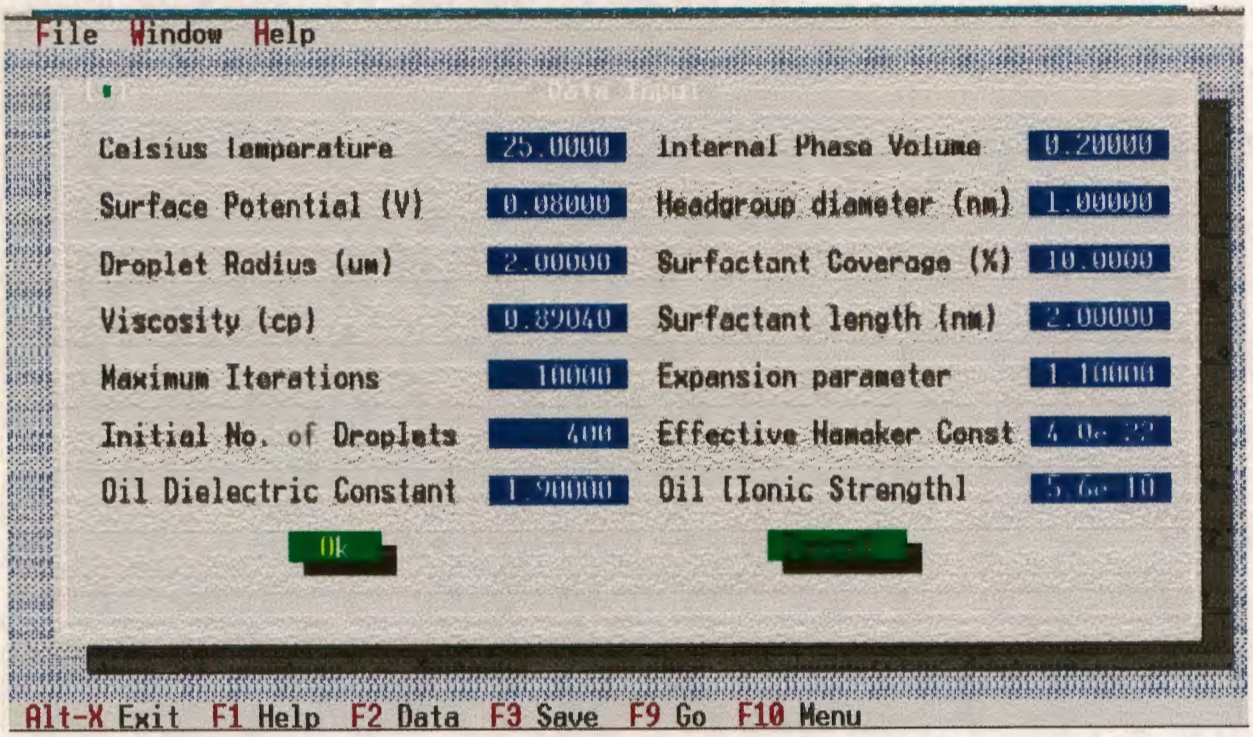

Figure 5.2
Screen capture of w/o emulsion computer program screen with the Data Input window open.

The Borland Pascal version 7 source code for this computer program is included in appendix 1, the executable (STREAC.EXE) is supplied on disk 1 of the included 1.44 Mb diskettes and the equations used are given in appendix 6. Appendix 7 has instructions on how to execute STREAC as well as a complete listing of the files on disk 1. A concurrent program which calculates the rate of coalescence has been written. This model which we have not refined is included in appendix 3.

5.3.1 INPUT PARAMETERS

Table 5.2 lists the emulsion experimental parameters needed to perform the simulated coalescence. The default value for each parameter, that is used in most simulations is included in the table. Reasons for choosing the default values for our experimental system are included.

Table 5.2 List of input values to calculate emulsion coalescence.

symbol	Description	default value	units
A_{eff}	effective Hamaker constant	4×10^{-22}	J
a_1	initial radius of particles	2	μm
α	expansion parameter for surfactant in emulsion	1.1	-
ε_r	relative permittivity of organic phase	1.9 (heptane)	-
η	oil phase viscosity	0.8904	centipoise
d_s	minimum distance between surfactant centres on droplet surface	1	nm
I	ionic strength of organic phase	5.6×10^{-10}	mol dm^{-3}
l	average length of surfactant in emulsion	2	nm
MI	maximum number of iterations to be performed	10000	-
N	number of emulsion particles to be analyzed	400	-
%cov	Initial percentage surfactant coverage	10	%
T	temperature of emulsion	25	°C
ϕ	internal phase volume ratio of emulsion	0.2	-
ψ_1	initial surface potential of particles	0.08	V

- **MI**, the maximum number of iterations to be performed, and the number of emulsion particles, N, can be varied per simulation. As these values are increased, the size distribution becomes more accurate at the cost of an increase in computational time per simulation.
- Experimentally for our emulsion system, the emulsion droplet radius, a, varied from 2μm upwards, mostly as a function of the shearing time and rate. When predicting emulsion stability this parameter was varied from 1μm up, as the initial droplet radius before initial coalescence would be less than 2μm.
- The temperature, **T**, for all experimental and theoretical experiments was kept at 25°C.
- The internal phase ratio, ϕ, was varied between 0.1 and 0.7 throughout the experimental and theoretical experiments.
- The default value for the effective Hamaker Constant, A_{eff}, is a literature value given for water in benzene / carbon tetrachloride emulsions[7] (see discussion section 2.3.1).

- The oil phase viscosity, η, for heptane was obtained from the literature.[8]
- The relative permittivity for the organic phase can normally be obtained from the literature. If the solvent used is not pure, this would have to be determined. The default value for heptane, ε_r, was determined experimentally (section 4.4.1).
- The expansion parameter, α, for the surfactant in the specified emulsion can vary around 1. For non-aqueous dispersions to be stable, this value needs to be greater than 1.[1,9]
- The minimum distance between surfactant centres, d_s, is referred to as the headgroup diameter in the input screen and is dependent on the size of the surfactant headgroup and the affinity between headgroups. This parameter is used purely to determine the point at which the surface becomes saturated with surfactant molecules and micellisation starts occurring in the organic phase. The default value of 1nm is a reasonable value for a bifunctional polar headgroup.
- The average surfactant length or monolayer thickness, l, is dependent on the surfactant and the organic phase. The average monolayer thickness, measured by ellipsometry for the Crill surfactant used in our experimental studies is 1.8nm and hence a default value of 2nm was used.
- In an oil continuous system, the thickness of the double layer is several microns. Hence the values of κ range from 0.1 to 1.0 μm^{-1}.[10] Using our input parameters this translates into an ionic strength, I, in the range of $(2.0 \times 10^{-9} - 2.0 \times 10^{-11})M$. The ionic strength may be calculated through chemical speciation.
- The initial percentage coverage, **%cov**, is proportional to the surfactant concentration. For emulsion systems, this parameter is hard to determine. For dispersions in which the particle is solid this parameter is determined more easily. D.H.Napper obtained surface coverage by initially preparing a dispersion freed from excess surfactant, the percentage coverage was assumed to be 100% and the reduction in coverage was calculated as the dispersions were grown in the absence of additional surfactant.[9]
- The surface potential of the water droplets, ψ, was obtained from a literature value for water droplets in a water in benzene emulsion.[10]

5.3.2 OUTPUT PARAMETERS

The conditions under which a computational run terminates are shown in Table 5.3. A computational run terminates when the emulsion is declared stable or unstable or the input parameters are not applicable to the model.

The first criterium is based on the input parameter MI which can be varied at will. If a very large value is given then this criterium will become meaningless and one of the other criteria will result in program termination. Giving a small value can be useful when doing a comparative study and when wanting the size distribution and output values after a set number of iterations.

The second criterium, number of consecutive non-effective collisions that would determine whether an emulsion is stable should be related to the number of droplets. For this criterium a value of $0.625N$ was chosen, as a reasonable value to confirm stability and not to increase computing time unnecessarily. For our default value of 400 droplets this translates into 250 consecutive non-effective collisions.

Table 5.3 Criteria used when terminating a computational run with the corresponding emulsion stability predicted.

criteria	reason for termination of computational run	stability
1	Number of collisions exceeds MI	stable
2	Consecutive non-effective collisions exceeds $0.625N$	stable
3	Internal phase volume ratio exceeds 0.74	not determined
4	Termination by user	not determined
5	Maximum droplet radius exceeds $6.7a_i$	unstable
6	Total number of droplets decreases below 4	unstable

The third criterium relates to a non-dilute emulsion. Under these conditions the model is not applicable and the program terminates.

At any stage during the iterative process the user can terminate the program and view the output values and distribution. However a facility to then continue from that point onwards with the iterations is not available and a new simulation would have to be started.

The fifth criterium is related to the restriction imposed by the 300 channels ($6.7 = 300^{1/3}$). For our default values where an initial sample of 400 droplets was used this value was not found to be restrictive and the emulsions were determined to be unstable due to criterium number 6 and not 5. As the initial droplet sample is increased this parameter could start becoming restrictive and could be increased in the source code depending on the memory constraints of the personal computer being used.

Table 5.4 Annotations to Figure 5.3, describing the output parameters from a computational run.

Parameter	Description	Possible values
A1	Number of consecutive non-effective collisions at end of computational run	1 - (0.625*N* + 1)
A2	Maximum number of consecutive non-effective collisions that occurred during the computational run	1 - (0.625*N* + 1)
A3	Total number of collisions performed during the computational run	1 - (MI + 1)
A4	Experimentally, the time it would take to perform the run.	
A5	Maximum droplet radius at the end of a computational run	a_1 - $6.7a_1$
A6	Reason for termination of computational run	More than 0.625*N* non-effective collisions Phase separation occurred Emulsion not dilute Termination by user
A7	Stability of emulsion at the end of a computational run	Stable Unstable Not determined

The sixth criterium, when the total number of droplets decreases to less than four droplets, is under all circumstances a good indication that the emulsion is unstable.

The output parameters and volume distribution displayed on the screen at the end of a computational run are shown in Figure 5.3 with the annotation described in Table 5.4. These parameters are referred to when discussing stability trends. The volume distribution is plotted in histogram form to compare with experimental droplet distribution data obtain using laser particle sizing or other techniques. For each channel or droplet radius the total volume of all droplets of that radius is plotted. Hence if one droplet was present in each channel, the histogram would show a positive slope.

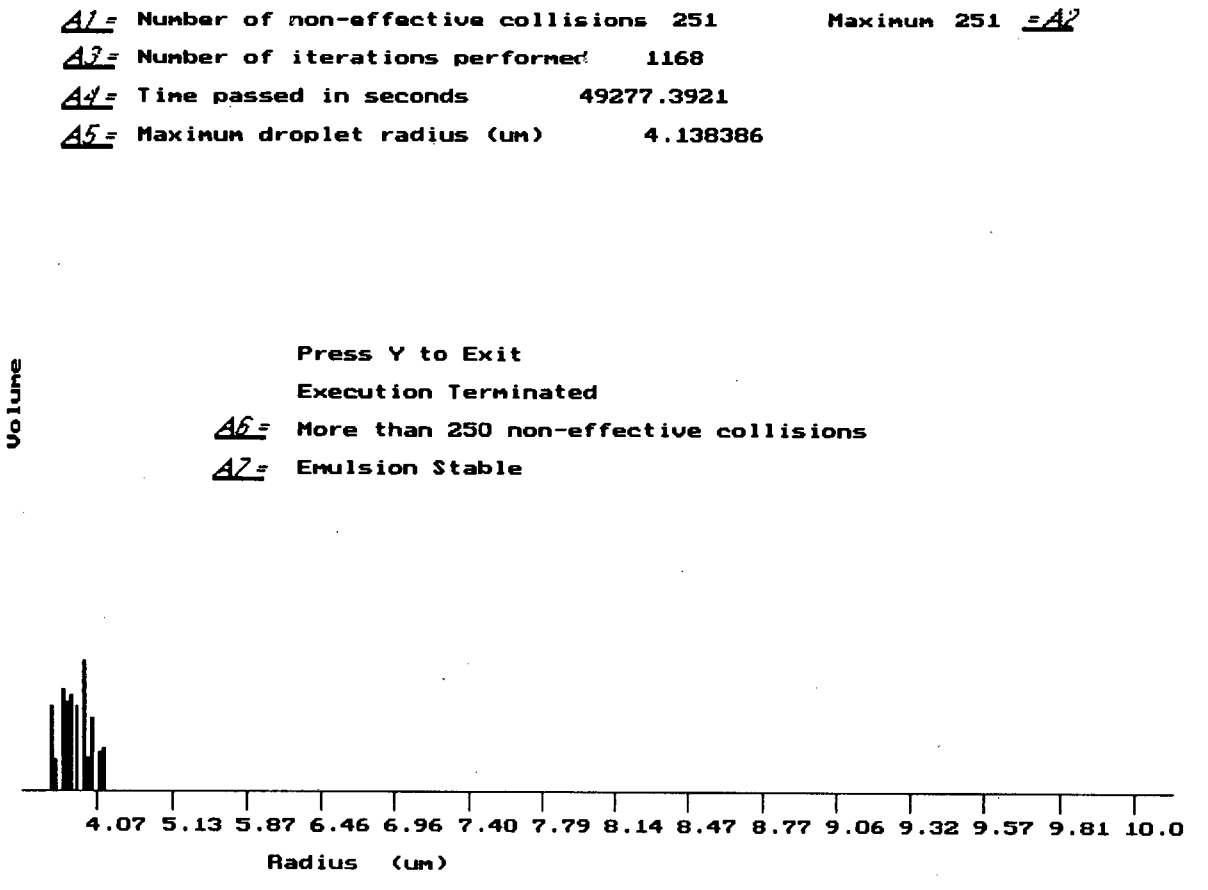

Figure 5.3
Screen output from a typical computational run showing the output parameters.

5.4 VALIDATION OF COMPUTER MODEL

To quantitatively validate a computer model, it is necessary to be able to compare an observed and a calculated result. The validation of complex systems is not always easy because of the lack of usable experimental data available in the literature. Reasons for the lack of experimental data include:

- Experimental results of complex systems are hard to obtain and/or interpret.
- Because of the natural stochastic processes at work in complex systems, experimental results are often not reproducible.
- Experimental measurements of input parameters are often hard to obtain.

Other modelling programs such as ECCLES, a human blood plasma speciation model, have similar validation problems.[11] The ECCLES model calculates the speciation of species in solution that can not be measured experimentally. Often the only validation is the correlation of predicted effects with clinical results. Another model is the Uranium model which has been used extensively to study the speciation of radioactive species but can't be validated experimentally without a nuclear accident.[12]

Prior to this model, bulk emulsion stability was predicted using the coagulation energy barrier between two initial droplets. If the droplets were predicted to coagulate, the emulsion was predicted to be unstable and *vice versa*. The model adds an iterative and stochastic approach to emulsion predictions. Our first test of the model is to see if bulk emulsion stability predictions agree with trends predicted by the initial coagulation energy barrier. If there are differences they need to be explained. The results of these tests are presented in this section.

The second test is to qualitatively test the stability predictions of the model against experimental data trends, in line with how other models are validated. Because of the lack of reliable quantitative experimental data in the literature, experimental data for a simple emulsion system was obtained in this work. The validation of the model against experimental trends from the literature and our work is presented in this section.

The next step in the validation is to quantitatively validate our model. To this end, particle size distributions before and after coalescence would have to be compared with size distribution data predicted using our model. In our experimental studies we have used the Malvern 2600 particle size analyzer to obtain particles size distributions. This technique presented many problems. Although size distribution data was obtained after emulsion stabilization with respect to initial coalescence, initial size distribution data was hard to obtain because of the speed of initial coalescence. As is the case with all models, your results or predictions are only as good as your input data. To obtain similar size distribution data from our model, good input data is needed. Certain input parameters are hard to determine accurately such as the ionic strength of the organic phase, the interfacial charge density and the Hamaker constant for the system. Estimates of these were used in the model but more work needs to be done in improving the estimates of these parameters.

This model mimics the stochastic processes in nature and therefore no two computational runs are identical. For this reason all runs are repeated at least five times and the average value as well as the spread of values are plotted.

5.4.1 THE STABILITY THEORY OF W/O EMULSION DROPLETS

The stability theory of w/o emulsion droplets has been developed in chapter two. Table 5.5 lists the effect changing one of the input parameters would have on the coagulation energy barrier between two droplets. If one assumed that the initial energy barrier between droplets determined the stability of the emulsion, then noting the trends displayed in Table 5.5, it would appear that emulsion stability theory predicts that the most stable emulsion would have the following properties:

- large emulsion droplets with a high surface potential
- high ionic strength and relative permittivity of the organic phase
- high density of long surfactant molecules
- low Hamaker Constant
- low temperature.

In the following sections the differences between the bulk stability of emulsions as predicted using a stochastic iterative model will be compared with the stability theory predictions for the initial energy barrier between two droplets.

Table 5.5 List of experimental input parameters and the effect increasing the parameters has on the attractive, repulsive, steric and total initial interaction energy.

Parameter	E_A	E_R	E_S	E_T
A_{eff}	-			-
a_1	-	+	+	+
α			*	*
ε_r		+		+
T	+	-		*
ψ_1		+		+
ϕ		-		-
d_s			-	-
%cov			+	+
l			+	+
I		+		+

where + Increasing the value of the parameter increases the energy.
- Increasing the value of the parameter decreases the energy.
* Increasing the value of the parameter can decrease or increase the energy.

5.4.2 THE STOCHASTIC AND ITERATIVE APPROACH

Experimentally it has been found that the coalescence of emulsion droplets need not result in the complete separation of an emulsion into two distinct phases. This phenomenum is shown by the computer model where the particles formed by coalescence are found to be more stable than the precursor particles.

The parameters that change during an emulsion coagulation simulation are listed in Table 5.6. Hence if two droplets coalesce the radius, surface potential and surfactant coverage will increase. Increasing these parameters will considerably increase the stability of the new droplet. Figure 5.4 demonstrates the considerable increase in droplet stability as the droplets increase in size during a computational run.

Table 5.6 The effect droplet coagulation has on the energy barrier.

Parameter	Change in parameter as droplets coagulate	Resultant effect on Δ_T
N	decreases	no effect
a_x	increases	increases
ψ_x	increases	increases
ν_x	increases	increases

In contrast, Figure 5.5 shows that as the emulsion coalesces, the energy barrier between the remaining original droplets decreases, showing a decrease in stability. This effect can be explained in terms of the repulsive energy component. The repulsive energy barrier between two colliding droplets, droplets 1 and 2, contains electrostatic contributions not only from the two colliding droplets, but also from droplet 1 and its neighbouring droplets. As the average droplet surface charge and radius increases the electrostatic repulsion between droplet 1 and its neighbouring droplets increases with respect to the repulsion between droplet 1 and droplet 2. This results in a decrease in the energy barrier preventing droplets 1 and 2 from coagulating. This effect has been noted experimentally that the smaller droplets coagulate at the expense of the larger droplets. When starting off with a monodisperse sample of droplets the initial coalescence of the first two droplets is slow but the speed steadily increases until most of the original monodisperse droplets have coalesced to form larger droplets. The new droplets however are more resistant to coagulation.

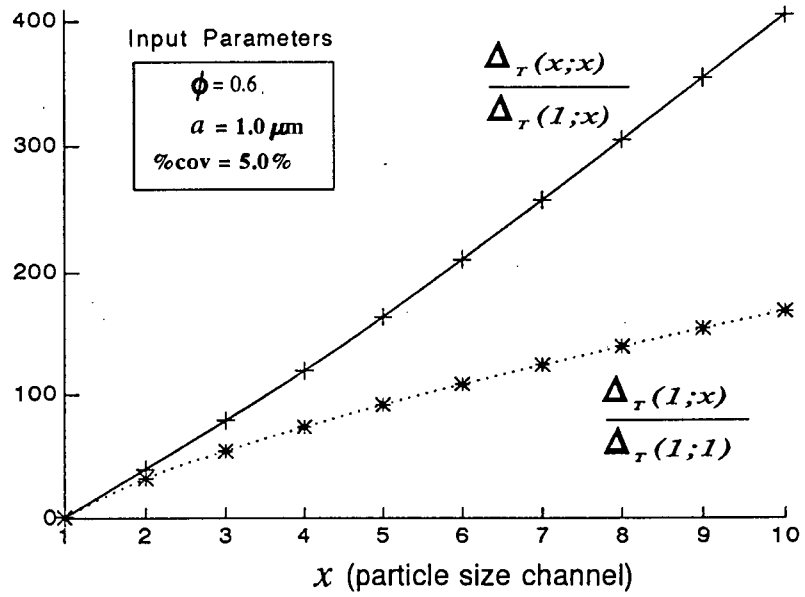

Figure 5.4

Plot of the relative energy barrier to coagulation versus the channel number of the droplet. All input parameters were the default values (Table 5.2) except for the parameters specified. (Δ_T(i;j) refers to the coagulation energy barrier for a droplet in channel i with a droplet in channel j)

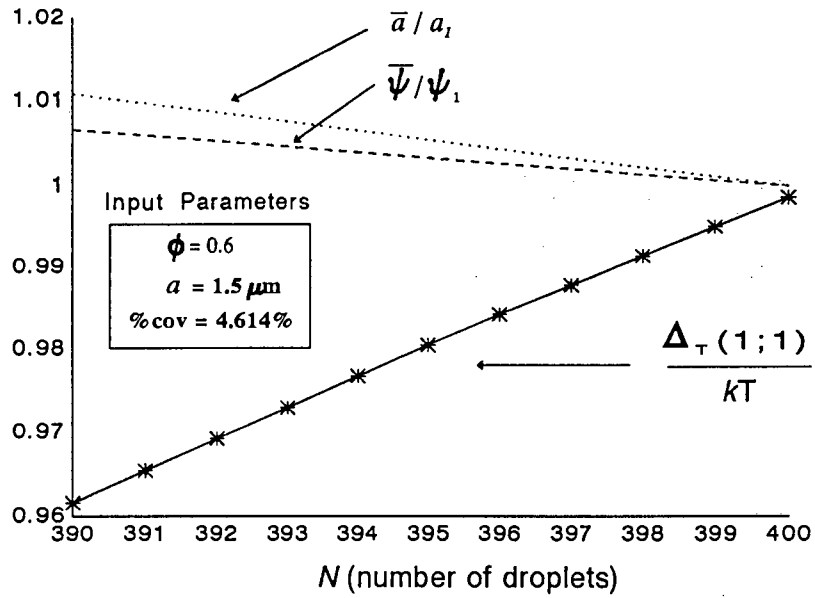

Figure 5.5

Plot of the Energy barrier to coagulation versus number of droplets, during a computational run. Included in the plot is the change in the average droplet size and surface potential. All input parameters were the default values (Table 5.2) except for the parameters specified. (Δ_T(1;1) refers to the coagulation energy barrier calculated between two droplets, both being in channel 1)

5.4.3 THE EFFECT OF SURFACTANT CONCENTRATION

Figure 5.6 and 5.7 show the effect surfactant concentration is predicted to have on emulsion stability. The time taken until the emulsion is determined to be stable and the largest droplet size when the emulsion is determined to be stable are both indications of the stability of the emulsion. Increasing the surfactant coverage resulted in smaller droplets in figure 5.6 and in a shorter stabilization time in figure 5.7. Both trends indicate that an increase in surfactant coverage results in more stable emulsions. Once the surfactant coverage increased above 6% the stability of the droplets was so great that the first 250 collisions were non-effective and no coalescence occurred. For surfactant coverage below 3%, some of the computational runs resulted in unstable emulsions.

According to the stability theory for emulsion droplets, an increase in surfactant concentration results in an increase in the steric energy barrier and hence an increase in the droplet stability. The same effect is observed using the computer model satisfying our first validation check. If one were to predict emulsion stability based purely on initial droplet coalescence, a surfactant coverage less than 6% would result in coagulation and hence an unstable emulsion. However the iterative model predicts that at surfactant coverage below 6%, although the initial droplets coagulate, the new larger droplets are more stable than their precursor droplets and stable emulsions can be obtained for surfactant coverage down to 2%.

Emulsion stability experimental results from the literature and this work are discussed in section 4.4.3.1. for the case of increasing the surfactant concentration. These results show that as the surfactant concentration increases the average droplet size decreases and then levels off. These experimental trends are predicted by the model (figures 5.6 and 5.7) satisfying our second validation check.

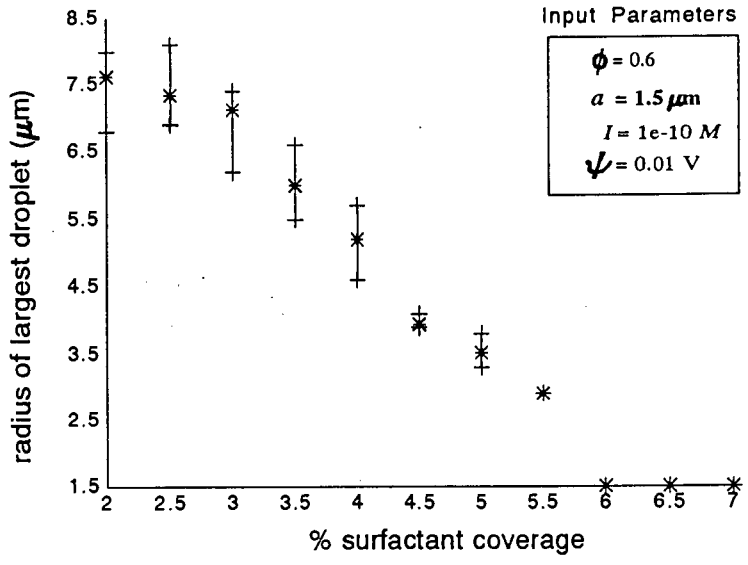

Figure 5.6

The effect of the surfactant coverage on the output parameter, largest droplet radius. All input parameters were the default values (Table 5.2) except for the parameters specified. The average, largest and smallest value for 5 computational runs in which the emulsion was determined to be stable, is plotted.

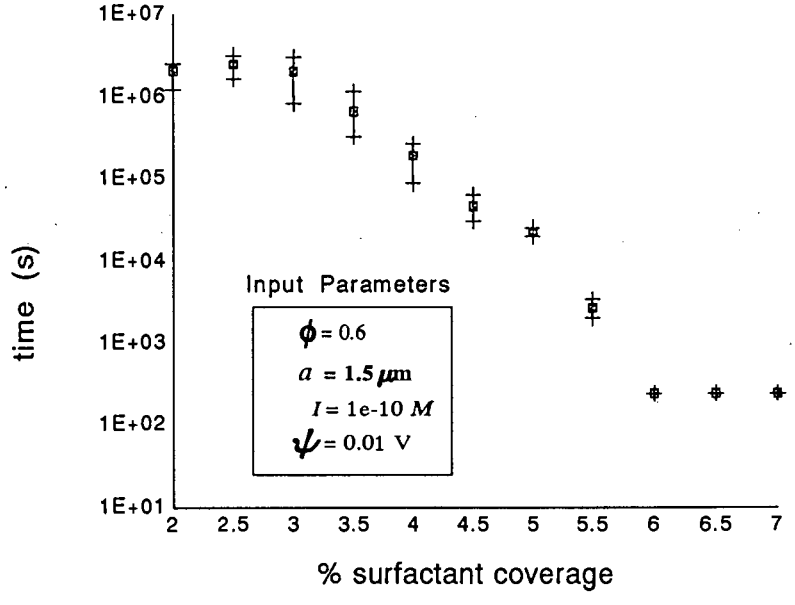

Figure 5.7

The effect of the surfactant coverage on the time taken before the emulsion is determined to be stable. All input parameters were the default values (Table 5.2) except for the parameters specified. The average, largest and smallest value for 5 computational runs in which the emulsion was determined to be stable, is plotted.

5.4.4 THE EFFECT OF IONIC STRENGTH

Figures 5.8 and 5.9 show the effect that the ionic strength of the organic phase is calculated to have on the stability of an emulsion. As the ionic strength of the organic phase increases so the radius of the largest droplet decreases, indicating an increase in stability of the emulsion. This is to be expected, as the theory of droplet stability predicts that an increase in the ionic strength will increase the electrostatic and hence total energy barrier. The number of iterations performed increases as the ionic strength decreases even though the extent of coalescence decreases, giving an indication of the number of non-effective collisions. For ionic strength values less than $1x10^{-9}M$ some of the computational runs resulted in unstable emulsions.

Malvern and creaming experimental results discussed in section 4.4.3.2 showed that as the ionic strength of the aqueous phase was increased, the droplet sizes in the emulsion decreased. In figure 5.8, the computer model predicts a similar trend in droplet size as the ionic strength of the organic phase increases.

At high ionic strength, experimental results show a levelling off of droplet sizes as the ionic strength of the aqueous phase increases. Increasing the ionic strength of the aqueous phase results in a corresponding increase in the ionic strength of the organic phase. However once the organic phase becomes saturated, increasing the salt concentration in the aqueous phase would not change the ionic strength of the organic phase. In this case the model would predict no change in droplet size, as the ionic strength of the aqueous phase increases. The correlation of experimental results and computational predictions is pleasing.

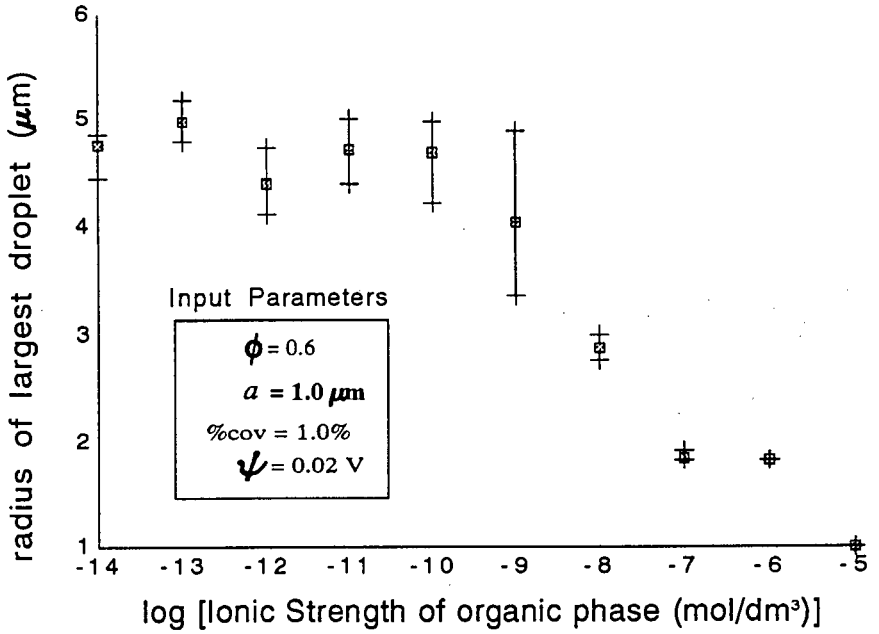

Figure 5.8

The effect of the ionic strength of the organic phase on the radius of the largest droplet. All input parameters were the default values (Table 5.2) except for the parameters specified. At each ionic strength the average, largest and smallest value for 5 computational runs in which the emulsion was determined as stable is plotted.

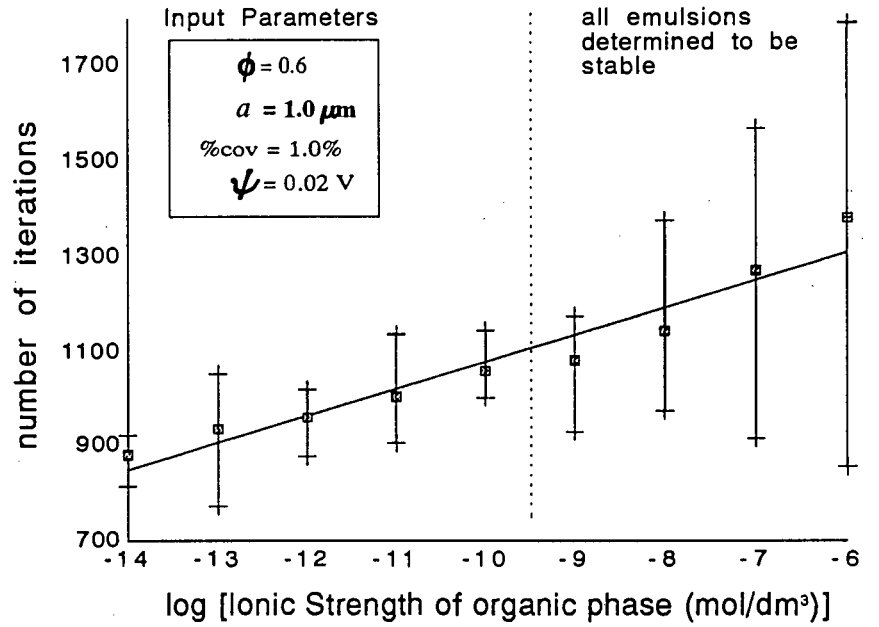

Figure 5.9

The effect of the ionic strength of the organic phase on the number of iterations performed. All input parameters were the default values (Table 5.2) except for the parameters specified. At each ionic strength the average, largest and smallest value for 5 computational runs in which the emulsion was determined as stable is plotted.

5.4.5 THE EFFECT OF DROPLET SIZE

The influence of droplet size on emulsion stability generally shows no clear pattern. Some workers have reported an increase in stability with drop size whereas others have reported the opposite. These findings have been explained by Davis *et al.* whose results have shown that for emulsions with small drop sizes increasing the drop size results in a decrease in stability whereas with larger droplets increasing the drop size results in an increase in stability.[13]

Figure 5.10 shows the effect the initial droplet radius is predicted to have on emulsion stability. As the initial droplet size increases, the radius of the largest droplet increases. This suggests that as the initial droplet radius increases, the stability of the emulsion decreases. In contrast as the initial droplet radius increases the coagulation energy barrier increases, which results in an increase in stability. When the energy barrier, Δ_T becomes greater than $1kT$, (above point z) a decrease in the largest droplet radius is observed. These results are echoed by Figure 5.11 which shows how initially the stabilization time increases as the radius increases, indicating an increase in the number of non-effective collisions. However when a_1 is greater than 1.5μm the time decreases as all collisions are then non-effective.

The experimental effects of changing the shearing time for emulsions is discussed in section 4.4.3.3. Experimentally an increase in shearing rate or shearing time translates into a decrease in the initial droplet radius. As the shearing time is increased, the resultant emulsions, upon stabilization, showed a decrease in droplet size. Hence decreasing the initial droplet radius resulted in an emulsions with decreased droplet sizes. In section 4.4.3.5 the effect of storage time on two emulsions with different initial droplet sizes is discussed. The emulsion which initially had smaller droplets appeared to be quite stable after 9 days while the emulsion with larger initial droplet sizes showed signs of breaking after this time.

When studying the effect of droplet sizes, the model shows its true potential. The droplet energy barrier theory simply predicts that emulsions with larger droplets will be more stable. However, the stochastic and iterative approach shows that this is not always the case, in agreement with the conflicting results obtained from real experimental systems.

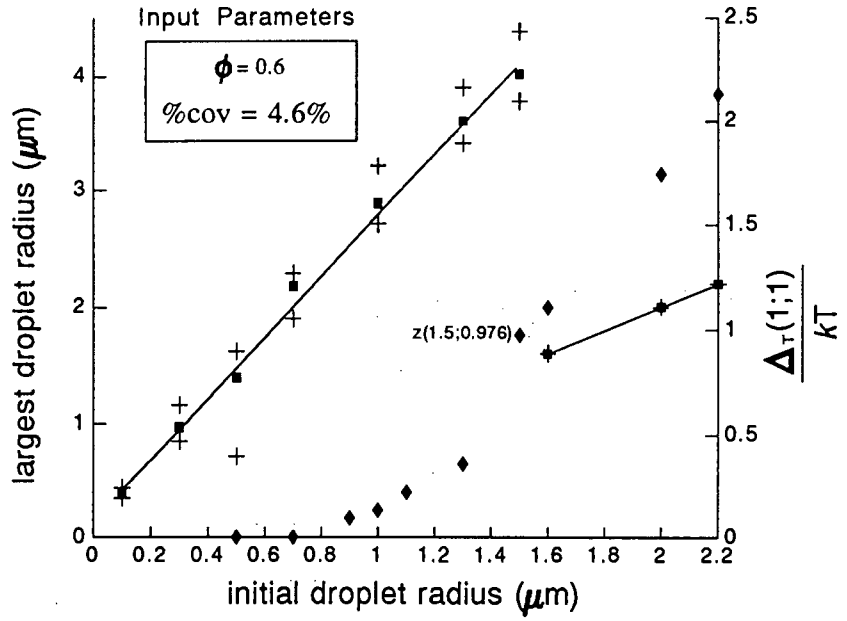

Figure 5.10

Plot of the output parameter, largest droplet radius, versus the input parameter, initial droplet radius. All input parameters were the default values (Table 5.2) except for the parameters specified. For each initial droplet radius the average, largest and smallest value for 5 computational runs in which the emulsion was determined to be stable, is plotted. Included in the plot is the coagulation energy barrier with its axis on the right of the plot.

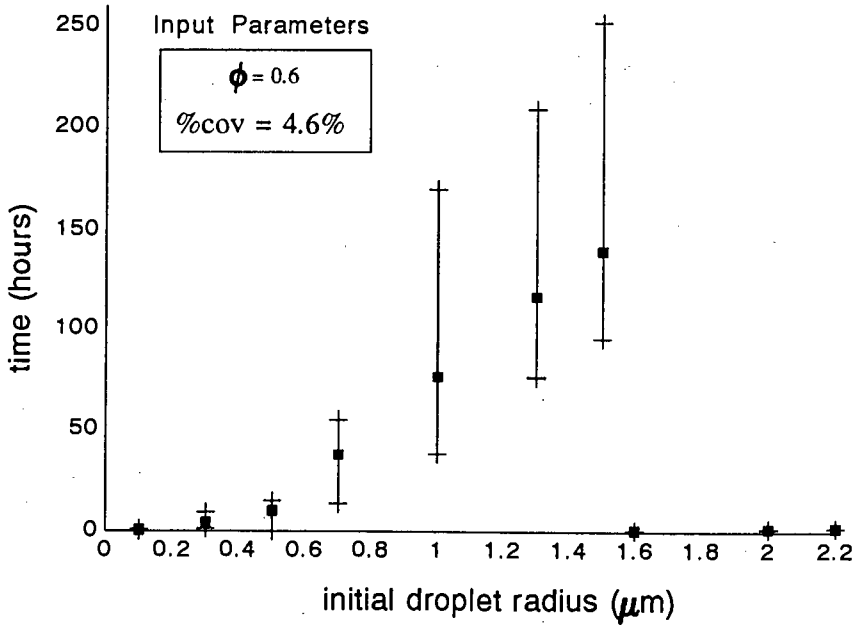

Figure 5.11

Plot of the output parameter, time, versus the input parameter, initial droplet radius. All input parameters were the default values (Table 5.2) except for the parameters specified. For each initial droplet radius the average, largest and smallest value for 5 computational runs in which the emulsion was determined to be stable, is plotted.

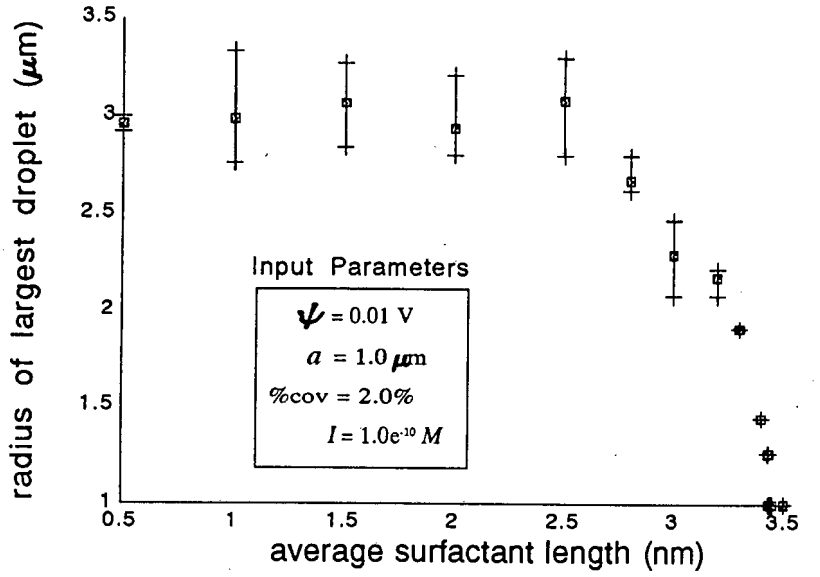

Figure 5.12

Plot of the output parameter, largest droplet radius, versus the input parameter, average surfactant length. All input parameters were the default values (Table 5.2) except for the parameters specified. For each surfactant length the average, largest and smallest value for 5 computational runs in which the emulsion was determined to be stable, is plotted.

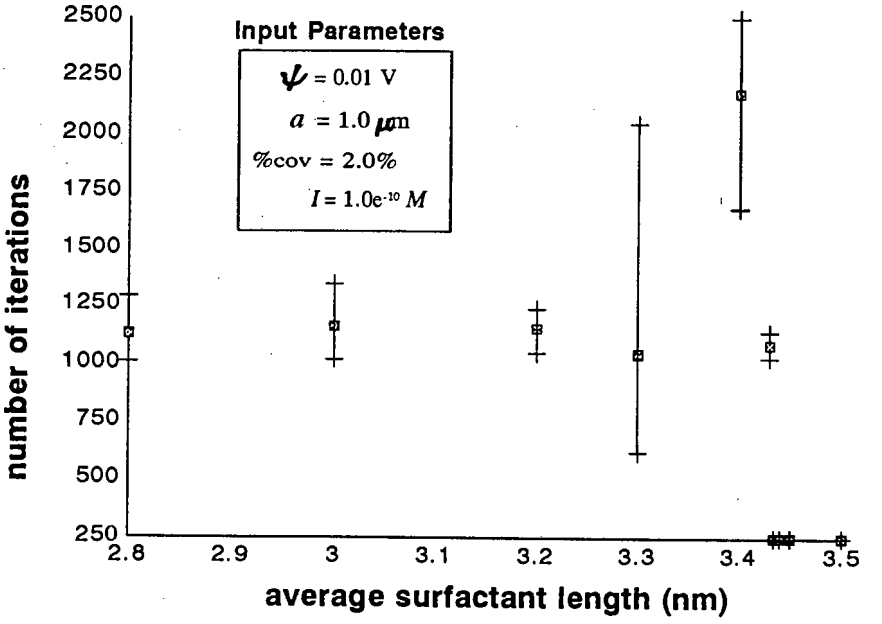

Figure 5.13

Plot of the output parameter, number of iterations, versus the input parameter, average surfactant length. All input parameters were the default values (Table 5.2) except for the parameters specified. For each surfactant length the average, largest and smallest value for 5 computational runs in which the emulsion was determined to be stable, is plotted.

5.4.6 THE EFFECT OF SURFACTANT LENGTH

The surfactant length is known to affect the stability of w/o emulsions. Data presented for colloidal dispersions in hydrocarbons by Mackor *et al.* showed that for their system, a surfactant length of 2nm gave a stable emulsion but a surfactant length of 1nm resulted in flocculation of the emulsion.[14] This is expected as the theoretical steric equations predict that the steric energy between two droplets increases as the surfactant length increases. Figure 5.12 shows computational results obtained for an emulsion system in which the steric effect dominated and the surfactant length was varied. As the surfactant length was decreased the radius of the largest droplet increased sharply and then levelled off. The initial increase in instability correlates well with experimental and theoretical results. The levelling off of the curve was found to be due to the electrostatic component of the energy barrier dominating in larger droplet sizes. Decreasing the surfactant length did not affect the energy barrier as the electrostatic maxima then determined the energy barrier. Figure 5.13 shows the effect of the surfactant length on the number of iterations. The initial decrease in surfactant length resulted in a steep increase in the number of iterations, due to an increase in the number of non-effective collisions. However once the electrostatic energy became the dominant term the number of iterations decreased and then levelled off.

5.4.7 THE EFFECT OF SURFACE POTENTIAL

Emulsion stability theory predicts that as the surface potential increases so the electrostatic energy barrier between two droplets increases and therefore the stability of the emulsion should increase. Experimental results published by Loh *et al.* show that for carbon suspensions in mineral oil an increase in the surface potential above 20-25 mV resulted in stable dispersions.[15] Figure 5.14 shows how increasing the surface potential is predicted to affect the stability of an emulsion. Surface potential values of less than 1mV resulted in unstable emulsions. As the surface potential was increased the radius of the largest droplet decreased, an indication of an increase in stability. These computational results agree well with the literature results and with initial droplet stability predictions.

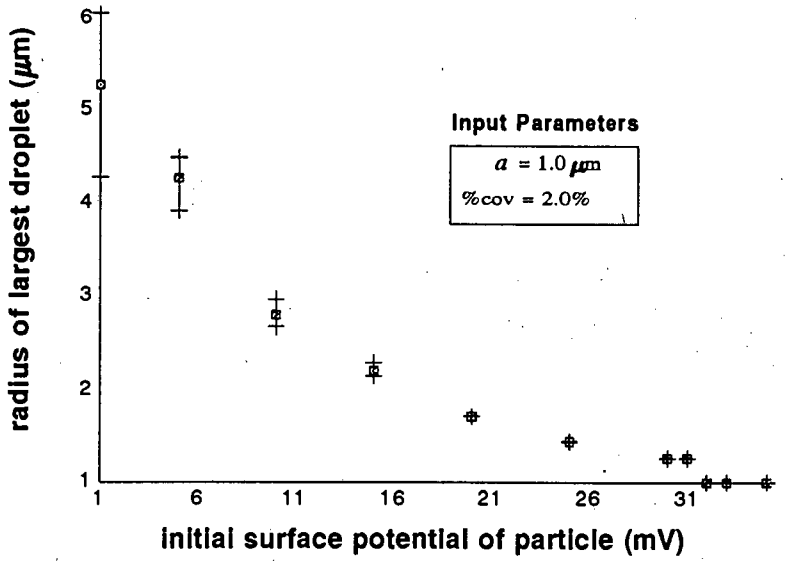

Figure 5.14

Plot of the output parameter, largest droplet radius, versus the input parameter, initial surface potential. All input parameters were the default values (Table 5.2) except for the parameters specified. For each initial surface potential the average, largest and smallest value for 5 computational runs in which the emulsion was determined to be stable, is plotted.

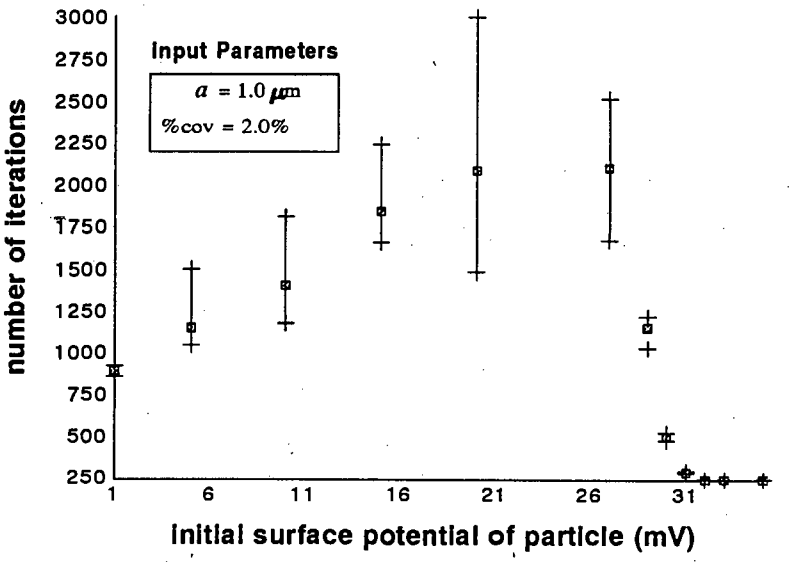

Figure 5.15

Plot of the output parameter, number of iterations, versus the input parameter, initial surface potential. All input parameters were the default values (Table 5.2) except for the parameters specified. For each initial surface potential the average, largest and smallest value for 5 computational runs in which the emulsion was determined to be stable, is plotted.

Figure 5.15 shows the corresponding effect increasing the surface potential has on the number of iterations. As the emulsion becomes more stable the number of iterations increase, giving an indication of a corresponding increase in the number of non-effective collisions. The number of iterations then steeply decreases as the emulsions become very stable and the final droplet radius is that for the corresponding channels 1 and 2.

5.5 COMPUTER MODEL PREDICTIONS

The validation of a computer model is never complete. As more experimental data becomes available it is used to test the predictions made by the model. In the process, the model can be refined and improved. Included in this refinement is the input data upon which the calculations are based. Some of the input data needed for the model to predict emulsion stability was not available in the literature. In these cases reasonable values were chosen based on chemical analogy. Thus the model could be used to highlight experimental deficiencies in the literature.

5.5.1 THE EFFECT OF RELATIVE PERMITTIVITY

The effect of the dielectric constant or relative permittivity of the organic phase on the stability of an emulsion as predicted by the model is depicted in figure 5.16. An increase in the dielectric constant will result in a corresponding increase in the electrostatic and total coagulation energy barrier. Therefore an increase in the dielectric constant should result in an increase in emulsion stability. Figure 5.16 demonstrates the model's prediction that the change in the dielectric constant results in a decrease in droplet sizes for a stabilized emulsion. The trends predicted by the stochastic iterative model agree with the trends predicted by initial droplet stability theory, but as yet has not been confirmed experimentally.

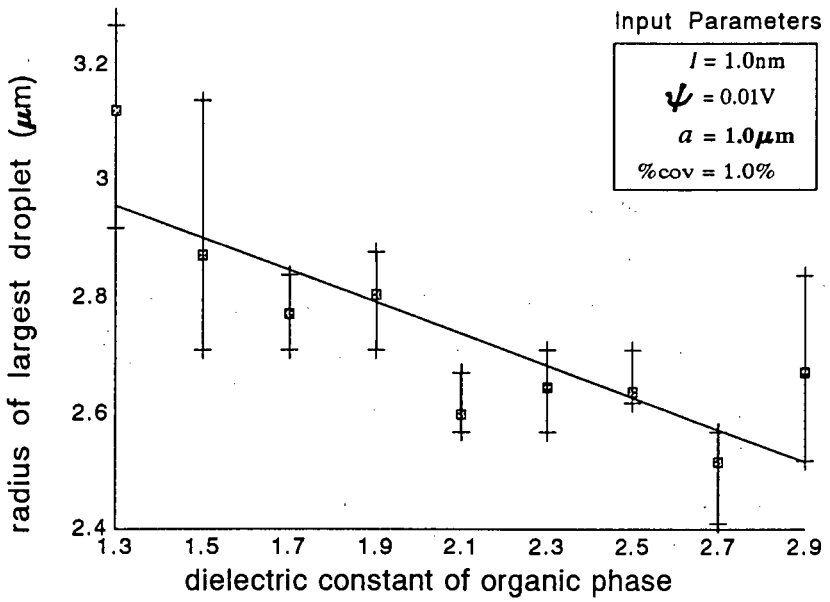

Figure 5.16

Plot of the output parameter, largest droplet radius, versus the input parameter, organic phase dielectric constant. All input parameters were the default values (Table 5.2) except for the parameters specified. The average, largest and smallest value for 5 computational runs in which the emulsion was determined to be stable, is plotted.

5.5.2 THE EFFECT OF THE EXPANSION PARAMETER

A change in the expansion parameter, α, can not be separated experimentally from a change in the average surfactant length in the emulsion. As the expansion parameter increases so the average surfactant length should increases. This relationship has not been expressed mathematically, as the average surfactant length is dependent on a combination of factors including surfactant-surfactant; surfactant-solvent and surfactant-droplet interactions. Theoretically an increase in the expansion parameter will generally result in a decrease in the energy barrier.

Figure 5.17 shows the increase in the largest droplet radius as predicted by the model for an increase in the expansion parameter. As the expansion parameter increases the droplet radius increases sharply and then levels off. The initial increase is as predicted from initial droplet stability predictions.

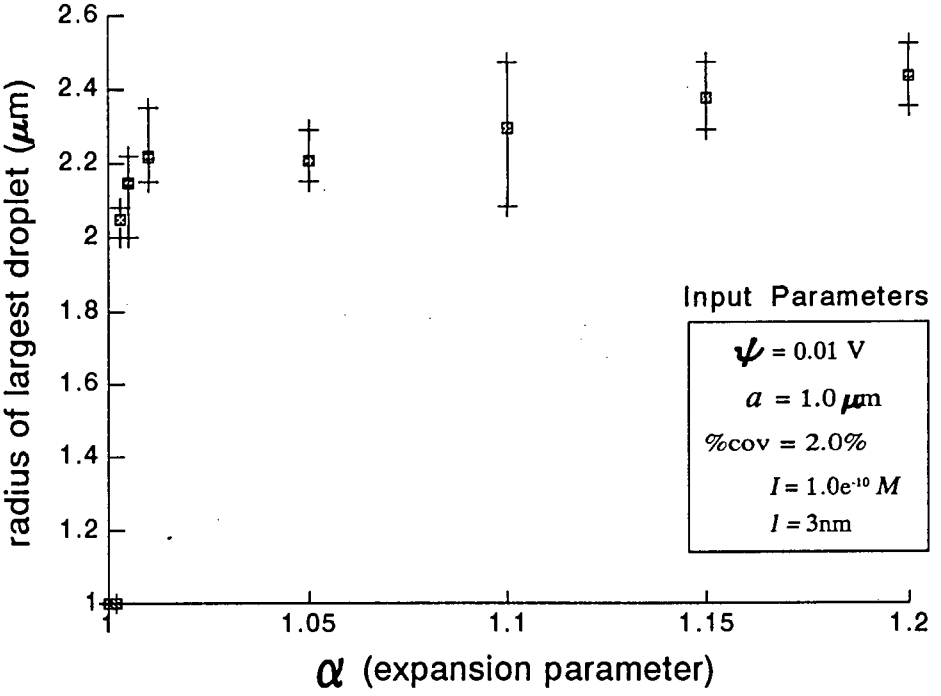

Figure 5.17

Plot of the output parameter, largest droplet radius, versus the input parameter, expansion parameter. All input parameters were the default values (Table 5.2) except for the parameters specified. The average, largest and smallest value for 5 computational runs in which the emulsion was determined to be stable, is plotted.

5.5.3 THE EFFECT OF THE INTERNAL PHASE VOLUME RATIO

The effect of the internal phase volume on emulsion stability as predicted by the computer model is shown in figure 5.18. As the internal phase volume increases, the distance between the droplets decreases, resulting in a decrease in the electrostatic energy barrier to coagulation. This would result in a decrease in the total energy barrier and consequent decreased emulsion stability. The average increase in the largest droplet radius as predicted by the model for an increase in the internal phase ratio is in agreement with predictions from initial energy barrier trends.

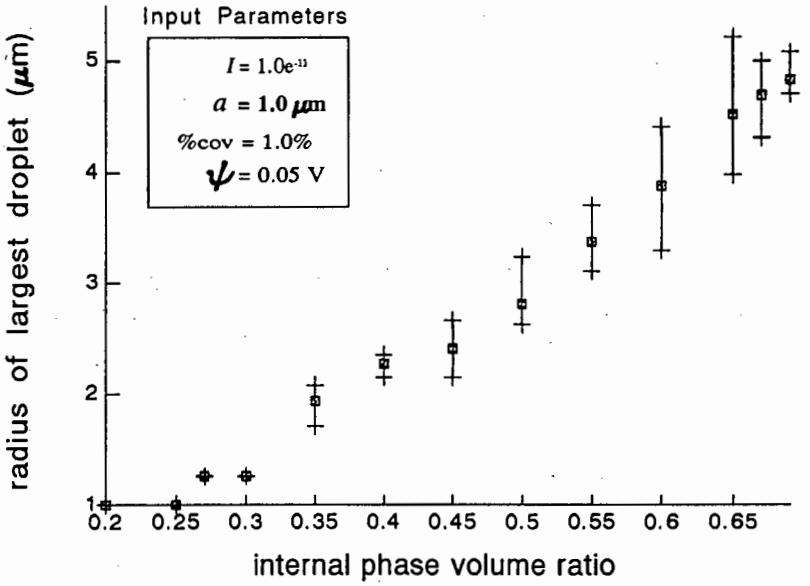

Figure 5.18

Plot of the output parameter, largest droplet radius, versus the input parameter, internal phase volume ratio. All input parameters were the default values (Table 5.2) except for the parameters specified. The average, largest and smallest value for 5 computational runs in which the emulsion was determined to be stable, is plotted.

5.6 CONCLUSIONS

The computer model developed in this section applies an iterative and stochastic approach to predicting emulsion stability. The energy functions developed in chapter two, which calculate the energy barrier to coagulation as a function of the interdroplet distance were incorporated into the model. The complexity of the energy functions precludes the analytical determination of the function maxima, so for any two droplets it is determined using a numerical maximization function. Adding to the complexity of the system is the random function which results in computational runs with identical input parameters giving different stable emulsion size distribution data.

Our first test of the model was to see if the bulk emulsion stability trends agreed with the trends predicted for the energy barrier between two droplets. In all cases except for the case of initial droplet size, the two trends agreed. For the case of initial droplet size, the complexity of the system was demonstrated. Although the energy function increases as a

function of the initial droplet radius, if the energy function maxima is less than the thermal energy, significant coagulation can occur. This results in an apparent decrease in emulsion stability as the initial droplet radius increases. The model also predicted that smaller droplets coagulate at the expense of larger droplets.

The model has distinct advantages over initial energy barrier predictions. Because of the increase in surfactant coverage and surface potential as droplets coagulate, the new droplets are inherently more stable than their precursor droplets. Where the initial coagulation energy barrier predicts that the initial droplets in an emulsion are unstable, the emulsion is not necessarily unstable. The model confirms experimental observations that emulsion which show initial coagulation can stabilize. The model predicts whether an emulsion will be stable or unstable. It will also predict the size distribution of the stable emulsion.

The second test was to qualitatively validate the model against experimental data trends from the literature and this work. For the following input data, stability trends from experimental data correlated well with predictions made by the model:

- varying the surfactant concentration
- varying the ionic strength of the organic phase
- varying the initial droplet size
- varying the surfactant length
- varying the surface potential

Thirdly, in the absence of experimental data with which to qualitatively validate the model, the following predictions were made:

- When electrostatic repulsion dominates, increasing the relative permittivity of the organic solvent results in an increase in emulsion stability.
- Increasing the expansion parameter above one, in the absence of increasing the surfactant length, results in a decrease in emulsion stability.
- Increasing the internal phase volume ratio results in a decrease in emulsion stability.

Whether these predictions are true, thereby validating the model further, only time will tell.

5.7 REFERENCES

1. Th.F.Tadros (1993), "Industrial Applications of Dispersions", *Adv.Colloid Interface Science*, **46**:1.
2. S.B.Hall, J.R Duffield and D.R.Williams (1991), "A Reassessment of the Applicability of the DLVO Theory as an Explanation for the Schulze-Hardy Rule for Colloid Aggregation", *J.Colloid Interface Science*, **143**:411.
3. S.B.Hall, J.R.Duffield and D.R.Williams (1991), "A Stochastic Computer Simulation of Emulsion Coalescence", *J.Colloid Interface Science*, **143**:416.
4. S.B.Hall, G.W.Gaskin, J.R.Duffield and D.R.Williams (1991), "An Interfacial Equilibria Model for the Electrokinetic Properties of a Fat Emulsion", *Int.J.Pharmaceutics*, **70**:251.
5. Paul Becher (1965), *Emulsions: Theory and Practice*, Reinhold Publishing Corporation, New York, 2nd Ed.
6. W.H.Press, B.P.Flannery, S.A.Teukolsky and W.T.Vetterling (1986), "Chapter 10. Minimization or Maximization of Functions", *Numerical Recipes (The Art of Scientific Computing)*, Cambridge University Press, New York.
7. W.Albers and J.Th.G.Overbeek (1960), "Stability of Emulsions of Water in Oil III. Flocculation and Redispersion of Water Droplets covered by amphipolar Monolayers", *J.Colloid Science*, **15**:489.
8. R.H.Perry and D.Green (1988), *Perry's Chemical Engineer's Handbook*, McGraw-Hill, Singapore, 6th Ed.
9. D.H.Napper (1970), "Flocculation Studies of Sterically Stabilized Dispersions", *J.Colloid Interface Science*, **32(1)**:106.
10. W.Albers and J.Th.G.Overbeek (1959), "Stability of Emulsions of Water in Oil. II. Charge as a Factor of Stabilization against Flocculation.", *J.Colloid Science*, **14**:510.
11. P.M.May, P.W.Linder and D.R.Williams (1977), "Computer Simulation of Metal-ion Equilibria: Models for the Low-molecular-weight Complex Distribution of Calcium(II), Magnesium(II), Manganese(II), Iron(III), Copper(II), Zinc(II), and Lead(II) Ions in Human Blood Plasma", *J.Chem.Soc.Dalton Trans.*:588.

12. D.R.Williams (1989), "Guest Editorial: Speciation and Legislation", *Chemical Speciation and Bioavailability*, **1(1)**:3.

13. S.S.Davis and A.Smith (1976), "The Stability of Hydrocarbon Oil Droplets at the Surfactant/Oil Interface", *Colloid & Polymer Science*, **254**:82.

14. E.L.Mackor (1951), "Letters to the Editors: A Theoretical Approach of the Colloid-Chemical Stability of Dispersions in Hydrocarbons", *J.Colloid Science*, **6**:492.

15. Chien-Cheng Loh and Wei-Ho Chen (1979), "Long Range Correlation Effect on the Percentage Lowering of Energy Barriers in W/O Emulsions", *J.Chinee Chem.Soc.*, **26**:101.

CHAPTER SIX
CONCLUSIONS

6.1 INITIAL OBJECTIVES

The two initial objectives of this research were:

- To perform a chemical speciation analysis of the aqueous phase of typical emulsion explosives.
- To develop a computer model which would be able to predict the lifetime of a w/o emulsion based on the emulsion formulation and certain physical properties of its components.

A flowchart which followed the progression of this thesis is given in Figure 6.1

6.2 THE SPECIATION OF THE AQUEOUS PHASE

To determine the speciation of the aqueous phase of a typical emulsion explosive, stability complexes of surfactant headgroups and the cations NH_4^+, Na^+, K^+ and Ca^{2+} in high ionic strength media had to be determined. The ligands propionate, succinate and mono-methyl succinate were chosen as model compounds of the headgroups of simple anionic surfactants.

Protonation constants for the ligands succinate, propionate and mono-methyl succinate were determined using glass electrode potentiometric techniques at 25°C in the following media (*M* and *m*, refer to molarity and molality respectively):

- 3*M* Et_4NBr
- 3*m* Et_4NBr
- 3*M* KNO_3
- 3*M* $NaNO_3$
- 3*M* NH_4NO_3
- 1*M* $Ca(NO_3)_2$

Et_4NBr was chosen as a reference electrolyte following the successes of Daniele *et al.* in studying weak complexation constants when using tetraalkylammonium salts as reference electrolytes.[1-2] These salts are known not to interact significantly with O-donor ligands.[3]

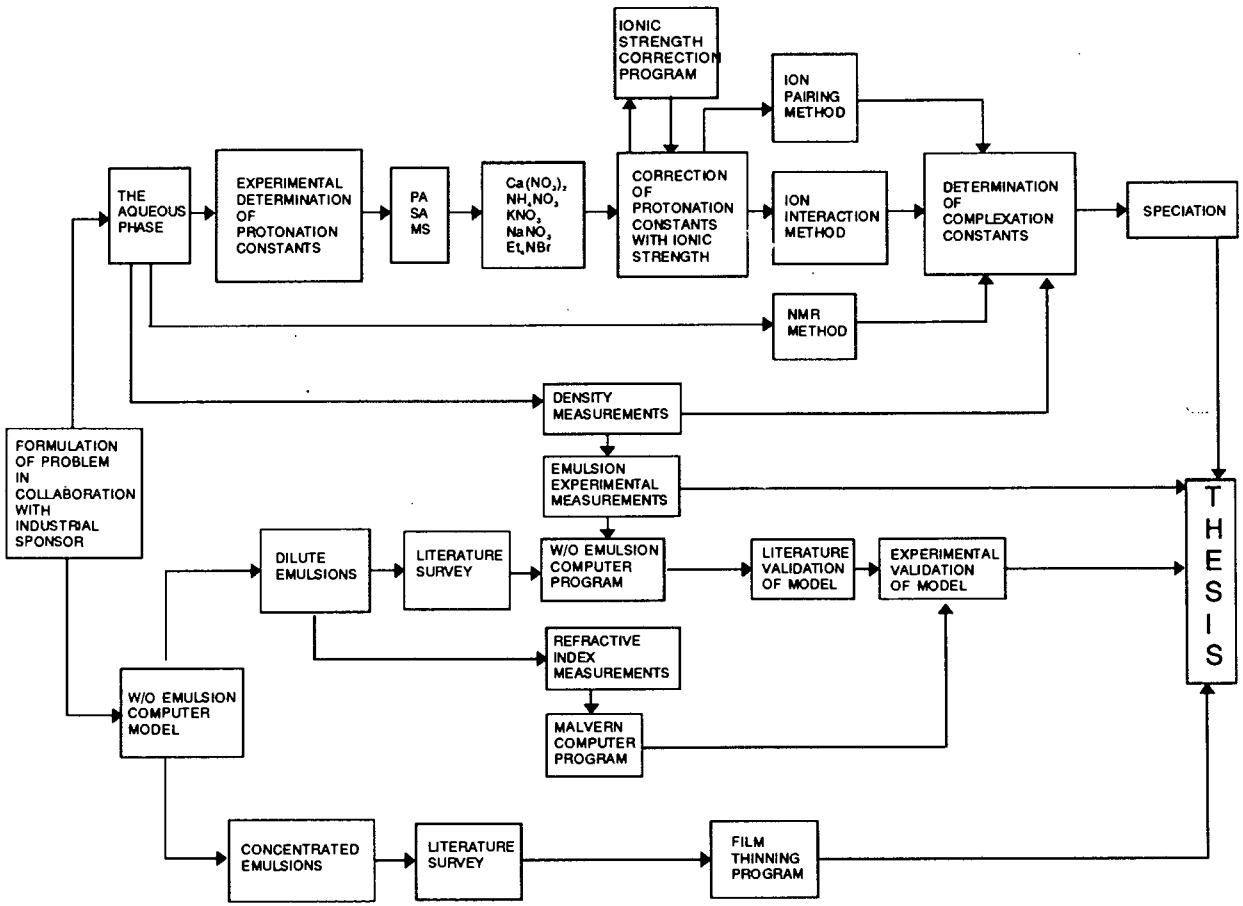

Figure 6.1

Flowchart of work included in this thesis. PA, SA and MS are abbreviations for propionic acid, succinic acid and mono-methyl succinate, respectively.

The protonation constants at the same molar ionic strength in the different media were found to follow the general trends with respect to ligand:

K_{011}(succinic acid) > K_{011}(propionic acid) > K_{011}(mono-methyl succinate) > K_{012}(succinic acid)

Each background medium was also found to affect the protonation equilibrium constants such that:

$K_{01r}(Et_4NBr) > K_{01r}(KNO_3) > K_{01r}(NaNO_3) > K_{01r}(NH_4NO_3) > K_{01r}(Ca(NO_3)_2)$

where r = 1 or 2

The ligands succinate and propionate are of importance in industrial and natural systems. Both are end products of amino acid, glucose and starch digestion and fermentation by bacteria under anaerobic conditions.[4,5] Systems containing succinate and propionate include dairy products especially cheese, the human and animal digestive systems, wastewater and sewage.[6-8] Therefore the protonation constants determined in this work can be used in chemical equilibrium modelling of these systems. Since being published these constants have already been entered into speciation databases such as JESS.[9,10]

To convert potentiometric data from one ionic strength to another a simplified Pitzer equation was derived from Pitzer's activity coefficient equations.[11] This equation and other equations derived for the ionic strength conversion have been included with Pitzer parameters in a computer program which performs ionic strength corrections. This program which can be used to convert stability constants from one ionic strength to another is supplied in diskette form.

To obtain complexation data between the ligands and the electrolyte cations, from the potentiometric data, three techniques were used:

- An equimolar ion pairing approach as used by Daniele *et al.*[12]
- An equimolal ion pairing approach derived in this work.
- A combined approach which was derived in this work from a combination of ion pairing effects and Pitzer's ion interaction equations.

Of the three techniques used the combined approach gave the more reliable complexation constants. With respect to cation binding, the complexation constants for propionate, succinate and mono-protonated succinate followed the trend:

$Ca^{2+} > NH_4^+ > K^+ > Na^+$

To verify the complexation constants obtained from potentiometric data, complexation constants for the ligands propionate and succinate at 25°C and at variable ionic strength were determined from NMR titrations. These results confirmed that specific binding occurs between the ligands and the cations. The constants obtained from NMR data were in the same range as those obtained using the combined approach.

Both NMR and potentiometric results, revealed unusual binding effects for the tetraethyl ammonium cation, indicating that more work needs to be done on this interesting ion.

Using the complexation constants obtained with the combined approach, it was possible to perform a speciation analysis of the aqueous phase of a typical water-in-oil emulsion used in emulsion explosives. The results showed that, in the pH range typical of these emulsions (pH ≈ 4.0), pH has a dramatic effect on the solution speciation. For this reason industrial emulsion explosives are buffered over a narrow pH range. The buffering of the solution controls the speciation of the surfactant headgroup and hence the nature of the emulsion interface. The protonation constants obtained for succinate and propionate in 3*M* NH_4NO_3 and at 25°C are listed below.

- log K_{011} (propionate) = 4.76; log K_{011} (succinate) = 5.15; log K_{012} (succinate) = 4.03;

Therefore propionate is predominantly protonated at pH values below 4.76 and predominantly deprotonated above pH 4.76.

The speciation analysis confirmed that although the complexation constants for propionate and succinate with the ammonium ion are small they can not be ignored at high ionic strength.

- In a 3.44*m* ionic strength system containing 3.44*m* NH_4NO_3 and 0.001*m* propionate at pH 7 and 25°C, 32% of the propionate is bound to NH_4^+.

The speciation analysis also confirmed that the presence of Ca^{2+} has a significant effect on the speciation of the system.

- In a 3.44*m* ionic strength system containing 2.58*m* NH_4NO_3, 0.29*m* $Ca(NO_3)_2$ and 0.001*m* propionate at pH 7 and 25°C, 36% of the propionate is bound, 24% is bound to NH_4^+ and 11% to Ca^{2+}.

6.3 COMPUTER MODEL OF W/O EMULSION COAGULATION

To determine the stability of droplets in a w/o emulsion, the coagulation energy barrier between any two droplets needs to be calculated. A literature survey in this area identified the predominant inter droplet forces to be:

- van der Waals attraction,
- electrostatic repulsion and
- steric repulsion.

Although some of the equations needed to calculate the energy barrier were available in the literature, many had to be derived. The electrostatic interaction between dissimilar droplets in a w/o emulsion was derived in this work. Hesselink *et al.* solved the steric energy function between two flat interfaces.[13] Using their results an energy function for two interacting spheres was derived. This equation was then modified to cater for the rhomboidal flattening of droplets as two droplets collide and for the case of two dissimilar droplets coagulating.

In contrast to o/w emulsions, steric repulsion is a dominant force in stabilizing w/o emulsions. When combining predominant inter droplet forces, the energy interaction between droplets as a function of their inter droplet separation shows a double humped curve (figure 6.2). As two droplets approach the first energy barrier is dominated by electrostatic repulsion, while the second energy barrier is dominated by steric repulsion and van der Waals interaction.

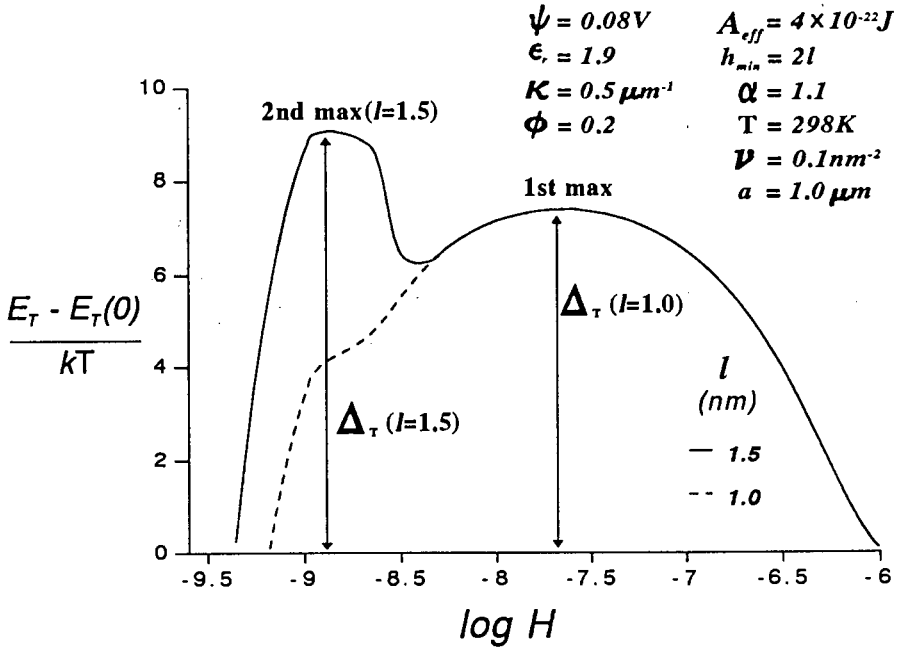

Figure 6.2

Plot of the dimensionless interaction energy between two emulsion droplets versus the log of the interdroplet distance. The effect of changing the surfactant length is shown. (T = 298K).

Depending on the experimental conditions, either both energy barriers are present or only the first or second is present. (In figure 6.2 the second energy barrier is absent for the case of l=1nm). Therefore depending on the experimental conditions, the coagulation energy barrier is dominated by either electrostatic or steric repulsion. If steric repulsion dominates, changing experimental conditions which only affect the electrostatic repulsion will have no affect on the coagulation energy barrier and *visa versa.* This explains the often confusing experimental results obtained from w/o emulsion stability studies.[14]

The equations derived for the energy barrier to coagulation were incorporated into a computer program in order to model the process of emulsion coagulation. The computer model was designed to consider interactions between randomly selected pairs of droplets from an emulsion particle size distribution with statistical weighting depending on the total volume of the particles within each size range. For two droplets to coagulate, the thermal energy must be greater than the coagulation energy barrier.

In deriving the equations and in implementing these equations in the computer model, the following assumptions were made and limitations imposed.

- The surface potential of a drop remains constant during a collision.
- Steric forces are within the range ($1.2 > H\alpha/l > 2.5$).
- All surfactants are identical and are attached at the head with a single tail protruding into the nonaqueous solvent *i.e.* mixed or co-surfactants are not considered.
- Rhomboidal flattening of droplets occurs.
- The interparticle separation at which flattening starts occurring is twice the average surfactant length.
- The droplet distribution is initially mono-disperse.
- The rate of coagulation is determined by the rate of clumping.
- The inverse Debye length, κ, is greater than $1000m^{-1}$
- The internal phase ratio of the emulsion is less than 0.74

To validate the model, it was necessary to collect experimental data on emulsions. A simple emulsion system was chosen. The emulsions were prepared with n-heptane as the organic phase, CRILL 43 (a nonionic surfactant blend) as the surfactant and a high ionic strength ammonium nitrate solution as the aqueous phase. Changes in droplet sizes as formulation parameters changed were monitored and the following results obtained:

- Changes in pH had little effect on droplet sizes.
- Increasing the salt concentration resulted in an initial decrease and then increase in droplet sizes.
- Increasing the shearing time resulted in decreases in droplet sizes. The effect was strong initially but gradually decreased.
- Increasing the surfactant concentration resulted in a decrease in droplet size. The effect was strong initially but gradually decreased.

To obtain the experimental droplet size data, three techniques were used; creaming, laser particle sizing and optical microscopy. Equations were developed to obtain droplet size data from droplet creaming data. Using these equations, the creaming technique was found to be a fast, inexpensive and effective technique for obtaining emulsion droplet size data. This technique can now be used to study size distribution data for emulsion systems,

complementing other sizing techniques.

In order to obtain size distribution data from Malvern 2600D light intensity data, a program had to be written to cater for anomalous diffraction effects. These effects occur when the refractive index of the droplets and the surrounding media is similar. Although more recent laser particle sizing instruments are now available which perform this function they were not accessible at the time this work was carried out. Already a modified version of this program is being used commercially by a local chemical company.

6.3.1 COMPUTER MODEL PREDICTIONS

The computer model uses a stochastic and iterative approach in determining bulk emulsion stability. In the past bulk emulsion stability has been predicted from the stability of the initial emulsion droplets. Equations which were developed in this work to determine the stability of two interacting droplets were incorporated into the model. Trends in the model's predicted stability of an emulsion were initially compared against trends in the initial droplet energy barrier. Emulsion stability in both cases is predicted to improve when making the following formulation changes:

- increasing the ionic strength of the organic phase
- increasing the concentration of the surfactant until 100% surfactant coverage is obtained
- increasing the length of the surfactant
- changing the organic solvent so as to decrease the effective Hamaker constant

In contrast to the initial droplet energy equations, changing the initial droplet size was predicted to either decrease or increase the stability of the emulsion.

Although both methods of predicting emulsion stability showed similar trends, the model showed distinct advantages over initial droplet stability theory. In many cases droplet stability theory predicts coagulation of the initial droplets and therefore it is concluded that the emulsion is unstable. Experimental observations have shown that emulsions that initially coagulate can stabilize as the larger droplets are often more stable than their precursor

droplets. The model confirms these experimental observations and is able to predict the true stability of the bulk emulsion. In addition, the model is able to predict the droplet size distribution of the stabilized emulsion.

The largest droplet size in the emulsion, once the emulsion was declared stable was used as a measure of droplet stability. For the following formulation changes the predictions of emulsion stability trends correlated well with experimental trends:

- the effect of surfactant concentration
- the effect of the ionic strength of the organic phase
- the effect of initial droplet sizes
- the effect of surfactant length
- the effect of surface potential

6.4 FUTURE WORK

The nature of a model infers that its validation is never complete. As experimental data is obtained it can be used against the models predictions to test and improve the model, this is a continual process until the model is no longer a model but a true reflection of the real system.

More work needs to be done to experimentally validate the computer model further. Although a qualitative validation of the model was performed for many input parameters, the model could not be validated quantitatively. Some of the experimental input parameters such as the effective Hamaker constant and the ionic strength of the organic phase are hard to measure and experimental techniques are needed to determine these accurately. An experimental method which will allow for the rapid determination of emulsion droplet sizes after shearing and prior to initial coalescence is also needed. This would then allow for the quantitative validation of the model.

The qualitative predictions made by the model were in agreement with experimental emulsion stability trends that were available from the literature and our work. In order to validate the model each input parameter was varied in isolation. However, the real power of the model comes to the fore when changing multiple parameters and manipulating the predominant forces. Because of the two step kinetic process of emulsion coagulation, if an input parameter which only affects steric repulsion is changed and the stability of the system is determined to the greater extent by electrostatic repulsion, the stability of the emulsion should not be affected and *visa versa*.

Speciation results showed that the form of the interface and the ionic strength of the aqueous phase is determined by the speciation of the aqueous phase. However, the relationship between the aqueous and organic phases was not determined. The ionic strength of the aqueous phase prior to emulsification, will affect the input parameters: ionic strength of organic phase and surface potential of the particles. Similarly, the form of the surfactant will affect the input parameters: initial particle radius, expansion parameter for surfactant in emulsion, average length of surfactant in emulsion. If these effects could be quantified, the calculation and measurement of input parameters would be greatly simplified.

The model could also be extended and improved to include different surfactant types, such as surfactants with two hydrocarbon tails, as well as the case of surfactant blends. The model is also limited to emulsions in which the rate of coagulation was determined by the rate of clumping. In concentrated emulsions the rate of coagulation is predominantly determined by the rate of coalescence, which is dependent on the rate of thinning of the thin film between two clumped droplets.[15] Initial attempts to include this mechanism in the model are presented in appendices two and three. However before this can be used much more work needs to be done.

6.5 REFERENCES

1. A.De Robertis, C.De Stefano, C.Rigano and S.Sammartano (1990), "Thermodynamic Parameters for the Protonation of Carboxylic Acids in Aqueous Tetraethylammonium Iodide Solutions", *J.Solution Chemistry*, **19**:569.
2. P.G.Daniele, A.De Robertis, C.De Stefano and S.Sammartano (1985), "On the Possibility of Determining the Thermodynamic Parameters for the Formation of Weak Complexes using a Simple Model for the Dependence on Ionic Strength of Activity Coefficients: Na^+, K^+ and Ca^{++} Complexes of Low Molecular Weight Ligands in Aqueous Solution.", *J.Chem.Soc.Dalton Trans*:2353.
3. P.G.Daniele, C.Rigano and S.Sammartano (1982), "Studies on Sulphate Complexes. Part I. Potentiometric Investigations of Li^+, Na^+, K^+, Rb^+ and Cs^+ Complexes at 37 degrees C and $0.03<I<0.5$", *Inorganica Chimica Acta*, **63**:267.
4. S.A.Woskow and B.A.Glatz (1991), "Propionic Acid production by a propionic acid tolerant strain of Propionibacterium acidiopropionici in batch and semicontinuous fermentation.", *Appl.Environmental Microbiology*, **57**:2821.
5. N.S.Samuelov, R.Lamed and S.Lowe (1991), "Influence of CO_2-HCO_3^- levels and pH on growth succinate production and enzyme activities of Anaerobiospirillum succiniciporducens.", *Appl.Environmental Microbiology*, **57**:3013.
6. L.Ceccon (1990), "Quantitative determination of free volatile fatty acids from dairy products on a Nukol Capillary Column.", *J.Chromatogr.*, **519**:369.
7. D.G.Kennedy, P.B.Young and W.J.McCaughey (1991), "Rumen succinate production may ameliorate the effects of cobalt-vitamin B-12 deficiency on methylmalonyl CoA mutase in sheep.", *J.Nutrition*, **121**:1236.
8. B.Schink, "Mechanisms and kinetics of succinate and propionate degradation in anoxic freshwater sediments and sewage sludge.", *J.General Microbiology*, **131**:643.
9. P.M.May and K.Murray (1991), "Jess, a Joint Expert Speciation System- I.", *Talanta*, **38**:1409.
10. P.M.May and K.Murray (1991), "Jess, a Joint Expert Speciation System - II. The Thermodynamic Database.", *Talanta*, **38**:1419.

11. K.S.Pitzer (1977), "Electrolyte Theory - Improvements since Debye and Hückel", *Acc.Chem.Research*, **10**:371.

12. P.G.Daniele, A.De Robertis, C.De Stefano and S.Sammartano (1985), "On the Possibility of Determining the Thermodynamic Parameters for the Formation of Weak Complexes using a Simple Model for the Dependence on Ionic Strength of Activity Coefficients: Na^+, K^+ and Ca^{++} Complexes of Low Molecular Weight Ligands in Aqueous Solution.", *J.Chem.Soc.Dalton Trans*:2353.

13. F.Th.Hesselink, A.Vrij and J.Th.G.Overbeek (1971), "On the Theory of the Stabilization of Dispersions by Adsorbed Macromolecules.", *J.Phys.Chem.*, **75**:2094.

14. A.Sung and I.Piirma (1994), "Electrosteric Stabilization of Polymer Colloids", *Langmuir*, **10**:1393.

15. R.P.Borwankar, L.A.Lobo and D.T.Wasan (1992), "Emulsion Stability - Kinetics of Flocculation and Coalescence", *Colloids and Surfaces*, **69**:135.

APPENDICES

A1 STREAC.PAS - Source code of computer program STREAC (Stochastic Reverse-Emulsion Aggregation and Coalescence). Borland Pascal version 7.

```
{$N+}
{$M 65520,0,655360}
PROGRAM STREAC;

(*************************************************************************)
(*         W/O Emulsion Aggregation & Coalescence Program                *)
(*                        Lisa F Seymour                                 *)
(*                    University of Cape Town                            *)
(*                          Version 1.0                                  *)
(*                            1/6/96                                     *)
(*************************************************************************)

uses Crt, Graph, Objects, Drivers, Views, Menus, Dialogs, App;

const
  {PathToDrivers    = 'c:\tp\bgi';}
  Inputfile         = 'emul_in.dat';
  pi       = 3.14285;
  pi43     = 4.18879;      (*  4/3 times pi                              *)
  k0       = 1.381E-23;    (*  Boltzmann const J molecule-1 K-1          *)
  surf     = 4.17e-21;     (*  600*4.184/6.023e23 J molecule-1           *)
  RadDim   = 300;          (*  Radius dimension                          *)
  real_lim = 87;
  real_max = 6.1e37;
  real_min = 1.7e-38;
  MaxLines          = 100;
  cmNew             = 102;
  cmGo              = 103;
  cmHelp            = 106;
  cmAbout           = 107;
  cmSave            = 108;

TYPE
   real        = double;
   stype       = string[120];
   num_array   = array[1..RadDim] of real;
   int_array   = array[1..2] of word;
   word_array  = array[1..RadDim] of word;

  TMyApp = object(TApplication)
    procedure AboutDialog;
    procedure ErrorDialog(num:stype);
    procedure Go;
    procedure HandleEvent(var Event: TEvent); virtual;
    procedure HelpDialog;
    procedure InitMenuBar; virtual;
    procedure InitStatusLine; virtual;
    procedure NewDialog;
    procedure SaveData;
  end;

  PInterior = ^TInterior;
  TInterior = object(TScroller)
    constructor Init(var Bounds: TRect; AHScrollBar,
                     AVScrollBar: PScrollBar);
    procedure Draw; virtual;
  end;

  PDemoDialog = ^TDemoDialog;
  TDemoDialog = object(TDialog)
  end;

  DialogData = record
    Temperature,
    phi,
    psi,
```

```
    diam,
    Radius,
    InitCoverage,
    Viscosity,
    Length,
    MaxIt,
    alpha,
    Droplets,
    Hamaker,
    epsilon,
    Istr                : string[7];
  end;

VAR
   dev                                          : Text;
   DataRec                                      : DialogData;
   pretime, preKM, QM, QV,
   epsilon, kappa, psi_ave,
   hmin, maxnu, RR1, rad1, rad2,
   PrePV, PrePM, BB, CC, DD, E0,
   kT, phi, Hamaker, aq_vol, rad_ave            : real;
   MaxY, MaxX, LineCount, i, k, droplets        : word;
   IterationNo, numcol, MaxIt, Maxnc            : longint;
   rad, nu, psi                                 : num_array;
   Lines                                        : array[0..MaxLines - 1] of PString;
   x, number                                    : word_array;
   MyApp                                        : TMyApp;

{*************************************************************************}

FUNCTION DBRENT(ax,bx,cx,tol: real; VAR xmin: real): real; forward;
FUNCTION LOG(A:real):real; forward;
FUNCTION MAX(a,b: real): real; forward;
FUNCTION POWER(A,B:real):real; forward;
FUNCTION SIGN(a,b: real): real; forward;

PROCEDURE Axes(xname:num_array); forward;
PROCEDURE Chan_select (VAR Chan:int_array; Chanvol,probnum:num_array;
chanlow,chanhigh:word); forward;
PROCEDURE Energy_Barrier(VAR Collision:Boolean;  Chan:int_array); forward;
PROCEDURE Graph_Init; forward;
PROCEDURE InitData; forward;
PROCEDURE Load_Array(VAR convert:boolean); forward;
PROCEDURE Mnbrak(VAR ax,bx,cx,fa,fb,fc: real); forward;
PROCEDURE MyDfunc(VAR funcx,funcy,dfunc:real); forward;
PROCEDURE Myfunc(VAR funcx,funcy:real ); forward;
PROCEDURE RSwop(VAR R1, R2 : Real); forward;
PROCEDURE The_Rest; forward;

{*************************************************************************}

FUNCTION DBRENT(ax,bx,cx,tol: real; VAR xmin: real): real;
{This function was taken from Numerical Recipes by by W.T.Vetterling}
LABEL 1,2,3;
CONST
   itmax=100;
   zeps=1.0e-10;
VAR
   a,b,d,d1,d2: real;
   du,dv,dw,dx: real;
   e,fu,fv,fw,fx: real;
   iter: integer;
   olde,tol1,tol2: real;
   u,u1,u2,v,w,x,xm: real;
   ok1,ok2: boolean;

BEGIN
   IF ax < cx THEN a := ax ELSE a := cx;
   IF ax > cx THEN b := ax ELSE b := cx;
   v := bx;
   w := v;
   x := v;
   e := 0.0;
   mydfunc(x,fx,dx);
```

```
    fv := fx;
    fw := fx;
    dv := dx;
    dw := dx;
    FOR iter := 1 to itmax DO BEGIN
       xm := 0.5*(a+b);
       tol1 := tol*abs(x)+zeps;
       tol2 := 2.0*tol1;
       IF (abs(x-xm) <= (tol2-0.5*(b-a))) THEN GOTO 3;
       IF (abs(e) > tol1) THEN BEGIN
          d1 := 2.0*(b-a);
          d2 := d1;
          IF (dw <> dx) THEN  d1 := (w-x)*dx/(dx-dw);
          IF (dv <> dx) THEN  d2 := (v-x)*dx/(dx-dv);
          u1 := x+d1;
          u2 := x+d2;
          ok1 := ((a-u1)*(u1-b) > 0.0) AND (dx*d1 <= 0.0);
          ok2 := ((a-u2)*(u2-b) > 0.0) AND (dx*d2 <= 0.0);
          olde := e;
          e := d;
          IF (NOT (ok1 OR ok2)) THEN GOTO 1
          ELSE IF (ok1 AND ok2) THEN BEGIN
             IF (abs(d1) < abs(d2)) THEN BEGIN
                d := d1
             END ELSE BEGIN
                d := d2
             END
          END ELSE IF (ok1) THEN BEGIN
             d := d1
          END ELSE BEGIN
             d := d2
          END;
          IF (abs(d) > abs(0.5*olde)) THEN GOTO 1;
          u := x+d;
          IF (((u-a) < tol2) OR ((b-u) < tol2)) THEN BEGIN
             d := sign(tol1,xm-x)
          END;
          GOTO 2
       END;
1:     IF (dx >= 0.0) THEN e := a-x ELSE e := b-x;
       d := 0.5*e;
2:     IF (abs(d) >= tol1) THEN BEGIN
          u := x+d;
          mydfunc(u,fu,du)
       END ELSE BEGIN
          u := x+sign(tol1,d);
          mydfunc(u,fu,du);
          IF (fu > fx) THEN GOTO 3
       END;
       IF (fu <= fx) THEN BEGIN
          IF (u >= x) THEN a := x ELSE b := x;
          v := w;
          fv := fw;
          dv := dw;
          w := x;
          fw := fx;
          dw := dx;
          x := u;
          fx := fu;
          dx := du
       END ELSE BEGIN
          IF (u < x) THEN a := u ELSE b := u;
          IF ((fu <= fw) OR (w = x)) THEN BEGIN
             v := w;
             fv := fw;
             dv := dw;
             w := u;
             fw := fu;
             dw := du
          END ELSE IF ((fu < fv) OR (v = x) OR (v = w)) THEN BEGIN
             v := u;
             fv := fu;
             dv := du
          END
```

```
      END
   END;
3:   xmin := x;
   dbrent := fx
END;

{*****************************************************************************}

FUNCTION LOG(A:real):real;
BEGIN
   log:= ln(A)/ln(10);
END;

{*****************************************************************************}

FUNCTION MAX(a,b: real): real;
BEGIN
      IF (a > b) THEN max := a ELSE max := b
END;

{*****************************************************************************}

FUNCTION POWER(A,B:real):real;
VAR temp:real;
BEGIN
 temp:= B*ln(A);
 if temp < -real_lim then
     power := real_min
 else if temp > real_lim then
     power := real_max
 else
     power:= exp(temp);
END;

{*****************************************************************************}

FUNCTION SIGN(a,b: real): real;
BEGIN
      IF (b > 0.0) THEN sign := abs(a) ELSE sign := -abs(a)
END;

{*****************************************************************************}

PROCEDURE AXES( xname:num_array);
Var
    x      : word;
    s      : string[4];
    xscale : real;
    temp   : real;

Begin
  SetColor(yellow);
  SetTextStyle(DefaultFont,HorizDir,1);
  OutTextXY(360, MaxY+35,'Press Any Key To Terminate');
  SetColor(white);
  SetTextStyle(DefaultFont,VertDir,1);
  OutTextXY(20,200,'Volume');
  SetTextStyle(DefaultFont,HorizDir,1);
  OutTextXY(80,20,'Number of non-effective collisions          Maximum ');
  OutTextXY(80,60,'Time passed in seconds    ');
  OutTextXY(80,40,'Number of iterations performed ');
  Line(20,MaxY,MaxX-30,MaxY);
  OutTextXY(150,MaxY+35,'Radius  (um)' );
  xscale := RadDim/(MaxX-70);
  for i := 1 to 15 do
     Begin
       x := round((i*20)/xscale)+20;
       Line(x, Maxy, x, Maxy+10);
       temp := (xname[i*20]*1E6);
       Str(temp:4:2,s);
       OutTextXY(x-5, MaxY+15,S);
     end;
end; { of procedure AXES }
```

```
{*************************************************************************}

PROCEDURE Chan_select (Var Chan:int_array; Chanvol,probnum:num_array;
chanlow,chanhigh:word);
{  Procedure to randomly select two channels weighted by vol }

Var
  prob    : real;
  success : Boolean;
  k,i,j,swop     : word;
  starti  : word;
  Non_empty : word_array;

begin (* randomly choose two channels *)

(* order non empty channels  *)
 j := 0;
 For i := 1 to chanhigh do
  Begin
    If ( number[i] > 0) Then
      Begin
        Inc(j);
        Non_empty[j] := i;
      end;
  end;

  k:=1;
  while (k <=2) do
    begin;
      success:=false;
      prob:=random * aq_vol;
      i := 1;

      while success=false do
        begin
          if i > j then
            begin
              i := 1;
              prob := random * aq_vol;
              success := false;
            end;
          if (prob < probnum[Non_empty[i]]) then
            begin
              Chan[k] := non_empty[i];
              success := true;
              If ((number[non_empty[i]] = 1) and (k = 1)) Then
                Begin
                 While i < j  do
                  Begin
                    Non_empty[i] := Non_empty[i+1];
                    Inc(i);
                  end;
                 j := j-1;
                end;

            end;
          Inc(i);
        end; (* of while success=false *)
     Inc(k);
    end; (* of while k <= 2 *)
             if (Chan[2] > Chan [1]) then begin
                swop := Chan [1];
                Chan[1] := Chan[2];
                Chan[2] :=  swop;
             end
end; (* of choose two channels*)

{*************************************************************************}

PROCEDURE Energy_barrier( Var Collision:Boolean;  Chan:int_array);
{ procedure to calculate energy barrier }

CONST
   tol=1.0e-6;
```

```
   eql=1.0e-4;
VAR
  psi2, psi2_ave,
  H_max, HDIF, Emin, xmin,
  ax,bx,cx,fa,fb,fc,dbr          : real;
  nmin : integer;

begin (* calculate modified DLVO interaction *)
  rad1:=rad[chan[1]];
  rad2:=rad[chan[2]];
  H_max := (1.81/(power(phi,(1/3))) - 2) * rad_ave;
  RR1 := H_max +rad1 +rad2;
  prePV := 82.48*(nu[Chan[1]] + nu[Chan[2]])*kT;
  prePM := 32.03*preKm*(nu[Chan[1]]*nu[Chan[2]]);
  psi2_ave := psi[Chan[1]]*psi_ave;
  psi2 := psi[Chan[1]]*psi[Chan[2]];
  BB := kappa*(rad1+rad_ave);
  if BB >= real_lim then BB:= real_Max
                    else BB:= exp(BB);
  BB := BB*epsilon*psi2_ave*rad1*rad_ave/RR1;
  CC := -1.3*kappa*RR1;
  if CC <= -real_lim then CC:= real_min
                     else CC := exp(CC);
  CC := CC*BB*8.88*(1.3*kappa*RR1+1)/(RR1*RR1*kappa*kappa);
  DD := kappa*(rad1+rad2);
  if DD >= real_lim then DD:= real_Max
                    else DD:= exp(DD);
  DD := DD*epsilon*psi2*rad1*rad2;
  E0 := -kappa*RR1;
  if E0 <= -real_lim then E0:= real_min
                     else E0 := exp(E0);
  E0 := (E0*((DD/RR1) + 11*BB) + 2*CC)/kT;
  collision := true;

  nmin := 0;
  HDIF := (log(H_max) + 12)/100;
  WHILE (collision = true) and (nmin < 2) DO BEGIN
    if nmin = 0 then begin
       ax := -12;
       bx := ax + HDIF;
       nmin := 1;
    end else if nmin = 1 then begin
       bx := log(H_max) - HDIF;
       ax := bx - HDIF;
       nmin := 2;
    end;
    mnbrak(ax,bx,cx,fa,fb,fc);
    if (-fb) > 1 then collision := false;
    if (collision=true) and (fb<fa) and (fb<fc) then begin
      dbr := dbrent(ax,bx,cx,tol,xmin);
      myfunc(xmin,Emin);
      IF (-Emin) > 1 THEN collision :=false;
    end;
  END;
end; { of procedure energy_barrier }

{*****************************************************************************}

PROCEDURE graph_init;

var
   grDriver       : integer;
   grMode         : integer;
   ErrorCode      : integer;

Begin
  grDriver := Detect;
  Initgraph(grDriver,grMode,PathToDrivers);
  ErrorCode := GraphResult;
  If ErrorCode <> grOk then begin
    MyApp.Init;
    MyApp.ErrorDialog(GraphErrorMsg(ErrorCode));
    MyApp.Done;
    Halt(1);
```

```
    end;
  SetBkcolor(blue);
  SetColor(white);
  SetUserCharSize(3,1,3,1);
  MaxY := GetMaxY - 50;
  MaxX := GetMaxX + 20;
  end; { of procedure graph_init}

{*********************************************************************}

PROCEDURE InitData;
VAR junk:stype;
Begin
  {$I-}
  Assign(dev,inputfile);
  Reset(dev);
  {$I+}
  If IOResult <> 0 then begin
    MyApp.Init;
    junk:= 'Error reading ';
    junk:= junk + inputfile;
    junk:= junk + ' Inputting default data';
    MyApp.ErrorDialog(junk);
    MyApp.Done;
    With DataRec do begin
       Temperature := '25.0000';
       phi := '0.20000';
       psi := '0.08000';
       diam := '1.00000';
       Radius := '2.00000';
       InitCoverage := '10.0000';
       Viscosity := '0.89040';
       Length := '2.00000';
       MaxIt := '  10000';
       Alpha := '1.10000';
       Droplets := '    400';
       Hamaker := '4.0e-22';
       epsilon := '1.90000';
       Istr := '5.6e-10';
    end;
  end else with DataRec do begin
      readln(dev);
      read(dev,Temperature); readln(dev);
      read(dev,phi);  readln(dev);
      read(dev,psi); readln(dev);
      read(dev,diam);  readln(dev);
      read(dev,Radius); readln(dev);
      read(dev,InitCoverage); readln(dev);
      read(dev,Viscosity); readln(dev);
      read(dev,Length); readln(dev);
      read(dev,MaxIt); readln(dev);
      read(dev,alpha); readln(dev);
      read(dev,Droplets);  readln(dev);
      read(dev,Hamaker);  readln(dev);
      read(dev,epsilon);  readln(dev);
      read(dev,Istr);  readln(dev);
      Close(dev);
    end;
end; {* of procedure InitData *}

{*********************************************************************}

PROCEDURE load_array(VAR convert:boolean);

Var
   code                                    : integer;
   volume, Istr, diam, alpha, length,
   initcov, Viscosity, Temperature         : real;

Begin
  convert := true;
  Val(DataRec.Temperature,Temperature,code);
  if code <> 0 then convert :=false;
  Val(DataRec.radius,rad[1],code);
```

```
  if code <> 0 then convert :=false;
  Val(DataRec.Initcoverage,initcov,code);
  if code <> 0 then convert :=false;
  Val(DataRec.Viscosity,Viscosity,code);
  if code <> 0 then convert :=false;
  Val(DataRec.MaxIt,MaxIt,code);
  if code <> 0 then convert :=false;
  Val(DataRec.alpha,alpha,code);
  if code <> 0 then convert :=false;
  Val(Datarec.diam,diam,code);
  if code <> 0 then convert :=false;
  Val(DataRec.droplets,droplets,code);
  if code <> 0 then convert :=false;
  Val(DataRec.Hamaker,Hamaker,code);
  if code <> 0 then convert :=false;
  Val(DataRec.phi,phi,code);
  if code <> 0 then convert :=false;
  Val(DataRec.Istr,Istr,code);
  if code <> 0 then convert :=false;
  Val(DataRec.psi,psi[1],code);
  if code <> 0 then convert :=false;
  Val(DataRec.epsilon,epsilon,code);
  if code <> 0 then convert :=false;
  Val(DataRec.Length,Length,code);
  if code <> 0 then convert :=false;
  if convert = true then begin
    maxnc := round(droplets/1.6);
    Istr := Istr*1e3;
    epsilon := epsilon*8.854e-12;
    Viscosity := 0.1*Viscosity;
    Temperature := (Temperature + 273.18);
    diam := diam*1e-9;
    Length := length*1e-9;
    rad[1] := rad[1]*1e-6;
    nu[1] := initcov/(100*diam*diam);
    number[1] := droplets;
    aq_vol := number[1]*pi43*rad[1]*rad[1]*rad[1];
    volume := aq_vol/phi;
    kT := k0 * Temperature;
    pretime := 3*volume*Viscosity/(4*kT);
    kappa := sqrt((Istr*2.2394e9)/(epsilon*Temperature));
    if kappa < 1e3 then kappa :=1e3;
    maxnu := 1/(diam*diam);
    hmin := 2*length;
    preKM := power((2*pi/9),(3/2))*2*(alpha*alpha-1)*length*length*kT;
    QM := 2.467*alpha/length;
    QV := 4.414*alpha/length;
  end;
End; { of PROCEDURE load_array}

{*************************************************************************}

PROCEDURE mnbrak(VAR ax,bx,cx,fa,fb,fc: real);
LABEL 1;
CONST
   gold=1.618034;
   glimit=100.0;
   tiny=1.0e-20;
VAR
   ulim,u,r,q,fu: real;
   mcount       : integer;
BEGIN
   mcount := 0;
   myfunc(ax,fa);
   myfunc(bx,fb);
   IF (fb > fa) THEN BEGIN
      Rswop(ax,bx);
      Rswop(fa,fb);
   END;
   IF (-fa < 1) and (-fb < 1) then begin
   cx := bx+gold*(bx-ax);
   myfunc(cx,fc);
1: IF (fb >= fc) and (mcount < 50) THEN BEGIN
      if fb = fc then mcount:= mcount + 1;
```

```
      r := (bx-ax)*(fb-fc);
      q := (bx-cx)*(fb-fa);
      u := bx-((bx-cx)*q-(bx-ax)*r)/(2.0*sign(max(abs(q-r),tiny),q-r));
      ulim := bx+glimit*(cx-bx);
      IF ((bx-u)*(u-cx) > 0.0) THEN BEGIN
         myfunc(u,fu);
         IF (fu < fc) THEN BEGIN
            ax := bx;
            fa := fb;
            bx := u;
            fb := fu;
            GOTO 1
         END
         ELSE IF (fu > fb) THEN BEGIN
            cx := u;
            fc := fu;
            GOTO 1
         END;
         u := cx+gold*(cx-bx);
         myfunc(u,fu)
      END ELSE IF  ((cx-u)*(u-ulim) > 0.0) THEN BEGIN
         myfunc(u,fu);
         IF (fu < fc) THEN BEGIN
            bx := cx;
            cx := u;
            u := cx+gold*(cx-bx);
            fb := fc;
            fc := fu;
            myfunc(u,fu)
         END
      END ELSE IF  ((u-ulim)*(ulim-cx) >= 0.0) THEN BEGIN
         u := ulim;
         myfunc(u,fu)
      END ELSE BEGIN
         u := cx+gold*(cx-bx);
         myfunc(u,fu)
      END;
      ax := bx;
      bx := cx;
      cx := u;
      fa := fb;
      fb := fc;
      fc := fu;
      GOTO 1
   END
   end else begin
     cx := fc;
     fc := fa;
   end
END; {Of Procedure MNBrak}

{*****************************************************************************}

PROCEDURE MYDFUNC(VAR funcx,funcy,dfunc:real);
VAR
  HH, SS, preE, EE, h0,
  d2, ds, ds2, RS, sum,
  nx, ny, nz, n_a, n_b, n_g,
  fx, fy, dES, dER, dEA, PM, PV, EA, ER, ES :real;

  BEGIN
    HH := power(10,funcx);
    fy := rad2/rad1;
    SS := HH + rad1 + rad2;
    d2 := rad2*rad2+rad1*rad2
        + rad1*HH+rad2*HH+HH*HH/2;
    d2 := d2/(rad1+rad2+HH);
    ds := SS - d2;
    ds2 := ds - d2;
    RS := RR1 - SS;
   if RS > 0 then begin
    fx := (HH)/(2*rad1);
    EE := power((RR1*RS/3 + SS*SS),0.5);
    preE := -kappa*EE;
```

```
    if preE >= -real_lim then preE := BB*exp(preE)
                         else preE := BB*real_min;
    nx := fx*fx + fx*fy + fx;
    ny := nx + fy;
    nz := 2*fx + fy + 1;
    n_a := CC*exp(kappa*RS);
    n_b := -kappa*RS;
    if n_b >= -real_lim then n_b := CC*exp(n_b)
                        else n_b := CC*real_min;
    n_b := n_b + 6*BB*exp(kappa*(SS-2*RR1));
    n_g := n_a + n_b;
    n_a := n_a - n_b + 6*preE;
    n_b := n_g - preE*6*RS/EE;
    EA := -1*Hamaker*(fy/nx + fy/ny + 2*ln(nx/ny))/(12*kT);
    dEA := Hamaker*nz*fy*fy*fy/(24*rad1*nx*nx*ny*ny);
    ER := DD*exp(-kappa*SS)/SS;
    dER := -ER*(kappa*SS + 1)/SS;
    ER := (ER + n_a/(kappa*RS))/kT;
    dER := dER + n_a/(kappa*RS*RS) - n_b/RS;
    if HH > hmin then h0 := HH
                 else h0 := hmin;
    d2 := 2*d2 - h0;
    PM := -1*h0*QM;
    if PM >= -real_lim then PM := prePM*exp(PM)
                       else PM := 0;
    PV := -1*h0*QV;
    if PV >= -real_lim then PV := prePV*exp(PV)
                       else PV := 0;
    if HH > hmin then
      begin
        dES := (ds2/SS + 1)*(PM/QM + PV/QV - d2*PM - d2*PV);
        dES := dES + (PM*QM +PV*QV)*(d2*d2/SS - 2*rad2*rad2);
      end
    else
        dES := 2*ds*(PM/QM + PV/QV - PM*d2 - PV*d2)/SS;
    sum := PM*(QM*d2 - 1)/(QM*QM);
    sum := sum + PV*(QV*d2 - 1)/(QV*QV);
    ES := (PM+PV)*(4*rad2*rad2 - d2*d2)/(2*kT) + sum/kT;
    funcy := -(EA + ER + ES - E0);
    dfunc := -(dEA + dER + dES);
   end else begin
    funcx := log(RR1 - rad1 - rad2);
    funcy := 0;
    dfunc := 0;
   end;
END; {OF Procedure MYDFunc}

{*****************************************************************************}

PROCEDURE MYFUNC(VAR funcx,funcy:real);
VAR
  HH, SS, preE, EE, h0,
  d2, RS, sum, nx, ny, n_a,
  fx, fy, PM, PV, EA, ER, ES :real;

  BEGIN
   HH:=power(10,funcx);
   SS := HH + rad1 + rad2;
   RS := RR1 - SS;
   if RS > 0 then begin
    EE := power((RR1*RS/3 + SS*SS),0.5);
    preE := -kappa*EE;
    if preE >= -real_lim then preE := 6*BB*exp(preE)
                         else preE := 6*BB*real_min;
    n_a := kappa*RS;
    if n_a <= real_lim then n_a := CC*(exp(n_a) - exp(-n_a)) + preE
                       else n_a := CC*(real_max) + preE;
    preE := kappa*(SS-2*RR1);
    if preE >= -real_lim then preE := 6*BB*exp(preE)
                         else preE := 6*BB*real_min;
    n_a := n_a - preE;
    ER := -kappa*SS;
    if ER >= -real_lim then ER := exp(ER)
                       else ER := real_min;
```

```
    ER := (DD*ER/SS + n_a/(kappa*RS))/kT;
    if (-ER+E0) > 1 then funcy := (-ER+E0) else begin
       fy := rad2/rad1;
       fx := (HH)/(2*rad1);
       nx := fx*fx + fx*fy + fx;
       ny := nx + fy;
       EA := -1*Hamaker*(fy/nx + fy/ny + 2*ln(nx/ny))/(12*kT);
       if HH > hmin then h0 := HH
                else h0 := hmin;
       d2 := rad2*rad2 +rad1*rad2 +rad1*HH +rad2*HH+ HH*HH/2;
       d2 := 2*d2/(rad1+rad2+HH) - h0;
       PM := -1*h0*QM;
       if PM >= -real_lim then PM := prePM*exp(PM)
                  else PM := 0;
       PV := -1*h0*QV;
       if PV >= -real_lim then PV := prePV*exp(PV)
                  else PV := 0;
       sum := PM*(QM*d2 - 1)/(QM*QM) + PV*(QV*d2 - 1)/(QV*QV);
       ES := (PM+PV)*(4*rad2*rad2 - d2*d2)/(2*kT) + sum/kT;
       funcy := -(EA + ER + ES - E0);
    end
   end else begin
    funcy := 0;
    funcx := (RR1 - rad1 - rad2);
    funcx := log(funcx);
   end;
END; {End Of Procedure MyFunc}

{*****************************************************************************}

PROCEDURE RSWOP(Var R1, R2 : Real);
Var Temp : real;
Begin
  Temp := R1;
  R1 := R2;
  R2 := Temp;
End; {Of Procedure RSwop}

{*****************************************************************************}

PROCEDURE The_Rest;

CONST
  chanlow      : word = 1;
  chanhigh     : word = 1;

VAR
  time, oldq, newq,
  xscale, incr, initq          : real;
  vol, probnum, chanvol        : num_array;
  y, nc, cnew, maxineff        : word;
  answer                       : char;
  collision, maxsurf,
  success, dilute              : boolean;
  s,n,snc,smnc                 : string[10];
  maxrad,maxcol                : string[60];
  Chan                         : int_array;
  x                            : array[1..radDim] of word;   (* xaxis points*)

BEGIN
  time := 0;
  maxsurf := false;
  chanhigh := 1;
  chanlow := 1;
  vol[1] := pi43*(exp(3*ln(rad[1])));
  chanvol[1] := number[1]*vol[1];
  probnum[1] := chanvol[1];
  xscale := RadDim/(MaxX-70);
  x[1] := round(1/xscale) +21;
  oldq := 1 + kappa*rad[1];
  initq :=  psi[1]*oldq;
  psi_ave := psi[1];
  rad_ave := rad[1];
  for i:=2 to RadDim do
```

```
    begin
      number[i] := 0;
      incr := (exp( ln(i)/3 ));
      vol[i] := vol[1]*i;
      rad[i] := rad[1]*incr;
      newq := power(i,1/3)*(1 + power(i,1/3)*kappa*rad[1]);
      psi[i] := (psi[i-1]*oldq + initq)/newq;
      oldq := newq;
      nu[i] :=  nu[1]*incr;
      if nu[i] >= Maxnu then
      begin
         nu[i] := Maxnu;
         if maxsurf = false then
         begin
            maxsurf := true;
            Str((rad[i]*1e6):4:2,maxrad);
            maxrad := 'Micelle formation for radius > ' + maxrad;
            maxrad :=  maxrad + ' um';
         end;
      end;
      chanvol[i] := number[i]*vol[i];
      probnum[i] := probnum[(i-1)] + chanvol[i];
      x[i] := round(i/xscale) +21;
      if number[i] > 0 then
         chanhigh := i;
    end;
  AXES(rad); {******* runs procedure ***********}
  For i := chanlow to chanhigh do
     Begin
       y := round(MAXY*(1 - chanvol[i]/aq_vol));
       Bar(x[i],MAXY, x[i]+1,y);
     end;
  Randomize;
  dilute := true;
  if (phi > 0.74) then
      begin
           {********** emulsion not dilute - program does not apply *********}
           dilute := false;
      end;
  maxineff:=0;
  numcol:=0;
  IterationNo := 0;
  nc:=0;
  snc :=' ';
  WHILE  (keypressed = false) and (droplets >= 4 ) and (dilute = true)
      and (IterationNo <= MaxIt ) and (nc <= Maxnc) DO BEGIN
    Chan_select(Chan,chanvol,probnum,chanlow,chanhigh);  {******* runs procedure
***********}
    Energy_barrier(collision,Chan);                          {******* runs procedure
***********}
    time := time + pretime/sqr(droplets);
    Inc(nc);        (* no. ineffective collisions*)
    if collision then begin
       (* decriment array and calculate channel and nu for new particle *)
          nc := 0;
          psi_ave := 0;
          rad_ave := 0;
          dec(droplets);
          for k:= 1 to 2 do
            begin
              SetFillStyle(0,blue);
              y := round(MAXY*(1 - chanvol[Chan[k]]/aq_vol));
              Bar(x[Chan[k]],MAXY, x[Chan[k]]+1,y);
              Dec(number[Chan[k]]);
              chanvol[Chan[k]] := chanvol[Chan[k]] - vol[Chan[k]];
              SetFillStyle(1,white);
              y := round(MAXY*(1 - chanvol[Chan[k]]/aq_vol));
              Bar(x[Chan[k]],MAXY, x[Chan[k]]+1,y);
            end;
          cnew := Chan[1] + Chan[2];
          if (cnew < RadDim) then
            begin
              chanvol[cnew] := chanvol[cnew] + vol[cnew];
              Inc(number[cnew]);
```

```
            y := round(MAXY*(1 - chanvol[cnew]/aq_vol));
            Bar(x[cnew],MAXY, x[cnew]+1,y);
            chanlow := Chan[1];
            if ((cnew < RadDim) and (cnew > chanhigh)) then
               chanhigh := cnew;
            if chanlow = 1 then
               Begin
                  probnum[1] := chanvol[1];
                  for i:= 2 to chanhigh do
                      probnum[i] := probnum[(i-1)] + chanvol[i];
               end
            Else
                for i:= chanlow to chanhigh do
                    probnum[i] := probnum[(i-1)] + chanvol[i];
            Inc(numcol);
          end {* of if cnew <= RadDim *}
        else
            {********** phase separation ocurred ********}
            droplets:= 1;
        for k:= 1 to chanhigh do
          begin
            psi_ave := psi_ave + psi[k]*number[k];
            rad_ave := rad_ave + rad[k]*number[k];
          end;
        psi_ave := psi_ave/droplets;
        rad_ave := rad_ave/droplets;
   end else
        if IterationNo = 0 then begin
              nc := maxnc;
              time := time*maxnc;
              IterationNo := maxnc - 1;
        end;
   Inc(IterationNo);
   if nc > maxineff then maxineff := nc;
   SetColor(Blue);
   OutTextXY(315,60,s);
   OutTextXY(350,40,n);
   OutTextXY(365,20,snc);
   OutTextXY(515,20,smnc);
   SetColor(White);
   Str(time:8:7,s);
   Str((IterationNo),n);
   Str(nc,snc);
   Str(maxineff,smnc);
   OutTextXY(315,60,s);
   OutTextXY(350,40,n);
   OutTextXY(365,20,snc);
   OutTextXY(515,20,smnc);
END;
if (keypressed = true) then begin
    OutTextXY(round(MaxX/4),round(MaxY/2)+20,'Termination by User');
    OutTextXY(round(MaxX/4),round(MaxY/2)+40,'Stability not determined');
end else if (nc > Maxnc) Then begin
    Str(Maxnc,maxcol);
    maxcol := 'More than ' + maxcol + ' non-effective collisions';
    OutTextXY(round(MaxX/4),round(MaxY/2)+20,maxcol);
    OutTextXY(round(MaxX/4),round(MaxY/2)+40,'Emulsion Stable');
end Else If (dilute = false) Then begin
    OutTextXY(round(MaxX/4),round(MaxY/2)+20,'Emulsion not dilute');
    OutTextXY(round(MaxX/4),round(MaxY/2)+40,'Stability not determined');
end Else If (droplets < 4) Then begin
    OutTextXY(Round(MaxX/4),round(MaxY/2)+20,'Phase separation occurred');
    OutTextXY(round(MaxX/4),round(MaxY/2)+40,'Emulsion Unstable');
end Else If (IterationNo >= MaxIt) Then begin
    Str(MaxIt,maxcol);
    maxcol := 'More than ' + maxcol + ' iterations';
    OutTextXY(Round(MaxX/4),round(MaxY/2)+20,maxcol);
    OutTextXY(round(MaxX/4),round(MaxY/2)+40,'Emulsion Stable');
end;
If maxsurf = true then
  OutTextXY(round(MaxX/4),round(MaxY/2)-40,maxrad);
OutTextXY(round(MaxX/4),round(MaxY/2),'Execution Terminated');
OutTextXY(80,80,'Maximum droplet radius (um)    ');
Str((rad[chanhigh]*1e6):8:6,s);
```

```
  OutTextXY(350,80,s);
  Setcolor(blue);
  OutTextXY(360, MaxY+35,'Press Any Key To Terminate');
  Setcolor(yellow);
  OutTextXY(round(MaxX/4),round(MaxY/2)-20,'Press Y to Exit');
  REPEAT
    answer:=Readkey;
  UNTIL (answer = 'Y') or (answer = 'y');
  CloseGraph;
End; { of PROCEDURE the_rest }

{*********************************************************************}

CONSTRUCTOR TInterior.Init(var Bounds: TRect; AHScrollBar,
                           AVScrollBar: PScrollBar);
begin
  TScroller.Init(Bounds, AHScrollBar, AVScrollBar);
  Options := Options or ofFramed;
  SetLimit(128, LineCount);
end; {* of constructor TInterior.Init}

{*********************************************************************}

PROCEDURE TInterior.Draw;

var
  Color  : Byte;
  I, Y   : Integer;
  B      : TDrawBuffer;

begin
  Color := GetColor(1);
  for Y := 0 to Size.Y - 1 do
    begin
      MoveChar(B, ' ', Color, Size.X);
      i := Delta.Y + Y;
      if (I < LineCount) and (Lines[I] <> nil) then
         MoveStr(B, Copy(Lines[I]^, Delta.X + 1, Size.X), Color);
      WriteLine(0, Y, Size.X, 1, B);
    end;
end; {* of procedure TInterior}

{*********************************************************************}

PROCEDURE TMyApp.AboutDialog;
Var
  Bruce                    : PView;
  Dialog                   : PDemoDialog;
  R                        : TRect;
  C                        : Word;

Begin
  R.Assign(4,5,76,15);
  Dialog := New(PDemoDialog, Init(R, 'About Emulsion Coalescence Simulation Program
'));
  with Dialog^ do
    begin
      R.Assign(2, 2, 69, 3);
      Insert(New(PLabel, Init(R, ' ', Bruce)));
      R.Assign(2, 3, 69, 4);
      Insert(New(PLabel, Init(R, '       This program was written by Lisa Seymour
UCT, 1995', Bruce)));
      R.Assign(2, 4, 69, 5);
      Insert(New(PLabel, Init(R, '    in partial fulfillment of the requirement for
the degree', Bruce)));
      R.Assign(2, 5, 69, 6);
      Insert(New(PLabel, Init(R, '                          PhD in Chemistry ',
Bruce)));
      R.Assign(28,8,41,10);
      Insert(New(PButton, Init(R, ' ~O~k', cmOK, bfDefault)));
    end;
  C := DeskTop^.ExecView(Dialog);
  Dispose(Dialog, Done);
End; {* of procedure TMyApp.AboutDialog *}
```

```
{*********************************************************************}

PROCEDURE TMyApp.ErrorDialog(num:stype);
Var
  Bruce                       : PView;
  Dialog                      : PDemoDialog;
  R                           : TRect;
  C                           : Word;

Begin
  R.Assign(10,7,70,16);
  Dialog := New(PDemoDialog, Init(R, 'Runtime Error'));
  with Dialog^ do
    begin
      R.Assign(2, 3, 58, 4);
      Insert(New(PLabel, Init(R, num , Bruce)));
      R.Assign(22,6,38,8);
      Insert(New(PButton, Init(R, ' ~O~k', cmOK, bfDefault)));
    end;
  C := DeskTop^.ExecView(Dialog);
  Dispose(Dialog, Done);
End; {* of procedure TMyApp.ErrorDialog *}

{*********************************************************************}

PROCEDURE TMyapp.Go;
VAR convert:boolean;
Begin
  MyApp.Done;
  load_array(convert); (*load previous array from disc*)
  if convert = false then begin
    MyApp.Init;
    MyApp.ErrorDialog('Data not in correct format, must be right aligned');
    MyApp.NewDialog;
  end else begin
    graph_init;
    the_rest;   (*all calculations are carried out in 'the_rest'*)
    MyApp.Init;
    MyApp.run;
  end;
end;{* of Procedure TMyapp.Go *}

{*********************************************************************}

PROCEDURE TMyApp.HandleEvent(var Event: TEvent);
Begin
  TApplication.HandleEvent(Event);  {******* runs procedure ***********}
  if Event.What = evCommand then
   begin
      case Event.Command of
        cmNew: NewDialog;
        cmCancel: NewDialog;
        cmGo : Go;
        cmHelp : HelpDialog;
        cmAbout : AboutDialog;
        cmSave : SaveData;
      else
        Exit;
      end;
      ClearEvent(Event);
   end;
end; {* of procedure TMyApp.HandleEvent *}

{*********************************************************************}

PROCEDURE TMyApp.HelpDialog;
Var
  Bruce                       : PView;
  Dialog                      : PDemoDialog;
  R                           : TRect;
  C                           : Word;

Begin
  R.Assign(4,2,76,21);
```

```
  Dialog := New(PDemoDialog, Init(R, 'Emulsion Coalescence Simulation Program
Instructions'));
  with Dialog^ do
    begin
      R.Assign(1, 1, 71, 2);
      Insert(New(PLabel, Init(R, '   <F1>  This Help Screen', Bruce)));
      R.Assign(1, 2, 71, 3);
      Insert(New(PLabel, Init(R, '   <F2>  Edit the input data obtained from file
emul_in.dat', Bruce)));
      R.Assign(1, 3, 71, 4);
      Insert(New(PLabel, Init(R, '   <F3>  Save the Input data to file
emul_in.dat', Bruce)));
      R.Assign(1, 4, 71, 5);
      Insert(New(PLabel, Init(R, '   <F9>  Start the Simulation', Bruce)));
      R.Assign(1, 5, 71, 6);
      Insert(New(PLabel, Init(R, '  <F10>  To get to the Top Menu Commands
',Bruce)));
      R.Assign(1, 6, 71, 7);
      Insert(New(PLabel, Init(R, '<Alt-X>  Exit this program
             ', Bruce)));
      R.Assign(1, 7, 71, 8);
      Insert(New(PLabel, Init(R, '*  The text file emul_in.dat contains a more
comprehensive', Bruce)));
      R.Assign(1, 8, 71, 9);
      Insert(New(PLabel, Init(R, '   description of the input parameters.',
Bruce)));
      R.Assign(1, 9, 71,10);
      Insert(New(PLabel, Init(R, '********************** HOW TO MOVE AROUND
************************', Bruce)));
      R.Assign(1,10, 71,11);
      Insert(New(PLabel, Init(R, '*  Push the above function keys or select them
with a mouse to run.',Bruce)));
      R.Assign(1,11, 71, 12);
      Insert(New(PLabel, Init(R, '*  Press <Enter> or <Esc> or Select OK or Cancel
to close the active', Bruce)));
      R.Assign(1, 12, 71, 13);
      Insert(New(PLabel, Init(R, '   window.  Each active window has to be closed
to proceed!     ', Bruce)));
      R.Assign(1, 13, 71, 14);
      Insert(New(PLabel, Init(R, '*  Press the <Tab> and arrow keys or your mouse
to move around the', Bruce)));
      R.Assign(1, 14, 71, 15);
      Insert(New(PLabel, Init(R, '   data on the screen.
       ', Bruce)));
      R.Assign(1, 15, 71, 16);
      Insert(New(PLabel, Init(R, '*  Press <Alt> and the red letter of choice to
get to the top menu', Bruce)));
      R.Assign(1, 16, 71, 17);
      Insert(New(PLabel, Init(R, '   or use your mouse.
             ', Bruce)));
      R.Assign(28,17,41,19);
      Insert(New(PButton, Init(R, ' -O-k', cmOK, bfDefault)));
    end;
  C := DeskTop^.ExecView(Dialog);
  Dispose(Dialog, Done);
End; {* of procedure TMyApp.HelpDialog *}

{*********************************************************************}

PROCEDURE TMyApp.InitMenuBar;
var
  R: TRect;
begin
  GetExtent(R);
  R.B.Y := R.A.Y + 1;
  MenuBar := New(PMenuBar, Init(R, NewMenu(
    NewSubMenu('~F-ile', hcNoContext, NewMenu(
      NewItem('~D-ata', 'F2', kbF2, cmNew, hcNoContext,
      NewItem('~S-ave', 'F3', kbF3, cmSave, hcNoContext,
      NewItem('~G-o', 'F9', kbF9, cmGo, hcNoContext,
      NewLine(
      NewItem('E-x-it', 'Alt-X', kbAltX, cmQuit, hcNoContext,
      nil))))))),
    NewSubMenu('~W~indow', hcNoContext, NewMenu(
```

```
      NewItem('~D-ata', 'F2', kbF2, cmNew, hcNoContext,
      NewItem('~H-elp', 'F1', kbF1, cmHelp, hcNoContext,
      NewItem('~S-upport', 'F5', kbF5, cmAbout, hcNoContext,
      nil)))),
    NewSubMenu('~H-elp', hcNoContext, NewMenu(
      NewItem('~I-nfo','F1', kbF1, cmHelp, hcNoContext,
      NewItem('~S-upport','F5', kbF5, cmAbout, hcNoContext,
      nil))),
    nil))
  ))));
end; {* of procedure TMyApp.InitMenuBar *}

{*********************************************************************}

PROCEDURE TMyApp.InitStatusLine;
var
  R: TRect;
begin
  GetExtent(R);
  R.A.Y := R.B.Y - 1;
  StatusLine := New(PStatusLine, Init(R,
    NewStatusDef(0, $FFFF,
      NewStatusKey('', kbF10, cmMenu,
      NewStatusKey('~Alt-X~ Exit', kbAltX, cmQuit,
      NewStatusKey('~F1~ Help', kbF1, cmHelp,
      NewStatusKey('~F2~ Data', kbF2, cmNew,
      NewStatusKey('~F3~ Save', kbF3, cmSave,
      NewStatusKey('~F9~ Go', kbF9, cmGo,
      NewStatusKey('~F10~ Menu', kbF10, cmMenu,
      nil)))))))),
    nil)
  ));
end; {* of procedure TMyApp.InitStatusLine *}

{*********************************************************************}

PROCEDURE TMyApp.NewDialog;

var
  c1,c2,c3,
  c4,c5       :Integer;
  Bruce       : PView;
  Dialog      : PDemoDialog;
  R           : TRect;
  C           : Word;

begin
  R.Assign(3, 1, 77, 21);
  c1:=2;
  c2:=27;
  c3:=37;
  c4:=62;
  c5:=72;
  Dialog := New(PDemoDialog, Init(R, 'Data Input'));
  with Dialog^ do
    begin
      R.Assign(c2+1, 2, c3, 3);
      Bruce := New(PInputLine, Init(R, 7));
      Insert(Bruce);
      R.Assign(c1, 2, c2, 3);
      Insert(New(PLabel, Init(R, 'Celsius Temperature', Bruce)));
      R.Assign(c4+1, 2, c5, 3);
      Bruce := New(PInputLine, Init(R, 7));
      Insert(Bruce);
      R.Assign(c3+1, 2, c4, 3);
      Insert(New(PLabel, Init(R, 'Internal Phase Volume', Bruce)));
      R.Assign(c2+1, 4, c3, 5);
      Bruce := New(PInputLine, Init(R, 7));
      Insert(Bruce);
      R.Assign(c1, 4, c2, 5);
      Insert(New(PLabel, Init(R, 'Surface Potential (V)', Bruce)));
      R.Assign(c4+1, 4, c5, 5);
      Bruce := New(PInputLine, Init(R, 7));
      Insert(Bruce);
```

```
      R.Assign(c3+1, 4, c4, 5);
      Insert(New(PLabel, Init(R, 'Headgroup diameter (nm)', Bruce)));
      R.Assign(c2+1, 6, c3, 7);
      Bruce := New(PInputLine, Init(R, 7));
      Insert(Bruce);
      R.Assign(c1, 6, c2, 7);
      Insert(New(PLabel, Init(R, 'Droplet Radius (um)', Bruce)));
      R.Assign(c4+1, 6, c5, 7);
      Bruce := New(PInputLine, Init(R, 7));
      Insert(Bruce);
      R.Assign(c3+1, 6, c4, 7);
      Insert(New(PLabel, Init(R, 'Surfactant Coverage (%)', Bruce)));
      R.Assign(c2+1, 8, c3, 9);
      Bruce := New(PInputLine, Init(R, 7));
      Insert(Bruce);
      R.Assign(c1, 8, c2, 9);
      Insert(New(PLabel, Init(R, 'Viscosity (cp)', Bruce)));
      R.Assign(c4+1, 8, c5, 9);
      Bruce := New(PInputLine, Init(R, 7));
      Insert(Bruce);
      R.Assign(c3+1, 8, c4, 9);
      Insert(New(PLabel, Init(R, 'Surfactant length (nm)', Bruce)));
      R.Assign(c2+1, 10, c3, 11);
      Bruce := New(PInputLine, Init(R, 7));
      Insert(Bruce);
      R.Assign(c1, 10, c2, 11);
      Insert(New(PLabel, Init(R, 'Maximum Iterations', Bruce)));
      R.Assign(c4+1, 10, c5, 11);
      Bruce := New(PInputLine, Init(R, 7));
      Insert(Bruce);
      R.Assign(c3+1, 10, c4, 11);
      Insert(New(PLabel, Init(R, 'Expansion parameter', Bruce)));
      R.Assign(c2+1, 12, c3, 13);
      Bruce := New(PInputLine, Init(R, 7));
      Insert(Bruce);
      R.Assign(c1, 12, c2, 13);
      Insert(New(PLabel,Init(R, 'Initial No. of Droplets',Bruce)));
      R.Assign(c4+1, 12, c5, 13);
      Bruce := New(PInputLine, Init(R, 7));
      Insert(Bruce);
      R.Assign(c3+1, 12, c4, 13);
      Insert(New(PLabel,Init(R, 'Effective Hamaker Const',Bruce)));
      R.Assign(c2+1, 14, c3, 15);
      Bruce := New(PInputLine, Init(R, 7));
      Insert(Bruce);
      R.Assign(c1, 14, c2, 15);
      Insert(New(PLabel,Init(R, 'Oil Dielectric Constant',Bruce)));
      R.Assign(c4+1, 14, c5, 15);
      Bruce := New(PInputLine, Init(R, 7));
      Insert(Bruce);
      R.Assign(c3+1, 14, c4, 15);
      Insert(New(PLabel,Init(R, 'Oil [Ionic Strength]',Bruce)));
      R.Assign(14, 16, 22, 18);
      Insert(New(PButton, Init(R, '~O~k', cmOK, bfDefault)));
      R.Assign(45, 16, 56, 18);
      Insert(New(PButton, Init(R, 'Cancel', cmCancel, bfNormal)));
    end;
  Dialog^.SetData(DataRec);
  C := DeskTop^.ExecView(Dialog);
  if c <> cmCancel then Dialog^.GetData(DataRec);
  Dispose(Dialog, Done);
end; {* of procedure TMyApp.NewDialog *}

{*********************************************************************}

PROCEDURE TMyApp.SaveData;
Var junk:stype;
Begin
  junk :='Error writing to ';
  junk := junk + inputfile;
  junk := junk + ' aborting save';
  with DataRec do Begin
    {$I-}
    Assign(dev,inputfile);
```

```
    Rewrite(dev);
    {$I+}
    If IOResult <> 0 then
       MyApp.ErrorDialog(junk)
    else begin
      writeln(dev,'{INPUT FOR PROGRAM EMULSION.PAS}');
      write(dev,Temperature); writeln(dev,'    Temperature in Degrees Celsius');
      write(dev,phi);  writeln(dev,'    Internal Phase Volume Ratio');
      write(dev,psi); writeln(dev,'    Surface Potential in V');
      write(dev,diam);  writeln(dev,'    surfactant headgroup diameter (nm)');
      write(dev,Radius); writeln(dev,'    Radius of Droplets in micrometres');
      write(dev,InitCoverage); writeln(dev,'    Initial Percentage Surfactant
Coverage');
      write(dev,Viscosity); writeln(dev,'    Viscosity of Oil in centipoise');
      write(dev,Length); writeln(dev,'    Length of surfactant in nm');
      write(dev,MaxIt); writeln(dev,'    Maximum Number of Iterations to Perform
(integer)');
      write(dev,alpha); writeln(dev,'    Surfactant Expansion Parameter');
      write(dev,Droplets);  writeln(dev,'    Number of Droplets in Sample (integer
< 65535)');
      write(dev,Hamaker);  writeln(dev,'    Effective Hamaker Constant (J)');
      write(dev,epsilon);  writeln(dev,'    Dielectric Constant of Organic Phase');
      write(dev,Istr);  writeln(dev,'    Ionic Strength of oil in molarity');
      Close(dev);
    end;
  end;
end; {* of procedure TMYApp.SaveData *}

{*********************************************************************}

BEGIN (* MAIN *)
  InitData;
  MyApp.Init;
  MyApp.Run;
  MyApp.Done;
END. (** of PROGRAM Emulsion **)

{*********************************************************************}
```

A2 EMULSION COALESCENCE THEORY

The coalescence of two drops in an emulsion after clumping has occurred, can be split into two stages:[1,2]

a) drainage of the thin liquid film to a critical thickness

b) film rupture by surface instability followed by the two droplets uniting.

Experimental observations suggest that the stability of a concentrated emulsion is directly related to the stability of the thin film formed between the droplets and that the stability of this film is determined primarily by its rate of thinning (stage a).

In order to predict the lifetime of a thin emulsion film (between 10 - 100 nm), it is essential to know the rate of drainage as well as the critical thickness at which the film ruptures.

Reynolds idealized the drainage of a liquid film between two identical droplets by approximating the deformed area between the two droplets by two rigid disks. His prediction for the rate of drainage is known as the Reynolds rate of drainage and is expressed as follows:[3]

$$V_{Re} = \frac{8h^3 \Delta P}{3\mu r^2} \qquad \text{....A.1}$$

where ΔP is the capillary pressure causing drainage

h is the half film thickness

r is the film radius and

μ is the viscosity of the film liquid

This theory ties in with experimental results which have shown that stiff interfacial films of hydrolysis and surfactant association products are necessary for the stabilization of w/o emulsions. The irregular shape of stabilized water globules can be attributed to the stiffness of the interfacial film.[4]

Experimental studies have shown that for an emulsion film the assumption of a plane parallel film is only justified for film thicknesses < 200 nm and for film radii < 10^{-4} m.[5,6] The

Reynolds equation predicts the experimental thinning velocity at high surfactant concentrations and high values of E_s ($E_s > 10^6$) and K_σ ($K_\sigma > 10^8$ μPa.m^4.sec/kmol).

where K_σ is the variation of the interfacial tension with respect to surfactant concentration and
E_s is the dimensionless elasticity number.

At smaller values of K_σ and E_s the thinning velocity is much greater than that predicted by the Reynolds equation due to the mobility of the interfaces.

In our approach we have used the model predicted by Malhotra *et al.* which accounts for the effect of surface mobility on film drainage and predicts results which are in fair agreement with the experimental data for all the systems studied so far.[3,5-8] Their predicted velocity is given by equation A.2.

$$V = \frac{8h^3F}{3} - 8h\sum_{n=1}^{N} A_n \frac{e^{-\lambda_n h}}{1+\lambda_n h} J_0(\lambda_n) \qquad \text{....A.2}$$

where F is the force exerted by the film liquid
h is the dimensionless half film thickness
$J_0(x)$ is the first order Bessel function of index zero
$J_1(x)$ is the first order Bessel function of index one
λ_n is the nth root of $J_1(\lambda) = 0$
α_n is the nth root of $J_0(\alpha) = 0$
and the N A_k parameters can be solved from the following equations:

$$R(r,h) = \frac{4hFr}{\pi} \qquad \text{....A.3}$$

$$R(r,h) = \sum_{k=1}^{N} A_k[ak^1(r,h) + ak^2(r,h) + ak^3(r,h) - ak^4(r,h) - ak^5(r,h)] \qquad \text{....A.4}$$

$$ak^1(r,h) = \frac{e^{-\lambda_k h}}{(1+\lambda_k h)}\left[\frac{12r}{\lambda_k h} J_0(\lambda_k) + \frac{3}{h} J_1(\lambda_k r)\right] \qquad \text{....A.5}$$

$$ak^2(r,h) = \frac{e^{-\lambda_k h}}{(1+\lambda_k h)} 2V_i \lambda_k J_1(\lambda_k r) \qquad \text{....A.6}$$

$$ak^3(r,h) = \frac{e^{-\lambda_k h}}{(1+\lambda_k h)} V_s \lambda_k^2 J_1(\lambda_k r) \quad \text{....A.7}$$

$$ak^4(r,h) = \frac{E_s}{S_c} Q_k^N(r,h) \quad \text{....A.8}$$

$$ak^5(r,h) = [(K_\varepsilon + K_\kappa) P^N(r,h) - \frac{2}{r} K_\varepsilon R^N(r,h)] \, Q_k^N(r,h) \quad \text{....A.9}$$

$$P^N(r,h) = \sum_{j=1}^{N} A_j \frac{e^{-\lambda_j h}}{(1+\lambda_j h)} J_0(\lambda_j r) \quad \text{....A.10}$$

$$R^N(r,h) = \sum_{j=1}^{N} A_j \frac{e^{-\lambda_j h}}{(1+\lambda_j h)} J_1(\lambda_j r) \quad \text{....A.11}$$

$$Q_k^N(r,h) = 2P_k(h) J_0(\lambda_k) \sum_{n=1}^{N} \frac{X_n(h)}{Q_n(h)} \frac{\alpha_n^2}{(\alpha_n^2 - \lambda_k^2)} \frac{J_0(\alpha_n r)}{J_0(\lambda_n)} \quad \text{....A.12}$$

$$P_k(h) = A_d S_c \lambda_k \frac{e^{-\lambda_k h}}{(1+\lambda_k h)} \quad \text{....A.13}$$

$$Q_n(h) = \sinh(\alpha_n h)\alpha_n + A_d D_f X_n(h) \alpha_n^2 \quad \text{....A.14}$$

$$X_n(h) = K \left[\cosh(\alpha_n h) + \frac{\alpha_n \sinh(\alpha_n h)}{K_1}\right] \quad \text{....A.15}$$

where r is the dimensionless film radius

V_i is the ratio of drop phase viscosity to film phase viscosity

V_s is the interfacial viscosity number

S_c is the Schmidt number

K_ε is the gradient of interfacial shear viscosity

K_κ is the gradient of interfacial dilational viscosity

A_d is the adsorption number

D_f is the ratio of interfacial diffusivity to film phase diffusivity

K is an equilibrium constant

K_1 is a kinetic rate constant

At a given film thickness, h, for N values of r, the N A_k parameters can be solved by initially setting $P^N(r,h)$ and $R^N(r,h)$ to zero. Equation A.4 then reduces to a matrix of N linear

equations which can be solved by simple Gauss reduction.

A film normally ruptures at a critical thickness, h_{cr}, of several hundred angstroms.[8] Film rupture is caused by the growth of corrugations in the film caused by thermal fluctuations or by the spontaneous perturbation of the droplet shape.[9-11] These corrugations grow rapidly and holes are formed locally at their points of contact. The rate-determining step of film rupture is the hole formation. The stability of the film has been shown to decrease with temperature and film diameter and increase with interfacial tension and interdroplet repulsion.[9,12]

Interest in this phenomena was created when it was established experimentally that the thinning liquid film near film rupture was non-homogeneous in thickness. The amplitude of the unevenness was found to increase with film radius. Malhotra *et al.* proposed a relationship between the critical thickness and the film radius, neglecting drainage flow in the film.[10] This reduces to the following equation, when the electrostatic contribution is considered negligible:

$$h_{cr} = \sqrt[4]{\frac{3Ar^2}{8\sigma(2.4)^2}} \qquad \text{....A.16}$$

where A is the Hamaker constant

r is the film radius and

σ is the interfacial tension

In an alternate approach Tsekov *et al.*, proposed that the formation of holes is a random process and that statistical methods should be used to describe h_{cr}. Their approach takes into account van der Waals and capillary forces and is documented in the literature.[13-15]

A2.1 REFERENCES

1. G.W.Steven, H.R.C.Pratt and D.R.Tai (1990), "Droplet Coalescence in Aqueous Electrolyte Solutions", *J.Colloid Interface Science*, **136**:470.
2. A.Sheludko (1967), "Thin Liquid Films", *Adv.Colloid Interface Sci.*, **1**:391.
3. D.T.Wasan, A.D.Nikolov, L.A.Lobo, K.Koczo and D.A.Edwards (1992), "Foams, Thin Films and Surface Rheological Properties", *Progress in Surface Science*, **39**:119.
4. W.Albers and J.Th.G.Overbeek (1959), "Stability of Emulsions of Water in Oil. I. The Correlation between Electrokinetic Potential and Stability.", *J.Colloid Science*, **14**:501.
5. D.T.Wasan and A.K.Malhotra (1986), "Thin Liquid Surfactant Film Drainage Phenomena - A review", *AIChE Symp.Ser. No 252*, **82**:5.
6. Z.Zapryanov, A.K.Malhotra, N.Aderangi and D.T.Wasan (1983), "Emulsion Stability: An analysis of the effects of bulk and interfacial properties on film mobility and drainage rate", *Int.J.Multiphase Flow*, **9**:105.
7. A.K.Malhotra and D.T.Wasan (1987), "Effect of Film Size on Drainage of Foam and Emulsion Films", *AIChE Journal*, **33**:1533.
8. A.K.Malhotra and D.T.Wasan (1987), "Effects of Surfactant Adsorption-Desorption Kinetics and Interfacial Rheological Properties on the Rate of Drainage of Foam and Emulsion Films", *Chem.Eng.Comm.*, **55**:95.
9. E.Dickinson (1992), "Interfacial Interactions and the Stability of oil-in-water Emulsions", *Pure & Appl.Chem.*, **64**:1721.
10. A.K.Malhotra and D.T.Wasan (1986), "Stability of Foam and Emulsion Films: Effects of the Drainage and Film Size on Critical Thickness of Rupture", *Chem.Eng.Comm.*, **48**:35.
11. W.B.Krantz, D.T.Wasan and R.K.Jain (1986), "Thin Liquid Film Phenomena - Introduction", *AIChE Symp.Ser. No 252*, **82**:1.
12. S.S.Davis and A.Smith (1976), "The Stability of Hydrocarbon Oil Droplets at the Surfactant/Oil Interface", *Colloid & Polymer Science*, **254**:82.
13. B.P.Radoev, A.D.Scheludko and E.D.Manev (1983), "Critical Thickness of Thin Liquid Films: Theory and Experiment", *J.Colloid Interface Science*, **95**:254.
14. R.Tsekov and B.Radoev (1992), "Life Time of Nonthinning Liquid Films - Influence of the Surface Waves Spatial Correlations.", *Adv.Colloid Interface Science*, **38**:353.
15. R.Tsekov and B.Radoev (1992), "Rupture of Thinning Liquid Films - Influence of the Surface Wave's Spatial Correlations", *J.Chem.Soc.Faraday Trans.*, **88**:251.

A3 THIN.PAS - Source code of computer program which calculates film thinning. Turbo Pascal Version 6.

```
{$M 65520,0,655360}

PROGRAM VELOCITY;

 { THIS PROGRAM WAS WRITTEN BY LISA SEYMOUR, CHEMISTRY DEPARTMENT, UCT      }
 { FOR CALCULATING THE DRAINAGE VELOCITY FOR AN EMULSION FILM.  THE INPUT   }
 { FILE VEL_IN.DAT CONTAINS THE EMULSION AND FILM EXPERIMENTAL PARAMETERS   }
 { AND THE PROGRAM OUTPUTS THE VELOCITY AS A FUNCTION OF ITERATION NUMBER   }
 { TO THE OUTPUT FILE VEL_OUT.DAT AND GRAPHICALLY TO THE SCREEN.            }
 { THIS PROGRAM CONTAINS 5 FUNCTIONS AND 3 PROCEDURES WHICH ARE LISTED IN   }
 { ALPHABETICAL ORDER.  FUNCTIONS WHICH ARE USED IN THIS PROGRAM INCLUDE    }
 { CALCULATING HYPERBOLIC SIN AND COS, CALCULATING THE BESSEL FUNCTIONS J0  }
 { AND J1 AND THEIR ZERO ROOTS AND SOLVING A MATRIX OF N-LINEAR EQUATIONS   }
 { 3 UNITS ARE USED IN THE PROGRAM, ONE, TPGRAPH WAS WRITTEN AT UCT.        }

USES Crt,Graph,TPGraph;

 CONST
   InputFile = 'vel_in.dat';

 TYPE
   Type2D = array[1..50, 1..(50+1)] of real;
   Type1D = array[1..(50+1)] of real;

 VAR
   h,            { HALF FILM THICKNESS }
   Vs,           { INTERFACIAL VISCOSITY NUMBER }
   Vi,           { VISCOSITY RATIO OF DROP PHASE TO FILM PHASE }
   Ad,           { ADSORPTION NUMBER }
   Sc,           { SCHMIDT NUMBER }
   Es,           { DIMENSIONLESS ELASTICITY NUMBER }
   Df,           { DIFFUSIVITY RATIO OF INTERFACIAL TO FILM PHASE }
   K0,           { EQUILIBRIUM CONSTANT }
   K1,           { KINETIC RATE CONSTANT }
   F  : real;    { FORCE EXERTED BY FILM LIQUID }

   I,N,J,
   ErrCode,grDriver,grMode    : integer;
   S,alpha,lamda              : Type1D;
   Vre,V,sum,lam              : real;
   rest                       : Type2D;
   Num, PathToDrivers         : String[30];
   dev                        : Text;

{*****************************************************************************}

function COSH(x:real):real; { calculates hyperbolic cos }
 BEGIN
   cosh:= (exp(x) + exp(-x))/2;
 END; { of function cosh }

{*****************************************************************************}

function SINH(x:real):real; { calculates hyperbolic sin }
 BEGIN
   sinh:= (exp(x) - exp(-x))/2;
 END; { of function sinh}

{*****************************************************************************}

function POWER(A,B:real):real;
begin
 power:= exp(B*ln(A));
end;

{*****************************************************************************}

function J0(x:real):real; { calculates Bessel function J0(x) }
```

```
VAR
  big,temp,bit,term : real;

BEGIN
  if x > 25 then
   J0:= sqrt(2/(pi*x))*cos(x - pi/4)
  else
  begin;
    bit:= (x*x)/4;
    temp:=1;
    term:=1;
    I:=1;
    REPEAT
      term:= -1*term*bit/(I*I);
      temp:= temp + term;
      I:= I + 1;
    UNTIL abs(term) < 1E-38;
    J0:= temp;
  end;
END; {of function J0}

{*************************************************************************}

function J1(x:real):real;  { calculates the Bessel function J1(x) }
 VAR
   big,temp,bit,term  : real;
 BEGIN
   if x > 25 then
      J1:= sqrt(2/(pi*x))*cos(x - pi/2 - pi/4)
   else
   begin;
      term:= x/2;
      bit:= x*x/4;
      temp:= x/2;
      I:= 1;
      REPEAT
        term:= -1*bit*term/(I*(I+1));
        temp:= temp + term;
        I:= I + 1;
      UNTIL abs(term) < 1E-38;
      J1:= temp;
   end;
 END; {of function J1}

{*********************************************************************}

PROCEDURE DATAINPUT;
Begin
  Assign(dev,inputfile);
  Reset(dev);
  readln(dev);
  readln(dev,pathtodrivers);
  read(dev,h);  readln(dev);
  read(dev,Vs); readln(dev);
  read(dev,Vi); readln(dev);
  read(dev,Ad); readln(dev);
  read(dev,Sc); readln(dev);
  read(dev,Es); readln(dev);
  read(dev,Df); readln(dev);
  read(dev,K0); readln(dev);
  read(dev,K1); readln(dev);
  read(dev,F);  readln(dev);
  Close(dev);
end; {* of procedure DataInput *}

{*************************************************************************}

procedure MAT;  { calculates (N by N+1) matrix for N unknown Sk's }
 VAR
   half,sm0,r                  : Type1D;
   top,bot                     : Type2D;
   pre,pro,sumM,Xh,Qh,
   ak1,ak2,ak3,ak4,ak5,
   pk0,pk1,pk2,pk3,pk4,inc     : real;
```

```
  k,l,m                          : integer;
BEGIN
  inc := 1/(N+1);
  pre:=  -4*h*F/(pi);
  FOR l:= N downto 1 DO
    r[l] := inc*l;
  FOR m:= 1 to N DO
  BEGIN
    sm0[m]:= J0(lamda[m]);
    Xh:=  K0 * (cosh(alpha[m]*h) + K1*alpha[m]*sinh(alpha[m]*h));
    Qh:=  alpha[m] * (Ad*Df*Xh*alpha[m] + sinh(alpha[m]*h));
    half[m]:= (alpha[m]*alpha[m]*Xh) / (sm0[m]*Qh);
    FOR l:= 1 to N DO
      BEGIN
        top[m,l]:= J0(alpha[m]*r[l]);
        bot[m,l]:= (alpha[m]*alpha[m]) - (lamda[l]*lamda[l]);
      END;
  END;
  FOR k:= 1 to N do
  BEGIN
    rest[k,(N+1)]:= pre*r[k];
    pro:=   (exp(-lamda[k]*h))/(1 + lamda[k]*h);
    pk0:=   pro*12*sm0[k]/(h*lamda[k]);
    pk1:=   pro*3/h;
    pk2:=   pro*lamda[k]*2*Vi;
    pk3:=   pro*lamda[k]*lamda[k]*Vs;
    pk4:=   (Es/Sc)*pro*2*lamda[k]*Ad*Sc*sm0[k];
    FOR l:= 1 to N do
    BEGIN
      sumM:=0;
      FOR m:= 1 to N do
              sumM:= sumM + half[m]*top[m,l]/bot[m,k];
      ak1:=  pk0*r[l] + J1(lamda[k]*r[l])*pk1;
      ak2:=  J1(lamda[k]*r[l])*pk2;
      ak3:=  J1(lamda[k]*r[l])*pk3;
      ak4:=  pk4*sumM;
      ak5:=  0;
      rest[l,k]:= ak1 + ak2 + ak3 - ak4 - ak5 ;
    END;
  END;
END;{ of procedure MAT }

{*****************************************************************************}

procedure SOLVE  ;  { solves matrix of N-linear equations }
 VAR
  Mat             : Type1D;
  k,l,count,D     : integer;
  A,B             : real;
BEGIN
  FOR k:= 1 to N do
  BEGIN
    B:= 0;
    FOR l:= 1 to N do
    BEGIN
      A:= Abs(rest[k,l]);
      IF A > B THEN
        B:= A;
    END;
    S[k]:= B;
  END;
  FOR count:= 1 to N do
  BEGIN
    B:= 0;
    FOR k:= count to N do
    BEGIN
      A:= Abs(rest[k,count])/S[k];
      IF A > B THEN
      BEGIN
        B:= A;
        D:= k;
      END;
    END;
    A:= S[count];
```

```
    S[count]:= S[D];
    S[D]:= A;
    FOR k:= count to (N+1) DO
    BEGIN
      A:= rest[count,k];
      rest[count,k]:= rest[d,k];
      rest[d,k]:= A;
    END;
    FOR k:= (count+1) TO N DO
    BEGIN
      Mat[k]:= rest[k,count]/rest[count,count];
      rest[k,count]:= 0;
      FOR l:= (count+1) TO (N+1) DO
        rest[k,l]:= rest[k,l] - Mat[k]*rest[count,l];
    END;
  END;
  FOR k:= 1 to N do
    S[k]:= 0;
  FOR l:= N downto 1 do
  BEGIN
    A:= 0;
    FOR k:= 1 to N do
      A:= A + rest[l,k]*S[k];
    S[l]:= (rest[l,N+1] - A)/rest[l,l];
  END;
END;{of procedure solve}

{*****************************************************************************}

procedure ZERO; { calculates zero roots for the Bessel functions J0 and J1 }
 VAR
   bit0,bit1   : real;
 BEGIN
   FOR I:= 1 to N DO
   BEGIN
     bit0:= (I - 0.25)*pi;
     bit1:= (I + 0.25)*pi;
     alpha[I]:= bit0 + (1/(8*bit0)) - (31/(384*bit0*bit0*bit0));
     lamda[I]:= bit1 - (3/(8*bit1)) + (9/(384*bit1*bit1*bit1));
   END;
 END; { of procedure zero }

{*****************************************************************************}


BEGIN {program Main calculates velocity of thinning}

  DataInput;
  Assign(dev,'vel_out.dat');
  Rewrite(dev);
  grDriver := Detect;
  Initgraph(grDriver,grMode,PathToDrivers);
  ErrCode := GraphResult;
  if ErrCode = grOk then begin
   Vre:= 8*F*h*h*h/3;
   FOR N:= 30 downto 1 do
   Begin;
     Str(N,Num);
     ZERO;
     MAT;
     SOLVE;
     sum:= 0;
     FOR j:= 1 to N DO
       sum:= sum + S[j]*exp(-lamda[j]*h)*J0(lamda[j])/(1 + lamda[j]*h);
     V:= Vre - 8*h*sum;
     Writeln(dev,'iteration ',N,'   velocity = ',V);
     if N = 30 then begin
       SetWindow(0,30,V,Vre);
       ScOutTextXY(15,Vre/2,'calculating');
       ScMoveTo(30,V);
     end;
     ScLineTo(N,V);
     ScOutTextXY(N,V,Num);
   End;
```

```
    ScLineTo(0,Vre);
    ScOutTextXY(15,0,'press enter to return');
    readln;
    Writeln(dev,'iteration 0    velocity = ',Vre);
   end
   else writeln('graphics error');
   Close(dev);
END.
```

A4 CORPIT.PAS - Computer program which performs ionic strength corrections using our simplified Pitzer approach. Borland Pascal version 7.

```
{$M 65520,0,655360}

PROGRAM CORPIT;

 { THIS PROGRAM WAS WRITTEN BY LISA SEYMOUR, CHEMISTRY DEPARTMENT, UCT     }
 { FOR PERFORMING IONIC STRENGTH CHANGES ON STABILITY CONSTANTS USING A    }
 { SIMPLIFIED VERSION OF THE PITZER EQUATION WHICH WE HAVE DERIVED.        }
 { THIS PROGRAM CONTAINS 14 PROCEDURES WHICH ARE LISTED IN ALPHABETICAL    }
 { ORDER.  7 BINARY FILES ARE ASSOCIATED WITH THE PROGRAM.  THESE FILES    }
 { CONTAIN PITZER PARAMETERS - MOSTLY LITERATURE BUT SOME WERE CALCULATED. }
 { 3 UNITS ARE USED IN THE PROGRAM, ONE, TPGRAPH WAS WRITTEN AT UCT.       }
 { WHEN AN IONIC STRENGTH CORRECTION IS DONE THE GRAPHICAL DATA IS STORED  }
 { IN A FILE PIT.DAT WHICH CAN THEN BE IMPORTED INTO A GRAPHICAL PACKAGE   }

 USES Graph,TPGraph,Crt;
 TYPE
  JType = record
        logK0                      : real;
        beta0PP,beta1PP,C0PP       : real;
        H,p,q,r                    : integer;
        M,S                        : string[5];
        L                          : string[12];
      end;
  AXType = record
        beta1AX,C0AX               : real;
        A,X                        : string[5];
       end;
  ALType = record
        beta0AL,beta1AL,C0AL       : real;
        A                          : string[5];
        L                          : string[12];
       end;
  MXType = record
        beta0MX,beta1MX,C0MX       : real;
        M,X                        : string[5];
       end;
  HXType = record
        beta0HX,beta1HX,C0HX       : real;
        H                          : integer;
        X                          : string[5];
       end;
  MType  = record
        zM                         : integer;
        M                          : string[5];
       end;
  LType  = record
        zL                         : integer;
        L                          : string[12];
       end;

  VAR
  I,IS,g,dg,Deb,
  mP,mL,mH,mM,PH,TL,TM,mA,
  BPP,BAL,BHX,BMX,B,
  dBPP,dBAX,dBAL,dBHX,dBMX,dB,
  CPP,CAX,CAL,CHX,CMX,C,
  act,logK,logKI           : real;
  long,s,sum,zP,name,
  option,answer            : integer;
  reply,found,edit         : string[1];
  MF,tempM                 : MType;
  LF,tempL                 : LType;
  J,tempJ                  : JType;
  AX,tempAX                : AXType;
  AL,tempAL                : ALType;
  MX,tempMX                : MXType;
```

```
  HX,tempHX                : HXType;
  MFile                    : file of MType;
  LFile                    : file of LType;
  JFile                    : file of JType;
  AXFile                   : file of AXType;
  ALFile                   : file of ALType;
  MXFile                   : file of MXType;
  HXFile                   : file of HXType;

 PROCEDURE CONC; forward;
 PROCEDURE CORRECT; forward;
 PROCEDURE DRAW; forward;
 PROCEDURE EDITING; forward;
 PROCEDURE FIND; forward;
 PROCEDURE GUESS; forward;
 PROCEDURE LISTING; forward;
 PROCEDURE METAL; forward;
 PROCEDURE LIGAND; forward;
 PROCEDURE PITZER_CORRECT; forward;
 PROCEDURE PRODUCT; forward;
 PROCEDURE PROTON; forward;
 PROCEDURE SALT; forward;
 PROCEDURE SEARCH; forward;

{*************************************************************************}

 function power(A,B:real):real;
 begin
   power:= exp(B*ln(A));
 end;

{*************************************************************************}

 PROCEDURE CONC; { Input of concentrations }
 Begin
    CAX:= AX.C0AX/2;
    If J.p = 0 then
    begin
      CMX:= 0;
      TM:= 0;
      mM:= 0;
    end
    else
    begin
      Writeln('*************************************************************');
      Write('       Enter the free metal concentration  ');
      Readln(TM);
      mM:= TM;
      CMX:= MX.C0MX/(2*sqrt(MF.zM));
    end;
    if (J.q = 0) OR (LF.zL = 0) then
    begin
        TL:= 0;
        mL:= 0;
        CAL:= 0;
    end;
    if (J.q <> 0) then
    begin
        Writeln('*************************************************************');
        Write('       Enter the free ligand concentration  ');
        Readln(TL);
        if (LF.zL <> 0) then
        begin
          mL:= TL;
          CAL:= AL.C0AL/(2*sqrt(abs(LF.zL)));
        end;
    end;
    if J.r = 0 then
    begin
        PH:= 0;
        CHX:= 0;
        mH:= 0;
    end
    else
```

```
    begin
        Writeln('*************************************************************');
        Write('       Enter the pH of your solution         ');
        Readln(PH);
        mH := power(10,-PH);
        CHX:= HX.C0HX/2;
    end;
    if (zP <> 0) then
      begin
          mP:= TL/2;
          CPP:= J.C0PP/(2*sqrt(abs(zP)));
      end
    else
      begin
        mP := 0;
        CPP := 0;
      end;
 End; { of procedure conc }

{*************************************************************************}

 PROCEDURE CORRECT; { corrects logK to ionic strengths wanted }
 VAR
    LOGKC,
    act1, act2, act3, act4, act5     : real;
    V,W                              : integer;
    corr                             : array [1..10] of real;
 Begin
    If option = 1 then
    begin
      Writeln('*************************************************************');
      Writeln('Enter Molal Ionic Strength to correct to, Enter 0 to end');
      V:= 0;
      Repeat
        V:= V + 1;
        Write('molal ionic strength   ');
        Readln(corr[V]);
      Until corr[V] = 0;
      V:= V - 1;
    end
    else if (option=2) or (option=3) then
    begin
      V := 1;
      corr[1] := logKI;
    end;
    s:= J.r + J.p*sqr(MF.zM) + J.q*sqr(LF.zL) - sqr(zP);
    sum:= J.r + J.p*MF.zM + J.q*abs(LF.zL) - abs(zP);
    FOR W:= 1 to V do
     Begin
      I:= corr[W] ;
      mA:= I - (sqr(LF.zL)*mL + sqr(MF.zM)*mM + sqr(zP)*mP + mH)/2;
      IS:= sqrt(I);
      g:= (1 - (1 + 2*IS)*exp(-2*IS))/(2*I);
      dg:= -(1 - (1 + 2*IS + 2*I)*exp(-2*IS))/(2*I*I);
      dBAX:= dg*AX.beta1AX;
      IF J.p = 0 then
      begin
        BMX:= 0;
        dBMX:= 0;
      end
      else
      begin
        BMX:= MX.beta0MX + g*MX.beta1MX;
        dBMX:= dg*MX.beta1MX;
      end;
      IF (J.q = 0) OR (LF.zL = 0) THEN
      begin
        BAL:= 0;
        dBAL:=0;
      end
      else
      begin
        BAL:= AL.beta0AL + g*AL.beta1AL;
        dBAL:= dg*AL.beta1AL;
```

```
      end;
      IF J.r = 0 THEN
      begin
        BHX:= 0;
        dBHX:= 0;
      end
      else
      begin
        BHX:= HX.beta0HX + g*HX.beta1HX;
        dBHX:= dg*HX.beta1HX;
      end;
      IF zP = 0 THEN
      begin
        BPP:= 0;
        dBPP:=0;
      end
      else
      begin
        BPP:= J.beta0PP + g*J.beta1PP;
        dBPP:= dg*J.beta1PP;
      end;
      Deb:= s*-0.392*(IS/(1 + 1.2*IS) + 2*ln(1 + 1.2*IS)/1.2);
      B:= 2*mA*(J.q*BAL + J.r*BHX + J.p*BMX - BPP);
      dB:= s*mA*(mA*dBAX + mL*dBAL + mH*dBHX + mM*dBMX + mP*dBPP);
      C:= 2*mA*mA*(J.q*CAL + J.r*CHX + J.p*CMX - CPP) +
          sum*mA*(mA*CAX + mL*CAL + mH*CHX + mM*CMX + mP*CPP);
      act1:= mA*(2*J.q*BAL + s*mL*dBAL + 2*mA*J.q*CAL + sum*mL*CAL);
      act2:= 2*mA*J.r*BHX + s*mA*mH*dBHX + 2*mA*mA*J.r*CHX + sum*mA*mH*CHX ;
      act3:= s*mA*mA*dBAX + sum*mA*mA*CAX;
      act4:= 2*mA*J.p*BMX + 2*mA*mA*J.p*CMX + sum*mA*mM*CMX + s*mA*mM*dBMX;
      act5:= s*mA*mP*dBPP - 2*mA*mA*CPP - 2*mA*BPP + sum*mA*mP*CPP;
      act:= (Deb + act1 + act2 + act3 + act4 + act5)/2.302585;
      if option = 1 then begin
         logK := J.logK0 + act;
         logKc := J.logK0 + (Deb + act1 + act5)/2.302585;
      end
      else if (option=2) or (option=3) then
      begin
         J.logK0 := logK - act;
         Writeln('I(m) =  0  LOG Km =  ',J.logK0);
      end;
      Writeln('I(m)=',I:5:3,' log Km=',logK:3:5,' log Kcor=',logKc:3:5);
      Writeln('f(AX)=',act3:5:3,' f(AL)=',act1:5:3,' f(HX)=',act2:5:3,'
f(MX)=',act4:5:3,' f(J)=',act5:5:3);
    End;
 End; { of procedure Correct }

{*************************************************************************}

 PROCEDURE DRAW; {Plots logK versus the square root of ionic strength}
 TYPE
  pitzerType    =  array[1..240] of record
                  ions        : real;
                  lgK         : real;
                                end;
 VAR
  pitzer                      : pitzerType;
  DH                          : array [1..240] of real;
  STop,SITop,SBot,SIBot,S0    : string[11];
  Bot,IBot,Top                : real;
  Z,GrMode,GrDriver           : integer;
  Ishow,show                  : array [1..50] of real;
  pitzerFile                  : text;

 Begin
   Assign( pitzerFile, 'f:\turbop\pit.dat');
    for Z:= 1 to 50 do
      begin
        Ishow[Z] := 0;
        show[Z] := 0;
      end;
    Writeln('************************************************************');
    Writeln('Enter Experimental molal logK with corresponding molal ionic
strength');
```

```
 Writeln('Enter 0 to end');
 Z:= 0;
 Repeat
   Z:= Z + 1;
   Write('     ionic strength   ');
   Readln(Ishow[Z]);
   Write('     molal log K      ');
   Readln(show[Z]);
 Until Ishow[Z] = 0;
 Z:= Z - 1;
Bot:= J.logK0;
IBot:= 0;
FOR Z:= 1 to 240 do
Begin
   I:= 0.025*Z ;
   mA:= I - (sqr(LF.zL)*mL + sqr(MF.zM)*mM + sqr(zP)*mP+ mH)/2;
   IS:= sqrt(I);
   g:= (1 - (1 + 2*IS)*exp(-2*IS))/(2*I);
   dg:= -(1 - (1 + 2*IS + 2*I)*exp(-2*IS))/(2*I*I);
   dBAX:= dg*AX.beta1AX;
   IF J.p = 0 then
   begin
     BMX:= 0;
     dBMX:= 0;
   end
   else
   begin
     BMX:= MX.beta0MX + g*MX.beta1MX;
     dBMX:= dg*MX.beta1MX;
   end;
   IF (J.q = 0) OR (LF.zL = 0) THEN
   begin
     BAL:= 0;
     dBAL:=0;
   end
   else
   begin
     BAL:= AL.beta0AL + g*AL.beta1AL;
     dBAL:= dg*AL.beta1AL;
   end;
   IF J.r = 0 THEN
   begin
     BHX:= 0;
     dBHX:= 0;
   end
   else
   begin
     BHX:= HX.beta0HX + g*HX.beta1HX;
     dBHX:= dg*HX.beta1HX;
   end;
   IF zP = 0 THEN
   begin
     BPP:= 0;
     dBPP:=0;
   end
   else
   begin
     BPP:= J.beta0PP + g*J.beta1PP;
     dBPP:= dg*J.beta1PP;
   end;
   DH[Z]:= s*-0.392*(IS/(1 + 1.2*IS) + 2*ln(1 + 1.2*IS)/1.2);
   B:= 2*mA*(J.q*BAL + J.r*BHX + J.p*BMX - BPP);
   dB:= s*mA*(mA*dBAX + mL*dBAL + mH*dBHX + mM*dBMX + mP*dBPP);
   C:= (J.q*CAL + J.r*CHX + J.p*CMX - CPP);
   C:= 2*mA*mA*C;
   C:= C + sum*mA*(mA*CAX + mL*CAL + mH*CHX + mM*CMX + mP*CPP);
   act:= (DH[Z] + B + dB + C)/2.302585;
   logK:= J.logK0 + act;
   DH[Z]:= J.logK0 + (DH[Z])/2.302585;
   If (logK - Bot) < 0 then
   begin
      Bot:= logK;
      IBot:= I;
   end;
```

```
      pitzer[Z].ions:= IS;
      pitzer[Z].lgK:= logK;
   End;
   If (logK - J.logK0) > 0 then
     begin
       Top:= logK;
       Str(I:5:3,SITop);
       Str(logK:5:3,STop);
       STop:= SITop + ',' + STop;
     end
   Else
     begin
       Top := J.logK0;
       STop:= '';
     end;
   Str(Bot:5:3,SBot);
   Str(IBot:5:3,SIBot);
   SBot:= SIBot + ',' + SBot;
   Str(J.logK0,S0);
   S0:= '0.000,' + S0;
   Grdriver:= detect;
   Initgraph( Grdriver, Grmode,'f:\bp\bgi ');
   SetWindow(0,(pitzer[Z].ions + 0.5),(Bot - 0.5),(Top + 0.5));
   ScRectangle(0,(Bot - 0.5),(pitzer[Z].ions + 0.5),(Top + 0.5));
   ScMoveTo(0,J.logK0);
   SetColor(5);
   For Z:= 1 to 240 do
     ScLineTo(pitzer[Z].ions,pitzer[Z].lgK);
   ScMoveTo(0,J.logK0);
   SetColor(6);
    For Z:= 1 to 240 do
      ScLineTo(pitzer[Z].ions,DH[Z]);
   ScOutTextXY(pitzer[10].ions,DH[10],'D-H');
   SetColor(8);
   ScOutTextXY(0,J.logK0,S0);
   ScOutTextXY(pitzer[Z].ions,pitzer[Z].lgK,STop);
   ScOutTextXY(sqrt(IBot),Bot,SBot);
   SetColor(3);
   For Z:= 1 to 50 do
     begin
       if show[Z] <> 0 then

ScRectangle(sqrt(Ishow[Z])-0.01,show[Z]-0.01,sqrt(Ishow[Z])+0.01,show[Z]+0.01);
     end;
   Readln;
   CloseGraph;
   Rewrite( pitzerFile );
   Writeln(pitzerfile,J.p:2,J.M:5,'  ',J.q:2,J.L:12,'  ',J.r:2,'H');
      For Z:= 1 to 240 do
      begin
        Write(pitzerfile,pitzer[Z].ions);
        Writeln(pitzerfile,pitzer[Z].lgK);
      end;
  Close( pitzerFile );
End; { of procedure Draw }

{*****************************************************************************}

PROCEDURE EDITING; { for adding and editing pitzer parameters }
   Begin
    answer:= 0;
    repeat
        begin
           Writeln('************************************************************');
           Writeln('********************** ADDING AND EDITING ***************');
           Writeln('************************************************************');
           Writeln('Which parameters would you like to add/edit ?');
           Writeln('                1) salt parameters');
           Writeln('                2) ligand parameters');
           Writeln('                3) metal parameters');
           Writeln('                4) proton parameters');
           Writeln('                5) product parameters');
           Write('Enter the number of your choice   ');
           Readln(answer);
```

```
          Writeln('************************************************************');
        end;
    until (answer > 0) OR (answer < 6);
    Case answer of
    1:begin
        Writeln('(1:1) Electrolyte  Parameters:');
        Write('Enter the cation (< 5 chs )                    ');
        Readln(AX.A);
        for long := 1 to length(AX.A) do
               AX.A[long] := Upcase(AX.A[long]);
        Write('Enter the anion (< 5 chs )                     ');
        Readln(AX.X);
        for long := 1 to length(AX.X) do
               AX.X[long] := Upcase(AX.X[long]);
        SEARCH;
        SALT;
      end;
    2:begin
        Write('Enter the name of your ligand (< 12 chs )      ');
        Readln(LF.L);
        for long := 1 to length(LF.L) do
               LF.L[long] := Upcase(LF.L[long]);
        AL.L := LF.L;
        name := 2;
        FIND;
        Write('Enter your electrolyte cation (< 5 chs )       ');
        Readln(AL.A);
        for long := 1 to length(AL.A) do
               AL.A[long] := Upcase(AL.A[long]);
        SEARCH;
        LIGAND;
      end;
    3:begin
        Write('Enter the name of your metal (< 5 chs )        ');
        Readln(MF.M);
        for long := 1 to length(MF.M) do
               MF.M[long] := Upcase(MF.M[long]);
        MX.M := MF.M;
        name := 3;
        FIND;
        Write('Enter your electrolyte anion (< 5 chs )        ');
        Readln(MX.X);
        for long := 1 to length(MX.X) do
               MX.X[long] := Upcase(MX.X[long]);
        SEARCH;
        METAL;
      end;
    4:begin
        Write('Enter your electrolyte anion (< 5 chs )        ');
        Readln(HX.X);
        for long := 1 to length(HX.X) do
               HX.X[long] := Upcase(HX.X[long]);
        SEARCH;
        PROTON;
      end;
    5:begin
        GUESS;
        SEARCH;
        PRODUCT;
      end;
    End;
   End; { of procedure editing }

{*************************************************************************}

 PROCEDURE FIND; { Finds metal and ligand names }
 Begin
   Case name of
      3: Begin
            Reset(MFile);
            found := 'N';
            repeat
               If Eof (MFile) then
                 Begin
```

```
                Writeln('metal parameters are not on file');
                If (option = 2) or (option = 3) then
                begin
                  Write('Enter the charge of your metal          ');
                  Readln(MF.zM);
                  Write(MFile,MF);
                end;
              End
            Else
              Begin
                Read(MFile,tempM);
                If (tempM.M = MF.M) then
                begin
                  found := 'Y';
                  MF := tempM;
                end;
              End;
          until EoF(MFile) or (found = 'Y');
          Close(MFile);
      End;
    2: Begin
          Reset(LFile);
          found := 'N';
          repeat
            If (Eof (LFile)) and (found = 'N') then
              Begin
                Writeln('ligand parameters are not on file');
                If (option = 2) or (option = 3) then
                begin
                  Write('Enter the charge of your ligand         ');
                  Readln(LF.zL);
                  Write(LFile,LF);
                end;
              End
            Else
              Begin
                Read(LFile,tempL);
                If (tempL.L = LF.L) then
                begin
                  found := 'Y';
                  LF := tempL;
                end;
              End;
          until EoF(LFile) or (found = 'Y');
          Close(LFile);
      End;
  End;
End; { of Procedure Find )

{*************************************************************************}

PROCEDURE GUESS; {Input of complexation components}
Begin
      Writeln('*********************************************************');
      Write('Enter no of metal ions in complex            ');
      Readln(J.p);
      Write('Enter no of ligand ions in complex           ');
      Readln(J.q);
      Write('Enter no of protons in complex (- for OH)    ');
      Readln(J.r);
      If J.p > 0 then
        begin
          Write('Enter the name of your metal (< 5 chs)       ');
          Readln(J.M);
          for long := 1 to length(J.M) do
            J.M[long] := Upcase(J.M[long]);
          name := 3;
          MF.M := J.M;
          FIND;
        end
      else
        begin
          MF.zM := 0;
          J.M := '';
```

```
          end;
        If J.q > 0 then
          begin
            Write('Enter the name of your ligand (< 12 chs)      ');
            Readln(J.L);
            for long := 1 to length(J.L) do
               J.L[long] := Upcase(J.L[long]);
            name := 2;
            LF.L := J.L;
            FIND;
          end
        else
          begin
            LF.zL := 0;
            J.L := '';
          end;
      zP:= J.r + J.p*MF.zM + J.q*LF.zL;
    If zP < 0 then
          begin
            Write('Enter the electrolyte cation (< 5 chs )       ');
            Readln(J.S);
            for long := 1 to length(J.S) do
               J.S[long] := Upcase(J.S[long]);
            AX.A:= J.S
          end
    else if zP > 0 then
          begin
            Write('Enter the electrolyte anion (< 5 chs )        ');
            Readln(J.S);
            for long := 1 to length(J.S) do
               J.S[long] := Upcase(J.S[long]);
            AX.X:= J.S;
          end
    else if zP = 0 then
          J.S := '';
 End; { Of procedure Guess }

{*************************************************************************}

 PROCEDURE LIGAND; {Input of Ligand parameters}
 Begin
      Writeln('  beta(0) = ',AL.beta0AL:6:4);
      Writeln('  beta(1) = ',AL.beta1AL:6:4);
      Writeln('  C theta = ',AL.C0AL:6:5);
      Write('Do you wish to change your values (Y/N) ? ');
      Readln(edit);
      edit[1]:= Upcase(edit[1]);
      If edit = 'Y' then
      With AL do
      begin
        Write('       Enter beta(0)  ');
        Readln(beta0AL);
        Write('       Enter beta(1)  ');
        Readln(beta1AL);
        Write('       Enter C theta  ');
        Readln(C0AL);
      end;
     Write(ALFile,AL);
     Close(ALFile);
 End;{ of procedure Ligand }

{*************************************************************************}

 PROCEDURE LISTING; { for the listing of metals and ligands on file}
  Var
    Y   :  INTEGER;
  Begin
    case option of
    4 : Begin
          WRITELN('*************************************************');
          Writeln('**************** METALS ON FILE ******************');
          WRITELN('***************** WITH CHARGE ********************');
          Reset(MFile);
          Y:= 0;
```

```
        Repeat
          Y := Y + 1;
          Read(MFile,tempM);
          if Y <> 7 then
            Write(tempM.M:5,'  ',tempM.zM,'    ')
          else
            begin
              Writeln(tempM.M:5,'  ',tempM.zM);
              Y := 0;
            end;
        Until Eof(MFile);
        Close(MFile);
        Writeln;
      End;
  5 : Begin
        WRITELN('*****************************************************');
        Writeln('*************** LIGANDS ON FILE *****************');
        WRITELN('***************** WITH CHARGE *******************');
        Reset(LFile);
        Y:= 0;
        Repeat
          Y := Y + 1;
          Read(LFile,tempL);
          If Y <> 4 then
            Write(tempL.L:12,'  ',tempL.zL:2,'    ')
          else
            begin
              Writeln(tempL.L:12,'  ',tempL.zL:2);
              Y := 0;
            end;
        Until Eof(LFile);
        Close(LFile);
        Writeln;
      End;
  End;
 End; { of procedure listing }

{*************************************************************************}

 PROCEDURE METAL; {Input of Metal parameters}
 Begin
     Writeln('  beta(0) = ',MX.beta0MX:6:4);
     Writeln('  beta(1) = ',MX.beta1MX:6:4);
     Writeln('  C theta = ',MX.C0MX:6:5);
     Write('Do you wish to change your values (Y/N) ? ');
     Readln(edit);
     edit[1]:= Upcase(edit[1]);
     If edit = 'Y' then
      With MX do
      begin
        Write('       Enter beta(0)  ');
        Readln(beta0MX);
        Write('       Enter beta(1)  ');
        Readln(beta1MX);
        Write('       Enter C theta  ');
        Readln(C0MX);
      end;
      Write(MXFile,MX);
      Close(MXFile);
 End; { of procedure Metal }

{*************************************************************************}

 PROCEDURE PITZER_CORRECT; { performs ionic strength corrections }
    Begin
           Writeln('*************************************************************');
           Writeln('****************** PITZER EQUATION ***********************');
           Writeln('*************************************************************');
     AX.A := '';
     AX.X := '';
     GUESS;
     If AX.A = '' then
       begin
          Write('Enter the electrolyte cation (< 5 chs )          ');
```

```
        Readln(AX.A);
        for long := 1 to length(AX.A) do
              AX.A[long] := Upcase(AX.A[long]);
    end;
  If AX.X = '' then
    begin
       Write('Enter the electrolyte anion (< 5 chs )          ');
       Readln(AX.X);
       for long := 1 to length(AX.X) do
             AX.X[long] := Upcase(AX.X[long]);
    end;
  HX.X := AX.X;
  MX.X := AX.X;
  MX.M := J.M;
  AL.L := J.L;
  AL.A := AX.A;
  for answer := 1 to 5 do
    case answer of
      1: SEARCH;
      2: begin
         If (J.q > 0) and (LF.zL <> 0) then
           SEARCH
         else
           begin
                        AL.beta0AL := 0;
                        AL.beta1AL := 0;
                        AL.C0AL := 0;
           end;
         end;
      3: begin
         If (J.p > 0) and (MF.zM <> 0) then
           SEARCH
         else
           begin
                         MX.beta0MX := 0;
                         MX.beta1MX := 0;
                         MX.C0MX := 0;
           end;
         end;
      4: begin
         If J.r <> 0 then
           SEARCH
         else if J.r = 0 then
           begin
                         HX.beta0HX := 0;
                         HX.beta1HX := 0;
                         HX.C0HX := 0;
           end;
         end;
      5: SEARCH;
    end;
  if option = 1 then
   begin
    Writeln('************************************************************');
    Writeln('M=',J.p,' L=',J.q,' H=',J.r,'              logK0 =',J.logK0:13);
    Writeln('zL=',LF.zL,' zM=',MF.zM,'              Beta(1)AX=',AX.Beta1AX:13,'
C0AX=',AX.C0AX:13);
    Writeln('Beta(0)AL=',AL.beta0AL:13,' Beta(1)AL=',AL.beta1AL:13,'
C0AL=',AL.C0AL:13);
    Writeln('Beta(0)HX=',HX.beta0HX:13,' Beta(1)HX=',HX.beta1HX:13,'
C0HX=',HX.C0HX:13);
    Writeln('Beta(0)MX=',MX.beta0MX:13,' Beta(1)MX=',MX.beta1MX:13,'
C0MX=',MX.C0MX:13);
    Writeln('Beta(0)PP=',J.beta0PP:13,' Beta(1)PP=',J.beta1PP:13,'
C0PP=',J.C0PP:13);
    Writeln('************************************************************');
    Write('Would you like the ionic strength correction done (Y/N) ?  ');
    Readln(reply);
    reply[1]:=Upcase(reply[1]);
    If reply = 'Y' then
     begin
      CONC;
      CORRECT;
      DRAW;
```

```
      end;
    end;
  End; { of procedure pitzer_correct }

{*************************************************************************}

PROCEDURE PRODUCT; {Input of Product parameters}
Begin
  logKI := 0;
  Writeln('  log K0  = ',J.logK0);
  Write('  Do you wish to change your value (Y/N) ? ');
  Readln(edit);
  edit[1]:= Upcase(edit[1]);
  If edit = 'Y' then
    begin
      Write('  Enter molal log K for species MpLqHr           ');
      Readln(J.logK0);
      Write('  Enter the corresponding molal ionic strength   ');
      Readln(logKI);
    end;
  If zP = 0 then
    Writeln('Your product is uncharged no parameters needed ')
  else
    begin
      Writeln('  beta(0) = ',J.beta0PP:6:4);
      Writeln('  beta(1) = ',J.beta1PP:6:4);
      Writeln('  C theta = ',J.C0PP:6:5);
      Write('  Do you wish to change your values (Y/N) ? ');
      Readln(edit);
      edit[1]:= Upcase(edit[1]);
      If edit = 'Y' then
      with J do
       begin
         Writeln('Enter your product and electrolyte ion parameters');
         Write('       Enter beta(0)  ');
         Readln(beta0PP);
         Write('       Enter beta(1)  ');
         Readln(beta1PP);
         Write('       Enter C theta  ');
         Readln(C0PP);
       end;
    end;
  If logKI <> 0 then
    begin
           logK:= J.logK0;
           answer := 1;
           if zP >= 0 then
             begin
                 Write('Enter the cation (< 5 chs )   ');
                 Readln(AX.A);
                 for long := 1 to length(AX.A) do
                        AX.A[long] := Upcase(AX.A[long]);
             end;
           if zP <= 0 then
             begin
                 Write('Enter the anion (< 5 chs )    ');
                 Readln(AX.X);
                 for long := 1 to length(AX.X) do
                        AX.X[long] := Upcase(AX.X[long]);
             end;
           SEARCH;
           If J.q > 0 then
             begin
                 answer := 2;
                 AL.L := J.L;
                 AL.A := AX.A;
                 SEARCH;
             end;
           if J.p > 0 then
             begin
                 answer := 3;
                 MX.M := MF.M;
                 MX.X := AX.X;
                 SEARCH;
```

```
              end;
            if J.r > 0 then
              begin
                  answer := 4;
                  HX.X := AX.X;
                  SEARCH;
              end;
            if zP <> 0 then
              begin
                  answer := 5;
                  SEARCH;
              end;
            CONC;
            CORRECT;
      end;
    Write(JFile,J);
    Close(JFile);
 End;{ of procedure Product }

{*************************************************************************}

 PROCEDURE PROTON; {Input of Proton parameters}
 Begin
     Writeln('  beta(0) = ',HX.beta0HX:6:4);
     Writeln('  beta(1) = ',HX.beta1HX:6:4);
     Writeln('  C theta = ',HX.C0HX:6:5);
     Write('Do you wish to change your values (Y/N) ? ');
     Readln(edit);
     edit[1]:= Upcase(edit[1]);
     If edit = 'Y' then
        With HX do
        begin
          Write('       Enter beta(0)  ');
          Readln(beta0HX);
          Write('       Enter beta(1)  ');
          Readln(beta1HX);
          Write('       Enter C theta  ');
          Readln(C0HX);
     end;
     Write(HXFile,HX);
     Close(HXFile);
 End; { of procedure Proton }

{*************************************************************************}

 PROCEDURE SALT; {Input of electrolyte and ionic strength parameters}
 Begin
    Writeln('  beta(1) = ',AX.beta1AX:6:4);
    Writeln('  C theta = ',AX.C0AX:6:5);
    Write('Do you wish to change your values (Y/N) ? ');
    Readln(edit);
    edit[1]:= Upcase(edit[1]);
    If edit = 'Y' then
      begin
        Write('       Enter beta(1)       ');
        Readln(AX.beta1AX);
        Write('       Enter C theta       ');
        Readln(AX.C0AX);
      end;
   Write(AXFile,AX);
   Close(AXFile);
 End; { of procedure Salt }

{*************************************************************************}

 PROCEDURE SEARCH; { searches for the data in each file }
 Begin
   Case answer of
     1 :  Begin
                  Reset(AXFile);
                  found := 'N';
                  repeat
                    Read(AXFile,tempAX);
                    If (tempAX.A = AX.A) and (tempAX.X = AX.X) then
```

```
                    begin
                        found := 'Y';
                        AX := tempAX;
                        If (option = 3) or (option = 2) then
                          Seek( AXFile, FilePos(AXFile) - 1 );
                    end;
                until (Eof (AXFile)) or (found = 'Y');
                If (found = 'N') then
                    begin
                          Writeln('salt parameters are not on file');
                          AX.beta1AX := 0;
                          AX.C0AX := 0;
                    end;
                if (option = 1) then
                          Close(AXFile);
    End;
2 : Begin
                Reset(ALFile);
                found := 'N';
                repeat
                  Read(ALFile,tempAL);
                  If (tempAL.A = AL.A) and (tempAL.L = AL.L) then
                    begin
                       found := 'Y';
                       AL := tempAL;
                       If (option = 3) or (option = 2) then
                         Seek( ALFile, FilePos(ALFile) - 1 );
                    end;
                until (Eof (ALFile)) or (found = 'Y');
                If (found = 'N') then
                    begin
                         Writeln('Ligand parameters are not on file');
                         AL.beta0AL := 0;
                         AL.beta1AL := 0;
                         AL.C0AL := 0;
                    end;
                if (option = 1) then
                    Close(ALFile);
    End;
3 : Begin
                Reset(MXFile);
                found := 'N';
                repeat
                  Read(MXFile,tempMX);
                  If (tempMX.M = MX.M) and (tempMX.X = MX.X) then
                    begin
                        found := 'Y';
                        MX := tempMX;
                        If (option = 3) or (option = 2) then
                          Seek( MXFile, FilePos(MXFile) - 1 )
                    end;
                until (Eof (MXFile)) or (found = 'Y');
                If (found = 'N') then
                    begin
                          Writeln('metal parameters are not on file');
                          MX.beta0MX := 0;
                          MX.beta1MX := 0;
                          MX.C0MX := 0;
                    end;
                if (option = 1) then
                          Close(MXFile);
     End;
4 : Begin
                Reset(HXFile);
                found := 'N';
                repeat
                  Read(HXFile,tempHX);
                  If (tempHX.X = HX.X) then
                    begin
                        found := 'Y';
                        HX := tempHX;
                        If (option = 3) or (option = 2) then
                          Seek( HXFile, FilePos(HXFile) - 1 )
                    end;
```

```
                    until (Eof (HXFile)) or (found = 'Y');
                    If (found = 'N') then
                        begin
                              Writeln('proton parameters are not on file');
                              HX.beta0HX := 0;
                              HX.beta1HX := 0;
                              HX.C0HX := 0;
                        end;
                    if (option = 1) then
                              Close(HXFile);
          End;
      5   :  Begin
                    Reset(JFile);
                    found := 'N';
                    repeat
                      Read(JFile,tempJ);
                      If (tempJ.p=J.p) and (tempJ.q=J.q) and (tempJ.r=J.r) then
                        If (tempJ.S=J.S) and (tempJ.M=J.M) and (tempJ.L=J.L) then
                          begin
                            found := 'Y';
                            J := tempJ;
                            If (option = 3) or (option = 2) then
                              Seek( JFile, FilePos(JFile) - 1 )
                          end;
                    until (Eof (JFile)) or (found = 'Y');
                    If (found = 'N') then
                        begin
                              Writeln('  product parameters are not on file');
                              J.beta0PP := 0;
                              J.beta1PP := 0;
                              J.C0PP := 0;
                              J.logK0 := 0;
                        end;
                    if (option = 1) then
                              Close(JFile);
          End;
    End;
  End; { of procedure search }

{*************************************************************************}

BEGIN {Program Main};
  CloseGraph;
  ClrScr;
  Writeln('************************************************************');
  Writeln('*************** PROGRAMME PITZER ************************');
  Writeln('*********** this program performs ionic strength ***********');
  Writeln('****** corrections using a simplified Pitzer equation ******');
  Writeln('****** Pitzer parameters for ligand metal systems can ******');
  Writeln('*************** be stored on records on file ***************');
  Writeln('************************************************************');
  Assign ( LFile, 'L.bin' );
  Assign ( MFile, 'M.bin' );
  Assign ( AXFile, 'AX.bin' );
  Assign ( ALFile, 'AL.bin' );
  Assign ( MXFile, 'MX.bin' );
  Assign ( HXFile, 'HX.bin' );
  Assign ( JFile, 'J.bin' );
  Repeat
     Writeln('************************************************************');
     Writeln( 'Would you like to 0) Exit this program');
     Writeln( '                  or 1) Use existing parameters');
     Writeln( '                  or 2) Add new parameters');
     Writeln( '                  or 3) Edit parameters');
     Writeln( '                  or 4) List metal names');
     Writeln( '                  or 5) List ligand names');
     Writeln('************************************************************');
     Write( 'Enter the number of your choice     ');
     Readln(option);
     ClrScr;
     If (option = 2) or (option = 3) then
        EDITING;
     If (option = 4) or (option = 5) then
        LISTING;
```

```
    If option = 1 then
       PITZER_CORRECT;
  Until (option = 0) ;
END. { of program Main }
```

A5 MALVERN.PAS - Source code of computer program which corrects Malvern 2600D light data to account for anomolous diffraction. Turbo Pascal Version 6.

```
{*************************************************************************}

PROGRAM MALVERN;

{ THIS PROGRAM WAS WRITTEN BY LISA.F.SEYMOUR 1994 FOR A MALVERN 2600 LASER  }
{ PARTICLE SIZER.  IT WAS WRITTEN SPECIFICALLY FOR A 100MMM LENS AND        }
{ HAS MATRIX FILES ASSOCIATED WITH IT THAT HAVE BEEN CALCULATED FOR HEPTANE }
{ AT 20OC TO BE THE REFERENCE MEDIUM. THIS PROGRAM USES OBJECTS WITH 8      }
{ ASSOCIATED PROCEDURES AND THE MAIN BODY CONTAINS 12 PROCEDURES AND 3      }
{ FUNCTIONS. ALL ARE LISTED IN ALPHABETICAL ORDER                           }
{ A CUBIC SPLINE INTERPOLATION IS USED TO SMOOTH THE DATA GRAPHICALLY.      }

USES  Dos, Printer, TPGraph, Crt, Graph, Objects,
      Drivers, Views, Menus, Dialogs, App;

CONST
  MaxLines          = 100;
  cmFileOpen        = 100;
  cmNewDialog       = 102;
  cmGo              = 103;
  cmFileSave        = 104;
  cmFileSaveas      = 105;
  cmHelp            = 107;
  cmAbout           = 108;
  np                = 50;
  xmax              = 16;

TYPE
  stype        =   string[100];
  xtype        =   array [0..xmax] of real;
  qtype        =   array [1..xmax] of real;
  atype        =   array [1..xmax-1, 1..xmax] of real;

  TMyApp = object(TApplication)
    procedure AboutDialog;
    procedure HandleEvent(var Event: TEvent); virtual;
    procedure InitMenuBar; virtual;
    procedure InitStatusLine; virtual;
    procedure HelpDialog;
    procedure NewDialog;
    procedure Go;
  end;

  PInterior = ^TInterior;
  TInterior = object(TScroller)
    constructor Init(var Bounds: TRect; AHScrollBar,
                     AVScrollBar: PScrollBar);
    procedure Draw; virtual;
  end;

  PDemoDialog = ^TDemoDialog;
  TDemoDialog = object(TDialog)
  end;

  DialogData = record
    KilH, KilL, InputName, n_int, n_ext, path : string[128];
  end;

VAR
   Ch                        : Char;
   i                         : integer;
   LineCount                 : word;
   Lines                     : array[0..MaxLines - 1] of PString;
   DataRec                   : DialogData;
   MyApp                     : TMyApp;
```

```
{*********************************************************************}

PROCEDURE AXES( junk:stype; x:xtype; y:qtype; logdiff:real ); forward;
PROCEDURE CALCULATE( junk:stype; a:atype; x:xtype; lm:qtype ); forward;
PROCEDURE DATA_INPUT; forward;
PROCEDURE GRAPH_INIT; forward;
PROCEDURE INITDATA; forward;
PROCEDURE ISWAP( Var I1, I2 :Integer ); forward;
PROCEDURE MULT_MAT( Var v1:qtype; mat:atype; v2:qtype ); forward;
PROCEDURE NORML( Var v:qtype ); forward;
PROCEDURE NORMV( Var v:qtype ); forward;
PROCEDURE PRNSCRN( X1,Y1,X2,Y2 :Integer; FormFeed:Boolean ); forward;
PROCEDURE SMOOTH( x:xtype; y:qtype; Var ds,d1,d3,d4,d5,d9,kd:real); forward;
PROCEDURE STATS (junk:stype ;x:xtype ;q,lc,lm:qtype;
ds,d1,d3,d4,d5,d9,kd,error:real); forward;

{*********************************************************************}

 function log(A:real):real;
 begin
   log:= ln(A)/(ln(10));
 end;

{*********************************************************************}

 function newerror(v1,v2:qtype):real;
 var temp : real;
 begin
   temp := 0;
   for i := 1 to 15 do
     temp := temp + sqr(v1[i] - v2[i]);
   if temp <= 1 then
     temp := 1;
   newerror:= log(temp);
 end;

{*************************************************************************}

 function power(A,B:real):real;
 begin
   power:= exp(B*ln(A));
 end;

{*********************************************************************}

PROCEDURE AXES( junk:stype; x:xtype; y:qtype; logdiff:real );
Var
    maxx        : real;
    minx        : real;
    peak        : real;
    dx          : real;
    temp        : real;
    maxi        : integer;
    info        : stype;
    size        : string[5];

Begin

SetViewPort(round(0.2*getmaxX),round(0.2*getmaxY),round(0.8*getmaxX),round(0.8*getm
axY),false);
  minx := log(x[xmax]);
  maxx := log(x[0]);
  dx := (maxx - minx)/10;
  SetWindow(minx,maxx,0,1);
  SetColor(green);
  ScOutTextXY((minx-3*dx),1.26,'UCT PHYSICS MALVERN SOFTWARE ');
  SetColor(white);
  Screctangle(minx,0,maxx,1);
  SetTextStyle(0,VertDir,1);
  ScOutTextXY(minx-0.4,0.6,'Volume %');
  SetTextStyle(0,HorizDir,1);
  ScOutTextXY(minx-0.2,1,'100');
  ScOutTextXY(minx-0.2,0,'0');
  ScOutTextXY(minx-0.2,0.5,'50');
```

```
  ScOutTextXY((minx+2.5*dx),-0.12,'Particle Diameter (um)');
  ScOutTextXY((minx-dx),1.1,junk);
  for i := 1 to 10 do
    begin
     ScLine(minx,(0.1*i),minx+0.02,(0.1*i));
     ScLine(maxx,(0.1*i),maxx-0.02,(0.1*i));
    end;
  temp := 0;
  for i := 1 to xmax do
    if y[i] > temp then
      begin
          maxi := i;
          temp := y[i];
      end;
  peak := (x[maxi] + x[maxi-1])/2;
  str(logdiff:5:3,size);
  info := 'log diff = '+ size;
  str((100*temp):4:1,size);
  info := info + '  Max % = '+ size;
  str(peak:4:2,size);
  info := info + ' at band centered at '+ size + ' um';
  ScOutTextXY(minx-dx,1.18,info);
  for i := 1 to 15 do
     Begin
        temp := log(x[i]);
        if (i mod 4) = 0 then
          begin
            Str(x[i]:4:2,size);
            ScOutTextXY(temp-0.4*dx,-0.04, size);
            ScLine(temp,0,temp,-0.015);
          end;
     end;
  Str(x[0]:4:2,size);
  ScOutTextXY(log(x[0])-0.5*dx,-0.04, size);
  ScLine(log(x[0]),0,log(x[0]),-0.01);
  ScLine(log(x[0]),0,log(x[0]),-0.015);
end; { of procedure AXES }

{*************************************************************************}

PROCEDURE CALCULATE ( junk:stype ; a:atype ; x:xtype ; lm:qtype );
Var
  error, olderror                  : real;
  lc, q, templc, tempq             : qtype;
  count                            : integer;
  ds, d1, d3, d4, d5, d9, kd       : real;

Begin
  norml(lm);
  for i := 1 to 15 do
      tempq[i] := lm[i]/a[i,i];                          { estimate volume }
  tempq[16] := 1.5*(2*tempq[15] - tempq[14]);
  if tempq[16] < 0 then
    tempq[16] := 0;
  normv(tempq);
  mult_mat(templc,a,tempq);
  norml(templc);
  error := newerror(templc,lm);                          { calculate error }
  count := 0;
  repeat                                                 { iteration loop 1 }
      olderror := error;
      count := count + 1;
      writeln('1  ',count,'  ',olderror);
      for i := 1 to 16 do
        begin
          lc[i] := templc[i];
          q[i] := tempq[i];
          tempq[i] := sqr(q[i]);                         { square volume }
        end;
      normv(tempq);
      mult_mat(templc,a,tempq);
      norml(templc);
      error := newerror(templc,lm);
  until (olderror <= error);
```

```
  error := olderror;
  for i := 1 to 16 do
    begin
      tempq[i] := q[i];
      templc[i] := lc[i];
    end;
  count := 0;
  repeat                                                    { iteration loop 2 }
      olderror := error;
      count := count + 1;
      writeln('2  ',count,'  ',olderror);
      for i := 1 to 15 do
        begin
          lc[i] := templc[i];
          q[i] := tempq[i];
          if templc[i+1] > 0 then
            tempq[i] := q[i]*(sqr(lm[i]/lc[i]) + sqr(lm[i+1]/templc[i+1]))
          else
            tempq[i] := q[i]*(sqr(lm[i]/lc[i]));
        end;
      lc[16] := templc[16];
      q[16] := tempq[16];
      if lc[16] > 0 then
        tempq[16] := q[16]*2*sqr(lm[16]/lc[16])          { refine volume }
      else
        tempq[16] := q[16]*2;
      normv(tempq);
      mult_mat(templc,a,tempq);
      norml(templc);
      error := newerror(templc,lm);
  until (olderror <= error) or (count > 5000);
  error := olderror;
  delay(1000);
  If (DataRec.KilH='Y') or (DataRec.KilH='y') then
    If (q[1] > q[2]) and (q[2] < 1e-2) then
    begin
      q[1] := 0;
      normv(q);
    end;
  If (DataRec.KilL='Y') or (DataRec.KilL='y') then
    begin
      q[16] := 0;
      normv(q);
    end;
  GRAPH_INIT;                                               { plot graph }
  AXES( junk, x, q, error );
  SMOOTH( x, q, ds, d1, d3, d4, d5, d9, kd);
  STATS( junk, x, q, lc, lm, ds, d1, d3, d4, d5, d9, kd, error);
End;

{*****************************************************************************}

PROCEDURE DATA_INPUT;
Var
  l1, l2, temp                    : real;
  inputfile, afile                : text;
  sym                             : char;
  info                            : string[22];
  junk                            : stype;
  k, run, lens, first, code       : integer;
  a                               : atype;
  x                               : xtype;
  lm                              : qtype;
Begin
  {$I-}
  If DataRec.n_ext = '1.3875' then
    begin
      Val(Datarec.n_int,temp,code);
      str((temp*10000):5:0,junk);
      junk := 'ri' + junk + '.100';
      Assign (afile, junk);
    end
  else begin
    junk := 'pil.100';
```

```
  Assign (afile, junk);
end;
Reset( afile );
{$I+}
If IOResult <> 0 then begin
  If (IOResult = 5) or (IOResult = 12) then
  junk := 'Incorrect Matrix File Type or File Access Denied'
  Else
  junk := 'Matrix File not found    ' + junk;
  writeln(junk);
  Halt(1);
end
else begin
  Readln( afile, junk );
  Readln( afile, junk );
  for k := 1 to 16 do
    begin
      if k = 1 then
        begin
          readln( afile, x[1], x[0]);
          x[0] := x[0]*2;
        end
      else
        readln( afile, x[k], temp);                    { read sizes  }
      x[k]:= x[k]*2;
      for i := 1 to 15 do                              { read matrix }
        readln( afile, a[i,k], temp, temp);
      readln( afile );
    end;
  Close( afile );
  x[16] := x[15] - 0.1;
  Writeln('size bands');
  for i:= 0 to 16 do
    Writeln(i,x[i]);
  writeln;
end;
{$I-}
Assign (inputfile, Datarec.inputname);
Reset( inputfile );
If IOResult <> 0 then begin
  If (IOResult = 5) or (IOResult = 12) then
  junk := 'Incorrect Malvern File Type or File Access Denied'
  Else
  junk := 'Malvern Text File not found';
  writeln(junk);
  Halt(1);
end
{$I+}
else begin
  Write('Enter first record number    ');
  readln(first);
  for k:= 1 to (first-1) do
    begin
        read(inputfile, run, temp);
        for i:= 1 to 15 do
          read(inputfile, l1, l2);
        readln(inputfile, temp, info, lens, temp);
    end;
  repeat
    read(inputfile, run, temp);
    str(temp:6:4,junk);
    junk := 'obscur = ' + junk;
    if run > 0 then
      begin
        for i:= 1 to 15 do
          begin
            read(inputfile, l1, l2);
            lm[i] := (l1 + l2)/2;
          end;
        readln(inputfile, temp, info, lens, temp);
        junk := junk + ' ' + info + '  lens = ';
        str(lens,info);
        junk := junk + info;
        str(run,info);
```

```
          junk := 'run = ' + info + '   ' + junk;
          CALCULATE( junk, a, x, lm );
        end;
    until Eof(inputfile) or (Ch = 'X') or (Ch = 'x');
    Close( inputfile );
  end;
End; { of procedure data_input }

{*************************************************************************}

PROCEDURE GRAPH_INIT;
Var
   grDriver : integer;
   grMode : integer;
   ErrorCode : integer;

Begin
  grDriver := Detect;
  Initgraph(grDriver,grMode,DataRec.path);
  ErrorCode := GraphResult;
  If ErrorCode <> grOk then begin
    writeln('graph error',GraphErrorMsg(ErrorCode));
    Readln;
    Halt(1);
    end;
  SetBkcolor(blue);
  SetColor(white);
  SetUserCharSize(3,1,3,1);
End; { of procedure graph_init}

{*************************************************************************}

PROCEDURE INITDATA;
Begin
  with DataRec do
     Begin
       KilH := 'N';
       KilL := 'N';
       InputName := '21nov94.txt';
       n_int := '1.343';
       n_ext := '1.3875';
       path := 'g:\bgi';
     end;
End; {* of procedure InitData *}

{*************************************************************************}

PROCEDURE ISWAP(Var I1, I2 : Integer);
Var Temp : Integer;
Begin
  Temp := I1;
  I1 := I2;
  I2 := Temp;
End;

{*************************************************************************}

PROCEDURE MULT_MAT(Var v1:qtype ; mat:atype ; v2:qtype );
Var num  : integer;
    temp : real;
Begin
  for i := 1 to 15 do
    begin
      temp:= 0;
      for num := 1 to 16 do
        temp := temp + mat[i,num]*v2[num];
      v1[i] := temp;
    end;
End;

{*************************************************************************}

PROCEDURE NORML(Var v:qtype );
Var
```

```
   temp,no : real;
Begin
   temp := 0;
   v[16] := 2*v[15] - v[14];
   if v[16] <= 0 then
     v[16] := 0;
   for i := 1 to 16 do
    if v[i] > temp then
      temp := v[i];
   no := 2047/temp;
   for i := 1 to 16 do
    v[i] := v[i]*no;
End;

{*************************************************************************}

PROCEDURE NORMV(Var v:qtype );
Var
  temp : real;
Begin
  temp := 0;
  for i := 1 to 16 do
    temp := temp + v[i];
  for i := 1 to 16 do
    v[i] := v[i]/temp;
End;

{*************************************************************************}

PROCEDURE PRNSCRN(X1,Y1,X2,Y2 : Integer; FormFeed : Boolean);
Var
    Ar                              : Array[0..7] of Integer;
    Temp, N2, N1, Num, N, A, B, C   : Integer;
    QuitDump                        : Boolean;

Begin
  If X1 > X2 then ISwap(X1,X2);
  If Y1 > Y2 then ISwap(Y1,Y2);
  QuitDump := False;
  Ar[0] := 128;  Ar[1] := 64;
  Ar[2] := 32;   Ar[3] := 16;
  Ar[4] := 8;    Ar[5] := 4;
  Ar[6] := 2;    Ar[7] := 1;
  N2 := (X2-X1+1) div 256;
  N1 := (X2-X1+1) - N2*256;
  Write(Lst,Chr(27),'@',Chr(13));
  Write(Lst,Chr(27),'A',Chr(8));
  Write(Lst,Chr(27),'1');
  For A := (Y1 div 8) to (Y2 div 8) do If Not QuitDump then
    Begin
      Write(Lst,Chr(27),'*',Chr(4),Chr(N1),Chr(N2));
      For B := X1 to X2 do
        Begin
          Num := 0;
          For C := 0 to 7 do
            Begin
              N := A * 8 + C;
              If GetPixel(B,N) <> Black then
                 If (N >= Y1) and (N <= Y2) then Num := Num + Ar[C];
            End;
          Write(Lst,Chr(Num));
          If KeyPressed then
                  QuitDump := True;
        End;
        WriteLN(Lst);
    End;
  Write(Lst,Chr(27),'3');
  If FormFeed then Write(Lst,Chr(12));
End;

{*************************************************************************}

PROCEDURE SMOOTH( x:xtype; y:qtype; Var ds, d1, d3, d4, d5, d9, kd : real);
VAR
```

```
  k                                                    : integer;
  alpha, beta, C, S, N, g, e, f, miny, mean,
  T, BB, CC, dt, tt, newx, newy, maxy, oldy, oldx      : real;
  D, costh, sinth, deltax, deltay, sum, lgx            : xtype;

Begin
  d1 := 0;
  d3 := 0;
  d4 := 0;
  d5 := 0;
  d9 := 0;
  kd := 0;
  sum[xmax] := 0;
  for i := xmax-1 downto 0 do
      sum[i] := sum[i+1] + y[i+1];
  for i := 0 to xmax do begin
      lgx[i] := log(x[i]);
  end;
  k := 1;
  deltax[0] := lgx[1] - lgx[0];
  deltay[0] := sum[1] - sum[0];
  d[0] := sqrt(sqr(deltax[0]) + sqr(deltay[0]));
  oldx := lgx[1];
  oldy := 1;
  for k := 1 to xmax-1 do
    begin
      deltax[k] := lgx[k+1] - lgx[k];
      deltay[k] := sum[k+1] - sum[k];
      d[k] := sqrt(sqr(deltax[k]) + sqr(deltay[k]));
      alpha := sqr(d[k]);
      beta := sqr(d[k-1]);
      C := deltax[k-1]*alpha + deltax[k]*beta;
      S := deltay[k-1]*alpha + deltay[k]*beta;
      N := sqrt(sqr(C) + sqr(S));
      costh[k] := C/N;
      sinth[k] := S/N;
    end;
  alpha := d[1]*(2*d[0]+d[1]);
  beta := -sqr(d[0]);
  C := deltax[0]*alpha + deltax[1]*beta;
  S := deltay[0]*alpha + deltay[1]*beta;
  N := sqrt(sqr(C) + sqr(S));
  costh[0] := C/N;
  sinth[0] := S/N;
  alpha := -sqr(d[xmax-1]);
  beta := d[xmax-2] * (d[xmax-2] + 2*d[xmax-1]);;
  C := deltax[xmax-2]*alpha + deltax[xmax-1]*beta;
  S := deltay[xmax-2]*alpha + deltay[xmax-1]*beta;
  N := sqrt(sqr(C) + sqr(S));
  costh[xmax] := C/N;
  sinth[xmax] := S/N;
  for k := 0 to xmax-1 do
    begin
      g := sqr(deltax[k]) + sqr(deltay[k]);
      e := 7 - costh[k]*costh[k+1] - sinth[k]*sinth[k+1];
      f := deltax[k]*(costh[k]+costh[k+1]) + deltay[k]*(sinth[k]+sinth[k+1]);
      T := (sqrt(f*f + 2*e*g) - f) * 3/e;
      BB := 6*deltax[k]/(T*T*T) - 3*(costh[k]+costh[k+1])/(T*T);
      CC := 6*deltay[k]/(T*T*T) - 3*(sinth[k]+sinth[k+1])/(T*T);
      dt := T/np;
      for i := 0 to np do
        begin
          tt := i*dt;
          newx := lgx[k] + costh[k]*tt + BB*(T*tt*tt/2 - tt*tt*tt/3)
                       + tt*tt*(costh[k+1]-costh[k])/(2*T);
          newy := sum[k] + sinth[k]*tt + CC*(T*tt*tt/2 - tt*tt*tt/3)
                       + tt*tt*(sinth[k+1]-sinth[k])/(2*T);
          if (newy < 0) or (newy > oldy) then
            newy := oldy;
          if k <> 15 then
            begin
               ScMoveTo(oldx,oldy);
               ScLineTo(newX,newY);
            end;
```

```
          if (oldy > 0.1) and (newy < 0.1) then
             d1 := power(10,oldx) + (0.1 - oldy)*(oldx - newx)/(oldy - newy);
          if (oldy > 0.5) and (newy < 0.5) then
             d5 := power(10,oldx) + (0.5 - oldy)*(oldx - newx)/(oldy - newy);
          if (oldy > 0.9) and (newy < 0.9) then
             d9 := power(10,oldx) + (0.9 - oldy)*(oldx - newx)/(oldy - newy);
         { mean := (power(10,newx) + power(10,oldx))/2; }
         { d3 := d3 + (oldy-newy)/mean; }
         { d4 := d4 + (oldy-newy)*mean; }
         { kd := kd + (oldy-newy)*mean*mean/4;}
          oldy := newy;
          oldx := newx;
        end;
    end;
  { d3 := 1/d3;}
  ds := (d9 - d1)/d5;
  for i:= 1 to 15 do
       ScRectangle(lgx[i],y[i],lgx[i-1],0);
  for i:= 1 to 16 do
    begin
       mean := (x[i] + x[i-1])/2;
       kd := kd + y[i]*mean*mean/4;
       d3 := d3 + y[i]/mean;
       d4 := d4 + y[i]*mean;
    end;
  SetColor(yellow);
  mean := 1.1*log(x[16]) - 0.1*log(x[0]);
  ScOutTextXY(mean,-0.2,'Press Y to Print, X to Exit, or any Other Key to
Continue');
  REPEAT
  UNTIL KeyPressed;
  Ch := Readkey;
  SetViewPort(0,0,GetMaxX,GetMaxY,ClipOn);
  If (Ch = 'Y') or (Ch = 'y') then
    PrnScrn(0,0,getmaxX,round(getmaxY*0.9),False);
  CloseGraph;
  d3 := 1/d3;
  ds := (d9 - d1)/d5;
END;

{*****************************************************************************}

 PROCEDURE STATS (junk:stype ;x:xtype ;q,lc,lm:qtype;
ds,d1,d3,d4,d5,d9,kd,error:real);
 Var
   Dev                              : text;

 Begin
  If (Ch = 'Y') or (Ch = 'y') then
    Assign(Dev, 'Lpt1')
  Else
    AssignCrt(Dev);
  If (Ch <> 'X') and (Ch <> 'x') then
    Begin
    Rewrite(Dev);                                        { output stats }
    Writeln (Dev,'
_____________________________________________________________________________');
    Writeln (Dev,' |       ',junk,'          |');
    Writeln (Dev,'
_____________________________________________________________________________');
    Writeln (Dev,' |  High Size   V%  |  High Size   V%  |  High Size   V%  |  High
Size   V%  |');
    for i := 1 to 4 do
      Writeln (Dev,' |',x[i-1]:9:2, (q[i]*100):8:2,  ' |', x[i+3]:9:2,
(q[i+4]*100):8:2,
            ' |',x[i+7]:9:2, (q[i+8]*100):8:2,' |', x[i+11]:9:2,
(q[i+12]*100):8:2,' |');
    Writeln (Dev,'
-----------------------------------------------------------------------------');
    Writeln (Dev,' |  D[v,0.1] = ',d1:6:2,' um  ',
             '   D[v,0.5] = ',d5:6:2,' um  ',
             '   D[v,0.9] = ',d9:6:2,' um   |');
    Writeln (Dev,' |   D[4,3]  = ',d4:6:2,' um  ',
             '    D[3,2]  = ',d3:6:2,' um  ',
```

```
            '     Span    = ',ds:6:2,'       |');
    Writeln (Dev,' |                  log diff = ',error:5:3,
             '           R[5,3]  = ',kd:6:2,' um^2              |');
    Writeln (Dev,'
-------------------------------------------------------------------------------');
    Close(Dev);
    Writeln('Press Enter');
    readln;
    GRAPH_INIT;
    SetViewPort(round(0.2*getmaxX),round(0.1*getmaxY),
          round(0.8*getmaxX),round(0.5*getmaxY),false);
    SetWindow(0,17,0,2047);                                    { plot lc and lm }
    Screctangle(0,0,17,2047);
    ScOutTextXY(-2,2200,junk);
    ScLine(1,1150,2,1150);
    ScOutTextXY(3,1200,'measured ');
    ScMoveTo(1,lm[1]);
    for i := 2 to 16 do
        ScLineTo(i,lm[i]);
    SetColor(yellow);
    SetLineStyle(DottedLn,0,NormWidth);
    ScLine(1,950,2,950);
    ScOutTextXY(3,1000,'calculated ');
    ScMoveTo(1,lc[1]);
    for i := 2 to 16 do
       SclineTo(i,lc[i]);
    ScOutTextXY(-2,2400,'  Press Y to Print, X to Exit or any Other Key to
Continue');
    SetColor(green);
    ScOutTextXY(1,1400,'LIGHT ENERGY');
    repeat
    until keypressed;
    Ch := Readkey;
    SetViewPort(0,0,GetMaxX,GetMaxY,ClipOn);
    If (Ch = 'Y') or (Ch = 'y') then
      PrnScrn(0,round(getmaxY*0.05),getmaxX,round(getmaxY*0.5),False);
    CloseGraph;
    End;
End; { of procedure statistics }

{*************************************************************************}

CONSTRUCTOR TInterior.Init(var Bounds: TRect; AHScrollBar,
                           AVScrollBar: PScrollBar);
begin
  TScroller.Init(Bounds, AHScrollBar, AVScrollBar);
  Options := Options or ofFramed;
  SetLimit(128, LineCount);
end; {* of constructor TInterior.Init}

{*************************************************************************}

PROCEDURE TInterior.Draw;
Var
  Color: Byte;
  I, Y: Integer;
  B: TDrawBuffer;
Begin
  Color := GetColor(1);
  for Y := 0 to Size.Y - 1 do
    begin
      MoveChar(B, ' ', Color, Size.X);
      i := Delta.Y + Y;
      if (I < LineCount) and (Lines[I] <> nil) then
         MoveStr(B, Copy(Lines[I]^, Delta.X + 1, Size.X), Color);
      WriteLine(0, Y, Size.X, 1, B);
    end;
End; {* of procedure TInterior}

{*************************************************************************}

PROCEDURE TMyapp.Go;
Begin
  MyApp.Done;
```

```
  data_input;
  MyApp.Init;
  MyApp.run;
End;{* of Procedure TMyapp.Go *}

{*********************************************************************}

PROCEDURE TMyApp.HandleEvent(var Event: TEvent);
Begin
  TApplication.HandleEvent(Event);  {******* runs procedure ***********}
  if Event.What = evCommand then
   begin
      case Event.Command of
        cmNewDialog: NewDialog;
        cmGo : Go;
        cmHelp: HelpDialog;
        cmAbout: AboutDialog;
      else
        Exit;
      end;
      ClearEvent(Event);
   end;
End; {* of procedure TMyApp.HandleEvent *}

{*********************************************************************}

PROCEDURE TMyApp.InitMenuBar;
Var
  R: TRect;
Begin
  GetExtent(R);
  R.B.Y := R.A.Y + 1;
  MenuBar := New(PMenuBar, Init(R, NewMenu(
    NewSubMenu('~F~ile', hcNoContext, NewMenu(
      NewItem('~D~ata', 'F2', kbF2, cmNewDialog, hcNoContext,
      NewItem('S~a~ve as ...', 'F5',kbF5,  cmFileSaveAs, hcNoContext,
      NewLine(
      NewItem('E~x~it', 'Alt-X', kbAltX, cmQuit, hcNoContext,
      nil))))),
    NewSubMenu('~W~indow', hcNoContext, NewMenu(
      NewItem('~N~ext', 'F6', kbF6, cmNext, hcNoContext,
      NewItem('~D~ata', 'F2', kbF2, cmNewDialog, hcNoContext,
      nil))),
    NewSubMenu('~H~elp', hcNoContext, NewMenu(
      NewItem('~I~nfo','F1', kbF1, cmHelp, hcNoContext,
      NewItem('~S~upport','F10', kbF10, cmAbout, hcNoContext,
      nil))),
    nil)))
  )));
End; {* of procedure TMyApp.InitMenuBar *}

{*********************************************************************}

PROCEDURE TMyApp.InitStatusLine;
Var
  R: TRect;
Begin
  GetExtent(R);
  R.A.Y := R.B.Y - 1;
  StatusLine := New(PStatusLine, Init(R,
    NewStatusDef(0, $FFFF,
      NewStatusKey('', kbF10, cmMenu,
      NewStatusKey('~Alt-X~ Exit', kbAltX, cmQuit,
      NewStatusKey('~F2~ Data', kbF2, cmNewDialog,
      NewStatusKey('~F9~ Go', kbF9, cmGo,
      NewStatusKey('~F1~ Help', kbF1, cmHelp,
      nil))))),
    nil)
  ));
End; {* of procedure TMyApp.InitStatusLine *}

{*********************************************************************}

PROCEDURE TMyApp.NewDialog;
```

```
Var
  Bruce: PView;
  Dialog: PDemoDialog;
  R: TRect;
  C: Word;
Begin
  R.Assign(10, 2, 70, 21);
  Dialog := New(PDemoDialog, Init(R, 'Data Input'));
  with Dialog^ do
    begin
      R.Assign(26, 2, 55, 3);
      Bruce := New(PInputLine, Init(R, 128));
      Insert(Bruce);
      R.Assign(2, 2, 24, 3);
      Insert(New(PLabel, Init(R, 'Kill High Data (Y/N)', Bruce)));
      R.Assign(26, 4, 55, 5);
      Bruce := New(PInputLine, Init(R, 128));
      Insert(Bruce);
      R.Assign(2, 4, 24, 5);
      Insert(New(PLabel, Init(R, 'Kill Low Data (Y/N)', Bruce)));
      R.Assign(26, 6, 55, 7);
      Bruce := New(PInputLine, Init(R, 128));
      Insert(Bruce);
      R.Assign(2, 6, 24, 7);
      Insert(New(PLabel, Init(R, 'Data File Name', Bruce)));
      R.Assign(26, 8, 55, 9);
      Bruce := New(PInputLine, Init(R, 128));
      Insert(Bruce);
      R.Assign(2, 8, 24, 9);
      Insert(New(PLabel, Init(R, 'n particles *', Bruce)));
      R.Assign(26, 10, 55, 11);
      Bruce := New(PInputLine, Init(R, 128));
      Insert(Bruce);
      R.Assign(2, 10, 24, 11);
      Insert(New(PLabel, Init(R, 'n solvent *', Bruce)));
      R.Assign(26, 12, 55, 13);
      Bruce := New(PInputLine, Init(R, 128));
      Insert(Bruce);
      R.Assign(2, 12, 24, 13);
      Insert(New(PLabel, Init(R, 'Path to Drivers', Bruce)));
      R.Assign(2, 14, 55, 15);
      Insert(New(PLabel, Init(R, '*    n = refractive index', Bruce)));
      R.Assign(8, 16, 16, 18);
      Insert(New(PButton, Init(R, '~O~k', cmOK, bfDefault)));
      R.Assign(36, 16, 46, 18);
      Insert(New(PButton, Init(R, 'Cancel', cmCancel, bfNormal)));
    end;
  Dialog^.SetData(DataRec);
  C := DeskTop^.ExecView(Dialog);
  if c <> cmCancel then Dialog^.GetData(DataRec);
  Dispose(Dialog, Done);
End; {* of procedure TMyApp.NewDialog *}

{*********************************************************************}

PROCEDURE TMyApp.AboutDialog;
Var
  Bruce                    : PView;
  Dialog                   : PDemoDialog;
  R                        : TRect;
  C                        : Word;
  dx                       : Integer;

Begin
  R.Assign(4,2,76,21);
  dx := ROUND((76-4)/2);
  Dialog := New(PDemoDialog, Init(R, 'About Shape Correction Program '));
  with Dialog^ do
    begin
      R.Assign(2, 2, 69, 3);
      Insert(New(PLabel, Init(R, ' ', Bruce)));
      R.Assign(2, 3, 69, 4);
      Insert(New(PLabel, Init(R, '      This program was written by Lisa Seymour,
UCT  1995 ', Bruce)));
```

```
      R.Assign(2, 4, 69, 5);
      Insert(New(PLabel, Init(R, '            As part of her PhD in chemistry ',
Bruce)));
      R.Assign(2, 5, 69, 6);
      Insert(New(PLabel, Init(R, ' ', Bruce)));
      R.Assign(DX-8,16,DX+5,18);
      Insert(New(PButton, Init(R, ' -O-k', cmOK, bfDefault)));
    end;
  C := DeskTop^.ExecView(Dialog);
  Dispose(Dialog, Done);
End; {* of procedure TMyApp.AboutDialog *}

{*****************************************************************}

PROCEDURE TMyApp.HelpDialog;
Var
  Bruce                    : PView;
  Dialog                   : PDemoDialog;
  R                        : TRect;
  C                        : Word;
  dx                       : Integer;

Begin
  R.Assign(4,2,76,21);
  dx := ROUND((76-4)/2);
  Dialog := New(PDemoDialog, Init(R, 'Malvern 2600 Correction Program
Instructions'));
  with Dialog^ do
    begin
      R.Assign(1, 1, 71, 2);
      Insert(New(PLabel, Init(R, '   <F2>  Enter the correct data such as the
malvern file name and ', Bruce)));
      R.Assign(1, 2, 71, 3);
      Insert(New(PLabel, Init(R, '         refractive indeces of your two phases as
well as the path', Bruce)));
      R.Assign(1, 3, 71, 4);
      Insert(New(PLabel, Init(R, '         to your turbo pascal graphics screen
drivers.          ', Bruce)));
      R.Assign(1, 4, 71, 5);
      Insert(New(PLabel, Init(R, '   <F9>  Apply Corrections to Malvern light Data
            ', Bruce)));
      R.Assign(1, 5, 71, 6);
      Insert(New(PLabel, Init(R, '<Alt-X>  Exit this program
            ', Bruce)));
      R.Assign(1, 6, 71, 7);
      Insert(New(PLabel, Init(R, '*  Before using this program, the relevant
Malvern data files', Bruce)));
      R.Assign(1, 7, 71, 8);
      Insert(New(PLabel, Init(R, '   must be converted to text using the Malvern
Spreadsheet Command', Bruce)));
      R.Assign(1, 8, 71, 9);
      Insert(New(PLabel, Init(R, '   with a long precision of 8 digits and spaces
as delimeters.', Bruce)));
      R.Assign(1, 9, 71,10);
      Insert(New(PLabel, Init(R, '********************** HOW TO MOVE AROUND
**********************', Bruce)));
      R.Assign(1,10, 71,11);
      Insert(New(PLabel, Init(R, '*  Push the above function keys or select them
with a mouse to run.',Bruce)));
      R.Assign(1,11, 71, 12);
      Insert(New(PLabel, Init(R, '*  Press <Enter> or <Esc> or Select OK or Cancel
to close the active', Bruce)));
      R.Assign(1, 12, 71, 13);
      Insert(New(PLabel, Init(R, '   window.  Each active window has to be closed
to proceed!      ', Bruce)));
      R.Assign(1, 13, 71, 14);
      Insert(New(PLabel, Init(R, '*  Press the <Tab> and arrow keys or your mouse
to move around the', Bruce)));
      R.Assign(1, 14, 71, 15);
      Insert(New(PLabel, Init(R, '   data on the screen.
       ', Bruce)));
      R.Assign(1, 15, 71, 16);
      Insert(New(PLabel, Init(R, '*  Press <Alt> and the red letter of choice to
get to the top menu', Bruce)));
```

```
      R.Assign(1, 16, 71, 17);
      Insert(New(PLabel, Init(R, '   or use your mouse.
            ', Bruce)));
      R.Assign(DX-8,17,DX+5,19);
      Insert(New(PButton, Init(R, ' ~O-k', cmOK, bfDefault)));
    end;
  C := DeskTop^.ExecView(Dialog);
  Dispose(Dialog, Done);
End; {* of procedure TMyApp.HelpDialog *}

{*************************************************************************}

BEGIN { PROGRAM MAIN }
  InitData;
  MyApp.Init;
  MyApp.Run;
  MyApp.Done;
END.

{*************************************************************************}
```

A6 EQUATIONS FOR THE INTERACTION ENERGY BETWEEN DROPLETS

The total interaction energy with its first and second derivative form with respect to s are presented here to assist with computation. The energy is calculated for droplet 1 with droplet 2, the droplet with which it has been chosen to collide, and for droplet 1 with all other droplets within its sphere of interaction. In each case the radius of droplet 1 is equal to or greater than the radius of droplet 2.

$$E_T = E_A + E_R + E_S$$

$$E_A = -\frac{A_{eff}}{12}\left(\frac{y}{n_x} + \frac{y}{n_y} + 2\ln\frac{n_x}{n_y}\right) \qquad E_A' = \frac{A_{eff} n_z y^3}{24 a_1^2 n_x^2 n_y^2} \qquad E_A'' = \frac{A_{eff} y^3 (n_x n_y - (n_x + n_y) n_z^2)}{24 a_1^2 n_x^2 n_y^2}$$

$$E_R = \frac{De^{-\kappa s}}{s} + \frac{n_\alpha}{\kappa(r-s)} \qquad E_R(0) = \frac{De^{-\kappa r}}{r} + 11Be^{-\kappa r} + 2C$$

$$E_R' = -\frac{De^{-\kappa s}(\kappa s+1)}{s^2} + \frac{n_\alpha}{\kappa(r-s)^2} - \frac{n_\beta}{(r-s)}$$

$$E_R'' = \frac{De^{-\kappa s}(\kappa^2 s^2 + 2\kappa s + 2)}{s^3} + \frac{2n_\alpha}{\kappa(r-s)^3} - \frac{2n_\beta}{(r-s)^2} - \frac{\kappa n_\gamma}{(r-s)}$$

$$E_S = [4a_2^2 - (2d-h_0)^2]\frac{(P_V+P_M)}{2} + q^2 sum \qquad E_S' = -q(P_V+P_M) + 2q sum \qquad E_S'' = -(P_V+P_M) + 2sum$$

$$sum = \frac{P_V}{C_V^2}\left[e^{-C_V} + \frac{(2d-h_0)}{q}C_V - 1 - \frac{(2d-h_0-q)}{q}C_V e^{-C_V}\right] + \frac{P_M}{C_M^2}\left[e^{-C_M} + \frac{(2d-h_0)}{q}C_M - 1 - \frac{(2d-h_0-q)}{q}C_M e^{-C_M}\right]$$

$$n_\alpha = Ce^{\kappa(r-s)} - Ce^{\kappa(s-r)} - 6Be^{\kappa(s-2r)} + 6Be^{-\kappa E}$$

$$n_\beta = Ce^{\kappa(r-s)} + Ce^{\kappa(s-r)} + 6Be^{\kappa(s-2r)} + B(6s-r)\frac{e^{-\kappa E}}{E}$$

$$n_\gamma = Ce^{\kappa(r-s)} + Ce^{\kappa(s-r)} + 6Be^{\kappa(s-2r)} + \frac{Be^{-\kappa E}}{\kappa}\left(\frac{6}{E} - \frac{(\kappa E+1)}{6E^3}\right)$$

$$n_x = x^2 + xy + x \qquad n_y = x^2 + xy + x + y \qquad n_z = 2x + y + 1$$

$$\bar{\psi} = \frac{\sum_i \psi_i}{N} \qquad \bar{a} = \frac{\sum_i a_i}{N}$$

$$x = \frac{H}{2a_1} \qquad y = \frac{a_2}{a_1}$$

$$q = a_1 + a_2 + H - h_0 \qquad s = a_1 + a_2 + H$$

$$V_1 = 52.51 \qquad M_1 = 20.39 \qquad V_2 = 4.414 \qquad M_2 = 2.467$$

$$K_V = (\nu_1 + \nu_2)kT \qquad C_V = V_2\frac{q\alpha}{l} \qquad P_V = \frac{\pi}{2}V_1 K_V\, e^{-V_2\frac{h_0\alpha}{l}}$$

$$2d = \frac{(2a_2^2 + 2a_1a_2 + 2a_1H + 2a_2H + H^2)}{(a_1 + a_2 + H)}$$

$$r = \frac{1.81\bar{a}}{\sqrt[3]{\phi}} \qquad \kappa = \sqrt{\frac{2F^2I_{SI}}{\varepsilon_r\varepsilon_0 RT}}$$

$$K_M = 2\left(\frac{2\pi}{9}\right)^{\frac{3}{2}}(\alpha^2-1)l^2\nu_1\nu_2 kT \qquad C_M = M_2\frac{q\alpha}{l} \qquad P_M = \frac{\pi}{2}M_1 K_M\, e^{-M_2\frac{h_0\alpha}{l}}$$

$$B = \frac{\varepsilon_r\varepsilon_0\psi_1\bar{\psi}a_1\bar{a}e^{\kappa(a_1+\bar{a})}}{r}$$

$$C = \frac{\varepsilon_r\varepsilon_0\psi_1\bar{\psi}a_1\bar{a}e^{\kappa(a_1+\bar{a})}}{r}\,\frac{8.88(1.3\kappa r+1)e^{-1.3\kappa r}}{\kappa^2 r^2}$$

$$D = \varepsilon_r\varepsilon_0\psi_1\psi_2 a_1a_2e^{\kappa(a_1+a_2)} \qquad E = \sqrt{\frac{r^2}{3} - \frac{rs}{3} + s^2}$$

$$\text{if } H > h_{min} \quad h_0 = H \quad \text{else} \quad h_0 = h_{min}$$

$$\nu = \frac{\%\ surfactant\ coverage}{100d_s^2} \qquad \nu_{max} = \frac{1}{d_s^2}$$

where
a_i is the radius of droplet i (m)
α is the expansion parameter for the surfactant in the organic solvent
ν_i is the surfactant concentration for droplet i (m^{-2})
ψ_i is the surface potential of droplet i (V)
ϕ is the internal phase volume ratio of the emulsion
d_s is the diameter of the surfactant headgroup (m)
h_{min} is the minimum thickness of the emulsion bilayer (m)
I_{SI} is the ionic strength of the organic phase (mol m^{-3})
r is the maximum distance between the centres of droplet 1 and droplet 2 (m)
s is the distance between the centres of droplet 1 and droplet 2 (m)
H is the theoretical interparticle separation between droplet 1 and droplet 2 (m)
N is the total number of droplets
A_{eff} is the effective Hamaker constant in the medium (J)
κ is the inverse Debye length (m^{-1})
ε_r is the relative permittivity of the organic phase
ε_0 is the permittivity of a vacuum ($C^2\ J^{-1}\ m^{-1}$)

A7 INCLUDED 1.44MB DISKETTES

Two 1.44Mb diskettes with three computer programs have been included with this thesis. Instructions on how to execute the computer programs as well as a listing of the contents of the diskettes are given in this section. In all cases the programs have been compiled for a Microsoft DOS environment and can be executed from the diskettes or can be transferred locally to another computer drive. When following the instructions, note the following conventions:

- A bold typeface is used for commands you need to enter from the keyboard.
- Angular brackets are used to denote special keys, *i.e.* **<Enter>** refers to pressing the key labelled **Enter**.
- A hyphen is used when two keys need to be pressed simultaneously, *i.e.* **<Alt-X>** refers to pressing the key labelled **Alt** and **X** simultaneously.

To execute any program follow the following procedure:

- Insert the appropriate diskette into your 1.44Mb disk drive.
- Change to this drive.
- Enter the name of the executable file.

If you would like to run these program from your local or networked drive follow this procedure:

- Copy the entire content of the diskette into the subdirectory of your choice. Remember to copy the BGI subdirectory with its files.
- Move to the subdirectory.
- Enter the name of the executable file.

There is a bug in Borland Pascal when executing graphics. If you have a subdirectory anywhere on your local drive named BGI, the graphics will not display properly. To get around this, rename your subdirectory for the period of testing these programs.

A7.1 STREAC.EXE

STREAC is an acronym for "Stochastic Reverse Emulsion Aggregation and Coalescence". This program predicts the extent of aggregation and coalescence and hence stability of a w/o emulsion based on its formulation. The program is discussed in chapter 5.

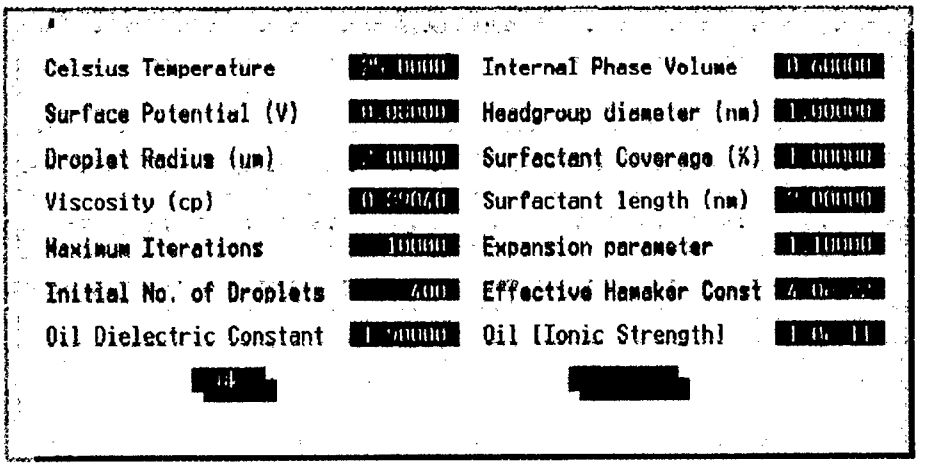

Figure A1
Screen capture of STREAC Data Input Window with test input data.

A7.1.1 Procedure for executing STREAC.EXE

The procedure below can be used to test STREAC. The procedure uses the test input data given in the file EMUL_IN.DAT and displayed in Figure A1.

1 Insert disk 1 into your 1.44Mb disk drive.

2 Move to this drive. (If this is your A: drive type **A: <Enter>**)

3 Type: **STREAC <Enter>**. The Menu will be displayed.

4 Press: **<F2>**. The Data Input Window as depicted in figure A1 will be displayed.

5 Press: **<Enter>**. The Menu will be displayed.

6 Press: **<F9>**. The iterations will start and a histogram of the particle size distribution will be displayed graphically.

7 Once the iterations are completed, press: **Y** to return to the Menu.

8 Repeat steps 4-7, varying the input parameter "Internal Phase Volume" to 0.2, 0.7 and 0.8. To vary an input parameter in the Data Input window, **<Tab>** to the appropriate field and type the new value or select the field with your mouse and press **<Insert>** before typing the new value.

9 Press: **<Alt-X>** to exit STREAC.

A7.2 MALVERN.EXE

This program converts light intensity data obtained from a Malvern 2600 sample run into size distribution data. The theory of this program is described in detail in section 4.2. To use this program to perform the conversion you would need the following two input files:

- The Malvern light intensity output file for your sample. This is obtained using the Malvern 2600 spreadsheet command.
- The refractive index matrix file which is specific to the refractive index of the particles, the refractive index of the surrounding medium and the Malvern lens used.

The file 1343.TXT contains experimental light data for 12 emulsion samples which can be used to test the program and as an example of the input data format. For this test data, a 100mm lens was used, the refractive index of the organic phase was 1.3875 and the refractive index of the aqueous particles was 1.343.

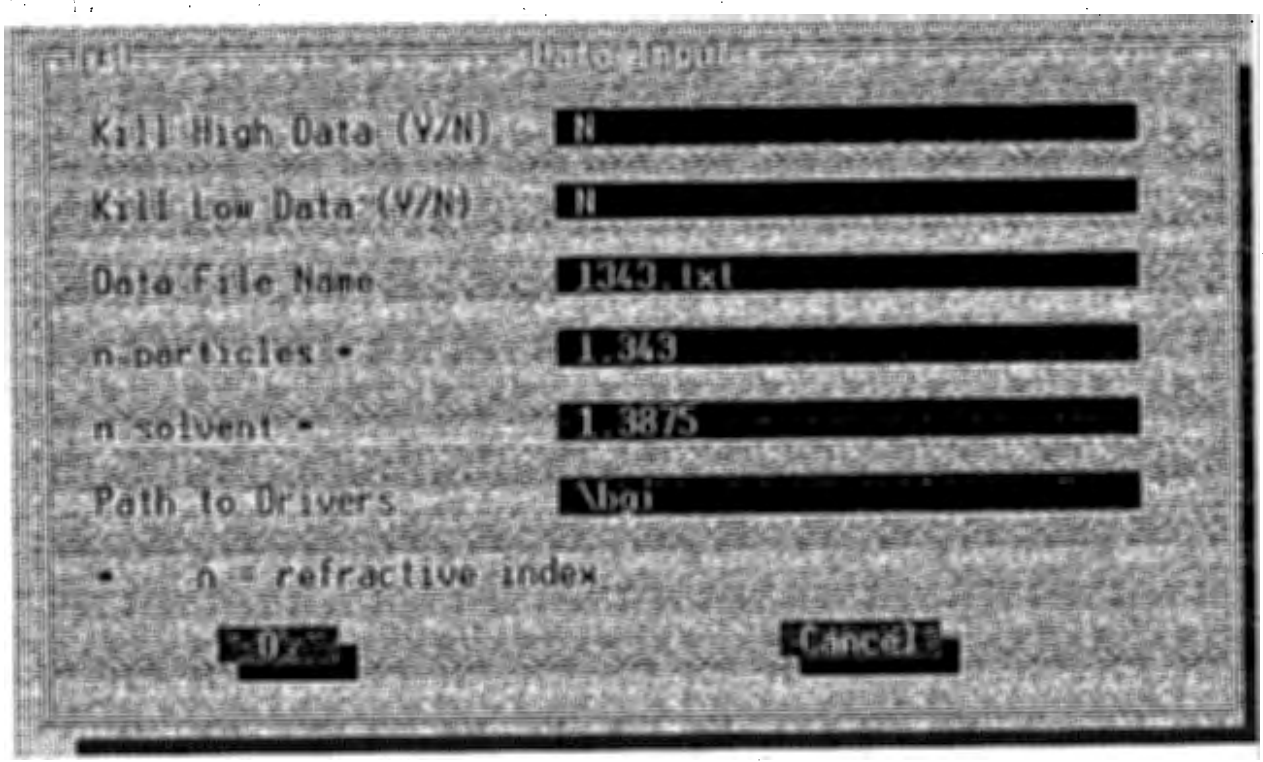

Figure A2

Screen capture of the default data input window showing the input parameters for the test data.

A7.2.1 Procedure for executing MALVERN.EXE

The procedure below can be used to test the MALVERN program. This procedure uses the default data as displayed in Figure A2.

1 Insert disk 2 into your 1.44Mb disk drive.

2 Move to this drive. (If this is your A: drive type **A: <Enter>**)

3 Type: **MALVERN <Enter>**. The Menu will be displayed.

4 Press: **<F9>**. The 16 size bands will be displayed to the screen and you should be prompted for a record number.

5 Type: **1 <Enter>**. As the least squares regression is performed the number of iterations will be displayed on your screen. Once the iterations are complete a histogram of the size distribution for the first record will be shown on your screen.

6 Press: **<Enter>**. A Table of size distribution data will be displayed on your screen.

7 Press: **<Enter>**. The fit between the measured and calculated light intensity data will be presented graphically.

8 Press: **<Enter>**. The histogram for the second record will be presented.

9 Repeat steps 6-8 at your leisure.

10 Press: **X** to return to the Menu.

11 Press: **<Alt-X>** to exit the program.

A7.3 CORPIT.EXE

This program can be used to convert stability constants from one ionic strength to other ionic strengths using the simplified Pitzer approach as documented in Section 3.3.4. This program has a standard DOS-text menu system which prompts you to enter a choice. The standard menu is shown in figure A3.

```
************************************************************
*************** PROGRAMME PITZER ***************************
*********** this program performs ionic strength ***********
****** corrections using a simplified Pitzer equation ******
****** Pitzer parameters for ligand metal systems can ******
************** be stored on records on file **************
************************************************************
************************************************************
Would you like to 0) Exit this program
                  or 1) Use existing parameters
                  or 2) Add new parameters
                  or 3) Edit parameters
                  or 4) List metal names
                  or 5) List ligand names
************************************************************
Enter the number of your choice
```

Figure A3

Standard Menu for CORPIT.EXE

The binary files which are associated with this program contain Pitzer parameters. To edit or add new Pitzer parameters choose options 2 or 3 from the menu. Options 4 and 5 list the metal and ligands for which Pitzer parameters are available in the binary files. The program is case-insensitive.

A7.3.1 Procedure for executing CORPIT.EXE

This procedure uses the program CORPIT to convert the protonation constant of propionate from an ionic strength of 0 to 3 molal NaCl.

1 Insert disk 1 into your local 1.44Mb disk drive.

2 Move to this drive. (If this is your A: drive type **A: <Enter>**)

3 Type: **CORPIT <Enter>**. The Menu will be displayed.

4 Type: **1 <Enter>**.

5 Follow the steps as displayed in Figure A4.

```
************************************************************
****************** PITZER EQUATION *************************
************************************************************
************************************************************
Enter no of metal ions in complex              0
Enter no of ligand ions in complex             1
Enter no of protons in complex (- for OH)      1
Enter the name of your ligand (< 12 chs)       propionate
Enter the electrolyte cation (< 5 chs )          na
Enter the electrolyte anion (< 5 chs )           cl
************************************************************
M=0 L=1 H=1              logK0 = 4.868000E+00
zL=-1 zM=0               Beta(1)AX= 2.664000E-01 C0AX= 1.270000E-03
Beta(0)AL= 1.043000E-01 Beta(1)AL= 2.940000E-01 C0AL= 0.000000E+00
Beta(0)HX= 1.775000E-01 Beta(1)HX= 2.945000E-01 C0HX= 8.000000E-04
Beta(0)MX= 0.000000E+00 Beta(1)MX= 0.000000E+00 C0MX= 0.000000E+00
Beta(0)PP= 0.000000E+00 Beta(1)PP= 0.000000E+00 C0PP= 0.000000E+00
************************************************************
Would you like the ionic strength correction done (Y/N) ?  y
************************************************************
       Enter the free ligand concentration  0.001
************************************************************
       Enter the pH of your solution          7
************************************************************
Enter Molal Ionic Strength to correct to, Enter 0 to end
molal ionic strength   3
molal ionic strength   0
I(m)=3.000 log Km=4.92264 log Kcor=4.41987
f(AX)=-0.168 f(AL)=0.879 f(HX)=1.325 f(MX)=0.000 f(J)=0.000
************************************************************
Enter Experimental molal logK with corresponding molal ionic strength
Enter 0 to end
     ionic strength   0
     molal log K      0
```

Figure A4

An example of the text output for an ionic strength correction. The protonation constant for propionate corrected to 3 molal sodium chloride is presented.

6 A graphical plot of the change in the protonation constant of propionate as the salt concentration increases will be presented to your screen. The co-ordinates for all points on the plot are written to a text file PIT.DAT which can then be used as input into any graphical program.

7 Press: **<Enter>**. The Menu will be displayed.

8 Type: **0 <Enter>** to exit the program.

A7.4 CONTENTS OF DISK 1

Table A1 lists the contents of disk 1. Disk 1 contains all the necessary files to execute the programs STREAC and CORPIT.

Table A1 Contents of Disk 1:

DIR	FILENAME	EXT	bytes	date	time	Description
	AX	BIN	432	16/06/95	14:50	CORPIT electrolyte parameters
	AL	BIN	740	17/05/94	15:56	CORPIT cation-ligand parameters
	HX	BIN	156	04/05/94	16:33	CORPIT proton-anion parameters
	J	BIN	741	11/05/94	15:05	CORPIT product parameters
	L	BIN	105	23/02/93	13:45	CORPIT ligand parameters
	M	BIN	80	21/05/93	11:52	CORPIT metal parameters
	MX	BIN	270	21/05/93	11:52	CORPIT metal-ligand parameters
	PIT	DAT	8,670	26/06/96	16:50	CORPIT graphical output file
	EMUL_IN	DAT	679	30/06/96	10:46	STREAC input data file
	CORPIT	EXE	55,680	16/06/96	15:21	CORPIT program executable
	STREAC	EXE	104,912	17/06/96	14:57	STREAC program executable
	TPGRAPH	TPU	6,048	16/06/96	15:40	graphical unit
BGI	IBM8514	BGI	9,926	27/10/92	7:00	graphical drivers for various monitors
	CGA	BGI	6,250	27/10/92	7:00	
	EGAVGA	BGI	5,527	27/10/92	7:00	
	HERC	BGI	6,122	27/10/92	7:00	
	ATT	BGI	6,266	27/10/92	7:00	
	PC3270	BGI	6,042	27/10/92	7:00	
	VESA16	BGI	6,345	27/10/92	7:00	
TOTAL	19		224,992			

A7.4 CONTENTS OF DISK 2

The contents of disk 2 are listed in Table A2. Disk 2 contains all the necessary files to execute the program MALVERN. When analyzing our emulsions using the Malvern 2600 particle sizer, the refractive index of the droplets in the emulsions varied between 1.333 and 1.424. A scattering matrix file specific to each refractive index had to be produced. The naming of these 101 files RI133000.100 - RI142900.100 correlates to the refractive index of the droplets (1.33 - 1.429). In all our Malvern experimental studies a 100mm lens was used and therefore the matrix files have an extension of 100 and can not be used for experimental data obtained using different lenses. The file MALV_IN.TXT contains Malvern light data for 99 experimental records. This file can be used as an input file to demonstrate the program. The refractive index of the droplets for these records varies between 1.333 and 1.424.

Table A2 Contents of Disk 2:

DIR	FILENAME	EXT	bytes	date	time	Description
	RI13300	100	11,898	22/11/93	8:35	matrix files for 100mm lens
	RI13320	100	11,898	11/12/93	14:29	
	RI13330	100	11,911	08/11/93	12:18	
	RI13340	100	11,898	11/12/93	14:29	
	RI13350	100	11,898	28/11/93	11:26	
	RI13360	100	11,898	06/12/93	8:18	
	RI13370	100	11,898	11/12/93	14:29	
	RI13380	100	11,898	07/12/93	14:11	
	RI13390	100	11,898	13/12/93	14:40	
	RI13400	100	11,898	22/11/93	16:59	
	RI13410	100	11,898	08/12/93	13:22	
	RI13420	100	11,898	11/12/93	14:29	
	RI13430	100	11,898	29/11/93	11:30	
	RI13440	100	11,898	30/11/93	11:13	
	RI13450	100	11,898	28/11/93	11:27	
	RI13460	100	11,898	06/12/93	8:18	

DIR	FILENAME	EXT	bytes	* date	time	Description
	RI13470	100	11,898	11/12/93	14:29	
	RI13480	100	11,898	07/12/93	14:11	
	RI13490	100	11,898	13/12/93	14:40	
	RI13500	100	11,898	23/11/93	9:23	
	RI13510	100	11,898	08/12/93	13:22	
	RI13520	100	11,898	11/12/93	14:30	
	RI13530	100	11,898	29/11/93	11:30	
	RI13540	100	11,898	30/11/93	11:13	
	RI13550	100	11,898	28/11/93	11:27	
	RI13560	100	11,898	06/12/93	8:18	
	RI13570	100	11,898	11/12/93	14:30	
	RI13580	100	11,898	07/12/93	14:11	
	RI13581	100	11,900	10/11/93	8:28	
	RI13590	100	11,898	13/12/93	14:41	
	RI13600	100	11,898	23/11/93	9:23	
	RI13610	100	11,898	08/12/93	13:22	
	RI13620	100	11,898	11/12/93	14:34	
	RI13630	100	11,898	29/11/93	11:30	
	RI13640	100	11,898	30/11/93	11:14	
	RI13650	100	11,898	28/11/93	11:27	
	RI13660	100	11,898	06/12/93	8:19	
	RI13670	100	11,898	13/12/93	14:42	
	RI13680	100	11,898	07/12/93	14:11	
	RI13690	100	11,898	13/12/93	14:41	
	RI13700	100	11,898	23/11/93	9:23	
	RI13710	100	11,898	08/12/93	13:22	
	RI13720	100	11,898	11/12/93	14:34	
	RI13730	100	11,898	29/11/93	11:30	
	RI13740	100	11,898	01/12/93	8:25	
	RI13750	100	11,898	28/11/93	11:27	
	RI13760	100	11,898	06/12/93	8:19	
	RI13770	100	11,898	13/12/93	14:43	
	RI13780	100	11,898	07/12/93	14:12	

DIR	FILENAME	EXT	bytes	date	time	Description
	RI13790	100	11,898	13/12/93	14:41	
	RI13800	100	11,898	23/11/93	9:24	
	RI13810	100	11,898	08/12/93	13:22	
	RI13820	100	11,898	11/12/93	14:34	
	RI13830	100	11,898	29/11/93	11:30	
	RI13840	100	11,898	01/12/93	8:25	
	RI13850	100	11,898	28/11/93	11:27	
	RI13851	100	11,898	10/11/93	8:29	
	RI13860	100	11,898	06/12/93	8:19	
	RI13870	100	11,898	13/12/93	14:43	
	RI13880	100	11,898	07/12/93	14:12	
	RI13890	100	11,898	13/12/93	14:41	
	RI13900	100	11,898	24/11/93	8:33	
	RI13910	100	11,898	08/12/93	13:23	
	RI13920	100	11,898	11/12/93	14:34	
	RI13930	100	11,898	29/11/93	11:30	
	RI13940	100	11,898	01/12/93	8:25	
	RI13950	100	11,898	28/11/93	11:27	
	RI13960	100	11,898	06/12/93	8:19	
	RI13970	100	11,898	13/12/93	14:43	
	RI13980	100	11,898	07/12/93	14:12	
	RI13990	100	11,898	13/12/93	14:41	
	RI14000	100	11,898	24/11/93	8:33	
	RI14010	100	11,898	08/12/93	13:23	
	RI14020	100	11,898	11/12/93	14:30	
	RI14030	100	11,898	29/11/93	11:31	
	RI14040	100	11,898	02/12/93	8:11	
	RI14050	100	11,898	28/11/93	11:28	
	RI14060	100	11,898	06/12/93	8:19	
	RI14070	100	11,898	13/12/93	14:43	
	RI14080	100	11,898	07/12/93	14:12	
	RI14090	100	11,898	13/12/93	14:42	
	RI14100	100	11,898	24/11/93	8:34	

DIR	FILENAME	EXT	bytes	date	time	Description
	RI14110	100	11,898	02/12/93	8:11	
	RI14120	100	11,898	11/12/93	14:30	
	RI14130	100	11,898	29/11/93	11:31	
	RI14140	100	11,898	02/12/93	8:12	
	RI14150	100	11,898	28/11/93	11:28	
	RI14160	100	11,898	06/12/93	8:19	
	RI14170	100	11,898	13/12/93	14:43	
	RI14180	100	11,898	09/12/93	12:42	
	RI14190	100	11,898	13/12/93	14:42	
	RI14200	100	11,898	24/11/93	8:34	
	RI14210	100	11,898	09/12/93	12:43	
	RI14220	100	11,898	11/12/93	14:31	
	RI14230	100	11,901	16/12/93	10:53	
	RI14240	100	11,898	14/12/93	14:48	
	RI14250	100	11,898	14/12/93	14:48	
	RI14260	100	11,898	06/12/93	8:20	
	RI14270	100	11,898	13/12/93	14:43	
	RI14280	100	11,898	02/12/93	8:12	
	RI14290	100	11,898	13/12/93	14:42	
	PIL	100	11,891	11/11/93	8:28	matrix file: particle in liquid
	MALVERN	EXE	95,984	20/06/96	10:25	MALVERN program executable
	TPGRAPH	TPU	6,048	20/06/96	10:25	graphical unit
	1343	TXT	3,800	20/06/96	10:11	light energy: aqueous refractive index=1.343
	1379	TXT	631	20/06/96	10:19	light energy: aqueous refractive index=1.379
	MALV_IN	TXT	29,102	15/06/96	16:49	light energy: aqueous refractive index varies
BGI	EGAVGA	BGI	5,527	27/10/92	7:00	graphical drivers for various monitors
	ATT	BGI	6,266	27/10/92	7:00	
	CGA	BGI	6,250	27/10/92	7:00	
	HERC	BGI	6,122	27/10/92	7:00	
	IBM8514	BGI	9,926	27/10/92	7:00	
	PC3270	BGI	6,042	27/10/92	7:00	
	VESA16	BGI	6,345	27/10/92	7:00	
TOTAL	114		1,395,650			